CORA Cork Open Research Archive
Cartlann Taighde Oscailte Chorcaí

Title	Decarbonisation of whiskey distilleries in a circular economy: investigating biorefinery systems for valorisation of distillery by-products
Authors	Hackula, Anga Awonke
Publication date	2024
Original Citation	Hackula, A. A. 2024. Decarbonisation of whiskey distilleries in a circular economy: investigating biorefinery systems for valorisation of distillery by-products. PhD Thesis, University College Cork.
Type of publication	Doctoral thesis
Rights	© 2024, Anga Awonke Hackula. - https://creativecommons.org/licenses/by/4.0/
Download date	2026-11-02 00:12:38
Item downloaded from	https://hdl.handle.net/10468/16421



UCC
University College Cork, Ireland
Coláiste na hOllscoile Corcaigh

Molluscoid na hÉireann, Corcaigh

National University of Ireland, Cork



Decarbonisation of whiskey distilleries in a circular economy: investigating biorefinery systems for valorisation of distillery by-products

Thesis presented by

Anga Awonke Hackula, BTech, PDBA, MEngSc

ORCID: 0000-0002-2227-7807

for the degree of

Doctor of Philosophy (Civil, Structural and Environmental Engineering)

University College Cork

Civil, Structural and Environmental Engineering

Head of School/Department: Professor Jorge Oliveira

Supervisors: Dr. David Wall, Dr. Richard O'Shea & Professor Jerry Murphy

May 2024

Table of Contents

Declaration xiii

Acknowledgements xiv

Abstract xvi

Thesis outputs xvii

Contribution to the papers xx

Abbreviations / Nomenclature xxi

1.0 Introduction 1

1.1 Introduction and background to thesis 1

1.2 Thesis aims and objectives 4

1.3 Thesis outline in brief 5

References 12

2.0 Literature review 15

2.1 The circular economy 15

2.2 Overview of the whiskey production process and the by-products generated 16

2.3 Anaerobic digestion and dark fermentation 17

2.3.1 Anaerobic digestion and dark fermentation 17

2.3.2 Digester configuration and operational considerations 21

2.4 Single-phase versus two-phase anaerobic digesters 24

2.5 Influence of operating conditions on dark fermentation and anaerobic digestion 25

2.6 Ammonia toxicity in dark fermentation and anaerobic digestion of whiskey by-products 34

2.7 Biogas end-use at a distillery 35

2.8 Demand-driven biogas production and relevance to distilleries 36

2.9 Carbonaceous additives as a means of improving dark fermentation and anaerobic digestion performance 40

2.10 Cascading biorefinery systems 46

2.11 Conclusion 46

References 47

3.0 Design, construction, and concept validation of a laboratory-scale two-phase reactor to valorise whiskey distillery by-products 60

Abstract 60

3.1 Anaerobic digestion of whiskey by-products 61

3.2 Objectives 64

3.3 Material and methods 65

3.3.1 Characteristics of the inoculum and whiskey by-products 65

3.3.2 LBR-EGSB system components 66

3.3.3 Issues and modifications 74

3.3.4 Calculating the maximum organic loading rate of the EGSB 76

3.3.5 LBR start-up/leaching trials 78

3.3.6 EGSB start-up trials 78

3.3.7 Analytical methods 79

3.4 Results and discussion 81

3.4.1 Trends in reactor stability 81

3.4.2 Trends in treatment efficiency 82

3.4.3 Biogas quality and estimated methane yield 83

3.4.4 Reactor considerations and future research 85

3.5 Conclusion 87

References 88

4.0 Two-phase anaerobic digestion for enhanced valorisation of whiskey distillery by-products 94

Abstract 94

4.1 Introduction 95

4.2 Material and methods 98

4.2.1 Inocula 98

4.2.2 Characteristics of the modified whiskey by-products 98

4.2.3 Biochemical methane potential assays 99

4.2.4 Continuously stirred tank reactor trials 101

4.2.5 Leach bed reactor with expanded granular sludge bed experimental trials 103

4.2.6 Analytical methods 106

4.3 Results and discussion 108

4.3.1 Theoretical and batch biochemical methane potential 108

4.3.2 Continuous trial results 111

4.3.3 Potential to offset natural gas consumption at the distillery 115

4.3.4 Estimating the value of volatile fatty acids produced from whiskey by-products 116

4.3.5 Reactor selection considerations and future research 120

4.4 Conclusion 122

References 123

5.0 Developing distillery biorefineries through dark fermentation of whiskey production by-products: the effect of organic loading rate on decarbonisation pathways 129

Abstract 129

5.1 Introduction 130

5.2 Materials and methods 134

5.2.1 Inoculum and feedstock characteristics 134

5.2.2 Biohydrogen potential assays 135

5.2.3 Continuous dark fermentation trials 135

5.2.4 Offsetting fossil fuel usage through a biorefinery approach 136

5.2.5 Analytical methods 137

5.3 Results and discussion 138

5.3.1 Specific biohydrogen and VFA yields from batch trials 138

5.3.2 Continuous dark fermentation trials 141

5.3.3 Acidogenesis performance 146
5.3.4 Considerations of dark fermentation of whiskey by-products 147
5.3.5 Biogenic carbon dioxide for beer carbonisation 148
5.3.6 Biogenic hydrogen for heating and distribution transport 150
5.3.7 Volatile fatty acid usage for beer packaging 153
5.3.8 Limitations and future research 154
5.4 Conclusion 155
References 157
6.0 Assessing two-phase anaerobic digestion systems for demand-driven electricity and biobutanol transport fuel at a large distillery 165
Abstract 165
6.1 Introduction 166
6.2 Materials and methods 172
6.2.1 Methods and analysis overview 172
6.2.2 Inocula and whiskey by-product characteristics 173
6.2.3 Demand-driven operation CSTR trials 175
6.2.4 LBR-EGSB demand-driven operation trials 176
6.2.5 Evaluating biogas production flexibility 178
6.2.6 Analytical methods 180
6.2.7 Demand-driven biogas kinetics 182
6.3 Results and discussion 184
6.3.1 Observations on reactor stability 184

6.3.2 Reactor and methane production efficiency....185
6.3.3 Flexibility of the two-phase reactors....190
6.3.4 Kinetics and biogas production of two-phase demand-driven systems 193
6.3.5 Demand-driven thermal and electrical production....195
6.3.6 Biobutanol for distribution transport....197
6.4 Conclusion 200
References....201
7.0 Investigating the effects of whiskey-barrel derived biochar addition to anaerobic digestion at a distillery: a study on energy yield and system efficiency .207
Abstract....207
7.1 Introduction....208
7.2 Materials and methods 211
7.2.1 Biochar production....211
7.2.2 Inoculum and feedstocks....212
7.2.3 Batch biomethane experiments 213
7.2.4 Characterisation of biomass and biochar 215
7.2.5 Gas production kinetic analysis 215
7.2.6 Biodegradability index and substrate energy yield calculation 216
7.2.7 DNA extraction and sequencing 217
7.2.8 Conventional AD system and integrated AD-pyrolysis system energy efficiency....217

7.2.9 Statistical significance....223
7.3 Results and discussion....223
7.3.1 Biochar production and properties....223
7.3.2 Fourier transform infrared spectroscopy observations....225
7.3.3 Whiskey barrel-derived biochar and biomethane production....226
7.3.4 Assessing the kinetics of biochar addition on the biomethane potential....230
7.3.5 Observations in microbial taxonomy....233
7.3.6 Evaluation of system energy efficiencies....234
7.4 Conclusion....237
Data availability....238
References....239
8.0 A comparison of carbonaceous additives in two-phase anaerobic digestion for enhanced biohythane production....246
Abstract....246
8.1 Introduction....247
8.2 Materials and methods....251
8.2.1 Methodology and analytical framework....251
8.2.2 Inoculum and feedstock....254
8.2.3 Carbonaceous materials....254
8.2.4 Biohydrogen and biomethane batch experimental trials....255
8.2.5 Analytical methods....258

8.2.6 Gas production kinetic analysis 259
8.2.7 Statistical significance 260
8.2.8 Biohythane energy recovery and emissions analysis 260
8.3 Results and discussions 262
8.3.1 Comparison of carbonaceous material characteristics 262
8.3.2 Biochar effects on biohydrogen and volatile fatty acid production 264
8.3.3 Biochar effects on biomethane production and kinetics 268
8.3.4 Assessing biohythane energy recovery and distillery emissions savings 273
8.3.5 Future research and limitations 277
8.4 Conclusions 278
References 280
9.0 Enhancing demand-driven biogas applications at a distillery through the addition of digestate-derived biochar 287
Abstract 287
9.1 Introduction 288
9.2 Materials and methods 292
9.2.1 Research approach and analytical structure 292
9.2.2 Inoculum and substrate characteristics 294
9.2.3 Biochar additives 294
9.2.4 Specific methane activity experiments 295
9.2.5 Two-phase demand-driven biogas production experiments 298

9.2.6 Demand-driven biogas production flexibility metrics 299
9.2.7 Kinetic analysis for demand-driven biogas production 302
9.2.8 Methods of analysis 303
9.3 Results and discussion 305
9.3.1 Biochar characteristics 305
9.3.2 Specific methane activity observations 306
9.3.3 Continuous two-phase anaerobic digestion trials 308
9.3.4 CSTR performance and VFA yields 308
9.3.5 Demand-driven biogas production with biochar addition 311
9.3.6 Opportunities and considerations at a distillery 315
9.4 Conclusion 317
References 318
10.0 Discussion - decarbonisation of whiskey distilleries through cascading biorefinery systems 324
10.1 Distillery cascading biorefinery concept from research 324
10.2 Furthering the cascading biorefinery approach at the distillery 326
10.3 Limitations of the system 329
10.4 Conclusion 329
References 331
11.0 Conclusions and recommendations 333
11.1 Conclusions 333
11.2 Recommendations and research implications 336

11.2.1 Policy 336
11.2.2 Industry 337
11.2.3 Community 338
11.2.4 Future research 339
Appendices 344
Appendix A 344
Appendix A.1: Theoretical substrate composition calculation of mWBM 344
Appendix A.2: Specific methane activity (SMA) of granular sludge 347
Appendix A.3: Optimum HRT to produce VFA-Rich leachate 349
Appendix A.4: EGSB Acclimatisation Experimental Trials 352
Appendix A.5: Theoretical LBR-EGSB biogas yield 354
Appendix References 355
Appendix B 356
Appendix B.1: Biochemical methane production (BMP) of the whiskey by-products 356
Appendix B.2: Continuous trials experimental data 357
Appendix C 360
Appendix C.1: Experimental results from dark fermentation trials at different loading rates 360
Appendix C.2: Biogenic carbon dioxide utilisation potential 363
Appendix C.3: Biogenic hydrogen utilisation potential 364
Appendix C.4: Volatile fatty acid utilisation potential 366

Appendix D 368
Appendix D.1: VFA to COD conversion factors 368
Appendix D.2: Potential butanol production and diesel blend from VFA production 369
Appendix D.3: LBR-EGSB specific methane yield estimation 374
Appendix D.4: CSTR specific methane yield 377
Appendix E 378
Appendix E.1: Properties of the mixed whiskey by-products and inoculum 378
Appendix E.2: DNA extraction and sequencing 379
Appendix E.3: Taxonomic marker gene amplicon sequence processing and analysis 380
Appendix E.4: Mass and energy balance of single-phase anaerobic digestion system without biochar 381
Appendix E.5: Mass and energy balance of integrated anaerobic digestion system and pyrolysis system with biochar at 300 ^{o}C 383
Appendix E.6: Observations in microbial taxonomy 386
Appendix F 400
Appendix F.1: Biohythane energy consumption 400
Appendix F.2: VFA to COD conversion factors 401
Appendix F.3: Carbon dioxide emissions reduction of different scenarios of WBChar 402
Appendix G 407

Appendix G.1: Preliminary dosage study 407

Declaration

This is to certify that the work I am submitting is my own and has not been submitted for another degree, either at University College Cork or elsewhere. All external references and sources are clearly acknowledged and identified within the contents. I have read and understood the regulations of University College Cork concerning plagiarism and intellectual property.

Signature: _____

Date: May 2024

Acknowledgements

As the long walk on my PhD journey comes to an end, I reflect on the path traversed and find this moment ripe to thank all the people that have lent a hand to get me to this point.

First and foremost, my sincerest gratitude to my main supervisor, Dr David Wall. Your unwavering patience, guidance, and advice have been the bedrock of my academic journey in Ireland. Your passion and wordsmithery continually inspire me. Thank you for giving me the freedom to explore any intellectual rabbit hole I found myself in, purely out of academic curiosity. To my other supervisors, Dr Richard O'Shea and Professor Jerry D. Murphy, thank you for your consistent support, sage advice, and gentle nudges when I deviated off course. Your wealth of knowledge, passion and enthusiasm for all things research are admirable and an inspiration.

I would also like to express my gratitude to my co-authors and collaborators at UCC and beyond, namely, Rajas Shinde, Xue Ning, Daniel Hickey, Stephen A. Jackson, Chen Deng, Gillian Collins, and Niall O'Leary. This thesis owes much of its depth and breadth to your contributions. Special thanks are due to Dr Xihui Kang and Dr Benteng Wu for their patience with my "1001 questions" about laboratory work and research advice.

No journey is complete without companionship of fellow travellers. The experience would not have been the same without the shared moments over hotpots, pints, lunches (some free), travels, and time shared together through the peaks and troughs of my PhD journey. A major shoutout to Anna O'Regan, Nathan Gray, Davis Rusmanis, Yunfei Li, Jorge Diaz Huerta, Archishman Bose, Maria Eduarda da Silva Sabedotti, Lily Purcell, Ankita Singh Gaur, Shabila Perveen, Vera O'Riordan, Clara Felberbauer, Paritosh Kunwar, Imke Sich, Gracie Vaughan-Wenner, Kathy Larrea, Emily Nauman (Tschida), John Williams, Rachel McGuire (Broos), and Raffaella Pizzichetti. Your friendship throughout the PhD has created countless fond memories and laughter, making the journey extremely enjoyable.

To my beloved LENA, my source of boundless joy and occasional sleepless nights, I am grateful for the countless memories we have shared.

I extend my deepest thanks to my friends back at home, who have kept me connected to my roots and providing unwavering support from South Africa, Sozizwe “King Sozi” Maqoma, Adrian “Silas” Kusambiza-Kiingi, Marloné “Kitty” Nel, Zipozonke “Mphora” Mpumlwana, Mandla “Power” Tutani, and Freddy Mdledle.

Finally, I would like to express my profound gratitude to my family, the bedrock of my existence – my siblings Xolisa and Oyisa, and especially my parents, Mzuvukile and Nombulelo Hackula. I could never adequately thank you enough for your never-waning, unconditional love, and support, which have sustained me through life’s trials and triumphs and this PhD journey. I am eternally grateful for the foundation you have provided, allowing me to explore the world with boundless curiosity and pursue my dreams without reservation.

Abstract

Decarbonisation of industrial processes is necessary to mitigate the detrimental impacts of anthropogenic climate change. Innovative technological solutions are sought that will allow for both a reduced carbon footprint and increased security of supply. The whiskey production industry produces by-products that are currently used linearly for animal feed. This thesis examines the use of by-products generated from whiskey production to enact a circular economy philosophy, which may be of further benefit to a distillery. This was achieved by examining various technologies, namely anaerobic digestion (AD), dark fermentation, and pyrolysis, in a cascading biorefinery concept.

Central to the evaluation of the whiskey by-product valorisation through anaerobic digestion was the development of a novel two-phase anaerobic digestion system, termed a leach bed reactor – expanded granular sludge bed (LBR-EGSB). Several design modifications, including the implementation of a cost-effective siphon-actuated leachate attenuation system, advanced the configuration beyond comparable designs. The LBR-EGSB could successfully convert the by-products into volatile fatty acids (VFAs) and methane-rich biogas (75 $\%_{vol}$). The LBR-EGSB was compared to traditional anaerobic digesters for energy production capabilities, showing similar biomethane potential, which could satisfy approximately 44 % of the thermal energy demand of a large distillery operating in Ireland.

Furthermore, the research investigated the potential of a biorefinery utilising dark fermentation, whereby the whiskey by-products were converted into biogenic carbon dioxide for use in beer carbonation, biohydrogen for use as transport or heating fuel, and VFAs for use as bioplastic beer packaging. A 50 million-litre whiskey distillery could satisfy approximately half of the carbon dioxide requirement of the Irish brewing industry. Biohydrogen was found to be best suited as a transport fuel. The VFAs could be processed into bioplastics which could completely satisfy beer packaging demand in Ireland.

Continuous VFA production and demand-driven biogas production to generate electricity during peak demand hours were also evaluated. The systems analysed were a two-phase continuously stirred tank reactor (CSTR) and the designed LBR-EGSB. Both systems exhibited continuous VFA production (up to 10.4 g. $L^{-1}_{Leachate}$) and rapid biogas production, achieving peak biogas flow rates within 30 minutes. A theoretical evaluation of processing butyric acid into biobutanol, to be blended with diesel, could produce a more sustainable transport fuel than diesel, reducing distillery-associated transport emissions by 16 %. Additionally, the novel use of whiskey barrel-derived biochar was compared to commercial carbonaceous materials, revealing its efficacy in enhancing biohydrogen and biomethane production by 15% and reducing methane production lag time, thereby advancing the understanding of pyrolysis parameters' impact on anaerobic digestion.

Overall, this thesis demonstrates that integrating AD systems, biochar application, and innovative biorefinery concepts can significantly enhance the sustainability of whiskey distilleries, proposing a pathway for modern circular economy strategies and decarbonisation of the whiskey distillery industry.

Thesis outputs

Peer-reviewed journal articles

Chapter 3:

Hackula, A., O'Shea, R., Murphy, J. D., & Wall, D. M. (2023). Design, Construction, and Concept Validation of a Laboratory-Scale Two-phase Reactor to Valorize Whiskey Distillery By-products. *ACS Engineering Au*. https://doi.org/10.1021/ACSENGINEERINGAU.3C00006

Chapter 4:

Hackula, A., Shinde, R., Hickey, D., O'Shea, R., Murphy, J. D., & Wall, D. M. (2023). Two-phase anaerobic digestion for enhanced valorisation of whiskey distillery by-products. *Bioresource Technology*, 129239. https://doi.org/10.1016/J.BIORTECH.2023.129239

Chapter 5:

Hackula, A., O'Shea, R., Murphy, J. D., & Wall, D. M. (2024). Developing distillery biorefineries through dark fermentation of whiskey production by-products: the effect of organic loading rate on decarbonisation pathways. *Energy Conversion and Management, 301*, 118064. https://doi.org/10.1016/j.enconman.2024.118064

Chapter 6:

Hackula, A., Shinde, R., O'Shea, R., Murphy, J. D., & Wall, D. M. (2024). Assessing two-phase anaerobic digestion systems for demand-driven electricity and biobutanol transport fuel at a large distillery. *Journal of Cleaner Production*, 140974. https://doi.org/10.1016/j.jclepro.2024.140974

Chapter 7:

Hackula, A., Ning, X., Collins, G., Jackson, S. A., O'Leary, N. D., Deng, C., ... & Wall, D. M. (2024). Investigating the effects of whiskey-barrel derived biochar addition to anaerobic digestion at a distillery: A study on energy yield and system efficiency. *Energy Conversion and Management: X*, 100654 https://doi.org/10.1016/j.ecmx.2024.100654

Chapter 8:

Hackula, A., Ning, X., O'Shea, R., Murphy, J. D., & Wall, D. M. (2024). A comparison of carbonaceous additives in two-phase anaerobic digestion for enhanced biohythane production. *To be submitted*

Chapter 9:

Hackula, A., Shinde, R., O'Shea, R., Murphy, J. D., & Wall, D. M. (2024). Enhancing demand-driven biogas applications at a distillery through the addition of digestate-derived Biochar. *To be submitted*

Co-authored peer-reviewed publications

Ning, X., Deng, C., Hickey, D. T., Hackula, A., O'Shea, R., Wall, D. M., Lin, R., & Murphy, J. D. (2023). Improving biomethane production from biochar-supplemented two-stage anaerobic digestion of on-farm feedstocks. *Journal of Cleaner Production*, 138723. https://doi.org/10.1016/j.jclepro.2023.138723

Shinde, R., Hackula, A., O'Shea, R., Barth, S., Murphy, J. D., & Wall, D. M. (2023). Demand-driven biogas production from Upflow Anaerobic Sludge Blanket (UASB) reactors to balance the power grid. *Bioresource Technology*, 385, 129364. https://doi.org/10.1016/j.biortech.2023.129364

Paritosh, K., & Hackula, A. (2024). Decarbonising distillery wastewater treatment: Experimental investigation of biochar-assisted anaerobic conversion and financial assessment. *Energy Conversion and Management*, 318, 118893. https://doi.org/10.1016/J.ENCONMAN.2024.118893

Conference oral presentations

Hackula, A., O'Shea, R., Murphy, J.D., Wall, D. M., Two-phase anaerobic digestion for valorisation of whiskey distillery by-products in a circular economy. Presented at the 18th IWA World Conference on Anaerobic Digestion (IWA AD18) in Istanbul, Türkiye. 2-6 June 2024

Hackula, A., O'Shea, R., Wall, D. M., Decarbonisation of Whiskey Distilleries in a Circular Economy (2022). Presented at the 32nd Irish Environmental Researchers Colloquium, Belfast. 21 June 2022.

Poster presentations

Hackula, A., Shinde, R., Hickey, D., O'Shea, R., Murphy, J.D.,Wall, D. M., Valorisation of whiskey by-products through anaerobic digestion systems (2023). Poster presented at the 4th International Conference for Bioresource Technology for Bioenergy, Bioproducts & Environmental Sustainability (BIORESTEC23). 14-15 May 2023.

Other presentations

Hackula, A., Valorisation of whiskey by-products through anaerobic digestion systems (2022). Environmental Research Institute (ERI) Early Career Researcher's Presentation Lunch. 18 October 2022.

Hackula, A., Valorisation of whiskey by-products through anaerobic digestion systems (2022). Environmental Research Institute (ERI) Postgraduate Research Symposium. 25 October 2022.

Contribution to the papers

Chapter 3: I was the first author of the paper. I conceptualised, designed, constructed, and conceptually validated the two-phase anaerobic digester through experimental trials over 12 months. I also did the data collection, data analysis, and interpretation of results for the paper.

Chapter 4: I was the first author of the paper. I conceptualised the study and operated three anaerobic digesters through experimental trials. I also undertook the data collection, data analysis, and interpretation of results for the paper. I also undertook the approximate VFA value analysis.

Chapter 5: I was the first author of the paper. I conceptualised the study and operated three dark fermenters for the experimental trials. I also undertook the data collection, data analysis, and interpretation of results for the paper. I was responsible for the theoretical biorefinery analysis.

Chapter 6: I was the first author of the paper. I conceptualised the study and operated two anaerobic digesters for the experimental trials. I also undertook the data collection, data analysis, and interpretation of results for the paper. I was responsible for the theoretical biobutanol biorefinery analysis.

Chapter 7: I was the first author of the paper. I conceptualised the study, produced the biochar, and operated the biochemical methane potential (BMP) batch trials. I also undertook the data collection, data analysis, and interpretation of results for the paper. I was responsible for the theoretical energy analysis.

Chapter 8: I was the first author of the paper. I conceptualised the study, produced the biochar, and operated the biochemical methane potential (BMP) batch trials. I also undertook the data collection, data analysis, and interpretation of results for the paper. I was responsible for the theoretical energy recovery and emissions savings analysis.

Chapter 9: I was the first author of the paper. I conceptualised the study, produced the biochar, and operated the reactor trials. I also undertook the data collection, data analysis, and interpretation of results for the paper.

Abbreviations / Nomenclature

Abbreviation	Meaning
$\%CH_{4vol}$	Methane content in the biogas on a volumetric basis
$\%CO_{2vol}$	Carbon dioxide content in the biogas on a volumetric basis
$\%H_{2vol}$	Hydrogen content in the biogas on a volumetric basis
$\%_{vol}$	Percentage on a volume basis
AD	Anaerobic digestion
C1a	Dark fermenter of the two-phase CSTR
C1b	Methanogenic reactor of the two-phase CSTR
CEAP	Circular economy action plan
CH_4	Methane
CHON	Chemical composition
CHP	Combined heat and power
CO_2	Carbon dioxide
COD	Chemical oxygen demand
COD_{eff}	COD removal efficiency
COD_{VFA}	COD equivalent of the volatile fatty acids (VFAs)
CSTR	Continuously stirred tank reactor
DIET	Direct interspecies electron transfer
EGSB	Expanded granular sludge bed
EU	European Union
FAN	Free ammonia nitrogen
FOS/TAC	Alkalinity ratio
GLS	Gas-liquid-separator
HRT	Hydraulic retention time
H_2	Hydrogen gas
k	The rate constant of decay
k_1	The rate constant of the easily degradable portion (x)
k_2	The rate constant of the remaining portion of the substrate without the easily degradable portion
LBR	Leach bed reactor
LBR-AF	Leach bed reactor with a downstream anaerobic filter
LBR-EGSB	Leach bed reactor-expanded granular sludge bed
LBR-UASB	Leach bed reactor with a downstream upflow anaerobic sludge blanket
$m_{bpr_{down}}$	The slope of the ramp down
$m_{bpr_{up}}$	The slope of the ramp-up in percentage per hour (%. h^{-1})
mWBM	Mixed whiskey by-products
OLA	Original litre of alcohol
OLR	Organic loading rate
PHAs	Polyhydroxyalkanoates
R_m	Maximum specific biogas production rate

SMY	Specific methane yield
SRT	Solid retention time
STP	Standard temperature and pressure
t	at a specific time
TAN	Total ammoniacal nitrogen
TS	Total solids
UASB	Upflow anaerobic sludge blanket
v(t)	The cumulative gas production per unit reactor volume
VFAs	Volatile fatty acids
Vmax	The final specific biogas production
VS	Volatile solids
VS_{eff}	VS destruction efficiency
ww	Wet weight
x	Easily degradable portion in the substrate
X_{eff}	The COD removal efficiency or the VS destruction efficiency
Δt	Difference in time
Y_{bpr}	Biogas production rate
$Y_{bpr_{ave}}$	Average daily biogas production rate

1.0 Introduction

1.1 Introduction and background to thesis

The greenhouse gas emissions from fossil fuel usage have necessitated the development of renewable energy technologies to mitigate climate change. Legislation such as the 'Fit for 55 package', which refers to the European Union's (EU) target to cut net greenhouse gas emissions by a minimum of 55 % by 2030, emphasises the urgency of climate change mitigation (European Council et al., 2024). Circular economy strategies have been touted as a crucial strategy in facilitating the EU's transition to a cleaner and more competitive region (Deutz, 2020). The adoption of the circular economy action plan (CEAP) by the EU accentuates the importance of circular economy strategies (European Commission, 2020). Contrary to the "take, make, discard" approach of the linear economy process, circular economy processes seek to reuse, recover, recycle, and reintroduce resources while meeting economic and social targets (Calisto Friant et al., 2021). Industry, particularly the food and beverage industry, has been pinpointed as a sector with the potential to convert linear processes into circular processes (European Commission, 2020).

The Republic of Ireland (hereon referred to as Ireland), which is part of the EU, will require energy systems which align with the EU targets. Ireland has responded by committing to a 51 % reduction in greenhouse gas emissions by 2023 and climate neutrality by 2050 (Government of Ireland et al., 2023). The Irish Climate Action Plan provides a comprehensive framework to succeed in these objectives (Government of Ireland et al., 2023). Within this framework, the Irish government

has set out sub-targets of 35 % greenhouse gas emission reductions from industry (Government of Ireland et al., 2023). The food, beverage, and tobacco sector alone produced approximately 1.1 Mt CO_2eq in 2022 (Environmental Protection Agency, 2023). It is imperative that low-carbon circular economy strategies are implemented within large sectors, such as the Irish whiskey industry, to achieve these national and regional targets (Gunes et al., 2019).

Ireland has a mature alcohol beverage industry and a prominent whiskey industry. The whiskey production process typically results in three by-products: a solid residue termed draff, a liquid residue termed thin stillage, and a solid-liquid residue termed thick stillage. These by-products are primarily processed into animal feed. (Kang et al., 2020). However, an alternative approach which may further valorise whiskey by-products is through biorefinery technologies such as anaerobic digestion (AD), dark fermentation, and pyrolysis.

Anaerobic digestion is the process of biological degradation of biomass in the absence of oxygen, which yields methane-rich biogas and digestate. Biogas, which typically consists of 50-60 % methane and 50-40 % carbon dioxide (CO_2), can be used for heat as well as combined heat and power (CHP). Removal of CO_2, referred to as biogas upgrading, results in biomethane. Biomethane has similar energy content to natural gas and, as such, can be used in similar applications (Ó Seilacher et al., 2023). Biomethane is seen as a critical energy vector to Ireland's ambition to achieve national targets (Government of Ireland et al., 2023). This perspective was echoed by the release of Ireland's National Biomethane Strategy 2024, which proposed a target of 5.7 TWh per annum of indigenously produced biomethane

(Department of Agriculture and Department of Environment, 2024). Different feedstocks have innate characteristics that influence the efficacy of anaerobic digestion. Further investigation on a case-by-case basis is required to determine the suitability of AD technology for specific feedstocks.

Dark fermentation is the microbial conversion of organic matter in the absence of oxygen and light and produces biohydrogen and volatile fatty acids (VFAs). Biohydrogen shares application similarities with biomethane. However, its combustion is often termed a “clean burn” as the primary by-product is water vapour (Wang et al., 2018). The release of the Irish National Hydrogen Strategy, which projects up to 39 TWh demand by 2050, emphasises the importance of biohydrogen (Department of the Environment Climate and Communications, 2023). VFAs, which include acetic, propionic, and butyric acids, serve as key ingredients for chemical synthesis and other biorefinery uses, such as biobased plastics (Atasoy et al., 2018). The Irish Bioeconomy Action Plan 2023-2025 highlights VFAs and other derivatives as key constituents to the path to net-zero by 2050 (Department of the Environment et al., 2023).

Pyrolysis is the thermochemical degradation of biomass at elevated temperatures in the absence of oxygen and yields biochar, bio-oil, and syngas. Biochar has various uses, such as a soil amendment, and has been deemed a negative emissions technology when applied to land (IPCC, 2022). The other pyrolysis products can be used for heat and other applications after further processing (Deng et al., 2020). All these technologies are seen as critical in terms of deploying circular economy practices and achieving national targets.

Biorefinery technologies have variable results due to the different characteristics of the feedstocks under investigation. For example, whiskey distilleries use different cereals and processes to produce whiskey, which ultimately results in different by-products being produced. As the efficacy of the products generated from these technologies is dependent on the characteristics of the feedstock, there is a scientific need to evaluate distillery generated by-products for these technologies and progress their use within the context of a large distillery. This thesis of work investigates these technologies within the context of a large distillery seeking to decarbonise its processes.

1.2 Thesis aims and objectives

The overarching aim of this thesis is to investigate various biorefinery technologies as a means of valorising whiskey by-products generated at a large distillery in Ireland while simultaneously providing a decarbonisation pathway.

The main objectives of the thesis are as follows:

1. To design, construct, and conceptually validate a leach bed reactor with a downstream expanded granular sludge bed (LBR-EGSB);
2. To establish and compare energy and materials recovery potential from the whiskey by-products utilising various anaerobic digestion systems;
3. To conceptualise and evaluate a dark fermentation biorefinery approach using whiskey by-products;
4. To evaluate and compare demand-driven biogas operation of different anaerobic digestion systems processing whiskey by-products;

5. To produce whiskey barrel-derived biochar at various pyrolysis temperatures and evaluate its impact on biomethane production;
6. To evaluate and compare the effect of carbonaceous additives on two-phase anaerobic digestion of whiskey by-products;
7. To produce digestate-derived biochar and assess its impact on demand-driven biogas production;
8. To conceptualise an integrated, circular economy-based biorefinery at a distillery to maximise the use of resources.

1.3 Thesis outline in brief

The thesis follows the publication-based model and consists of 11 chapters and additional appendices. Each chapter consists of an abstract, introduction, materials and methods, results, and a conclusion to form a cohesive narrative in the context of the thesis. Still, it can also be read as a standalone chapter. Figure 1.1 illustrates the outline of the thesis.

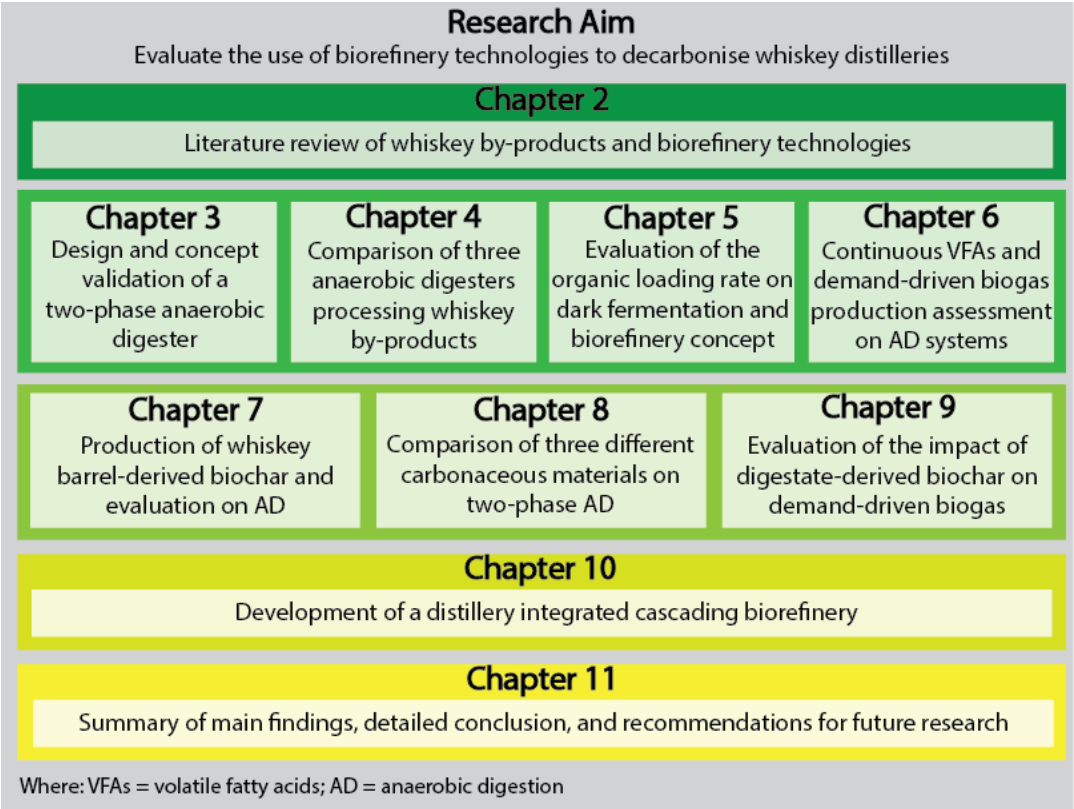


Figure 1.1: Thesis overview and link between chapters

Chapter 1 defines the scope of the thesis and its relevance within the EU and Irish policy context, as well as the overall aims and objectives of the thesis. Chapter 2 provides the background information through a comprehensive literature review to enable the reader to synthesise Chapters 3 to 9, which are all original works of research. Chapters 3 to 9 of this thesis are presented in their publication (or under review) format. Minor adjustments were made to ensure uniformity within the thesis and improve the reader experience. Chapter 10 is a discussion that combines the research undertaken in Chapters 3 to 9 with other biorefinery technologies to develop an integrated, cascading distillery biorefinery. Each chapter was categorised to address the research objectives as outlined in Section 1.2. The common theme of the thesis is the decarbonisation of a whiskey distillery using process by-products and biorefinery technologies to reduce its carbon footprint. A brief overview of Chapters 2 to 11 is provided below:

Chapter 2: Literature review

The objective of this chapter is to provide an in-depth exploration of the framework of this thesis, including the policy framework, various applications of whiskey by-products, and technologies used with respect to valorisation of whiskey by-products. It also provides relevance to the thesis with respect to a distillery. This chapter will provide the reader with sufficient information to synthesize the chapters that follow in the thesis. More recent studies as compared to the subsequent chapters, will be referred to in this chapter, highlighting insights of the works.

Chapter 3: Design, construction, and concept validation of a laboratory-scale two-phase reactor to valorise whiskey distillery by-products

In this chapter, a leach bed reactor connected to an expanded granular sludge bed (LBR-EGSB) was designed, commissioned, and conceptually validated to produce volatile fatty acids (VFAs) and biogas using whiskey by-products. Based on the literature review in Chapter 2, these by-products had not been evaluated on the system prior to this body of work. Several design improvements progress the LBR-EGSB beyond similar reactor designs. The LBR-EGSB could ultimately provide more by-product valorisation and decarbonisation opportunities than traditional anaerobic digestion systems for a whiskey distillery.

Chapter 4: Two-phase anaerobic digestion for enhanced valorisation of whiskey distillery by-products

This chapter explores and compares the valorisation of whiskey by-products in three anaerobic digestion systems, namely a continuously stirred tank reactor (CSTR), a two-phase CSTR and the LBR-EGSB, which was designed in the preceding chapter. The methane generated from whiskey by-products could displace natural gas and reduce the distillery's carbon footprint. The potential value of the volatile fatty acids (VFAs) produced in the two-phase systems was also evaluated. It may also be of interest to a distillery seeking to diversify its revenue streams.

Chapter 5: Developing distillery biorefineries through dark fermentation of whiskey production by-products: the effect of organic loading rate on decarbonisation pathways

The previous chapters focused on biomethane for the decarbonisation of a whiskey distillery. However, biorefinery approaches can arise at distilleries using dark fermentation to treat whiskey by-products and provide decarbonisation opportunities. A biorefinery leveraging dark fermentation can convert residues to biohydrogen, biogenic carbon dioxide, and VFAs. This chapter investigated the effect of the organic loading rate (OLR) on the production of VFAs and biogenic gases in dark fermentation. The experimental results were further explored through a case study of a large whiskey distillery to produce biogenic carbon dioxide, for use in beer carbonisation and the potential for biohydrogen to offset transport and heat-related emissions at the distillery. The biogenic carbon dioxide resource is seldom explored in literature, this body of work contributes to this knowledge gap. The dark fermentation biorefinery supports the distillery’s transition to circular production systems.

Chapter 6: Assessing two-phase anaerobic digestion systems for demand-driven electricity and biobutanol transport fuel at a large distillery

Anaerobic digestion and dark fermentation provide valorisation opportunities for a distillery. However, for a distillery to be able to avail of both VFAs and biogas, a demand-driven approach may be required to produce both products. Where the previous chapters only considered either VFA production or biogas, this chapter provides an approach to produce both through two-phase systems. In this demand-driven approach, VFAs are continuously produced, and biogas production is only produced when electricity demand is required. A theoretical conversion analysis of butyric acid into biobutanol was also evaluated for use as a transport fuel. To the best of the authors' knowledge, the use of butyric acid generated from distillery by-products as a transport fuel has not been explored in prior literature.

Chapter 7: Investigating the effects of whiskey-barrel derived biochar addition to anaerobic digestion at a distillery: a study on energy yield and system efficiency

The preceding chapters showed that the whiskey by-products are amenable to anaerobic digestion. Whiskey barrels are another by-product of the whiskey production process. Processing whiskey barrels into biochar provides a valorisation pathway for the whiskey barrels. Biochar has been explored in various studies as an additive to enhance anaerobic digestion. This chapter explores using the whiskey barrel-derived biochar as an additive for anaerobic digestion to boost methane yields, which is a novel approach for the usage of the material.

Chapter 8: A comparison of carbonaceous additives in two-phase anaerobic digestion for enhanced biohythane production

Biochar produced from whiskey barrels was proven to enhance biomethane production. Chapter 8 expands the scope of research to explore the versatility and efficacy of different carbonaceous additives in two-phase anaerobic digestion. The focus shifts towards the production of biohythane – a sustainable and higher-value blend of biohydrogen and biomethane – with the objective to further optimise energy recover from distillery residues. This chapter compares the impacts of various carbonaceous materials, namely commercial biochar, activated carbon, and, specifically, the whiskey barrel-derived biochar that proved to be effective in Chapter 7.

Chapter 9: Enhancing demand-driven biogas applications at a distillery through the addition of digestate-derived biochar

Chapter 9 explores two-phase anaerobic digestion with biochar-amended demand-driven biogas production. This chapter builds on higher VFA production of the CSTR dark fermenter system connected to a high-rate reactor (Chapters 3 to 6). Biochar was established as a valuable additive for improving anaerobic digestion (Chapters 7 to 8). The use of digestate-derived biochar in this chapter underscores a broader strategy of enhancing resource recovery, energy efficiency, and digestate management within a distillery's processes.

Chapter 10: Discuss - Decarbonisation of whiskey distilleries through cascading biorefinery systems

Chapter 10 aims to combine all the research within the thesis into a perspective cascading biorefinery system to achieve a near zero-waste distillery. This chapter explores the integration of additional technologies, namely duckweed cultivation and power to gas, to address digestate management and assist with the loss of animal feed from anaerobic digestion of whiskey by-products.

Chapter 11: Conclusions and recommendations

The final chapter of the thesis summarises the results of the prior chapters and provides detailed conclusions for distillery stakeholders. The insights are presented in an accessible manner to facilitate future research and for context for a broader audience. Lastly, the recommendations provide a platform for the expansion of the thesis for future research.

References

1. Atasoy, M., Owusu-Agyeman, I., Plaza, E., Cetecioglu, Z., 2018. Bio-based volatile fatty acid production and recovery from waste streams: Current status and future challenges. Bioresour Technol 268, 773–786. https://doi.org/10.1016/j.biortech.2018.07.042
2. Calisto Friant, M., Vermeulen, W.J.V., Salomone, R., 2021. Analysing European Union circular economy policies: words versus actions. Sustain Prod Consum 27, 337–353. https://doi.org/10.1016/J.SPC.2020.11.001
3. Deng, C., Lin, R., Kang, X., Wu, B., O'Shea, R., Murphy, J.D., 2020. Improving gaseous biofuel yield from seaweed through a cascading circular bioenergy system integrating anaerobic digestion and pyrolysis. Renewable and Sustainable Energy Reviews 128, 109895. https://doi.org/10.1016/j.rser.2020.109895
4. Department of Agriculture, F. and the M., Department of Environment, C. and C., 2024. Ireland's Draft National Biomethane Strategy.
5. Department of the Environment, C. and C., Department of Agriculture, F. and the M., Government of Ireland, 2023. Bioeconomy Action Plan 2023-2025.
6. Department of the Environment Climate and Communications, 2023. National Hydrogen Strategy.
7. Deutz, P., 2020. Circular Economy. International Encyclopedia of Human Geography 193–201. https://doi.org/10.1016/B978-0-08-102295-5.10630-4
8. Environmental Protection Agency, 2023. Manufacturing and industry | Environmental Protection Agency [WWW Document]. URL https://www.epa.ie/our-services/monitoring--assessment/climate-change/ghg/manufacturing-and-industry/ (accessed 4.23.24).

9. European Commission, 2020. Circular economy action plan [WWW Document]. URL https://ec.europa.eu/environment/strategy/circular-economy-action-plan_en (accessed 3.10.22).
10. European Council, Council of the European Union, 2024. Fit for 55 - The EU's plan for a green transition - Consilium [WWW Document]. URL https://www.consilium.europa.eu/en/policies/green-deal/fit-for-55/#what (accessed 4.23.24).
11. Government of Ireland, Department of the Environment, C. and C., 2023. Climate Action Plan 2024.
12. Gunes, B., Stokes, J., Davis, P., Connolly, C., Lawler, J., 2019. Pre-treatments to enhance biogas yield and quality from anaerobic digestion of whiskey distillery and brewery wastes: A review. Renewable and Sustainable Energy Reviews 113, 109281. https://doi.org/10.1016/j.rser.2019.109281
13. IPCC, 2022. Summary for Policymakers, Climate Change and Land. Cambridge University Press. https://doi.org/10.1017/9781009157988.001
14. Kang, X., Lin, R., O'Shea, R., Deng, C., Li, L., Sun, Y., Murphy, J.D., 2020. A perspective on decarbonizing whiskey using renewable gaseous biofuel in a circular bioeconomy process. J Clean Prod 255, 120211. https://doi.org/10.1016/j.jclepro.2020.120211
15. Ó Céileachair, D., O'Callaghan, S., Wall, D.M., Goulding, D., O'Connor, D., Murphy, J.D., O'Shea, R., 2023. Logistical considerations and challenges in deploying virtual biomethane pipelines to serve on-farm biogas plants. J Clean Prod 407, 137075. https://doi.org/10.1016/j.jclepro.2023.137075

16. Wang, H., Xu, J., Sheng, L., Liu, X., Lu, Y., Li, W., 2018. A review on bio-hydrogen production technology. Int J Energy Res 42, 3442–3453. https://doi.org/10.1002/er.4044

University College Cork, Ireland
Coláiste na hOllscoile Corcaigh

CORA
Cork Open Research Archive
Cartlann Taighde Oscailte Chorcaí

Hackular, A. A. 2024. Decarbonisation of whiskey distilleries in a circular economy: investigating biorefinery systems for valorisation of distillery by-products. PhD Thesis, University College Cork.

Please note that Chapter 2(pp. 15-59) is unavailable due to a request by the author.

CORA Cork Open Research Archive http://cora.ucc.ie

3.0 Design, construction, and concept validation of a laboratory-scale two-phase reactor to valorise whiskey distillery by-products

Anga Hackula, Richard O'Shea, Jerry D Murphy, David M Wall

SFI MaREI Centre for Energy, Climate and Marine Environmental Research Institute, University College Cork, Cork, Ireland
Civil, Structural, and Environmental Engineering, School of Engineering and Architecture, University College Cork, Cork, Ireland

Abstract

By-products generated from the whiskey distillation process consist of organic liquids with a high chemical oxygen demand (COD) and residues with a high-solids content. Low-carbon strategies that repurpose and valorise such by-products are now imperative to reduce the carbon footprint of the food and beverage industry. The operation of a two-phase anaerobic digester to produce volatile fatty acids (VFAs) and biogas may enable distilleries to transition towards a low-carbon bioeconomy. An example of such a system is a leach bed reactor connected to an expanded granular sludge bed (LBR-EGSB), which was designed, commissioned, and conceptually validated in this paper. Several design improvements progress the LBR-EGSB beyond previous reactor designs. An external gas-liquid-solid separator in the EGSB was used to capture any residual gases produced by the effluent and may reduce the amount of methane slippage and biomass washout. The implementation of a siphon-actuated leachate cup is a low-cost alternative that is less prone to actuation malfunction as compared to electrically actuated solenoid valves in previous reactor designs. Furthermore, replacing fresh water with the distillery's liquid by-products as leachate promotes a circular repurpose and reuse philosophy. The system proved to be effective in generating VFAs (10.3 g VFAs. $L^{-1}_{Leachate}$), in EGSB COD removal (96 %), and in producing methane-rich biogas (75 $\%_{vol}$), which is higher than values achieved by traditional anaerobic digestion systems. The LBR-EGSB could ultimately provide more by-product valorisation and decarbonisation opportunities than traditional anaerobic digestion systems for a whiskey distillery.

3.1 Anaerobic digestion of whiskey by-products

Greenhouse gas emissions from burning fossil fuels have accelerated climate change's adverse environmental and societal effects (Yamaka et al., 2021). Societal expectations have resulted in industries attempting to decarbonise and reduce their carbon footprint as part of their corporate social responsibility (Barrena Martínez et al., 2016). Anaerobic digestion (AD) is one technology that can offer a viable pathway to reducing industry's carbon footprint by converting biological secondary raw materials through the production of biogas, volatile fatty acids (VFAs), and bio-fertilisers (Abad et al., 2019).

For optimal digestion performance, the design of the reactor should consider not only biological parameters but also technical, environmental, and economic constraints (Nizami et al., 2011). Feedstock source, availability, inhibitors, and chemical composition will affect the digester configuration. Optimal digestion configurations seek to maximise the throughput of biological material, as quantified by the organic loading rate (OLR), whilst minimising the hydraulic retention time (HRT) for biogas production (Chernicharo, 2007). Maximising the throughput of feedstock to the digester within the confines of biological stability, maximises the organic loading rate, minimises the hydraulic retention time and reduces the digester volume and overall capital costs. Two-phase systems allow for additional valorisation pathways through VFA production while providing for biogas production (Castilla-Archilla et al., 2021; Wall et al., 2016). VFAs can be considered a valuable commodity with a high monetary value; for example, butyric acid and propionic acid may accrue market prices of 2,500 € and 2,250 € per tonne, respectively (Atasoy et al., 2018; Bastidas-Oyanedel et al., 2015). This additional

valorisation pathway could be of interest to industries which produce biological secondary raw materials, such as distillers, as it would diversify their revenue streams.

Distillery by-products are similar to brewery by-products but have more liquid derivatives (Gunes et al., 2019; Nigam, 2017). Thin and thick stillage constitute the liquid by-products; the primary solid by-product is termed draff. Draff is a lignocellulosic material due to its high lignin, cellulose, protein, and fibre content (Gunes et al., 2019). Several previous studies have established that both brewery and distillery by-products are amenable to anaerobic digestion. The traditional continuously stirred tank reactor (CSTR) can typically accommodate feedstocks of up to 12 % total solids (TS), as higher solids content could lead to stirring problems (Drosg, 2013). Thus, feedstocks such as draff with high initial solids content (TS >12 % on a wet weight (ww) basis) would need to be co-digested with liquid substrates such as thin stillage (or pre-treated to reduce the overall TS content) to be used in such a system (López-Gutiérrez et al., 2021).

Coupled configurations aim to overcome shortfalls in single-phase AD systems by leveraging the unique advantages of each system (Murphy and Thanasit Thamsiriroj, 2013). An example of a two-phase AD reactor is the leach bed reactor (LBR) coupled with an expanded granular sludge bed (EGSB), referred to as the LBR-EGSB. The LBR-EGSB system splits the anaerobic digestion process into two parts: hydrolysis and acidogenesis (VFA production), which take place in the LBR, and acetogenesis and methanogenesis (biogas production), which take place in the EGSB (Wall et al., 2016). Dry batch AD reactors, such as the LBR, which are characterised by simple design and operation with no mechanical stirring, are potentially more suitable to digest draff due to their ability to accept high solid content feedstocks (up

to 50 %ww)(Uke and Stentiford, 2013). Hydrolysis is achieved by leachate recirculation in the LBR. The liquid percolates through the organic matter and increases the leachate's VFA content (Chen and Huang, 2006). The VFAs-rich leachate can then be fed to the coupled EGSB, where biogas can be produced. The EGSB is akin to the upflow anaerobic sludge blanket (UASB). However, the EGSB has a higher aspect ratio (height-to-diameter ratio) of 20 (or more) which allows it to operate at higher upflow velocities as compared to UASBs (Chernicharo, 2007; Kato et al., 1994). Higher upflow velocities can equate to shorter HRTs. Low upflow velocities (0.1 m. hr^{-1}) were previously recommended for the operation of UASBs (Nizami et al., 2011).

Several studies have evaluated variations of the LBR-EGSB. The following design issues were highlighted in prior designs of similar systems: low upflow velocities as low upflow velocities decrease substrate-inoculum contact; malfunctioning leachate actuation systems resulting in reduced hydrolysis; and back pressure within the high-rate reactor resulting in gas leaks (Chernicharo, 2007; Nizami et al., 2011). The LBR-UASB has been used to evaluate grass, food waste, and common reeds, achieving specific methane yields of up to 340 L CH_4. kg^{-1} volatile solids (VS) added (±243 L CH_4. kg^{-1} chemical oxygen demand (COD) added using a conversion factor of 1.4 kg COD. kg^{-1} VS) (Browne and Murphy, 2014; Lehtomäki et al., 2008; Nizami et al., 2011). An LBR with a downstream anaerobic filter processed maize silage and reported a methane yield of 330 L CH_4. kg^{-1} VS_{added} (±236 L CH_4. kg^{-1} COD_{added})(Linke et al., 2015).

Studies have previously analysed coupled configurations for brewery and distillery by-products but primarily on the liquid by-products. Some coupled configurations that assessed distillery by-products include two-phase CSTRs, granular bed baffled

reactors, and two-phase UASBs, which reported specific methane yields of up to 202 L CH_4. kg^{-1} COD_{added} (Akunna, 2000; Uzal et al., 2003; Wu et al., 2015; Yeoh, 1997). A previous study using an LBR and a high-rate reactor (granular biomass reactor) evaluated pre-treated brewers spent grains (BSG) and reported a specific methane yield of 273 L CH_4. kg^{-1} VS_{added} (±195 L CH_4. kg^{-1} COD_{added}) but did not consider liquid brewery by-products (Panjičko et al., 2015). A two-phase EGSB reactor was used to evaluate continuous VFA production (8.4 g total VFA. L^{-1}) from brewers spent grain hydrolysate but again did not consider the liquid by-products (Castilla-Archilla et al., 2021). Thus, there is an evident gap in literature whereby both liquid and solid whiskey by-products are processed. The authors propose the development of an LBR-EGSB to produce VFAs and biogas.

3.2 Objectives

This paper aims to design, construct, and provide concept validation for a two-phase LBR-EGSB to produce VFAs and biogas from whiskey by-products. This work may be considered a holistic engineering study as opposed to the biological optimisation of the said system. However, concept validation will comprise of short experimental trials to ensure both the successful production of VFAs and biogas.

The innovation in this paper is that it is the first paper to use the two-phase anaerobic digester, LBR-EGSB, to valorise all liquid and solid by-products (draff, thin stillage and thick stillage) produced on-site at the distillery to produce VFAs and biogas. Furthermore, the paper will identify design improvements of the two-phase LBR-EGSB that may enhance the reactor performance beyond previously developed systems. The specific objectives of this paper are as follows:

1. Design and construct a laboratory-scale leach bed reactor with an extended granular sludge bed (LBR-EGSB) that can process distillery by-products;
2. Calculate key start-up operational parameters, detail any issues encountered, and outline mitigation modifications to the design;
3. Complete concept validation trials for the LBR-EGSB;
4. Measure the VFA profile (from the LBRs) and the COD removal rate (from the EGSB) when digesting distillery by-products.

3.3 Material and methods

3.3.1 Characteristics of the inoculum and whiskey by-products

The granular inoculum for the EGSBs was sourced from an operational mesophilic EGSB in Co. Cork, Ireland that processes dairy wastewater. A 3mm mesh sieve was used to isolate the solid granules, which were subsequently used to seed the EGSBs. Before start-up, the inoculum was degassed inside the reactor for 30 days. The total solids content of the inoculum was 10.4 %ww, of which 79.7 % of the total solids were volatile solids. The leach bed reactors were not inoculated (Nizami et al., 2011).

The whiskey by-products were sourced from an operational distillery and consisted of draff, thick stillage, and thin stillage, which are produced at a ratio of 1:9:10 on a wet weight basis per annum (Table 3.1). Due to the relatively high solids content of thick stillage (8.9 %ww compared to thin stillage (TS of 2.9 %ww)), a modified thick stillage was used for the experimental trials. Thick stillage was centrifuged to produce a dry fraction, termed cake maize (TS of 29.0 %ww), and a liquid fraction, termed centrate (TS of 3.5 %ww). The distillery currently implements this separation process. Subsequently, a mixed whiskey by-product mixture (mWBM) was created based on a draff, cake maize, centrate and thin stillage in a production ratio of

1:2:7:10 on a wet weight basis. Thus, mWBM consisted of 'dry' (draff, cake maize) and 'wet' (thin stillage, centrate) fractions. mWBM 'wet' was further sieved with a 0.76 mm sieve to remove any solid particles prior to experiments. The production rate of by-products from an existing whiskey distillery was used to inform the relative proportions of by-products for the operation of the LBR-EGSB.

Table 3.1: Whiskey by-products characteristics

		mWBM 'dry'[ab]		mWBM 'wet'[ac]		
			Thick stillage			
	Unit	Draff	Cake maize	Centrate	Thin stillage	Total mWBM[ah]
Quantity	(twwt. a^{-1})[g]	31,251	58,951	218,544[h]	322,813[h]	631,559
TS[d]	(%ww)	27.4	29.0	3.5	2.9	6.8
VS[e]	(% TS)	96.0	97.2	89.3	88.8	93.7
pH	pH	/	/	3.8	4.3	4.0
COD[f]	(g. L^{-1})	/	/	34.6	33.4	/

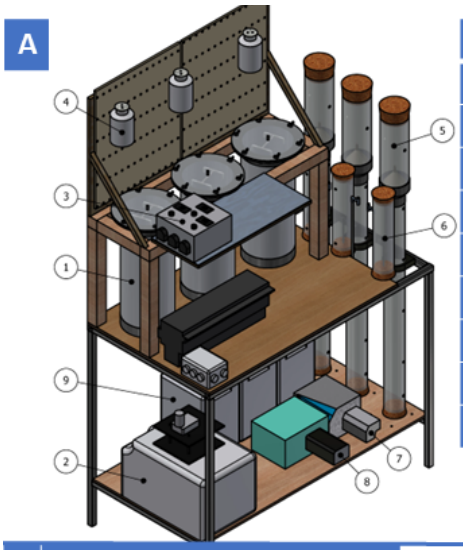
[a] mWBM = whiskey by-product mixture; [b] mWBM 'dry' = the solid fraction of mWBM (draff and cake maize); [c] mWBM 'wet' = the liquid fraction of mWBM (centrate and thin stillage); [d] TS = total solids on a wet weight basis; [e] VS = volatile solids on a total solids basis; [f] COD = chemical oxygen demand; [g] twwt. a^{-1}= tonne wet weight per annum; [h] theoretical value based on TS and VS annual quantities of the substrates and thick stillage (see Appendix A.1)

3.3.2 LBR-EGSB system components

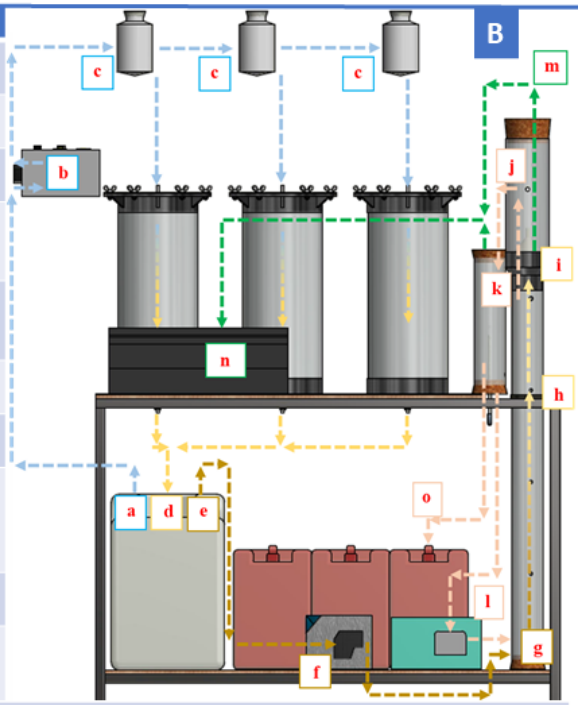
3.3.2.1 Overview of the LBR-EGSB concept

The LBR-EGSB system is similar to previous LBR-UASB configurations described in literature (Lehtomäki et al., 2008; Nizami et al., 2011). The primary difference is the higher upflow velocities in the EGSB, which can enable lower HRTs. The system designed herein consists of three LBRs (Figure 3.1A - component 1) and three EGSBs (Figure 3.1A - component 5). The LBRs were loaded with mWBM 'dry', and the leachate holding tank (Figure 3.1A - component 2) was loaded with mWBM 'wet'. A peristaltic pump transferred mWBM 'wet' from the leachate holding tank into the LBRs. Hydrolysis and acidogenesis occurred in the LBRs through percolation of mWBM 'wet' over mWBM 'dry'. During the leaching

process, the VFA content of mWBM ‘wet’ increases and is subsequently pumped with a peristaltic pump to the EGSBs, where VFAs are converted to biogas by methanogens. Figure 3.1 shows the detailed components and conceptual flow analysis of the LBR-EGSB.



#	QTY	COMPONENT
1	3	Leach bed reactors (LBR)
2	1	Leachate holding tank
3	1	LBR pump
4	3	Leachate holding cup
5	3	Expanded granular sludge beds (EGSB)
6	3	External gas-liquid-solid separator (GLSS)
7	1	EGSB pump
8	1	EGSB recirculation pump
9	3	EGSB effluent tank



#	DESCRIPTION
a	mWBM 'wet' is used as the initial leachate with minimal VFA content.
b	Leachate is pumped by a peristaltic pump to each LBR.
c	Each LBR leachate holding cup is supplied with leachate.
d	The VFA content of mWBM 'wet' increases as leaching of mWBM 'dry' occurs.
e	Steps A-D are repeated until the leachate reaches the maximum VFA concentration allowable to the EGSB.
f	The VFA-rich leachate is pumped to the EGSB using a peristaltic pump.
g	The VFA-rich leachate enters the EGSB and flows upward.
h	VFAs are consumed by the granular sludge and converted to biogas. The effluent from the EGSB has a reduced VFA content.
i	An initial gas-liquid-solid separator (GLSS) removes the gas from the EGSB.
j	The EGSB effluent with low VFA content leaves the EGSB at the 6L (1.2m) mark.
k	The EGSB effluent with low VFA content enters the external GLSS.
l	The EGSB effluent with low VFA content is recirculated back into the EGSB using a peristaltic pump.
m	Biogas from the EGSB exits from the top and flows to the gas measurement unit.
n	The biogas quantity is measure in a gas measurement unit.
o	Effluent from the EGSB exits into effluent tanks for disposal.

Figure 3.1: **A:** LBR-EGSB components; and **B**: conceptual flow analysis.

3.3.2.2 Leach bed reactors (LBRs)

Three identical leach bed reactors of 14.9 L volume were constructed with an outer diameter of 205 mm, an internal diameter of 195 mm, and a height of 500 mm (Figure 3.2A – component a). The design of a single LBR allows for approximately 668 g of mWBM 'dry' to be loaded. The feed housing cylinder (Figure 3.2A – component f) was made of PVC pipe with an inner diameter of 160mm and a height of 150mm. Approximately 5 L of headspace was left for the sprinkling of leachate over the feedstock, and an additional 2.5 L was left for leachate collection at the bottom of the LBR. Each LBR was wrapped with a heating mat and maintained at 37±1^{o}C (mesophilic temperature range).



Figure 3.2: LBR and leachate holding cup components. **A:** LBRs and the percolation system components: (a) LBR; (b) plastic bowl; (c) 1.5mm sieve; (d) 3mm sieve; (e) 4mm sieve;(f) feed housing cylinder (g) sprinkler head and (h) LBR lid. **B:** Leachate holding cup: (i) leachate inlet from the pump; (j) 250mL container; (k) inner tube at the bottom of the leachate holding cup (l) leachate outlet; (m) gas tube connected to LBR lid.

3.3.2.3 Percolation system

A multi-layer sieve was implemented to prevent solid particles from exiting the LBRs and clogging the leachate pump. The sieve hole diameters were 4 mm, 3 mm, and 1.5 mm, respectively, from top to bottom (Figure 3.2A - components c-e). In addition, mWBM 'dry' was added to the LBR in muslin cheesecloth to mitigate any washout of solid particles. The structural walls of the feed housing cylinder were made from PVC pipe, and the sieve surface was made of 2mm thick HDPE plastic. A 1.5 L round-bottomed plastic bowl (Figure 3.2A – component b) served as a funnel to direct the leachate to the outlet of the LBRs.

3.3.2.4 Leachate sprinkler

The leachate sprinkler (Figure 3.2A – component g) consisted of three T-shaped tube connectors and four L-shaped connectors made of polypropylene to distribute the leachate effectively into the LBR. The sprinkler was attached to the lid (Figure 3.2A – component h) of the LBRs. The overall sprinkler diameter was 120 mm.

3.3.2.5 Leachate holding tank

The LBR effluent (leachate) was collected in a 25 L drum, which served as the leachate holding tank. The mWBM 'wet' was introduced directly into this tank. The leachate holding tank also provided a sampling point from which the leachate could be analysed. When required, the leachate could be pumped from the holding tank to the LBRs and/or the EGSBs.

3.3.2.6 Leachate pump and sprinkling system

The leachate was recirculated from the leachate holding tank (see Section 2.2.5) to the LBRs (via a leachate holding cup) by a bespoke variable speed peristaltic pump

(45-180 L. d^{-1}) with three independent pump heads; each LBR received leachate independently. The sprinkling system consisted of tubing, tubing connectors, a leachate sprinkler, and the leachate holding cups (250 ml) (Figure 3.2B). The leachate was continuously pumped into the leachate holding cups. The leachate holding cups used a siphoning effect whereby, once the leachate reached 250 ml, the leachate emptied into the LBRs. The leachate holding cups had a gas outlet on top (Figure 3.2B – component m) connected to the top of the LBR headspace to allow for gas displacement in the leachate holding cup. As the hydrolysis process within the LBRs is the performance-limiting step of similar systems, malfunctioning of the leachate actuation system due to clogging, as mentioned in previous designs, would be alleviated. As previous designs used solenoid valves to initiate leachate discharge, the designed leachate holding cups are a cost-effective alternative requiring little specialised skill and are easily scalable.

3.3.2.7 EGSB reactors

Three identical EGSBs were constructed to provide triplicate reactors for experimental trials, each with a total height of 1,330 mm. Each EGSB consisted of two sections: a lower section (Figure 3.3a) 1,000 mm in length with an internal diameter of 74 mm and an upper section (Figure 3.3c) 330 mm long with an internal diameter of 104 mm. The two sections were connected by a pipe adapter coupling (100 mm length) which had negligible height contribution to the overall EGSB height after assembly (Figure 3.3b). The increase in cross-sectional area in the upper section would serve as a diffuser and reduce the fluid velocity inside the reactor to facilitate the settlement of the granular sludge. It was hypothesised that this would reduce sludge washout at higher upflow velocities. The total volume of each EGSB was 7.1 L with a working volume of 6 L. An influent inlet was placed 50 mm from

the bottom of the EGSBs to allow for space for rubber stoppers (Figure 3.3e). The rubber stoppers were used to seal the bottom of the reactors. Each EGSB had three sampling points located at 1 L (ca. 235 mm), 2 L (ca. 470 mm) and 3 L (ca. 705 mm) from the bottom of the reactor. The effluent point was located ca. 1,200 mm from the bottom of the reactor. The top of each EGSB was sealed using a 105 mm diameter rubber end stop (Figure 3.3d) with two gas outlets.

The leachate was pumped into each EGSB using a variable speed Ismatec Ecoline VS-MS/CA8-6 peristaltic pump. Establishing the leachate upflow velocity in the EGSB and, thereby, the maximum pump flow rate is a crucial design parameter. A low upflow velocity (0.2 m. hr^{-1}) was chosen for the commissioning trials to ensure little expansion of the granular sludge bed and minimal sludge washout (Chernicharo, 2007). It was hypothesised that higher upflow velocities would be possible after acclimatisation of the inoculum as inert and inactive sludge would exit the EGSB during the commissioning trial. However, the upflow velocity was still double the recommended upflow velocity (0.1 m. hr^{-1}) of UASBs (Nizami et al., 2011). The upflow velocity was established experimentally. A Watson Marlow 323U peristaltic pump was used to recirculate the EGSB effluent back into the EGSB through a Y-shaped connection that was also used for the leachate to maintain the required upflow velocity. The EGSBs were wrapped with heating mats (37±1 ^{o}C) to a height of 600 mm. The lower section contained a sludge bed height of 650 mm, but the EGSB was insulated with 13 mm insulation foam. Temperature checks indicated uniform heating of the entire bed.

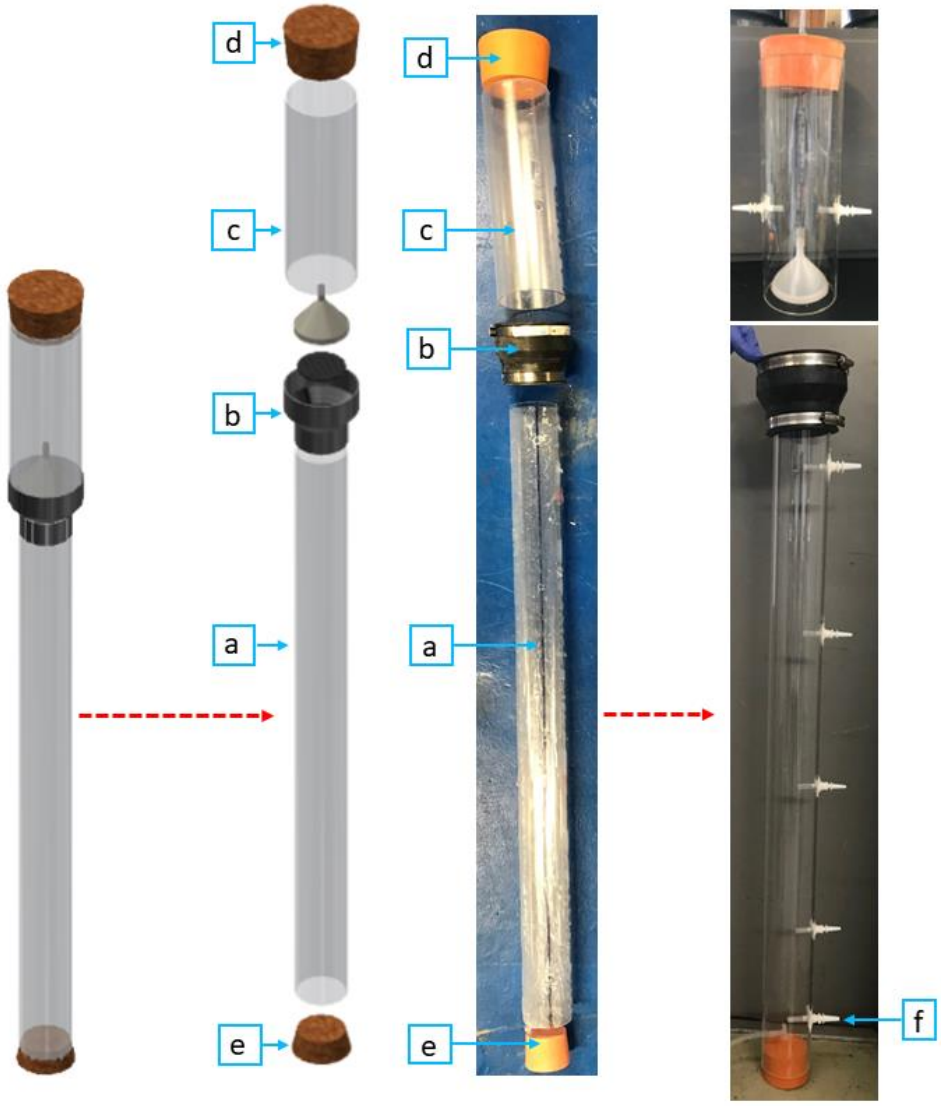


Figure 3.3: EGSB components and assembly: (a) EGSB lower section; (b) Pipe adapter coupling; (c) EGSB upper section; (d) top rubber stopper and EGSB gas outlet; and (e) bottom rubber stopper; (f) alternative recirculation inlet.

3.3.2.8 Gas-liquid-solid separator (GLSS)

The gas-liquid-solid separator (GLSS) separates and collects the biogas generated from the liquids and buoyant solids within the EGSB (Yasar et al., 2007). The EGSBs had internal and external gas-liquid-solid separators. The internal GLSS was an inverted polypropylene funnel (80 mm diameter) that was connected to the top gas outlet of the EGSB (Figure 3.4a). An additional gas outlet at the top of the EGSB

(Figure 3.4b) was made for any gases that may have bypassed the internal GLSS. Once the effluent exited the EGSB, it settled momentarily in the external GLSS (Figure 3.4h). The external GLSS was made of clear acrylic pipe with an inner diameter of 74 mm and a height of 300 mm. The external GLSS also served as a settling chamber for granular sludge washout. It was hypothesised that any gases that escaped with the washed-out sludge or from back pressure, as stated in previous designs, would be captured in the external GLSS. A gas outlet at the top of the external GLSS was connected to the two EGSB gas outlets (Figure 3.4c). The EGSB effluent was recirculated from the bottom of the external GLSS (Figure 3.4d). The gas outlets led to the biogas production measurement system. The effluent outlet (Figure 3.4e), which was approximately halfway inside the GLSS, had a U-tube connection that split into two points; one end pointed downwards toward a 5L effluent tank (Figure 3.4f), and the other pointed upwards toward the atmosphere (Figure 3.4g). The GLSS also allowed for back-pressure adjustment (see Section 3.4.3). This setup was used to avoid any siphoning effects and to avoid air entering the GLSS.

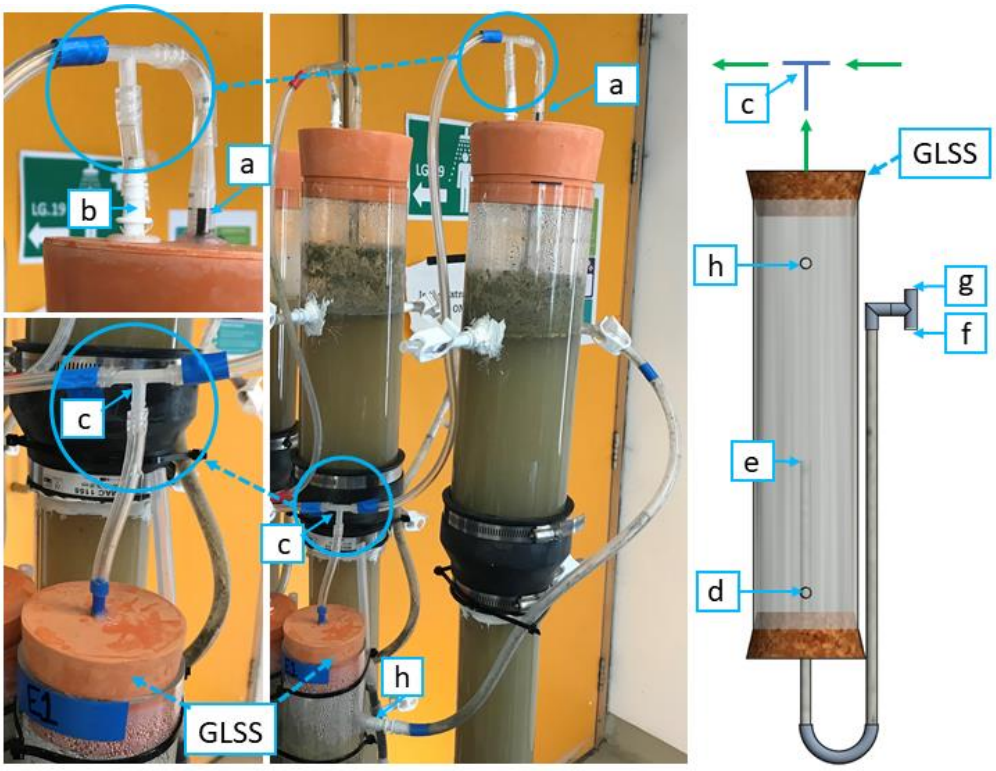


Figure 3.4: Gas-liquid-solid separator (GLSS) configuration: (a) internal GLSS outlet; (b) additional gas outlet; (c) GLSS T-shaped connection point; (d) GLSS recirculation point leads back into the EGSB; (e) effluent outlet; (f) effluent tank point; (g) atmosphere; and (h) GLSS inlet from EGSB effluent.

3.3.2.9 LBR-EGSB system capacity

The total system capacity for liquids was 25 L within the leachate tank and 44 L of solids within the LBRs. The working volume in the configuration proposed for the whiskey by-products was up to 24 L for liquids and up to 28 L for solids.

3.3.3 Issues and modifications

3.3.3.1 Sludge flotation

Sludge flotation caused the granular sludge bed to rise in the EGSB up to the expansion section. Sludge flotation occurred due to entrapped biogas within the hollow spaces of the sludge bed, creating a buoyant force on the granular sludge (Yoda and Nishimura, 1997). This resulted in fluid washout (±0.3 L) and clogging.

Any sludge washout during this phase was collected in the GLSS and reintroduced into the reactor. This issue was alleviated by changing the recirculation inlet to the EGSB from the same as the leachate to the lowest sample port of the EGSB, which is found on the opposite side of the EGSB influent and 50 mm higher than the influent port (see Figure 3.3f). It was hypothesised that this would assist in agitating the sludge bed and allow the entrapped biogas to escape.

3.3.3.2 Settling of mWBM 'wet' residual solids

Residual solids within mWBM 'wet' would congregate and coagulate at the bottom of the leachate holding tank and in the downstream tubing, resulting in clogging of the leachate pumping system. The leachate holding tank was subsequently fitted with a bespoke stirrer to allow for continuous agitation. This improvement may be unique to the leachate used in this system.

3.3.3.3 Pressure differences

Pressure differences between the EGSB internal gas-liquid-solid separator and the external gas-liquid-solid separator had to be continuously corrected (see Figure 3.5). As pressure was also needed to cause the effluent to exit the gas-liquid-solid separator, a balance was required between gas collection and effluent leaving the system; that is, equal pressure was needed to exit the system as was required to tip the gas meter. Clogging within the EGSB would result in the EGSB effluent rising beyond the effluent outlet and reducing the headspace of the EGSB. This would disturb the EGSB's pressure "sweet spot" to register gas production. The effluent port in the external gas-liquid-solid separator would be exposed, resulting in the biogas exiting the system via the external GLSS instead of being measured (Figure 3.5). This issue was addressed by replenishing the external GLSS liquid level with EGSB effluent from the EGSB effluent tank. The long-term solution was to separate

the gas outlet of the GLSS from the main EGSB and include a larger U-tube bend between the GLSS and EGSB.

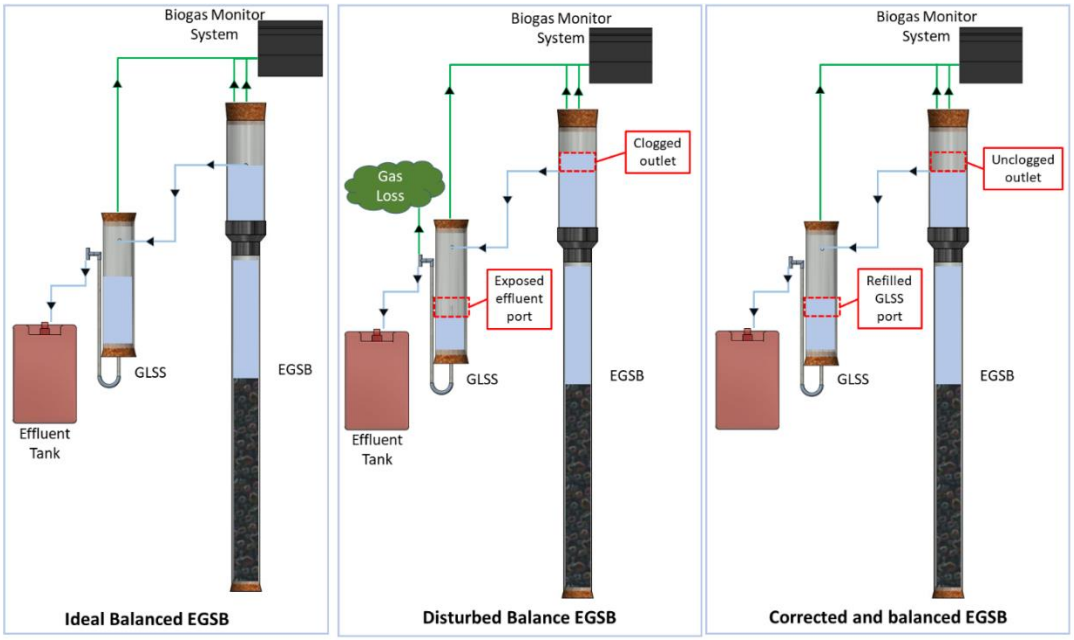


Figure 3.5: EGSB pressure balance correction.

3.3.4 Calculating the maximum organic loading rate of the EGSB

The maximum COD loading capacity of the EGSB is a critical design parameter for biogas production in an LBR-EGSB system (Lehtomäki et al., 2008). To maximise biogas production from the EGSB. Ideally, the maximum COD capacity should be fed to the reactor; this is based on the quantity of inoculum and the EGSB maximum upflow velocity (see Box 3.1). The COD capacity of the inoculum may increase with time as the inoculum adapts to the conditions of the substrate and as inert particles exit the reactors (Hussain et al., 2017).

Box 3.1: EGSB reactor COD capacity (adapted from (Nizami et al., 2011))
The inoculum used in the reactor determines the maximum COD capacity of the EGSB.

I. Start-up inoculum quantity

Inoculum TS (%)	=	10.4	%
Inoculum VS (%)	=	79.7	% of TS
Inoculum g VS. L^{-1} $_{inoculum}$	=	1L of inoculum x 10.4 % x 79.7 % (%VS)	
Inoculum g VS. L^{-1} $_{inoculum}$	=	82.9	g VS. L^{-1} $_{inoculum}$ (assuming 1 ml = 1 g)
Working Volume	=	6	L

A series of preliminary trials assessed the EGSB design VS concentration. The three EGSBs were inoculated with three inoculum concentrations: 15 g VS. $L^{-1}_{reactor}$ (Forbes et al., 2009), 25 g VS. $L^{-1}_{reactor}$ and 35 g VS. $L^{-1}_{reactor}$ (Nizami et al., 2011). The EGSB with 35 g VS. $L^{-1}_{reactor}$ was deemed best in terms of pH stability, biogas quantity and COD removal. 35 g VS. $L^{-1}_{reactor}$ of inoculum equates to 42 % of the reactor volume being filled with inoculum (remainder with distilled water) as assessed below:

EGSB designed VS concentration	=	35	g VS. L^{-1} reactor
Quantity of inoculum added	=	35	g VS. L^{-1} reactor / 82.9 g VS. L^{-1} x 6 L
Quantity of Inoculum added	=	2.5	L of inoculum
VS Mass of Inoculum	=	2.5 $L_{inoculum}$	x 82.9 g VS. L^{-1} inoculum
VS Mass of Inoculum	=	207.3	g VS of inoculum

II. EGSB maximum upflow velocity

Volume of EGSB	=	6	L
Effective height of EGSB	=	1.2	m
Upflow velocity (m. hr^{-1})	=	**0.2**	**m. hr^{-1}**
Leachate retention time (HRT)	=	1.2 m	/ 0.2 m. hr^{-1}
Leachate retention time (HRT)	=	6	hr – maximum without recirculation
Maximum influent flow rate	=	6 L /6 hr	
Maximum influent flow rate	=	1	L. hr^{-1} x 24 hr
Maximum influent flow rate	=	24	L. d^{-1}

III. COD capacity of the inoculum

COD capacity of the inoculum guides the organic loading rate of the EGSB at start-up.

Digestion activity of the inoculum	=	0.1[a]	g COD. g^{-1} $VS_{inoculum}$. d^{-1}
COD conversion efficiency of inoculum	=	75[a]	%
COD capacity of added inoculum	=	207.3[b]	g VS x 0.1 g COD. g^{-1} VS. d^{-1} x 75%
COD capacity of added inoculum	=	15.5	g COD. d^{-1}
Maximum start-up OLR	=	15.5	g COD. d^{-1} / 6 $L_{reactor}$
Maximum start-up OLR	=	2.6	g COD. L^{-1}. d^{-1}

[a] see Box S2; [b] attained from Box 3.1. I.

3.3.5 LBR start-up/leaching trials

The concept validation of VFA production from liquid and solid whiskey by-products within LBRs was evaluated through leaching trials. The leaching trials were phenomenological rather than optimised biological trials. The leaching trials also served as the commissioning of the LBRs. The LBRs and EGSBs were initially commissioned separately due to the anticipated long start-up time of the EGSBs and the variable VFA concentration of the leachate.

The LBRs were sequentially fed with 668 g of mWBM 'dry' every 5 days (Browne and Murphy, 2014). To mimic the liquid-to-solid ratio as produced at the distillery, approximately 4L of mWBM 'wet' was fed every 5 days directly into the leachate holding tank (see Figure 3.1A- component 2). The conceptual flow analysis (Figure 3.1B) shows the flow of the substrates within the system. The LBR leaching trials lasted 45 days. As such, each LBR was loaded three times, and mWBM 'dry' was digested for 15 days. This addition was enough to facilitate high recirculation rates of the LBR of 140 L. d^{-1} but resulted in the pooling of the LBRs. However, this pooling effect yielded higher VFA production than using a lower recirculation rate (60 L. d^{-1}) (Figure A2). After loading with feedstock, the LBR and leachate holding tank were flushed with nitrogen gas for 5 minutes to displace air from the headspace.

3.3.6 EGSB start-up trials

The EGSB were acclimatised to whiskey by-products prior to experimental trials (Figure A3). A short experimental trial (25 days) was undertaken as a concept validation and commissioning trial. As such, optimal biological performance was not the objective of the trial. Rather, fault finding, leak detection and design

modifications were the objectives of the trial. The EGSB was connected directly to the LBR leachate holding tank, after the LBR leaching trials. As the COD of the leachate varied, the average COD over the previous 7 days was used to set the OLR to ±2.6 g COD. L^{-1}. d^{-1} (HRT of 6 days) for the following week. Long HRTs and low OLRs are recommended for acclimatisation for wastewaters with COD concentrations greater than 5 g. L^{-1} (Chernicharo, 2007). For commissioning, only the COD removal and biogas quality were assessed. The EGSB were considered commissioned once the biogas quality was near constant, with less than 5 % variation (Akunna, 2000).

3.3.7 Analytical methods

The TS and VS content of mWBM and inoculum was analysed as per Standard Methods 2540 G (APHA, 2022). The pH of all samples was determined by a Mettler Toledo™ F20 pH meter. A gas chromatographer (Agilent GC 7890B) equipped with the DB-FFAP column (Ø 0.32 mm x 50 m) and the flame ionisation detector (FID) was used to evaluate the VFA concentration and composition (acetic acid, butyrate acid, and propionic acid) of the LBR leachate and the EGSB effluent. VFA samples were stored at -20 ^{o}C, thawed, and centrifuged at 11,000 rpm for 10 minutes prior to analysis (Kang et al., 2021). The biogas composition of the EGSB was measured by a gas chromatographer (Agilent GC 7890B) furnished with a thermal conductivity detector (TCD) and two fused silica capillary columns. Methane (CH_4) was detected by a CP-Molsieve 5A column (25 m x 0.32 mm x 30 µm film thickness), whereas carbon dioxide (CO_2) content was established by a GS-CarbonPLOT column (3 m x 0.32 x 3 µm film thickness).

The COD concentration of the LBR leachate and EGSB effluent was evaluated by Hach Lange cuvette test kits (LCK 914 and LCK514) and a Hach Lange

Spectrophotometer (DR 3900). COD samples were centrifuged at 11,000 rpm for 10 minutes and evaluated immediately.

The COD removal efficiency (COD_{eff}) of the EGSB was calculated as follows (Kang et al., 2021):

$$COD_{eff} = \frac{(COD_{in} - COD_{out})}{COD_{in}} \times 100\ \%$$

where: COD_{in} = leachate COD entering the EGSB; and COD_{out} = COD of the EGSB effluent.

Acidification of the leachate was calculated by converting the VFAs to the COD equivalent (VFAs-COD_{equiv}) and dividing it by the total COD of the leachate. The COD to VFA conversion efficiency was calculated by dividing VFAs-COD_{equiv} with the COD of mWBM 'wet' (33.9 g COD. L^{-1}).

The VS destruction efficiency ($VS_{dest\%}$) of the LBR was calculated as follows (Switzenbaum et al., 2003):

$$VS_{dest\%} = \frac{vs_{in} - vs_{out}}{vs_{out}} \times 100$$

where: VS_{in} = VS mass (in grams) of mWBM 'dry' before entering the LBR, and VS_{out} = VS mass of mWBM 'dry' out of the LBR.

Biogas production from the LBRs was not monitored as mostly carbon dioxide was expected. Biogas gas production from the EGSB was estimated based on the system removal efficiencies: the VS destruction efficiency and the COD removal efficiency.

3.4 Results and discussion

3.4.1 Trends in reactor stability

The pH range in the LBRs for the first 20 days was in the range of 3.81-4.02; thereafter, the pH settled into the range of 4.3-4.8 (Figure 3.6b). A gradual rise in pH was evident in studies utilising LBR systems in the treatment of grass, brewers spent grains and the organic fraction of municipal solid waste (Dogan et al., 2009). The average pH for the EGSB was 7.3 (Figure 3.7). Overall, the EGSB pH remained within the range for optimum methane production in the range of 7.0-7.6 (Gerardi, 2003).

The leachate COD steadily declined from 34.8 to 27.5 g. L^{-1} over the first 15 days, thereafter, values ranged between 27.7 and 32.4 g. L^{-1} (Figure 3.6b). The initial reduction in COD can be attributed to the LBRs not being completely anaerobic; such systems are often considered partially anaerobic. It was hypothesised that aerobic respiration within the system may have converted some of the COD to carbon dioxide. These findings concur with previous findings in the literature (Browne et al., 2013; Nizami et al., 2011).

The VFA concentrations (Figure 3.6a) in the leaching trials showed an increasing trend, reaching a peak concentration of 10,341 mg. L^{-1} by day 35. Thereafter, the VFAs ranged between 8,890-10,144 mg. L^{-1}. The VFAs concentration was higher than that reported in a study of VFA production from brewers spent grains hydrolysate (8.4 g VFA. L^{-1}) (Castilla-Archilla et al., 2021). The composition on day 35 approximated acetic acid at 20 %, butyric acid at 55 %, and propionic acid at 15 %, with small amounts of caproic acid (6 %) and other VFAs evident. Caproic acid concentrations reached 964.2 mg. L^{-1} on day 45. There was a gradual rise in VFAs

due to an accumulation of longer-chain VFAs (such as isovaleric acid and valeric acid) in the EGSB from 96.7 g VFA. L^{-1} to 747.6 g VFA. L^{-1}, however, this concentration is within the recommended process stability levels (<1 g VFA. L^{-1}) (Drosg, 2013).

3.4.2 Trends in treatment efficiency

Overall, the volatile solids content of mWBM 'dry' reduced over the 15-day digestion period by 20-33 %. The reduction in volatile solids content was higher than in a study evaluating grass in LBRs, which established a 19 % decrease in volatile solids content (Wall et al., 2016). However, it was lower than another study which investigated the organic fraction of municipal waste in LBRs, where 40 %VS destruction was reported(Uke and Stentiford, 2013). This evidences the difficulty or ease of degradation of specific feedstocks. The degree of acidification can be measured in two ways. First, by comparing the COD of the VFAs to the COD of mWBM 'wet' (termed the COD to VFA efficiency). On Day 35, when the leachate contained 10,341 mg tVFAs. L^{-1} (17.3 g VFA-COD_{equiv}. L^{-1}) and the COD of mWBM 'wet' was 33.9 g COD. L^{-1}, the COD to VFA efficiency was approximately 51 %. Secondly, the degree of acidification can also be measured by comparing the COD of the VFAs to the COD within the leachate (termed acidification). On day 35, when the leachate contained 29.6 g COD. L^{-1} and 17.3 g VFA-COD_{equiv}. L^{-1}, the acidification was approximately 58.4 %. This acidification was higher than that previously reported for cheese whey (up to 40 %), winery wastewater (14 %) and brewers spent grains hydrolysate (41 %)(Atasoy et al., 2018; Buitrón et al., 2019; Guarda et al., 2021). As the LBRs did not contain any inoculum, it can be assessed that leaching mWBM 'dry' with mWBM 'wet' as leachate can extract volatile content from the solid material for VFA production.

The EGSB COD removal efficiency (Figure 3.7) throughout the experimental trials remained high, with an average of 96 %. High COD removal efficiencies (>80 %) in high-rate reactors such as the EGSB are expected. A study where a two-phase EGSB processed fermentation wastewater reported a COD removal efficiency of 95 % (Wu et al., 2015). Another study that assessed distillery wastewater using a two-phase UASB reported a removal efficiency of 96 %(Uzal et al., 2003).

3.4.3 Biogas quality and estimated methane yield

The average methane content in the biogas was high at 75 $\%_{vol}$ (Figure 3.7). The methane content in the biogas was akin to that of a study evaluating ethanol wastewater in a two-phase UASB (75 %) (Jiraprasertwong et al., 2021). At peak VS destruction (33 %) (see Section 3.2) and EGSB COD removal efficiency (96 %), the estimated specific methane yield was 241 L CH_4. kg^{-1} $VS_{mWBM,}$ which is 53 % of the theoretical yield (459 L CH_4. kg^{-1} VS) with the current configuration (see Appendix A.5). This result is higher than a similar reactor degrading grass silage (204 L CH_4. kg^{-1} VS_{added}) but lower than a study degrading food waste (340 L CH_4. kg^{-1} VS_{added})(Browne and Murphy, 2014; Lehtomäki et al., 2008).

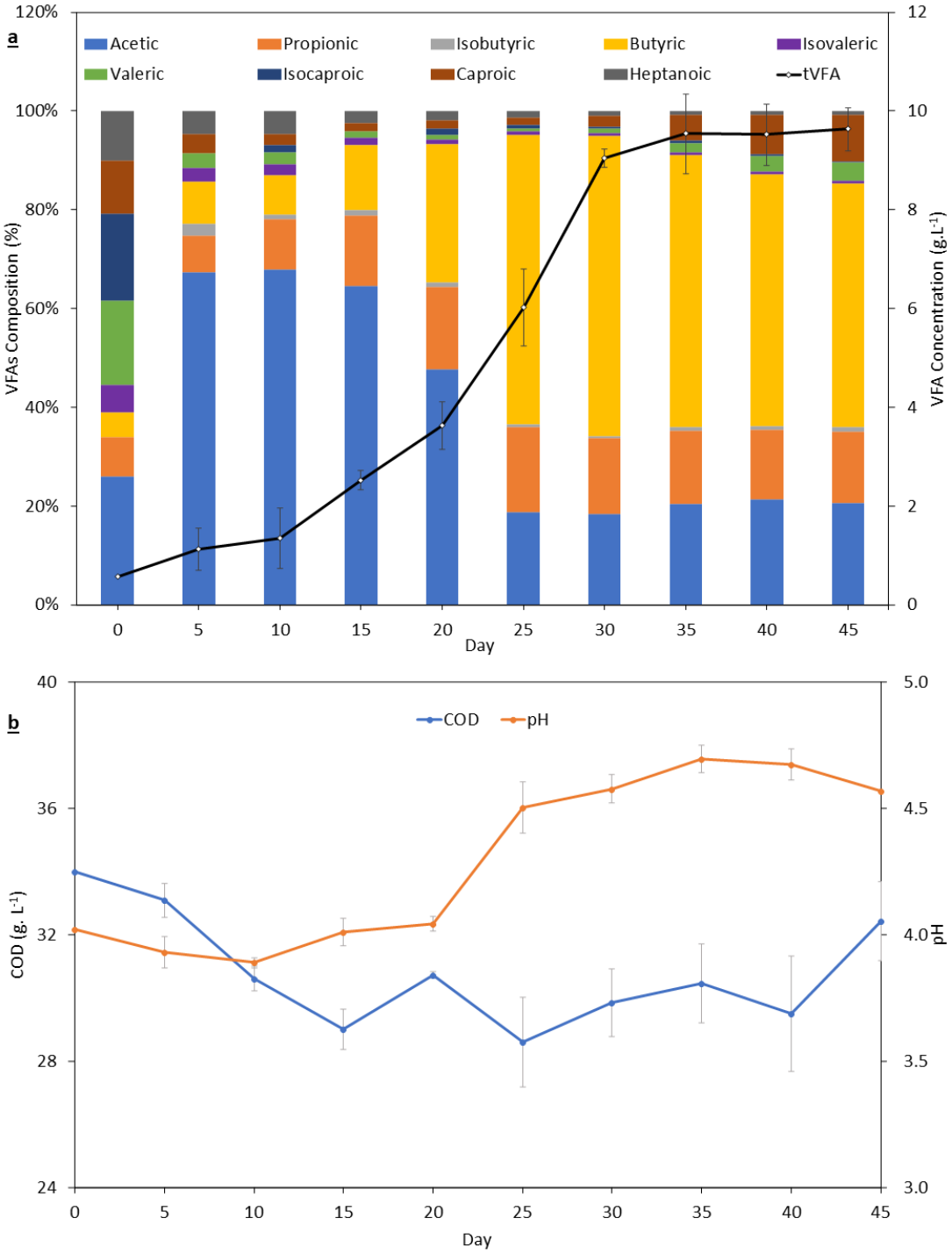


Figure 3.6: (a) Leachate VFA concentrations and composition, (b) leachate COD and pH from the leaching trials.

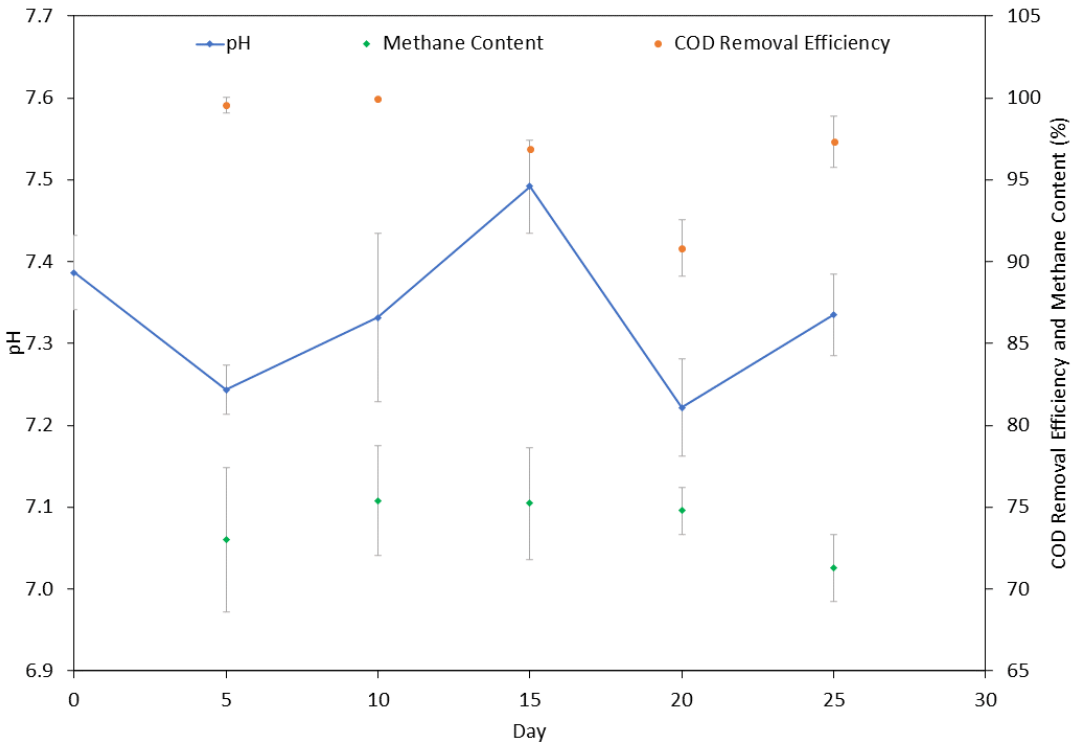


Figure 3.7: Expanded granular sludge bed (EGSB) stability and treatment efficiency.

3.4.4 Reactor considerations and future research

The LBR-EGSB reactor was shown to be capable of processing all solid (draff and cake maize) and liquid (thin stillage and centrate) distillery by-products (mWBM). The dry by-product fractions were suitable for the LBR, whilst the liquid by-product fractions provided suitable initial leachate. Implementing an EGSB allowed a doubling of upward velocities (0.2 m. hr^{-1}) compared to previous UASB studies; in essence, this may reduce the required footprint of an EGSB at the distillery. The implementation of an external gas-liquid-solid separator device to capture any residual gases produced by the effluent can potentially reduce the amount of methane slippage as compared to previous designs. The improved design of the LBR-EGSB can alleviate previous design flaws, namely, malfunctioning leachate actuation systems and low upflow velocities (0.1 $m.hr^{-1}$) recommended in the literature (Nigam, 2017; Wall et al., 2016).

Interestingly, while the LBR may not have been operated at optimum conditions, the VFA concentrations during the leaching process peaked at levels greater than 10 g VFA. L^{-1}. As hydrolysis is the limiting step of the performance of LBR-EGSB, a balance between VFA production, pH, and VS destruction in the LBR must be established. Increasing the overall VS destruction efficiency of the LBR would increase the overall performance of the reactor. Several options, such as thermal pretreatment, pH control, and bulk density additives, to name a few, are available and require further research (Hu et al., 2005; Hussain et al., 2017; Xu et al., 2012). While the design of the LBR is simple, a level of ambiguity in its operation is evident in literature. Some of these variables include adding or excluding inoculum in the LBRs, flooded or percolated LBR operation and recirculation of effluent from the downstream EGSB back to the LBRs (Browne et al., 2013; Nizami et al., 2010; Xu et al., 2012). The addition of the whiskey by-product liquids as leachate offers a unique opportunity beyond previous systems in which fresh water may be required for leaching. Overall, further research is required to establish the optimum operational conditions for the processing of both liquid and solid whiskey by-products in an LBR-EGSB.

While this study focused on the design and construction of the LBR-EGSB, the proof of concept was validated by the acidification of the leachate. A biological optimisation study over a more extended period would be required to establish the optimal (maximum) specific methane potential of the whiskey by-products in the LBR-EGSB.

3.5 Conclusion

A two-phase anaerobic reactor (termed LBR-EGSB) was designed, constructed, and conceptually validated to valorise liquid and solid distillery by-products. The work presented achieved the following:

1. The leach bed reactor with a downstream expanded granular sludge bed (LBR-EGSB) was designed and constructed to process whiskey by-products.
2. The operational start-up parameters for the LBR-EGSB included a hydraulic retention time of ±32 min for the leach bed reactor and an upflow velocity of 0.2 m. hr^{-1} for the expanded granular sludge bed reactor. The maximum organic loading rate was determined to be 2.6 g COD. $L^{-1}_{reactor}$. d^{-1} for the expanded granular sludge bed reactor. Reactor modifications were made for sludge flotation, settling of residual solids and pressure differential issues.
3. Phenomenological commissioning trials were conducted experimentally. The LBR-EGSB was considered commissioned once volatile fatty acid concentration levels and biogas methane content were stable.
4. High volatile fatty acid yields (10,341 mg. L^{-1}), acidification (58 %) and EGSB COD removal (96 %) were evident from the designed LBR-EGSB system when processing whiskey by-products. Methane-rich biogas (75%$_{vol}$ CH_4) was produced with an estimated yield of 241 L CH_4. kg^{-1} VS.

References

1. Abad, V., Avila, R., Vicent, T., Font, X., 2019. Promoting circular economy in the surroundings of an organic fraction of municipal solid waste anaerobic digestion treatment plant: Biogas production impact and economic factors. Bioresour Technol 283, 10–17. https://doi.org/10.1016/J.BIORTECH.2019.03.064
2. Akunna, J., 2000. Performance of a granular-bed anaerobic baffled reactor (GRABBR) treating whisky distillery wastewater. Bioresour Technol 74, 257–261. https://doi.org/10.1016/S0960-8524(00)00017-1
3. APHA, 2022. Standard Methods for the Examination of Water and Wastewater™, 24th ed. American Public Health Association, American Water Works Association, and Water Environment Federation.
4. Atasoy, M., Owusu-Agyeman, I., Plaza, E., Cetecioglu, Z., 2018. Bio-based volatile fatty acid production and recovery from waste streams: Current status and future challenges. Bioresour Technol 268, 773–786. https://doi.org/10.1016/j.biortech.2018.07.042
5. Barrena Martínez, J., López Fernández, M., Romero Fernández, P.M., 2016. Corporate social responsibility: Evolution through institutional and stakeholder perspectives. European Journal of Management and Business Economics 25, 8–14. https://doi.org/10.1016/J.REDEE.2015.11.002
6. Bastidas-Oyanedel, J.-R., Bonk, F., Thomsen, M.H., Schmidt, J.E., 2015. Dark fermentation biorefinery in the present and future (bio)chemical industry. Rev Environ Sci Biotechnol 14, 473–498. https://doi.org/10.1007/s11157-015-9369-3

7. Browne, J.D., Allen, E., Murphy, J.D., 2013. Improving hydrolysis of food waste in a leach bed reactor. Waste Management 33, 2470–2477. https://doi.org/10.1016/j.wasman.2013.06.025
8. Browne, J.D., Murphy, J.D., 2014. The impact of increasing organic loading in two phase digestion of food waste. Renew Energy 71, 69–76. https://doi.org/10.1016/j.renene.2014.05.026
9. Buitrón, G., Martínez-Valdez, F.J., Ojeda, F., 2019. Biogas Production from a Highly Organic Loaded Winery Effluent Through a Two-Stage Process. Bioenergy Res 12, 714–721. https://doi.org/10.1007/s12155-019-09984-7
10. Castilla-Archilla, J., Heiberger, J., Mills, S., Hilbig, J., Collins, G., Lens, P.N.L., 2021. Continuous Volatile Fatty Acid Production From Acid Brewery Spent Grain Leachate in Expanded Granular Sludge Bed Reactors. Front Sustain Food Syst 5. https://doi.org/10.3389/fsufs.2021.664944
11. Chen, T.-H., Huang, J.-L., 2006. Anaerobic treatment of poultry mortality in a temperature-phased leachbed–UASB system. Bioresour Technol 97, 1398–1410. https://doi.org/10.1016/j.biortech.2005.07.002
12. Chernicharo, C.A. de L., 2007. Anaerobic Reactors. IWA Publishing, London.
13. Dogan, E., Dunaev, T., Erguder, T.H., Demirer, G.N., 2009. Performance of leaching bed reactor converting the organic fraction of municipal solid waste to organic acids and alcohols. Chemosphere 74, 797–803. https://doi.org/10.1016/j.chemosphere.2008.10.028
14. Drosg, B., 2013. Process monitoring in biogas plants. IEA bioenergy Paris, France.
15. Forbes, C., O'Reilly, C., McLaughlin, L., Gilleran, G., Tuohy, M., Colleran, E., 2009. Application of high rate, high temperature anaerobic digestion to fungal

thermozyme hydrolysates from carbohydrate wastes. Water Res 43, 2531–2539. https://doi.org/10.1016/J.WATRES.2009.03.014

16. Gerardi, M.H., 2003. The Microbiology of Anaerobic Digesters. The Microbiology of Anaerobic Digesters. https://doi.org/10.1002/0471468967
17. Guarda, E.C., Oliveira, A.C., Antunes, S., Freitas, F., Castro, P.M.L., Duque, A.F., Reis, M.A.M., 2021. A Two-Stage Process for Conversion of Brewer's Spent Grain into Volatile Fatty Acids through Acidogenic Fermentation. Applied Sciences 11, 3222. https://doi.org/10.3390/app11073222
18. Gunes, B., Stokes, J., Davis, P., Connolly, C., Lawler, J., 2019. Pre-treatments to enhance biogas yield and quality from anaerobic digestion of whiskey distillery and brewery wastes: A review. Renewable and Sustainable Energy Reviews 113, 109281. https://doi.org/10.1016/j.rser.2019.109281
19. Hu, Z.-H., Yu, H.-Q., Zhu, R.-F., 2005. Influence of particle size and pH on anaerobic degradation of cellulose by ruminal microbes. Int Biodeterior Biodegradation 55, 233–238. https://doi.org/10.1016/j.ibiod.2005.02.002
20. Hussain, A., Filiatrault, M., Guiot, S.R., 2017. Acidogenic digestion of food waste in a thermophilic leach bed reactor: Effect of pH and leachate recirculation rate on hydrolysis and volatile fatty acid production. Bioresour Technol 245, 1–9. https://doi.org/10.1016/J.BIORTECH.2017.08.130
21. Jiraprasertwong, A., Karnchanapaisal, P., Seneesrisakul, K., Rangsunvigit, P., Chavadej, S., 2021. High process activity of a two-phase UASB (upflow anaerobic sludge blanket) receiving ethanol wastewater: Operational conditions in relation to granulation development. Biomass Bioenergy 148, 106012. https://doi.org/10.1016/j.biombioe.2021.106012

22. Kang, X., Lin, R., Li, L., Wu, B., Deng, C., O'Shea, R., Sun, Y., Murphy, J.D., 2021. Assessment of pretreatment and digestion temperature on anaerobic digestion of whiskey byproducts and microbial taxonomy. Energy Convers Manag 243, 114331. https://doi.org/10.1016/j.enconman.2021.114331
23. Kato, M.T., Field, J.A., Versteeg, P., Lettinga, G., 1994. Feasibility of expanded granular sludge bed reactors for the anaerobic treatment of low-strength soluble wastewaters. Biotechnol Bioeng 44, 469–479. https://doi.org/10.1002/BIT.260440410
24. Lehtomäki, A., Huttunen, S., Lehtinen, T.M., Rintala, J.A., 2008. Anaerobic digestion of grass silage in batch leach bed processes for methane production. Bioresour Technol 99, 3267–3278. https://doi.org/10.1016/j.biortech.2007.04.072
25. Linke, B., Rodríguez-Abalde, Á., Jost, C., Krieg, A., 2015. Performance of a novel two-phase continuously fed leach bed reactor for demand-based biogas production from maize silage. Bioresour Technol 177, 34–40. https://doi.org/10.1016/j.biortech.2014.11.070
26. López-Gutiérrez, I., Montiel-Corona, V., Calderón-Soto, L.F., Palomo-Briones, R., Méndez-Acosta, H.O., Razo-Flores, E., Ontiveros-Valencia, A., Alatriste-Mondragón, F., 2021. Evaluation of the continuous methane production from an enzymatic agave bagasse hydrolysate in suspended (CSTR) and granular biomass systems (UASB). Fuel 304, 121406. https://doi.org/10.1016/j.fuel.2021.121406
27. Murphy, J.D., Thanasit Thamsiriroj, 2013. Fundamental science and engineering of the anaerobic digestion process for biogas production, in: The Biogas

Handbook. Woodhead Publishing, pp. 104–130. https://doi.org/10.1533/9780857097415.1.104

28. Nigam, P.S., 2017. An overview: Recycling of solid barley waste generated as a by-product in distillery and brewery. Waste Management 62, 255–261. https://doi.org/10.1016/J.WASMAN.2017.02.018
29. Nizami, A.-S., Singh, A., Murphy, J.D., 2011. Design, Commissioning, and Start-Up of a Sequentially Fed Leach Bed Reactor Complete with an Upflow Anaerobic Sludge Blanket Digesting Grass Silage. Energy & Fuels 25, 823–834. https://doi.org/10.1021/ef101739d
30. Nizami, A.S., Thamsiriroj, T., Singh, A., Murphy, J.D., 2010. Role of Leaching and Hydrolysis in a Two-Phase Grass Digestion System. Energy & Fuels 24, 4549–4559. https://doi.org/10.1021/ef100677s
31. Panjičko, M., Zupančič, G.D., Zelić, B., 2015. Anaerobic biodegradation of raw and pre-treated brewery spent grain utilizing solid state anaerobic digestion. Acta Chim Slov 62, 818–827. https://doi.org/10.17344/acsi.2015.1534
32. Switzenbaum, M.S., Farrell, J.B., Pincince, A.B., 2003. Relationship between the Van Kleeck and Mass-Balance Calculation of Volatile Solids Loss. Water Environment Research 75, 377–380.
33. Uke, M.N., Stentiford, E., 2013. Enhancement of the anaerobic hydrolysis and fermentation of municipal solid waste in leachbed reactors by varying flow direction during water addition and leachate recycle. Waste Management 33, 1425–1433. https://doi.org/10.1016/J.WASMAN.2013.02.020
34. Uzal, N., Gökçay, C.F., Demirer, G.N., 2003. Sequential (anaerobic/aerobic) biological treatment of malt whisky wastewater. Process Biochemistry 39, 279–286. https://doi.org/10.1016/S0032-9592(03)00071-2

35. Wall, D.M., Allen, E., O'Shea, R., O'Kiely, P., Murphy, J.D., 2016. Investigating two-phase digestion of grass silage for demand-driven biogas applications: Effect of particle size and rumen fluid addition. Renew Energy 86, 1215–1223. https://doi.org/10.1016/j.renene.2015.09.049

36. Wu, S., Dang, Y., Qiu, B., Liu, Z., Sun, D., 2015. Effective treatment of fermentation wastewater containing high concentration of sulfate by two-stage expanded granular sludge bed reactors. Int Biodeterior Biodegradation 104, 15–20. https://doi.org/10.1016/J.IBIOD.2015.04.015

37. Xu, S.Y., Karthikeyan, O.P., Selvam, A., Wong, J.W.C., 2012. Effect of inoculum to substrate ratio on the hydrolysis and acidification of food waste in leach bed reactor. Bioresour Technol 126, 425–430. https://doi.org/10.1016/J.BIORTECH.2011.12.059

38. Yamaka, W., Phadkantha, R., Rakpho, P., 2021. Economic and energy impacts on greenhouse gas emissions: A case study of China and the USA. Energy Reports 7, 240–247. https://doi.org/10.1016/J.EGYR.2021.06.040

39. Yasar, A., Ahmad, N., Chaudhry, M.N., Khan, A.A.A., 2007. Sludge granulation and efficiency of phase separator in UASB reactor treating combined industrial effluent. Journal of Environmental Sciences 19, 553–558. https://doi.org/10.1016/S1001-0742(07)60092-8

40. Yeoh, B.G., 1997. Two-phase anaerobic treatment of cane-molasses alcohol stillage. Water Science and Technology 36, 441–448. https://doi.org/10.1016/S0273-1223(97)00553-2

41. Yoda, M., Nishimura, S., 1997. Controlling granular sludge floatation in UASB reactors. Water Science and Technology 36, 165–173. https://doi.org/10.1016/S0273-1223(97)00520-9

4.0 Two-phase anaerobic digestion for enhanced valorisation of whiskey distillery by-products

Anga Hackula[a, b], Rajas Shinde[a,b,c], Daniel Hickey[a,b], Richard O'Shea[a,b], Jerry D Murphy[a,b], David M. Wall[a,b]

[a] SFI MaREI Centre for Energy, Climate and Marine, Environmental Research Institute, University College Cork, Cork, Ireland

[b] Civil, Structural and Environmental Engineering, School of Engineering and Architecture, University College Cork, Cork, Ireland

[c] Crops, Environment and Land Use Program, Crop Science Department, Teagasc, Oak
Park, Carlow, R93XE12 Co. Carlow, Ireland

Abstract

The valorisation of whiskey by-products was assessed and compared in three anaerobic digestion systems. The systems produced similar methane yields, which could satisfy up to 44 % of the thermal energy demand at a distillery. Using methane generated from by-products would displace natural gas and reduce the distillery's carbon footprint. Two-phase systems had higher methane content (±75 $\%_{vol}$) than the traditional system (54 $\%_{vol}$) and unlocked opportunities for volatile fatty acid production. The potential value that could be generated from the extraction of butyric acid and caproic acid was approximately €6.76 million for a 50 million litre alcohol facility (0.14 € per original litre of alcohol). All three anaerobic digestion systems showed the potential to valorise whiskey by-products and convert current linear distillery production processes into circular repurpose and reuse production processes.

4.1 Introduction

The food and beverage sector incorporates several energy-intensive processes such as fermentation, evaporation, distillation, and heating in the production of their goods. By-products generated from these processes are often amenable to anaerobic digestion (AD). The AD technology offers a plausible pathway to the valorisation of organic residues through the production of biogas, volatile fatty acids (VFAs) and digestate (Atasoy et al., 2018). For example, distilleries produce by-products such as draff, thin stillage and thick stillage in the production of whiskey (O'Shea et al., 2020). AD can convert such organic feedstocks into biogas which can ultimately be used to replace onsite fossil fuel demand.

VFAs are an intermediate product of the AD process, produced from the feedstock after hydrolysis and acidogenesis. The primary VFAs produced in AD are acetic acid, propionic acid, and butyric acid. Low concentrations of caproic acid are typically generated from AD (Chen et al., 2017). If isolated, such platform chemicals can be used to produce high-value products such as bioplastics and bio-preservatives (Jiang et al., 2018). VFAs have a considerable global market value: ± $1.7 billion worldwide in 2021, projected to grow to ±$2.5 billion by 2029 (Fernández, 2022). Overall, AD systems could convert a distiller's linear processes into a circular repurpose and reuse model, as per Figure 4.1.

Numerous studies have investigated whiskey by-products for anaerobic digestion, but few have evaluated both liquid and solid whiskey by-products (Jackson et al., 2020; Kang et al., 2021). Traditional single-phase AD systems are unsuitable for both VFA and biogas production since all the microbial processes co-occur (Szaja et al., 2020).

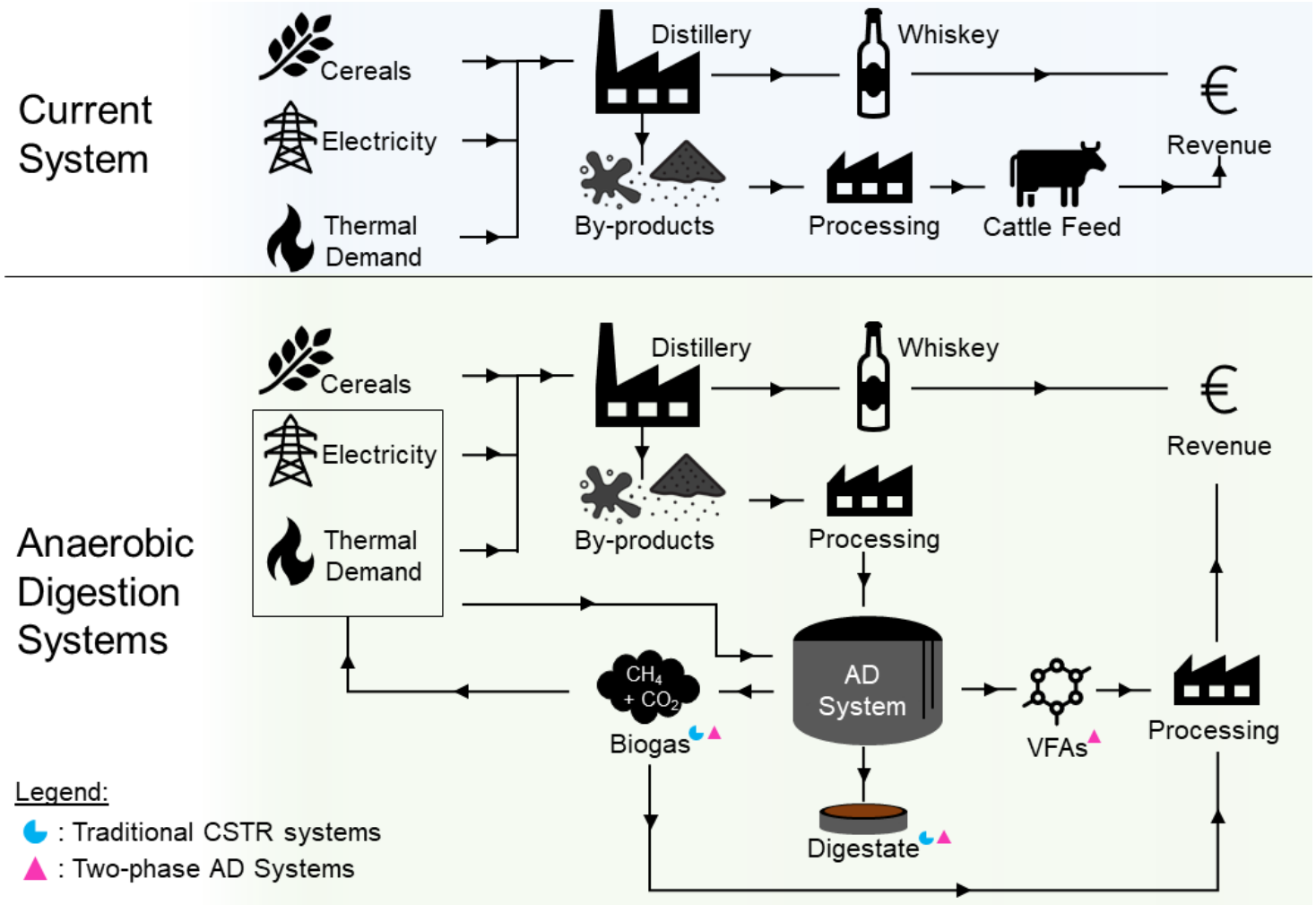


Figure 4.1: The current linear system and proposed circular reuse through anaerobic digestion systems at the distillery

Two-phase reactor configurations have the potential to split the AD process, whereby hydrolysis and acidogenesis occur in the first phase reactor (acidogenic reactor), and acetogenesis and methanogenesis occur in the second phase reactor (methanogenic reactor). Regardless of configuration, the bioavailability of essential nutrients and the microbial anaerobic consortia greatly influence the AD system's performance (Maroušek, J et al., 2020). Alternative two-phase AD systems, such as the leach bed reactor (LBR) coupled with a downstream expanded granular sludge blanket (EGSB), referred to as the LBR-EGSB, may provide further opportunities for valorising whiskey by-products. Previous studies have operated similar systems with grass, food waste, and brewer's spent grains (BSG) as feedstocks (Wall et al., 2016, Browne & Murphy, 2014, Panjičko et al., 2017). The brewery liquid by-products were not considered in the study by Panjičko et al. (2017).

There is a gap in the literature whereby both liquid and solid whiskey by-products are accounted for and assessed in different AD system configurations. This work will specifically look at three types of AD reactors: a traditional single-phase continuously stirred tank reactor (CSTR) referred to as C1, a two-phase CSTR (C2) and a more novel two-phase LBR-EGSB system. The innovation in this paper is that it is the first study, to the best of the authors' knowledge, to use and compare two-phase anaerobic digesters, LBR-EGSB and two-phase CSTR, as a means of valorising whiskey by-products to produce VFAs and biogas. The specific objectives of the paper are as follows: (1) to quantify the available by-products at a distillery site that can be used for anaerobic digestion; (2) to assess and compare the biogas production between three different AD systems; (3) to assess and compare the VFA production between the two-phase reactors; and (4)

to evaluate the potential application of AD systems at a distillery in terms of offsetting onsite fossil fuel use and the potential value of the VFAs produced.

4.2 Material and methods

4.2.1 Inocula

Cattle slurry was sourced as inoculum from a local farm for the biochemical methane potential (BMP) assays and the CSTR experimental trials. The inoculum was sieved with a 5mm mesh sieve to remove excess solid particles and immediately stored in a CSTR for one month to de-gas prior to both experimental trials. The inoculum for the acidogenic CSTR reactor (the first reactor of the two-phase CSTR) was preheated to 100 ^{o}C for 45 minutes to inhibit any methanogenic activity (Hussain et al., 2017). The total solids (TS) and volatile solids (VS) content of the slurry after sieving were 2 % on a wet weight basis (ww) and 73 %TS, respectively.

For the LBR-EGSB reactor, there was no inoculation of the LBRs. For the EGSB, 50 L of granular sludge inoculum was sourced from an operational mesophilic EGSB digesting cheese whey processing wastewater in Ireland. The granular sludge inoculum was submerged in distilled water for one month to de-gas at mesophilic conditions (37 ^{o}C). Subsequently, half of the EGSB (3 L) was seeded with the separated granular sludge, whilst distilled water was used for the remaining reactor volume. The granular sludge TS and VS content were 11 %ww and 89 %TS, respectively.

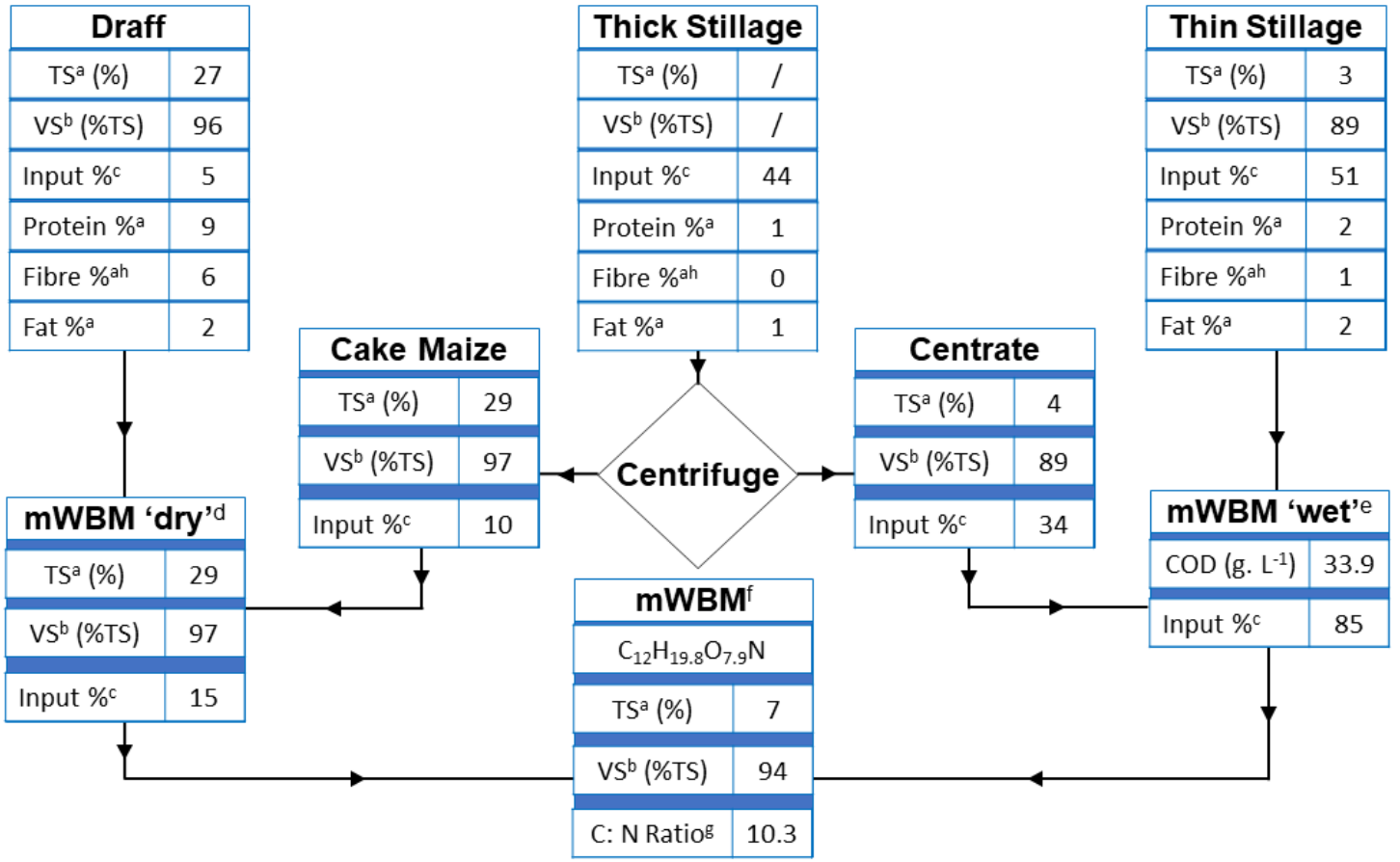
4.2.2 Characteristics of the modified whiskey by-products

The raw whiskey by-products generated from whiskey production are initially processed onsite. This culminates in the production of a mixed whiskey by-

product mixture (mWBM), which constitutes four substrates: draff, thin stillage, cake maize, and centrate. This mWBM can be further disaggregated into 'wet' and 'dry' fractions: mWBM 'wet' consists of the liquid fraction (thin stillage and centrate); mWBM 'dry' consists of the solid fraction (draff and cake maize). Figure 4.2 shows the material process flows to generate mWBM, along with the characteristics of mWBM and the individual substrates. mWBM 'wet' was sieved with a 0.76 mm sieve to remove any solid particles.

4.2.3 Biochemical methane potential assays

The BMP assay is a simple anaerobic batch process used to evaluate the maximum methane production of a particular substrate. BMP assays of mWBM were conducted in triplicate using the Bioprocess Control ^{TM} AMPTS II. The inoculum activity was assessed using cellulose powder (Sigma Aldrich) as a positive control (Kang et al., 2021). An inoculum control (without any addition of whiskey by-product substrate) was also assessed in triplicate to calculate the gas production from the inoculum. The BMP assays were conducted under mesophilic temperature (37±1 ^{o}C) conditions in a thermostatic water bath. A 2:1 inoculum-to-substrate ratio on a VS basis was used (Kang et al., 2021). The cumulative biomethane production was monitored on a gas volumetric unit part of the Bioprocess Control ^{TM} AMPTS II and converted to dry gas volumes at standard temperature and pressure (STP) of 0 ^{o}C and 101.325 kPa. The BMP assays were halted once the gas production ceased after 25 days.



[a] value on a wet weight basis; [b] VS= volatile solids on a total solids basis; [c] Input % = percentage contribution to distillery by-products on a wet weight basis; [d] mWBM 'dry' = solid fraction of the modified whiskey by-product mixture; [e] mWBM 'dry' = liquid fraction of the modified whiskey by-product mixture; [f] mWBM = modified whiskey by-product mixture ; [g] C:N Ratio= Carbon: Nitrogen ratio
[h] Fibre = Crude fibre

Figure 4.2: Whiskey by-products characteristics and material process flow

4.2.4 Continuously stirred tank reactor trials

Two laboratory-scale CSTR systems were operated with mWBM as feedstock. The first system consisted of a single reactor and thus was a single-phase mesophilic CSTR (C1) fed directly with mWBM. The second system consisted of two reactors in series (C2 a and b) and thus represented a two-phase mesophilic CSTR process. The first reactor (C2a) served as the acidogenic reactor and was fed with mWBM. The second reactor (C2b) was fed with the effluent generated from C2a and served as the methanogenesis reactor. All three reactors were manually pulse-fed five times per week. Initially, all CSTR reactors were fed at an organic loading rate (OLR) of 0.5 gVS. L^{-1}. d^{-1} for 15 days to allow the microbial community to adapt to the operating conditions as per previous literature (Jackson et al., 2020). The OLR was subsequently increased to 2.5 gVS. L^{-1}. d^{-1}. As VFA production was the objective for C2a, longer HRTs are recommended for the more valuable, longer-chain VFAs such as butyric acid and caproic acid (Ribau Teixeira et al., 2020). The hydraulic retention time (HRT) for C1, C2a and C2b was 25 days for each reactor. Only data from the second HRT is reported for both C1 and C2, as the first HRT was considered a means of reaching a steady state. Schematics of the process flow accounting for all distillery by-products used in a CSTR (C1) and a two-phase CSTR (C2) are illustrated in Figure 4.3.

The Bioprocess Control ^{TM} BioReactor Simulator was used for all three CSTR reactors. The operating volume of each reactor was 1.6 L with 0.5 L headspace. All reactors had vertically mounted stirrers that operated every five minutes to provide adequate mixing. The reactors were partially submerged in a thermostatic water bath, which kept the temperature constant (37±0.5 ^{o}C). The gas sampling port was subsequently connected to a Bioprocess Control ^{TM} BRS-B unit, which

continuously measured the biomethane production at STP of 0 °C and 101.325 kPa.

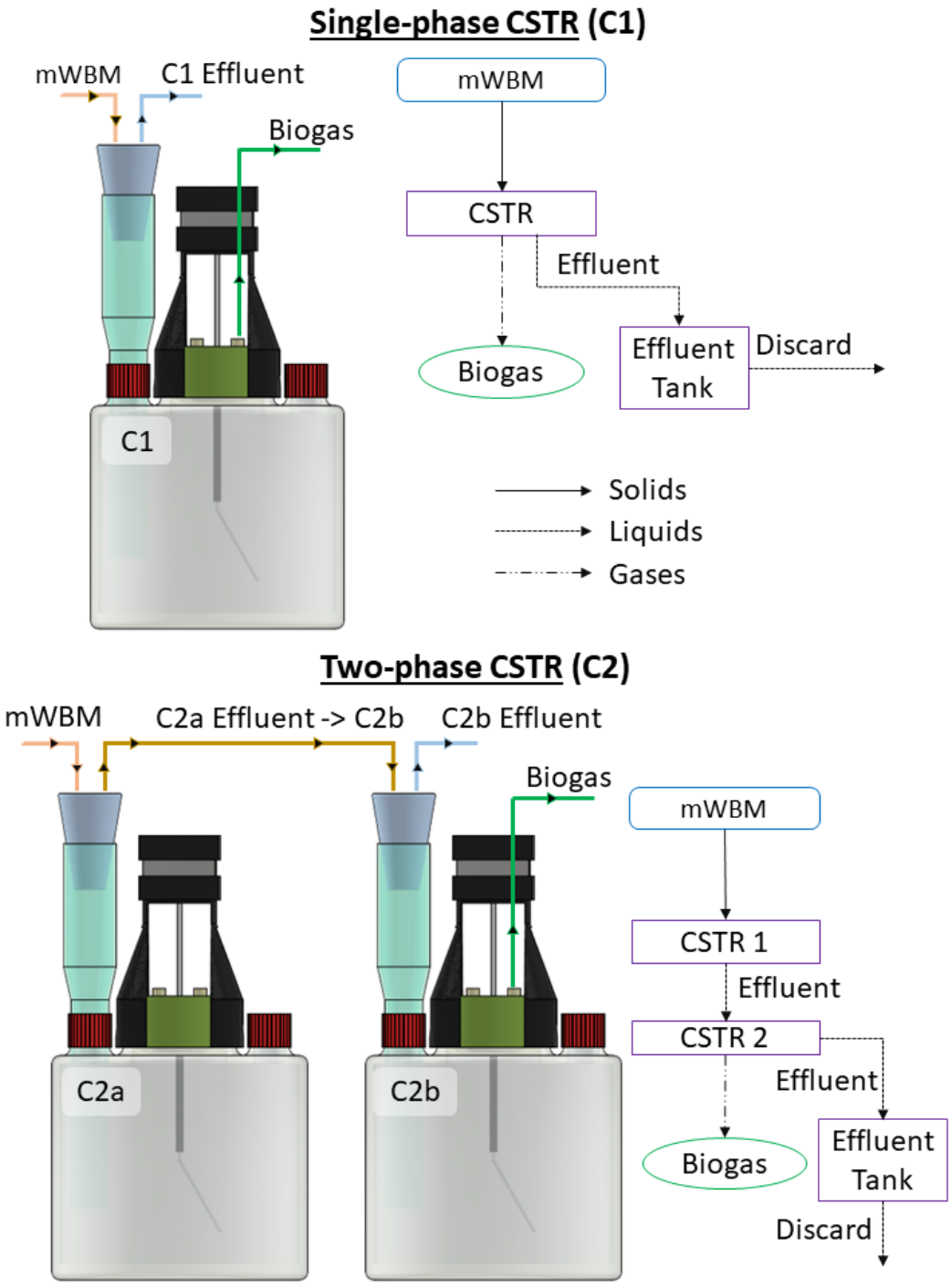


Figure 4.3: Materials process flow for mWBM for a single-phase and two-phase CSTR.

4.2.5 Leach bed reactor with expanded granular sludge bed experimental trials

The LBR-EGSB system (see Figure 4.4B) consisted of three LBRs (each of 5 L operating volume) and one EGSB (6 L operating volume). Hydrolysis occurs through enzymatic degradation of the solids into soluble chemical oxygen demand (which will be referred to as COD) by percolating the liquids over the solids in the LBRs. Further degradation results in acidification of the leachate, resulting in a VFA-rich leachate. The VFA-rich leachate is then converted to biogas in the EGSB. In essence, hydrolysis and acidogenesis (VFA production) occur in the LBRs, and acetogenesis and methanogenesis (biogas production) occur in the EGSB. The solids, referred to as mWBM 'dry', are suitable for digestion in the LBRs. The liquids, referred to as mWBM 'wet', are suitable to be used as liquid for the leaching process.

Each LBR was fed sequentially with 0.98 kg mWBM 'dry' every 7 days, resulting in a solid retention time of 21 days per LBR (7 days x 3 LBRs). The feeding regime was conducted as follows: LBR 1 was fed on day 0, LBR 2 was fed on day 7, LBR 3 was fed on day 14, and subsequently, LBR 1 was emptied and re-loaded on day 21. LBR 2 was emptied and re-loaded on day 28, and so on. Initially, 6.9 L of fresh mWBM 'wet' and 13.7 L of distilled water (20.6 L in total) was added to the leachate tank (25L capacity), which served as the initial leachate for the LBR-EGSB system. This was done to adjust the COD of the liquid from 33.9 g. L^{-1} to ~11.4 g. L^{-1}, which may stifle the hydrolysis process (Dogan et al., 2009). The leachate was pumped (Pump 1, Figure 4.4B) into siphon-actuated leachate holding cups situated above each LBR. The LBRs were operated in a 'flooded' manner over mWBM 'dry', whereby the liquid percolated through and exited the bottom

of the LBRs into the leachate tank. A high recirculation rate (±140 L. d^{-1}) established experimentally maintained the' flooded' operation.

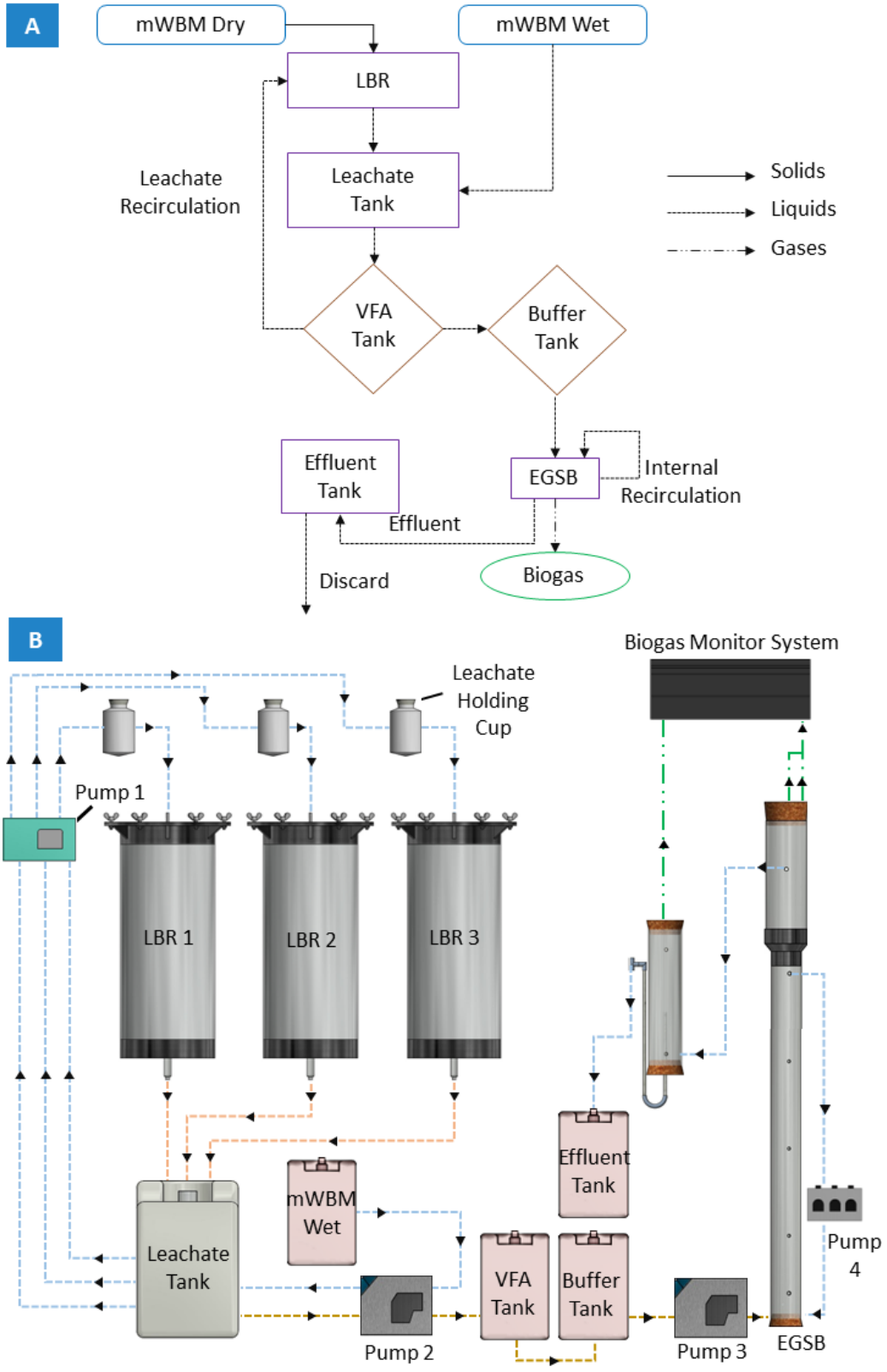


Figure 4.4: (A) Process flow of materials and (B) schematic of the LBR-EGSB for the use of whiskey by-products

Fresh mWBM ‘wet’ was continuously pumped (Pump 2, Figure 4.4B) into the leachate tank, providing 5.88 L of fresh mWBM ‘wet’ per week. Simultaneously, the same volume of leachate was continuously pumped (Pump 2, Figure 4.4B) into a VFA tank. In effect, the leachate remained in the leachate tank for 25 days. In total, 6.86 kg of mWBM (wet and dry) was introduced into the LBR and leachate tank every 7 days. The effective loading rate of the entire system was 5.3 gVS. $L^{-1}_{\text{working volume}}$. d^{-1} or 2.1 gVS. L^{-1}_{reactor}. d^{-1}.

The leachate in the VFA tank was manually transferred once a week to a buffer tank and would serve as the influent for the EGSB the following week (see Figure 4.4B). That is, the LBRs and leachate system were operated in an isolated manner, as opposed to being directly connected to the EGSB. This approach was used to reduce the impact of the anticipated dynamic nature of the leachate in terms of pH, VFA, and COD levels. VFA-rich leachate would be converted to biogas in the EGSB. The maximum OLR for the EGSB was 3.3 g COD. L^{-1}_{reactor}. d^{-1} (6.7 g COD. L^{-1}_{inoculum}. d^{-1}), and the HRT of the EGSB was 5 days. The EGSB was operated for 5 days and paused for 2 days, similar to the CSTRs. The maximum upflow velocity of the EGSB was 0.4 m. hr^{-1}, which was established experimentally. The upflow velocity was maintained through recirculation (Pump 4, Figure 4.4B).

Each LBR and the EGSB were fitted with heating mats to maintain mesophilic temperature conditions (37±0.5 ^{o}C). The EGSB biogas production was monitored by a Bioprocess Control ^{TM} BRS-B unit at STP (0 ^{o}C and 101.325 kPa).

A schematic of the material process flow accounting for all distillery by-products used in the LBR-EGSB is detailed in Figure 4.4A. This can be considered the

characterisation of the flow of materials at the distillery site if an LBR-EGSB system was implemented.

4.2.6 Analytical methods

Standard Methods 2540 G were used to determine the TS and VS content for the experimental trials (3). The elemental composition of the substrates was established by an elemental analyser equipped with a thermal conductivity detector (CE 440, Exeter Analytical). The COD concentrations were evaluated by Reagecon COD Vials (420721) and a Hach Spectrophotometer (DR 3900). As per Figure 4.2, the carbon: nitrogen (C: N) ratio of mWBM was 10.3, which is considered low and sub-optimal for AD (ideal C: N ratio is 20-30:1), which could result in ammonia inhibition and poor biomethane production performance (Li et al., 2011). Thus, ammonia levels were monitored for the experimental trials. Ammoniacal nitrogen (TAN) concentrations were measured using the Hach Lange AmVer™ Salicylate Test 'N Tube ™ Method (Hach Lange 10031). Free ammonia (FAN) was estimated according to the following formula (Hansen et al., 1998):

$$FAN = (TAN \times 1.2)/\left(1 + 10^{-\mathrm{pH}}/10^{-\left(0.09018+(2729.92/T)\right)}\right)$$

Where: FAN = free ammonia concentration (mg. L^{-1}); TAN = ammoniacal nitrogen (mg. L^{-1}); pH = pH Value; T= temperature (Kelvin)

The pH was measured using a Mettler Toledo™ F20 pH meter. Samples for VFA analysis were initially collected and then stored at -20 ^{o}C prior to analysis. The samples were subsequently thawed and centrifuged at 12,000 rpm for 10 minutes before testing. COD and TAN samples were similarly centrifuged prior to analysis. An Agilent GC (Agilent Technologies 7890B) with the DB-FFAP

column (Ø 0.32 mm x 50 m) and the flame ionization detector were used to evaluate the VFA composition and quantity.

The VS removal efficiency (VS_{eff}) and COD removal efficiency (COD_{eff}) were calculated as follows:

$$X_{eff} = \frac{(X_{in} - X_{out})}{X_{in}} \times 100$$

Where: X_{eff} is the relevant removal efficiency; X_{in} is either the mass of the COD in or the mass of VS introduced in the system, and X_{out} is either the mass of COD out or the mass of VS removed from the system.

The acidogenic reactors were evaluated based on acidification and COD-to-VFA efficiency. Acidification was measured by converting the individual VFAs to COD equivalents (COD_{VFA}) and dividing it by the COD within the reactor (Khatami et al., 2021). COD-to-VFA efficiency was calculated by dividing COD_{VFA} by the COD of mWBM (33.9 g COD. L^{-1}).

The alkalinity ratio (FOS/TAC) is an indicator of reactor stability (Drosg, 2013). The FOS/TAC was evaluated using a dual-point titration method that established the ratio between intermediate alkalinity and partial alkalinity. The Nordmann method established the FOS/TAC (Drosg, 2013).

The theoretical methane yield was estimated using the Buswell equation (Buswell & Hatfield, 1936):

$$C_n H_a O_b + \left(n - \frac{a}{4} - \frac{b}{2}\right) H_2O \rightarrow \left(\frac{n}{2} + \frac{a}{8} - \frac{b}{4}\right) CH_4 + \left(\frac{n}{2} - \frac{a}{8} + \frac{b}{4}\right) CO_2$$

The biodegradability index (BI) was calculated as the specific methane yield obtained from the respective experiment divided by the Buswell theoretical

methane yield. The biogas composition of the methanogenic reactors was analysed with an MRU Optima 7 BioGas Analyser (ca. 3 % error). The biogas of the acidogenic reactors was not measured as primarily carbon dioxide (CO_2), and trace amounts of hydrogen were expected.

An online statistical calculator called DataTAB.net was used to analyse the data for statistical difference (DATAtab Team, 2023). A two-sample, single-factor ANOVA parametric test was used with the significance level set to 0.05 for all tests.

The euro (€) to US dollar (US$) exchange rate was taken to be 1.10 € / US$ (Central Bank of Ireland, 2023).

4.3 Results and discussion

4.3.1 Theoretical and batch biochemical methane potential

A well-operating digester has a minimum of 70 % VS removal (Murphy & Thamsiriroj, 2013). Based on the known atomic weights of the elements, the following stoichiometric equation can be formulated for mWBM ($C_{12}H_{19.8}O_{7.9}N$) (see Figure 4.2). Using the Buswell Equation, the theoretical methane yield was projected to be 501 L. kg^{-1} VS_{added} mWBM, correlating to an energy content of 19.3 MJ. m^{-3} of biogas and a theoretical methane content in the biogas of 54 % (CH_4). The relationship between COD and VS for mWBM can be shown to be 1.5 kg COD. kg^{-1} VS.

Assessing the microbial consortium of the cattle slurry, the labile organic matter and the biodegradability of the whiskey by-products was undertaken through

BMP assays (Maroušek, 2014). The BMP assay ran for 25 days (see Appendix B.1). The specific methane yield from the BMP assays was 383.7±11.9 L. kg^{-1} $VS_{added,}$ equating to a biodegradability index (BI) of 77 %. These results are illustrated in Table 4.1 and are similar to previous batch experiments undertaken by Kang et al. (2021), which co-digested draff, thin stillage and thick stillage (389.1 L. kg^{-1}VS).

This suggests the centrifugation of thick stillage to centrate (the liquid fraction) and cake maize (the solid fraction) has negligible impact on the biodegradability of the whiskey by-products. The BI also suggests that mWBM is amenable to anaerobic digestion.

The BMP results can be considered representative of the maximum possible yield attainable from the mesophilic CSTRs. As the LBR-EGSB is operated under different conditions, the theoretical maximum can be estimated based on the VS removal and COD removal efficiencies in the literature. Assuming a VS removal efficiency of 70 % within the LBRs, 90 % COD removal efficiency in the EGSB, and 350 L CH_4. kg^{-1}COD, the theoretical methane yield for the LBR-EGSB can be calculated as 349.1 L CH_4. kg^{-1} VS. This equates to a BI of 70 %.

Table 4.1: Experimental results and comparison of the anaerobic digestion of whiskey by-products

		Single-phase CSTR	Two-phase CSTR		LBR-EGSB	
Parameter	**Unit**	**C1**	**C2a**	**C2b**	**LBRs**	**EGSB**
pH		7.3 ± 0.0	4.8 ± 0.0	7.5 ± 0.1	4.4 ± 0	7 ± 0.0
FOS/TAC[a]		0.3 ± 0.0		0.3 ± 0.2		0.4 ± 0.0
Effluent COD	g. L^{-1}	3.5 ± 0.1	31.3 ± 1.2	3.5 ± 1.6	26.3 ± 0.8	1.3 ± 0.0
% COD Rem[b]	%	90 ± 0	8 ± 0	89 ± 2	22 ± 3	94 ± 0
% VS Rem[c]	%	71 ± 0		79 ± 2	42 ± 4	-
TAN[d]	mg. L^{-1}	1,287 ± 20.5	639 ± 195	1,239 ± 312.4	161 ± 3.0	341 ± 40.7
VFAs[e]	mg. L^{-1}	210 ± 91.3	11,193 ± 669	338 ± 129.6	10,164 ± 33.9	378 ± 61.3
Acetic Acid	%	71 ± 0	25 ± 8	95.5 ± 0	20 ± 1	53 ± 0
Propionic Acid	%	13 ± 0	11 ± 1	0.6 ± 0	17 ± 0	37 ± 0
Butyric Acid	%	3 ± 0	35 ± 3	0.9 ± 0	45 ± 1	3 ± 1
Valeric Acid	%	-	12 ± 3	0.2 ± 0	7 ± 1	-
Caproic Acid	%	-	14 ± 3	0.3 ± 0	7 ± 0	-
VFA Production	**mg VFA. $g^{-1}VS_{added}$**	-	**176.3 ± 10.5**	-	**137.2 ± 8.0**	-
	mg VFA. $g^{-1}ww_{added}$	-	**11.2 ± 0.7**	-	**8.7 ± 0.5**	-
	g VFAs. L^{-1} OLA	-	**110**	-	**85.8**	-
$CH_4\%_{vol}$[f]	%	54 ± 1	76 ± 3		76 ± 2	
SMY[g]	**L CH_4. $kg^{-1}VS_{added}$**	**272.3 ± 4.4**	**268.9 ± 3.3**		**283.0 ± 2.1**	
	L CH_4. kg^{-1} ww_{added}	17.3 ± 0.3	17.1 ± 0.2		18.0 ± 0.1	
Theoretical Yield[h]	L CH_4. $kg^{-1}VS_{added}$		503			
BMP Maximum Yield[i]	L CH_4. $kg^{-1}VS_{added}$	383.7 ± 11.9	383.7 ±11.9		335.2	
BI%[j]	%	54	53		55	

[a] FOS/TAC = alkalinity ratio; [b] % COD Rem = COD removal efficiency; [c] % VS Rem = VS removal efficiency; [d] TAN = ammoniacal nitrogen; [e] VFAs = volatile fatty acids; [f] $CH_4\%_{vol}$ = methane content in biogas on a volume basis; [g] SMY = specific methane yield; [h] Theoretical yield = Buswell theoretical maximum yield; [i] BMP Maximum Yield = yield based on BMP assessment for methanogenic CSTRs and theoretical removal efficiencies for the LBR-EGSB; [j] BI% = biodegradability index based on the Buswell theoretical yield. (see Appendix B.2)

4.3.2 Continuous trial results

4.3.2.1 Trends in reactor stability

There was a significant difference ($p<0.05$) between the pH of the three methanogenic reactors (C1, C2b and the EGSB). However, it remained within recommended levels of 7.0-7.5 for biogas production (Gerardi, 2003). This could be due to the higher organic loading rate (6.7 g COD. $L^{-1}{}_{inoculum}$. d^{-1}) achieved in the EGSB as compared to C1 and C2b (±1.7 g COD. $L^{-1}{}_{inoculum}$. d^{-1}). C1 and C2b had a similar FOS/TAC ratio (~0.3), which was slightly lower than that of the EGSB (0.4) ($p<0.05$) (see Table 4.1). FOS/TAC values less than 0.3 are considered stable for methanogenesis. However, systems can be relatively stable at FOS/TAC values of up to 0.8 (Drosg, 2013). C1 and C2b exhibited dissimilar FOS/TAC and pH trends compared to a study evaluating whiskey by-products in a single-phase CSTR, which reported increasing FOS/TAC and declining pH throughout digestion (Jackson et al., 2020).

TAN concentrations were significantly higher in C1 and C2b (~1.2 g. L^{-1}) than in the EGSB (0.3 g. L^{-1}) ($p<0.05$). The observed difference in TAN concentrations could be due to less degradation of draff and cake maize in the LBR-EGSB as compared to C1 and C2b. A study evaluating thin stillage reported that TAN levels >1 g. L^{-1} reduced the reactor's biogas yield (Moestedt et al., 2016). However, TAN concentrations of less than 5 g. L^{-1} are still considered stable for AD (Drosg, 2013). The estimated FAN concentrations for the CSTRs remained below 70 mg. L^{-1}, but significantly higher than levels within the EGSB (<6 mg. L^{-1}). A broad range of FAN inhibition limits is reported in the literature, between 1.5-150 mg. L^{-1} (Angelidaki et al., 2004; Hansen et al., 1998). The VFA

concentrations remained within the recommended stability levels for methanogenesis at less than 0.4 g. L^{-1} with no statistical significance between the three methanogenic reactors ($p>0.05$) (Drosg, 2013).

Both acidogenic reactors (C2a and LBRs) exhibited pH stability: C2a at pH 4.8 and the LBR at pH 4.4 ($p<0.05$). The slightly higher pH within C2a would suggest higher concentrations of less acidic or mildly acidic VFAs, such as caproic acid, as compared to the LBRs. The COD range for C2a was 29.2-32.2 g. L^{-1} and for the LBR was 25.6-27.0 g. L^{-1} ($p<0.05$). Higher COD losses in the LBRs were expected as these reactors are often considered partially aerobic, resulting in aerobic respiration and the production of CO_2 (which was not measured) (Wall et al., 2016). As FAN levels depend on pH, temperature and TAN concentrations, the FAN concentrations in both acidogenic reactors were estimated to be negligible (<1 mg. L^{-1}). This can be attributed to the low pH in both acidogenic reactors.

4.3.2.2 Anaerobic digestion efficiency

All methanogenic reactors had high COD removal. The EGSB exhibited slightly higher COD removal efficiency (94 %), followed by C1 (90 %) and then C2b (89 %) (see Table 4.1). There was no statistical significance between C1 and C2b ($p>0.05$), however, there was between C1, C2b and the EGSB ($p<0.05$). This was expected as recirculation rates within the EGSB increased contact between the granular sludge inoculum and the substrate (Jiraprasertwong et al., 2019). The COD removal efficiency from all three AD systems was on the higher end of that observed in the literature (Jackson et al., 2020; Jiraprasertwong et al., 2019). There was evident COD loss in both acidogenic reactors, more so in the LBRs (22 %) than in C2a (8 %) ($p>0.05$). This loss could be due to the degradation of the

feedstock in cellular nourishment for growth and reproduction (Gerardi, 2003). The VS removal efficiency was significantly higher (±30 % more) in the two CSTR systems than in the LBR-EGSB system (42 %). As the LBR-EGSB was slightly more acidic, this may have partially stifled the hydrolysis process (Dogan et al., 2009). A range of VS removal efficiencies on similar LBR-EGSB systems are reported in the literature (27-90 %) (Browne & Murphy, 2014; Jagadabhi et al., 2011). A possible cause of the differences in VS removal efficiencies could be the composition of the different feedstocks and the different operational conditions of the LBR. The overall VS and COD removal efficiencies for each system were C1 (78 %), C2 (82 %) and the LBR-EGSB (67 %).

4.3.2.3 Trends in biogas and volatile fatty acid production

Similar specific methane yields were observed for the mesophilic reactors: C1 at 272.3 L CH_4. kg^{-1}VS, C2b at 268.9 L CH_4. kg^{-1}VS, and the LBR-EGSB at 283 L CH_4. kg^{-1}VS ($p>0.05$) (see Appendix B2). These values are within the range reported for various studies digesting by-products from breweries or distilleries (82-423 L CH_4. kg^{-1}VS) (Yeoh, 1997; Jiraprasertwong et al., 2019). The TAN concentrations may have resulted in lower methane yields for C1 and C2, as suggested in the literature (Moestedt et al., 2016). Improving the VS destruction of the LBR-EGSB would improve the realised specific methane yield. The biogas from both two-phase systems was rich in methane (±75 $\%_{vol}$) with no significant difference observed ($p>0.05$). In contrast, the average methane content in the biogas from C1 was similar to the theoretical methane content (54 $\%_{vol}$) (see Section 4.3.1). Several studies reported similar methane content from single-phase and two-phase systems processing similar feedstocks (Yeoh, 1997; Jiraprasertwong et al., 2019).

The VFA concentrations for C2a and the LBR were 11.2 g. L^{-1} and 10.2 g. L^{-1}, respectively. Previous studies processing similar feedstocks reported VFA concentrations of up to 10.5 g. L^{-1} (Jiraprasertwong et al., 2019). The average specific VFA yield of C2a was 176.3 mg VFA. g^{-1}VS, while for the LBRs, the value was 137.2 mg VFA. g^{-1} VS ($p<0.05$). It was hypothesized that this difference is due to lower VS destruction and COD loss within the LBRs. Previous studies digesting similar feedstocks reported VFA yields between 104 and 234 mg VFA. g^{-1}VS (Ribau Teixeira et al., 2020; 6). The COD-to-VFA efficiency (based on the COD of mWBM wet) for C2a (56 %) was higher than that of the LBRs (50 %). A possible reason for lower COD-to-VFA efficiency in the LBRs could be due to aerobic respiration within the LBRs due to their partially aerobic nature. The COD-to-VFA efficiency was higher than several works digesting similar feedstocks, which reported ranges of 16-43 % (Yeoh, 1997). A single study reported higher COD-to-VFA efficiency when treating thermally pretreated brewer's spent grains (68 %) (Ribau Teixeira et al., 2020). This study may have realised higher COD-to-VFA efficiency due to the thermal pretreatment, which broke down the rigid lignin structure of brewer's spent grains (Kang et al., 2021).

High acidification (a metric based on reactor COD) was evident in both reactors. The acidification in the LBRs (65 %) was slightly higher than C2a (61 %). This level of acidification is much higher than the rates reported from winery wastewater (up to 14 %), cheese whey (up to 40 %), and brewer's spent grain hydrolysate (up to 41 %) (Atasoy et al., 2018; Buitrón et al., 2019; Guarda et al., 2021). However, acidification of up to 81 % has been reported from raw brewer's spent grains (Ribau Teixeira et al., 2020). The higher acidification in the study by

Ribau Teixeira et al. (2020) could potentially be due to the thermal pretreatment applied in the study. The main VFAs for both acidogenic reactors were butyric acid and acetic acid (see Table 4.1). Interestingly, caproic acid (1.5 g VFA. L^{-1}) was the next most prominent VFA in C2a, which was almost double the caproic acid concentration (0.8 g VFA. L^{-1}) found in the LBRs. This could be due to differences in the microbial community of the reactors. Caproic acid and butyric acid are of interest due to their commercial value, estimated at €2,500 per tonne for both VFAs (5).

4.3.3 Potential to offset natural gas consumption at the distillery

The following assumptions were made for calculating the potential to offset natural gas consumption at the distillery via the aforementioned three AD systems in this analysis:

- A large distillery that produces 50 million L of original litres of alcohol (OLA) per annum.
- An original litre of alcohol produces 10.3 kg of mWBM (O'Shea et al., 2020).
- The natural gas required per litre of whiskey is 4.2 kWh. L^{-1}_{OLA} (O'Shea et al., 2020).
- The energy value of methane is 9.92 kWh. m^{-3} (35.7 MJ. m^{-3}).

The potential natural gas displacement at the distillery can be estimated for each AD system based on the data generated in Table 4.1. The second phase of the two-phase CSTR (C2b) will be used to illustrate this analysis:

If the specific methane yield of C2b is 17.1 L CH_4. kg^{-1} ww, the potential methane production from the whiskey by-products produced onsite (516.5 ww ktonnes)

from a two-phase CSTR is **8,832,150 m^3 CH_4. a^{-1}**. The thermal energy generated from the methane produced in C2b is **87.6 GWh. a^{-1}** (at 9.9 kWh. m^{-3} assuming 100 % efficiency in producing thermal energy from the biogas). The methane produced in C2b is enough to produce **21.1 million OLA**. The methane produced from C2b can meet **42 %** of the thermal demand of the distillery. A similar calculation was undertaken for the single-phase CSTR (C1) and the LBR-EGSB. Table 4.2 summarises the potential natural gas offset from all three AD systems.

The potential for natural gas offset through the implementation of the different systems would most likely reduce depending on the technology efficiency in utilising the biogas. As each distillery may have different requirements, further research is required to establish which biogas utilisation pathway best satisfies the distiller's demands.

4.3.4 Estimating the value of volatile fatty acids produced from whiskey by-products

A rudimentary estimation of the potential value of the VFAs produced from whiskey by-products was generated based on the following assumptions:

- A large distillery that produces 50 million L of original litres of alcohol (OLA) per annum.
- An original litre of alcohol produces 10.3 kg of mWBM (O'Shea et al., 2020).
- The VFA separation efficiency is 95 % (Aydin et al., 2018)

- Only the acidogenic reactors in the two-phase reactors would extract VFAs (C2a and the LBR). The methanogenic reactors are neglected for this analysis.

- Only butyric acid and caproic acid are extracted as they have the highest commercial value from the prominent VFAs found in the reactors mentioned above (€2,500 (US$ 2,750) per tonne for both VFAs) (Bastidas-Oytanedel et al., 2015).

The two-phase CSTR (C2a) acidogenic reactor is used to illustrate the analysis. The specific VFA production of C2a is 11.2 mg VFA. g^{-1}ww (see Table 4.1). Approximately 516.5 ww ktonnes of mWBM is produced per annum (see Section 3.2.4): with a VFA separation efficiency of 95 %, this would yield **5.5 ktonnes VFAs per annum (110 g VFAs. L^{-1}_{OLA}).** Using the average percentage composition of the effluent of C2a (see Table 4.1), the quantity of butyric acid is 35 % (1.9 ktonnes per annum), and caproic acid 14 % (770.0 tonnes per annum); 2.7 kt per annum of relevant VFAs can be produced in C2a. The combined potential value of VFAs production of butyric and caproic acid in C2a is **€ 6.76 million** (0.14 €. L^{-1}_{OLA}) or US$ 7.44 million (0.15 US$. L^{-1}_{OLA}). A similar calculation was made for the acidogenic reactor of the LBR-EGSB as per Table 4.2.

Extraction techniques of the VFAs may limit the realised revenue from the systems, which would require additional research. As VFAs have a broad

application, a thorough techno-economic analysis and VFA utilisation pathway would need to be undertaken to meet the distiller's objectives.

Table 4.2: Summary of the potential natural gas offset and VFAs production value for the distillery

		Units	C1[d]	C2[e]	LBR-EGSB[f]
Potential natural gas offset	Distillery Annual Production	million L_{OLA}		50	
	Annual Energy Requirement[a]	$GWh.a^{-1}$		208	
	Annual Whiskey By-Products[a]	kt mWBM. a^{-1}		516.5	
	Specific Methane Yield[b]	$m^3 CH_4$. t^{-1}mWBM	17.3 ± 0.3	17.1 ± 0.2	18.0 ± 0.1
	Energy Yield	GWh. a^{-1}	88.6 ± 1.4	87.6 ± 1.0	92.2 ± 0.6
	Whiskey Offset Potential	million L_{OLA}	21.3 ± 0.3	21.1 ± 0.2	22.2 ± 0.1
	Natural Gas Offset	**%**	**43 ± 1**	**42 ± 0**	**44 ± 0**
Potential value of VFAs	Specific VFA Yield[b]	kg VFAs. t^{-1}mWBM	-	11.2 ± 0.7	8.7 ± 0.5
	Potential VFA Yield[b]	kt VFAs. a^{-1}		5.50 ± 0.3	4.29 ± 0.0
	Butyric Acid Value[c]	million € (US$)[g]		4.8 ± 0.0 (5.3)	4.8 ± 0.0 (5.1)
	Caproic Acid Value[c]	million € (US$)[g]		1.9 ± 0.0 (2.1)	0.8 ± 0.0 (0.8)
	Total VFA Value	**million € (US$)[g]**		**6.8 ± 0.0 (7.4)**	**5.6 ± 0.0 (6.1)**
	Specific VFA Value	**€. L^{-1}_{OLA} (US$)[g]**		**0.14 ± 0.0 (0.15)**	**0.11 ± 0.0 (0.12)**

[a] Data taken from (O'Shea et al., 2020); [b] yield taken pro rata based on experimental trials; [c] Assuming €2,500 per tonne for both VFAs (5); [d] C1 = single-phase continuously stirred tank reactor; [e] C2 = two-phase continuously stirred tank reactor; [f] LBR-EGSB = two-phase leach bed reactor with expanded granular sludge bed [g] 1 EUR = 1.1 USD (Central Bank of Ireland, 2023)

4.3.5 Reactor selection considerations and future research

All three reactors have advantages and limitations that a distillery must consider before selecting the most suitable system. In terms of reactor stability, all methanogenic reactors were stable in terms of pH and FOS/TAC. Potential ammonia inhibition may be more of a concern for the CSTR systems than the LBR-EGSB. All three reactors could benefit from artificial intelligence to automate and take operational decisions (Zvarikova et al., 2020). For example, an automatic reduction or seize feeding order if the FOS/TAC, pH, and/or the biogas quality change significantly from the nominal conditions. These decisions should be based on data and provide developers with intelligent, dynamic and interactive operation systems which could reduce operational costs and reactor failures (Zvarikova et al., 2020). The two-phase CSTR had the highest overall removal efficiency (combined COD and VS removal), while the LBR-EGSB had the lowest. This means the two-phase CSTR system requires less digestate management post-treatment than the LBR-EGSB.

All three reactors produced similar methane yields (269-283 L CH_4. kg^{-1}VS). The methane content in both two-phase systems was much higher (>20 %) than the traditional CSTR. Thus, less energy would be required for CO_2 removal in the two-phase system biogas. The traditional CSTR system is a well-established technology and poses less of an investment “risk” as opposed to the two-phase LBR-EGSB system. As the traditional CSTR is a single reactor, the associated capital and operational costs would be significantly less than the two-phase systems. However, the traditional CSTR forgoes the potential revenue from VFA production. While the

two-phase CSTR system had a higher VFA yield than the LBR-EGSB, the simplicity of the LBR with no rotating components could result in less maintenance downtime.

Possible shortcomings of this study could include the pulse-feeding of both CSTR systems. These systems are typically continuously fed with effluent being continuously removed. The feeding regime in this study may have caused minor shock loading each time the reactors were fed. All three methanogenic reactors were fed 5 days and paused for two days. This operation may have benefitted the stability of the reactors. A commercial operator would operate continuously to increase the utility of the reactor. The operational difference may impact the stability of the reactors, which would affect the realised biogas. In the two-phase systems, the acidogenic reactor effluent volume was the same as the methanogenic reactor. To produce both VFAs and biogas, a larger acidogenic reactor than the methanogenic reactor would be required. Alternatively, operating the methanogenic reactor in a demand-driven manner, where biogas is only produced when required, would allow for the extraction of both VFAs and biogas. Currently, VFA production is predominantly from fossil fuels. The VFAs from the proposed systems would have to be competitively priced or supported through legislation for adoption by potential consumers.

All three systems could achieve higher biogas or VFA yields through further optimisation. Several techniques, such as feedstock pretreatments and additives, could be implemented to increase yields. Biogas produced from the acidogenic reactors was not monitored in this study. Biogenic CO_2 produced from these reactors

could be valuable, particularly in the food and beverage industry. Further research into the possible CO_2 and hydrogen yields achievable from the systems should be investigated. A techno-economic analysis of the systems is crucial to evaluate the financial feasibility of the different systems; however, this was considered out of scope for this study.

4.4 Conclusion

Three anaerobic digestion systems were evaluated and compared to valorise by-products generated at a whiskey distillery. From an energy perspective, a distillery seeking to reduce its natural gas consumption could use any of the proposed systems as similar specific methane yields were evident. However, two-phase systems could provide additional valorisation opportunities through volatile fatty acid production (worth up to 0.14 € per OLA). All three systems demonstrated benefits and limitations that may vary depending on a distillery's objectives. Ideally, a developer must align the distillery's objectives and the system's benefits.

References

1. Ahn, Y.-H., Min, K.-S., & Speece, R. E. (2001). Pre-acidification in anaerobic sludge bed process treating brewery wastewater. *Water Research*, *35*(18), 4267–4276. https://doi.org/10.1016/S0043-1354(01)00171-3
2. Angelidaki, I., & Sanders, W. (2004). Assessment of the anaerobic biodegradability of macropollutants. *Re/Views in Environmental Science & Bio/Technology 2004 3:2*, *3*(2), 117–129. https://doi.org/10.1007/S11157-004-2502-3
3. APHA, A. W. W. A. (1998). Standard methods for the examination of water and wastewater. In *American Public Health Association* (Vol. 20).
4. Aydin, S., Yesil, H., & Tugtas, A. E. (2018). Recovery of mixed volatile fatty acids from anaerobically fermented organic wastes by vapor permeation membrane contactors. *Bioresource Technology*, *250*, 548–555. https://doi.org/10.1016/J.BIORTECH.2017.11.061
5. Bastidas-Oyanedel, J. R., Bonk, F., Thomsen, M. H., & Schmidt, J. E. (2015). Dark fermentation biorefinery in the present and future (bio)chemical industry. *Reviews in Environmental Science and Biotechnology*, *14*(3), 473–498. https://doi.org/10.1007/S11157-015-9369-3/TABLES/3
6. Blonskaja, V., Menert, A., & Vilu, R. (2003). Use of two-stage anaerobic treatment for distillery waste. *Advances in Environmental Research*, *7*(3), 671–678. https://doi.org/10.1016/S1093-0191(02)00038-2
7. Browne, J. D., & Murphy, J. D. (2014). The impact of increasing organic loading in two phase digestion of food waste. *Renewable Energy*, *71*, 69–76. https://doi.org/10.1016/j.renene.2014.05.026

8. Buitrón, G., Martínez-Valdez, F. J., & Ojeda, F. (2019). Biogas Production from a Highly Organic Loaded Winery Effluent Through a Two-Stage Process. *BioEnergy Research*, *12*(3), 714–721. https://doi.org/10.1007/s12155-019-09984-7
9. Buswell, A. M., & Hatfield, W. D. (1936). *State of Illinois Department of Registration And Education Division of The State Water Survey Anaerobic Fermentations*. https://www.isws.illinois.edu/pubdoc/B/ISWSB-32.pdf
10. Chen, W. S., Strik, D. P. B. T. B., Buisman, C. J. N., & Kroeze, C. (2017). Production of Caproic Acid from Mixed Organic Waste: An Environmental Life Cycle Perspective. *Environmental Science and Technology*, *51*(12), 7159–7168. https://doi.org/10.1021/ACS.EST.6B06220/ASSET/IMAGES/LARGE/ES-2016-06220E_0003.JPEG
11. Central Bank of Ireland. (2023). *Euro Exchange Rate | Central Bank of Ireland*. Annual Averages / Meáin Bhliantúla 2001-Present | Xls 291 KB. https://www.centralbank.ie/statistics/interest-rates-exchange-rates/exchange-rates
12. DATAtab Team (2023). DATAtab: Online Statistics Calculator. DATAtab e.U. Graz, Austria. URL https://datatab.net
13. Dogan, E., Dunaev, T., Erguder, T. H., & Demirer, G. N. (2009). Performance of leaching bed reactor converting the organic fraction of municipal solid waste to organic acids and alcohols. *Chemosphere*, *74*(6), 797–803. https://doi.org/10.1016/j.chemosphere.2008.10.028
14. Drosg, B. (2013). *Process monitoring in biogas plants*. IEA Bioenergy.

15. Fernández, L. (2022). • *Propionic acid market value worldwide 2015-2029 | Statista*. https://www.statista.com/statistics/1244417/global-market-value-propionic-acid/
16. Gerardi, M. H. (2003). The Microbiology of Anaerobic Digesters. *The Microbiology of Anaerobic Digesters*. https://doi.org/10.1002/0471468967
17. Guarda, E. C., Oliveira, A. C., Antunes, S., Freitas, F., Castro, P. M. L., Duque, A. F., & Reis, M. A. M. (2021). A Two-Stage Process for Conversion of Brewer's Spent Grain into Volatile Fatty Acids through Acidogenic Fermentation. *Applied Sciences*, *11*(7), 3222. https://doi.org/10.3390/app11073222
18. Hansen, K. H., Anglelidaki, I., & Ahring, B. K. (1998). Anaerobic digestion of swine manure: inhibition by ammonia. *Water Research*, *32*(1), 5–12. https://doi.org/10.1016/S0043-1354(97)00201-7
19. Hussain, A., Filiatrault, M., & Guiot, S. R. (2017). Acidogenic digestion of food waste in a thermophilic leach bed reactor: Effect of pH and leachate recirculation rate on hydrolysis and volatile fatty acid production. *Bioresource Technology*, *245*, 1–9. https://doi.org/10.1016/j.biortech.2017.08.130
20. Jackson, S. A., Kang, X., O'Shea, R., O'Leary, N., Murphy, J. D., & Dobson, A. D. W. (2020). Anaerobic digestion performance and microbial community structures in biogas production from whiskey distillers organic by-products. *Bioresource Technology Reports*, *12*, 100565. https://doi.org/10.1016/j.biteb.2020.100565
21. Jagadabhi, P. S., Kaparaju, P., & Rintala, J. (2011). Two-stage anaerobic digestion of tomato, cucumber, common reed and grass silage in leach-bed

reactors and upflow anaerobic sludge blanket reactors. *Bioresource Technology*, *102*(7), 4726–4733. https://doi.org/10.1016/j.biortech.2011.01.052

22. Jiang, L., Fu, H., Yang, H. K., Xu, W., Wang, J., & Yang, S. T. (2018). Butyric acid: Applications and recent advances in its bioproduction. *Biotechnology Advances*, *36*(8), 2101–2117. https://doi.org/10.1016/J.BIOTECHADV.2018.09.005
23. Jiraprasertwong, A., Maitriwong, K., & Chavadej, S. (2019). Production of biogas from cassava wastewater using a three-stage upflow anaerobic sludge blanket (UASB) reactor. *Renewable Energy*, *130*, 191–205. https://doi.org/10.1016/J.RENENE.2018.06.034
24. Kang, X., Lin, R., Li, L., Wu, B., Deng, C., O'Shea, R., Sun, Y., & Murphy, J. D. (2021). Assessment of pretreatment and digestion temperature on anaerobic digestion of whiskey byproducts and microbial taxonomy. *Energy Conversion and Management*, *243*, 114331. https://doi.org/10.1016/j.enconman.2021.114331
25. Khatami, K., Atasoy, M., Ludtke, M., Baresel, C., Eyice, Ö., & Cetecioglu, Z. (2021). Bioconversion of food waste to volatile fatty acids: Impact of microbial community, pH and retention time. *Chemosphere*, *275*, 129981. https://doi.org/10.1016/j.chemosphere.2021.129981
26. Li, Y., Park, S. Y., & Zhu, J. (2011). Solid-state anaerobic digestion for methane production from organic waste. *Renewable and Sustainable Energy Reviews*, *15*(1), 821–826. https://doi.org/10.1016/j.rser.2010.07.042
27. Maroušek, J. (2014). Biotechnological Partition of the Grass Silage to Streamline its Complex Energy Utilization. *International Journal of Green Energy*, 11(9), 962–968. https://doi.org/10.1080/15435075.2013.833930

28. Maroušek, J., Strunecký, O., Kolář, L., Vochozka, M., Kopecký, M., Maroušková, A., ... & Cera, E. (2020). Advances in nutrient management make it possible to accelerate biogas production and thus improve the economy of food waste processing. *Energy Sources, Part A: Recovery, Utilization, and Environmental Effects*, 1-10. https://doi.org/10.1080/15567036.2020.1776796
29. Moestedt, J., Müller, B., Westerholm, M., & Schnürer, A. (2016). Ammonia threshold for inhibition of anaerobic digestion of thin stillage and the importance of organic loading rate. *Microbial Biotechnology*, *9*(2), 180–194. https://doi.org/10.1111/1751-7915.12330
30. O'Shea, R., Lin, R., Wall, D. M., Browne, J. D., & Murphy, J. D. (2020). Using biogas to reduce natural gas consumption and greenhouse gas emissions at a large distillery. *Applied Energy*, *279*, 115812. https://doi.org/10.1016/j.apenergy.2020.115812
31. Panjičko, M., Zupančič, G. D., Fanedl, L., Logar, R. M., Tišma, M., & Zelić, B. (2017). Biogas production from brewery spent grain as a mono-substrate in a two-stage process composed of solid-state anaerobic digestion and granular biomass reactors. *Journal of Cleaner Production*, *166*, 519–529. https://doi.org/10.1016/j.jclepro.2017.07.197
32. Ribau Teixeira, M., Guarda, E. C., Freitas, E. B., Galinha, C. F., Duque, A. F., & Reis, M. A. M. (2020). Valorization of raw brewers' spent grain through the production of volatile fatty acids. *New Biotechnology*, *57*, 4–10. https://doi.org/10.1016/j.nbt.2020.01.007
33. Szaja, A., Montusiewicz, A., Lebiocka, M., & Bis, M. (2020). The effect of brewery spent grain application on biogas yields and kinetics in co-digestion

with sewage sludge. *PeerJ*, *8*, e10590. https://doi.org/10.7717/PEERJ.10590/SUPP-1

34. Uzal, N., Gökçay, C. F., & Demirer, G. N. (2003). Sequential (anaerobic/aerobic) biological treatment of malt whisky wastewater. *Process Biochemistry*, *39*(3), 279–286. https://doi.org/10.1016/S0032-9592(03)00071-2
35. Wall, D. M., Allen, E., O'Shea, R., O'Kiely, P., & Murphy, J. D. (2016). Investigating two-phase digestion of grass silage for demand-driven biogas applications: Effect of particle size and rumen fluid addition. *Renewable Energy*, *86*, 1215–1223. https://doi.org/10.1016/j.renene.2015.09.049
36. Yeoh, B. G. (1997). Two-phase anaerobic treatment of cane-molasses alcohol stillage. *Water Science and Technology*, *36*(6–7), 441–448. https://doi.org/10.1016/S0273-1223(97)00553-2
37. Zvarikova, K., Rowland, M., & Krulicky, T. (2021). Sustainable Industry 4.0 Wireless Networks, Smart Factory Performance, and Cognitive Automation in Cyber-Physical System-based Manufacturing. *Journal of Self-Governance and Management Economics*, 9(4), 7-20. https://doi.org/10.22381/jsme9420211

5.0 Developing distillery biorefineries through dark fermentation of whiskey production by-products: the effect of organic loading rate on decarbonisation pathways

Anga Hackula, Richard O'Shea, Jerry D. Murphy, David M. Wall

SFI MaREI Centre for Energy, Climate and Marine, Environmental Research Institute, University College Cork, Cork, Ireland

Civil, Structural and Environmental Engineering, School of Engineering and Architecture, University College Cork, Cork, Ireland

Abstract

Biorefinery approaches can arise at distilleries using dark fermentation to treat whiskey production by-products and provide decarbonisation opportunities. A biorefinery can convert residues to hydrogen, carbon dioxide and volatile fatty acids (VFAs). This study investigated the effect of organic loading rate (OLR) on the production of VFAs and biogas in dark fermentation. Similar yields of hydrogen (5.6-6.9 mL H_2. g^{-1} VS), carbon dioxide (18.3-24.9 mL CO_2. g^{-1} VS), and VFAs (141.7-155.0 mg VFA. g^{-1} VS) were found for all OLRs. However, the composition of VFAs altered; higher caproic acid levels (1.2 g. L^{-1}) were observed at low OLRs and higher valeric acid levels at high OLRs (2.0 g. L^{-1}). The most prominent VFAs were butyric acid and acetic acid across the OLR range. The biogenic carbon dioxide and hydrogen offset potential was also assessed. A 50 million-litre whiskey distillery could satisfy approximately half of the carbon dioxide requirement of the Irish brewing industry. Biogenic hydrogen was found to be best suited as a transport fuel. The biorefinery supports the distillery's transition to circular production systems.

5.1 Introduction

The ‘Fit for 55’ package signifies new EU legislation to assist in meeting net greenhouse gas (GHG) emissions reduction targets of at least 55 % by 2030 and highlights the urgency for climate change mitigation (Department of Environment, 2023). Circular economy strategies and, more specifically, biorefinery approaches can be leveraged in large industries, such as those in the food and beverage industry, to promote sustainable change and valorisation of organic residues. Technologies such as anaerobic digestion (AD) and dark fermentation are particularly relevant to such approaches.

AD is a biological process that breaks down organic residues in the absence of oxygen. In the intermediate phase of the AD process, known as dark fermentation, volatile fatty acids (VFAs), carbon dioxide (CO_2) and hydrogen (H_2) are produced. VFAs are platform chemicals for a diverse range of valuable bioproducts, such as food additives and chemical solvents (Atasoy et al., 2018). Acetic acid, butyric acid, and propionic acid are the predominant VFAs generated (Atasoy et al., 2018). However, longer-chain VFAs can attract significant market prices: 1,070 € per tonne of valeric acid and 3,710 € per tonne of caproic acid (Hackula et al., 2023a; IndiaMART, 2023). VFAs can be used for polyhydroxyalkanoate (PHA) production, with a market price of up to 5,000 € per tonne (Crutchik et al., 2020). PHAs can be used to produce bioplastics, providing an alternative to fossil fuel-derived plastics. Whilst CO_2 is considered less economically valuable than VFAs and H_2 (5,000 € per tonne of green H_2), it still be considered very important in applications such as drinks carbonation (Dinh et al., 2021; International Energy Agency, 2019). To enhance sustainability, alternative biogenic CO_2 sources such as AD and dark fermentation could support future CO_2 demand.

H_2 is an additional output product from dark fermentation. Current H_2 production methods include water electrolysis, pyrolysis, and natural gas reforming (Wang et al., 2018). Biogenic H_2 production through dark fermentation has been suggested as an alternative transport fuel (Sganzerla et al., 2022). Several food and beverage industry sub-sectors, such as whiskey production, could benefit from integrating dark fermentation systems as a means of decarbonising their associated transport systems.

Whiskey and beer production share similarities in their by-products, both producing solid and liquid residues, which are typically used as animal feed (Gunes et al., 2019). Generally, a short hydraulic retention time (HRT) in dark fermentation promotes acidogenesis for H_2 and VFA production, but the yield of both products is dependent on the feedstock and the configuration of the reactor (Buitrón et al., 2019; Yang et al., 2022). In general, longer HRTs favour the production of the more valuable longer-chain VFAs (Buitrón et al., 2019). Thus, the optimum operating parameters must be established to produce the desired output. Several studies have evaluated the impact of the HRT on AD systems on the production of VFAs and/or H_2 from alcohol by-products. The VFA concentrations have typically ranged between 1.0 and 11.2 g. L^{-1} (Blonskaja et al., 2003; Ribau Teixeira et al., 2020). H_2 yields of up to 11.5 L H_2. kg^{-1} VS have been reported in the literature from the dark fermentation of alcohol by-products (Solera et al., 2002). These studies primarily focused on just the liquid by-products or just the solid by-products. One previous study co-digested liquid and solid brewery by-products for primarily H_2 production but neglected the potential biogenic CO_2 (Sganzerla et al., 2022). A previous study by the authors evaluated liquid and solid whiskey by-products as part of a two-phase AD system but did not report the potential for H_2 production (Hackula et al., 2023b).

The organic loading rate (OLR) is an essential operational parameter in AD systems. A high OLR and shorter HRT reduces the physical footprint required for the AD system and thus may require less investment. However, if the OLR is too high and the HRT is too short, microbial washout may occur in the AD system and reduce the overall performance or even lead to system failure (Gerardi, 2003). The OLR has also been reported to alter the VFA profile in terms of shorter or longer chain VFAs (Yang et al., 2022). In essence, varying the OLR could be a cost-effective means of delivering a favourable VFA composition for a given biorefinery depending on the product it wishes to produce.

To the best of the authors' knowledge, no previous studies have evaluated the impact of variable OLR on VFA production, H_2 production and the utilisation of the CO_2 from dark fermentation of liquid and solid distillery by-products. No prior studies have quantified the H_2 production and utilisation potential from dark fermentation for heating and/or transport at a distillery. This study addresses this knowledge gap through a distillery biorefinery concept based on dark fermentation. The proposed biorefinery would produce H_2 for either heating or use as a transport fuel for the distillery, CO_2 for beer carbonation, and bioplastic packaging for beer derived from VFAs, as illustrated in Figure 5.1.

The specific objectives of this study are to: (1) establish the maximum VFA and H_2 yield of whiskey by-products through batch trials and continuous dark fermentation experiments; (2) explore the potential of biogenic H_2 to offset fossil fuel use within the distillery in terms of heating and transportation; (3) explore the potential of biogenic CO_2 offsetting fossil CO_2 within the food and beverage industry, in particular for the carbonation of beer; (4) explore the potential of converting biogenic VFAs into PHAs for use as packaging for beer cans.

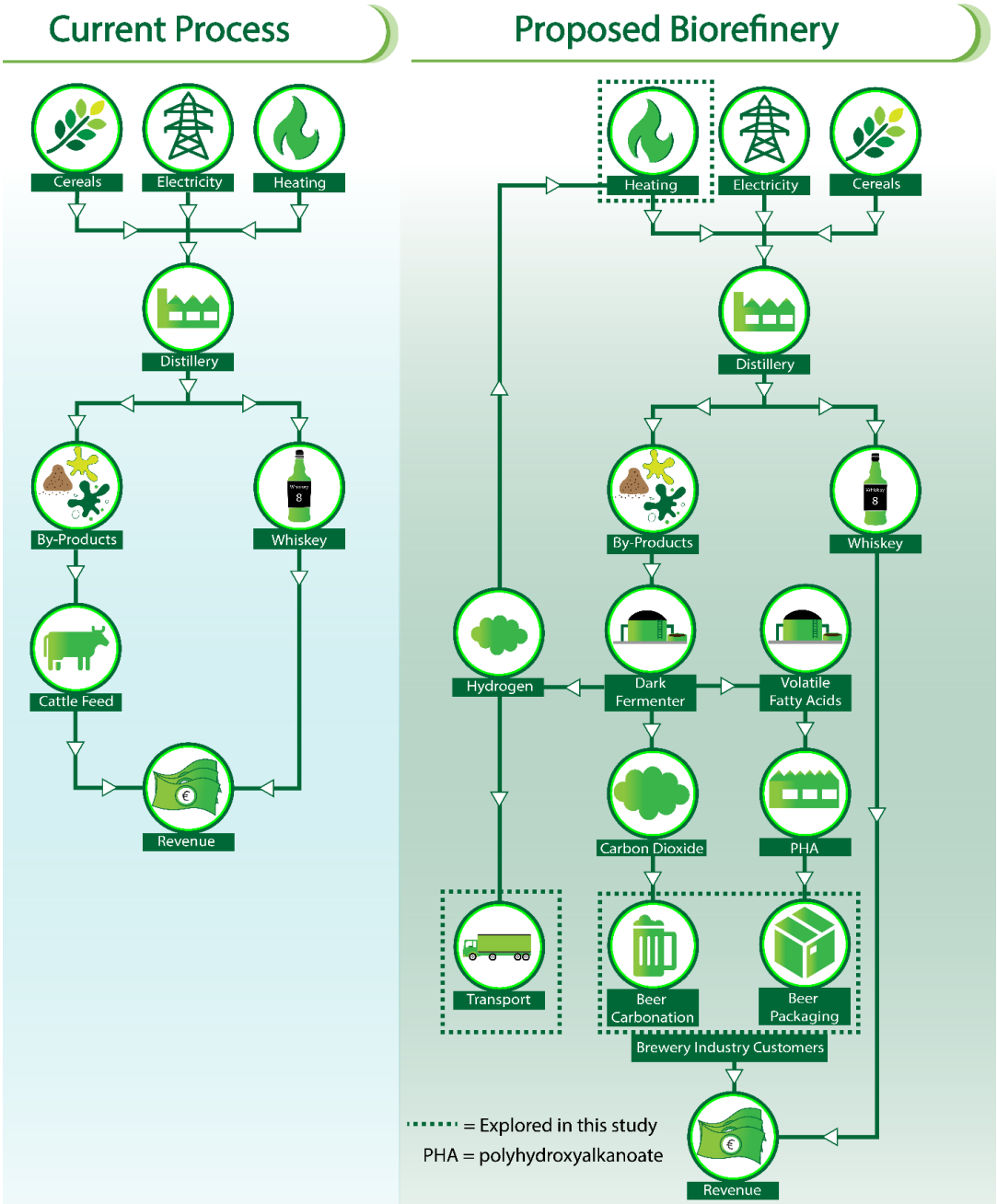


Figure 5.1: Illustration depicting the existing distillery process alongside the proposed biorefinery approach

5.2 Materials and methods

5.2.1 Inoculum and feedstock characteristics

Cattle slurry obtained from a farm in Co. Cork, Ireland, was used as inoculum for all dark fermentation trials. The slurry was filtered with a 5 mm mesh to remove any solid particulates. To inhibit the methanogens, the cattle slurry inoculum was preheated at 100 ^{o}C for 30 minutes (Deng et al., 2019). Subsequently, the pH was adjusted to pH 6.0 with 1M HCl solution (Dauptain et al., 2021). The total solids (TS) and volatile solids (VS) of the inoculum were 2.1 %ww and 1.4 %ww, respectively.

The solid whiskey by-products were comprised of draff and cake maize, whilst the liquid by-products comprised of centrate and thin stillage as described in a previous study and termed mixed whiskey by-products (Hackula et al., 2023a). Prior to experiments, 400 ml of the liquid by-products were added to the inoculum in batch mode for 30 days in a laboratory scale continuously stirred tank reactor to acclimatise the inoculum to the substrate. Table 5.1 shows the characteristics of the distillery by-products.

Table 5.1: Characteristics of the whiskey by-products

		Solids		Liquids		
	Unit	**Draff**	**Cake maize**	**Centrate**	**Thin stillage**	**mixed whiskey by-products**
% Breakdown[a]	%	5	10	34	51	
TS[b]	% ww	27.4	29.0	3.5	2.9	6.8
VS[c]	% TS	96.0	97.2	89.3	88.8	93.7
pH				3.8	4.3	4.0
COD[d]	g. L^{-1}			34.6	33.4	
Protein	% ww	9		1[e]	2	
Crude Fibre	% ww	6		0[e]	1	
Fat	% ww	2		1[e]	2	
CHON[f]						$C_{12}H_{19.8}O_{7.9}N$

[a] Percentage of by-products produced per tonne; [b] TS = total solids; [c] VS = volatile solids; [d] COD = soluble chemical oxygen demand; [e] values of cake maize and centrate taken prior to centrifugation; [f] CHON = carbon, hydrogen, oxygen and nitrogen composition (adapted from Hackula et al., 2023, Hackula et al., 2023b)

5.2.2 Biohydrogen potential assays

A simple batch biohydrogen potential (BHP) trial was undertaken to establish the maximum BHP and VFA yield of the by-product feedstock. The BHP trial represents the ideal conversion for the feedstock to biogenic H_2 and is used as a precursor to continuous trials (Carrillo-Reyes et al., 2019). The BHP test was set to a duration of 25 days, as suggested by a prior study evaluating a similar feedstock for VFAs and H_2 (Sganzerla et al., 2022). The BHP was conducted in triplicate using the Bioprocess Control ^{TM} AMPTS II system. In total, 1.81 g VS of the mixed whiskey by-products was placed in each bottle with 0.28 g VS of inoculum. This ratio was found to be suitable for hydrogen production in batch assays (Deng et al., 2019). The volume was adjusted to 200 ml with deionized water. An inoculum control group was also evaluated in triplicate to account for gas production from the inoculum and a positive control with cellulose. The pH was then adjusted to 6.0 with 1 mol L^{-1} HCl (Sganzerla et al., 2022). Mesophilic conditions (37±1 ^{o}C) were maintained by placing the bottles in a thermostatic water bath. All bottles were purged with nitrogen for 2 minutes to ensure anaerobic conditions.

5.2.3 Continuous dark fermentation trials

Continuous trials were conducted to simulate the real-world application of dark fermentation. Three 1 L working volume continuously stirred tank reactors (CSTRs) were manually pulse-fed mixed whiskey by-products five times a week for 40 days. To evaluate the impact of the organic loading rate (OLR) on the products of dark fermentation, three OLRs were evaluated: 5 g VS. L^{-1}. d^{-1} (referred to as reactor C5

with an HRT of 12 days), 10 g VS. L^{-1}. d^{-1} (referred to as reactor C10 with an HRT of 6 days) and 15 g VS. L^{-1}. d^{-1} (referred to as reactor C15 with an HRT of 4 days). The three OLRs were within the range (5-19 g VS. L^{-1}. d^{-1}) of studies evaluating dark fermentation of alcohol by-productions in CSTRs (Ribau Teixeira et al., 2020; Sittijunda et al., 2022). Mesophilic conditions (37±1 ^{o}C) were again maintained by placing the reactors in a thermostatic water bath. Detailed results can be found in Appendix C.1.

5.2.4 Offsetting fossil fuel usage through a biorefinery approach

The dark fermentation biorefinery proposed has the potential to offset fossil fuel-derived products. Biogenic H_2 was evaluated to offset either natural gas, which is used for heating, or diesel, which is used as a distribution transport fuel at the distillery. The biogenic CO_2 was considered to offset fossil fuel-derived CO_2 for carbonation in the beer brewing industry. Lastly, the conversion of the biogenic VFAs into PHAs was considered to offset current packaging methods within the beer industry. A theoretical evaluation of the offset potential of the biogenic H_2, CO_2, and converting biogenic VFAs into PHAs was undertaken by combining data from the continuous dark fermentation trials (see Section 5.2.2) and assumptions from the literature. The relevant assumptions are outlined in detail in Sections 5.3.3-5.3.5 to estimate the offset potential. More detailed calculations can also be found in Appendix C.2-C.4.

5.2.5 Analytical methods

The soluble COD (referred to as COD) of the CSTR effluent was monitored using Reagecon COD Cuvette Vials (420721) and a DR 3900 Hach Spectrometer. The TS and VS content of the whiskey by-products were assessed using conventional techniques APHA 2540 G (APHA, 2023). Ammoniacal nitrogen (TAN) levels were monitored using the Hach Lange AmVerTM Salicylate Test 'N Tube TM Method (Hach Lange 10031) and a DR 3900 Hach Spectrometer.

The pH was determined using a Mettler ToledoTM F20 pH meter. An Agilent GC (Agilent Technologies 7890B) fitted with a DB-FFAP column (0.32 mm x 50 m) and a flame ionization detector was used to assess the VFA concentration and composition of the CSTR effluent. Prior to analysis, samples for VFA analysis were collected and kept at -20 ^{o}C. The samples were defrosted at room temperature and centrifuged for 10 minutes at a speed of 12,000 rpm prior to testing. COD and TAN samples underwent a similar centrifugation procedure. An Agilent GC (Agilent Technologies 8860) fitted with a J&W GC packed column (2 mm x 1.8 m) was used to assess the biogas composition (CO_2, H_2 and methane (CH_4)). Biogas production for the batch trials was measured by the Bioprocess Control ^{TM} AMPTS II system, while a Bioprocess Control ^{TM} BRS-B unit was used for the continuous trial. Both systems reported the daily gas production at standard temperature and pressure (STP = 0 ^{o}C and 1 atm). The specific CO_2 yield and specific H_2 yield were calculated based on the percentages represented in the gas mixture. The COD reduction was calculated as follows:

$$COD_{red} = \frac{(COD_{in} - COD_{out})}{COD_{in}} \times 100$$

Where: COD_{red} is the COD reduction, COD_{in} is the COD of the substrate, and COD_{out} is the reactor effluent COD.

The acidification level in the continuous dark fermentation trials describes the proportion of the VFA equivalent COD (COD_{VFA}) within the reactor's effluent as calculated below. COD_{VFA} was calculated using stoichiometric COD conversion factors reported in the literature (Owusu-Agyeman et al., 2020):

$$Acidification\ level = \frac{COD_{VFA}}{COD_{effluent}} \times 100$$

Where: COD_{VFA} is the COD equivalent of VFAs, and $COD_{effluent}$ is the COD of the reactor effluent.

The COD-to-VFA conversion efficiency is a measure of how efficiently the reactors convert the initial substrate into VFAs and was calculated by the following formula:

$$\text{COD} - \text{to} - \text{VFA conversion efficiency} = \frac{COD_{VFA}}{COD_{influent}} \times 100$$

Where: COD_{VFA} is the COD equivalent of VFAs, and $COD_{influent}$ is the COD of mixed whiskey by-products (measured as 33.9 g COD. L^{-1}).

The data were tested for statistical difference using a two-sample, single-factor ANOVA parametric test with an online statistical calculator, DataTAB.net (DATAtab Team, 2023). The significance level of all tests was set to 0.05.

5.3 Results and discussion

5.3.1 Specific biohydrogen and VFA yields from batch trials

Gas production from the batch BHP assays ceased after 40 hours. The cumulative H_2 yield was 52.8±1.9 L H_2. kg^{-1} VS (2.4 mol H_2. kg^{-1} VS) (Figure 5.2A). The specific H_2

yield was within the range of specific H_2 yields from batch assays reported in the literature from similar feedstocks (3.9 - 145.5 L H_2. kg^{-1} VS) (Sganzerla et al., 2022; Sittijunda et al., 2022; Vanyan et al., 2022). The specific H_2 yield of the positive control group with cellulose as the substrate was 25.1 ± 0.6 L H_2. kg^{-1} VS. The specific H_2 yield of the positive control was within the range reported in the literature evaluating glucose and cellulose as the substrate (5.2 - 90.2 L H_2. kg^{-1} VS) (Carrillo-Reyes et al., 2019). The broad variance in results can be attributed to the nature of the inoculum, discrepancies in BHP methodology, such as initial pH, and other parameters such as the use of buffer solutions (Carrillo-Reyes et al., 2019).

On day 11, the primary VFAs were acetic acid (45 %), butyric acid (35 %), caproic acid (6 %) and propionic acid (4 %). The formation of propionic acid may follow a hydrogen-consuming pathway, resulting in lower H_2 yields (Angenent et al., 2004). Trace amounts of iso-butyric acid, iso-valeric, and valeric acid were found on day 11 (<80 mg. L^{-1} each). The peak specific VFA yield of 319.8 ± 22.2 mg VFAs. g^{-1} VS, equivalent to 2,889 mg VFA. L^{-1}, was found on day 11 (Figure 5.2B). The decline between days 11 and 15 could be attributed to the formation of a white-fungal substance in all three BHP assays, which was removed on day 13. Subsequently, the BHP assays were reclosed, purged with nitrogen, and continued. The trend was an increase in caproic acid concentrations ($p<0.05$) and a decrease in butyric acid concentrations ($p>0.05$). By the end of the trial, the specific VFA yield was 292.3 ± 5.2 mg VFAs. g^{-1} VS, equivalent to 2,640 mg VFA. L^{-1}. However, there was no significant difference in the specific VFA yield from day 11 until the end of the trial, on day 25 ($p>0.05$).

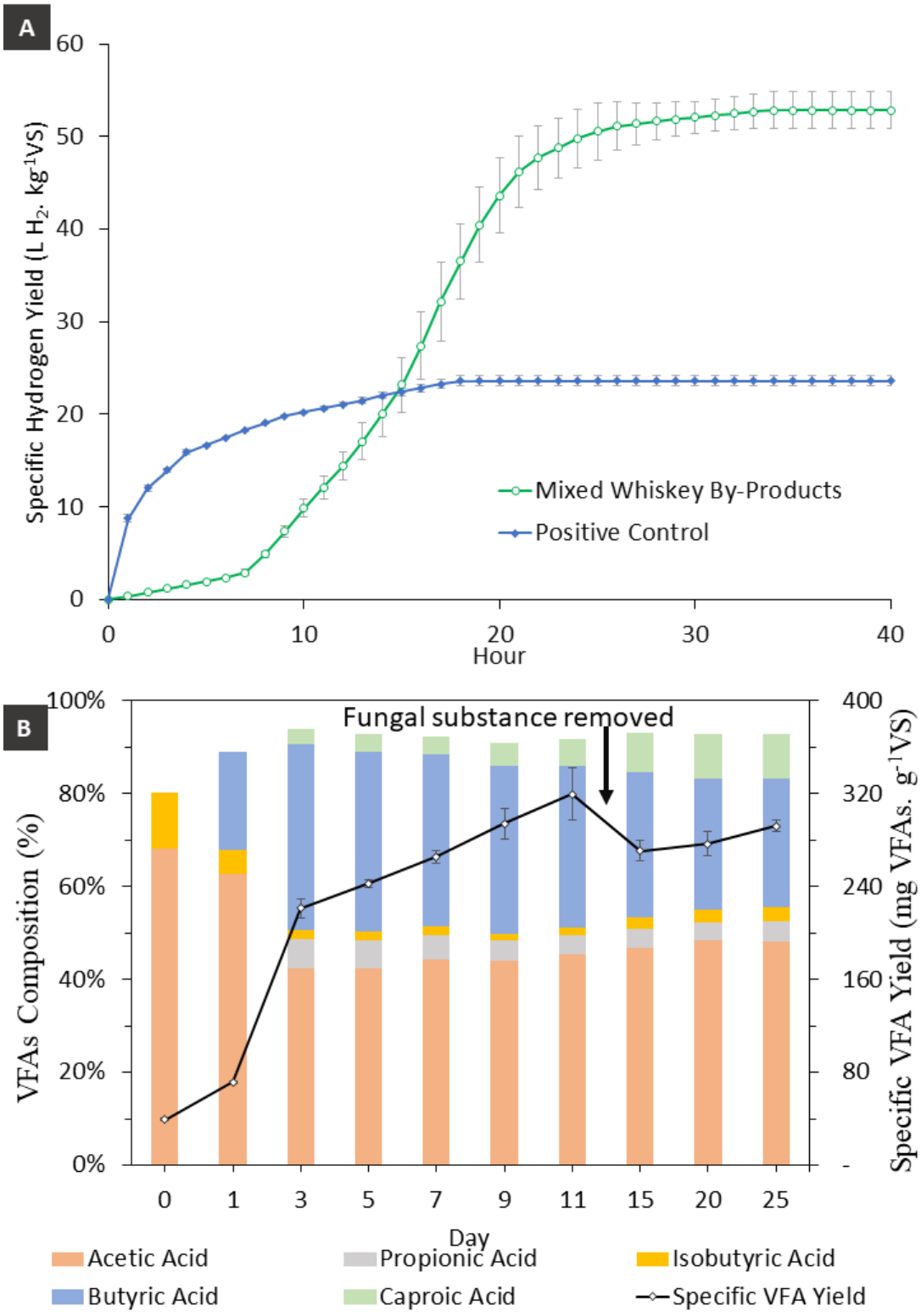


Figure 5.2: Biohydrogen potential and VFA yields from batch trials

5.3.2 Continuous dark fermentation trials

The pH for reactors C10 and C15 was slightly lower than in C5 (Table 5.2). This could be due to more pH-reducing acids, such as acetic acid, than pH-increasing acids, such as caproic acid, within the reactors in C10 and C15 compared to C5 (Candry et al., 2020).

Table 5.2: Continuous dark fermentation results

	Unit	C5	C10	C15
OLR[a]	kg VS. L^{-1}. d^{-1}	5	10	15
HRT[b]	d	12	6	4
pH		4.7 ± 0	4.5 ± 0	4.5 ± 0
COD	g. L^{-1}	26.1 ± 1	28.9 ± 1	27.3 ± 1
% COD Reduction[c]	%	23 ± 2	15 ± 2	19 ± 2
TAN[d]	mg. L^{-1}	468 ± 26	352 ± 43	337 ± 27
COD_{VFA}[e]	g. L^{-1}	15.4 ± 0	16.3 ± 1	16.4 ± 1
Acetic Acid	mg. L^{-1}	2,078 ± 104	2,244 ± 115	2,260 ± 149
Propionic Acid	mg. L^{-1}	989 ± 56	1,660 ± 158	1,878 ± 176
Butyric Acid	mg. L^{-1}	3,368 ± 127	3,167 ± 236	2,956 ± 116
Valeric Acid	mg. L^{-1}	1,132 ± 36	1,590 ± 160	2,011 ± 81
Caproic Acid	mg. L^{-1}	1,241 ± 37	604 ± 76	323 ± 26
COD-TO-VFA[f]	%	46 ± 1	48 ± 2	48 ± 2
Specific VFA Yield	mg VFA. g^{-1} VS	141.7 ± 4	153.3 ± 7	155.0 ± 6
	mg VFA. g^{-1} ww	9.0 ± 0	9.8 ± 1	9.9 ± 0
% H_2[g]	%	24 ± 2	23 ± 1	19 ± 2
Specific H_2 Yield	mL H_2. g^{-1} VS	6.3 ± 0	5.6 ± 1	6.9 ± 1
	mL H_2. g^{-1} ww	0.4 ± 0	0.3 ± 0	0.4 ± 0
Specific CO_2 Yield	mL CO_2. g^{-1} VS	19.4 ± 1	18.3 ± 4	24.9 ± 2
	mL CO_2. g^{-1} ww	1.2 ± 0	1.2 ± 0	1.6 ± 0

[a] OLR = Organic loading rate; [b] HRT = Hydraulic retention time; [c] % COD Reduction = Percentage COD reduced; [d] TAN = Ammoniacal nitrogen; [e] COD_{VFA} = COD equivalent of the VFAs; [f] COD-to-VFA = COD-to-VFA conversion efficiency (based on the initial COD of 33.9 g. L^{-1}); [g] % H_2 = Percentage of hydrogen in biogas

There was no significant difference in the COD of the effluent for all three reactors (Figure 5.3B) 26-29 g. L^{-1} ($p > 0.05$). Significantly lower TAN concentrations were observed with increasing OLR ($p<0.05$) and pH (see Table 5.2). The higher OLR (shorter HRT) resulted in less volatile solids conversion within the reactor, resulting

in lower TAN concentrations (see Table 5.2 and Figure 5.3B). This was evidenced by the significantly higher VS destruction observed in C5 (42 %), which was significantly different to both C10 and C15 ($p<0.05$) (see Figure 5.3B). There was no significant difference in terms of VS destruction between C15 and C10 ($p>0.05$). The average VFA concentrations were similar for C15 (9.9 g. L^{-1}) and C10 (9.8 g. L^{-1}). Lower VFA concentrations were observed in C5 (9.0 g. L^{-1}). However, there was no significant difference in the overall VFA concentration across the three reactors ($p>0.05$). The majority of VFA concentrations generated from treating alcohol by-products in the literature have ranged from 0.9 to 11.2 g. L^{-1}, however, much higher values above 24 g. L^{-1} have also been reported (Ribau Teixeira et al., 2020). These higher yields could be due to mechanical and thermal pretreatment of the solid alcohol by-products, which has been reported to break the recalcitrant lignin structure within draff and brewers spent grains (Kang et al., 2021).

Butyric acid was the major VFA in all three reactors, followed by acetic acid, suggesting a butyric-type fermentation pathway (Yang et al., 2022). In C15 and C10, valeric acid was the next most prominent VFA, followed by propionic acid. This was dissimilar to C5, which had higher concentrations of caproic acid, followed by valeric acid and propionic acid. Longer HRTs have been reported to favour longer-chain VFAs such as caproic acid (de Groof et al., 2021). The descending concentrations of caproic acid further illustrated this with increasing OLR in this study. The caproic acid concentrations were: C5 - 1,273 mg. L^{-1}; C10 - 660 mg. L^{-1}; and C15 - 319 mg. L^{-1} (see Appendix C.1) ($p<0.05$). A previous study of the same feedstock operating at a lower OLR of 2.5 kg VS. L^{-1}. d^{-1} (and HRT of 25 days) reported slightly higher caproic acid concentrations (ca. 1.6 g. L^{-1}) (Hackula et al.,

2023b). Caproic acid is of interest due to its market price (3,710 € per tonne) and partial insolubility in water (IndiaMART, 2023; Bastidas-Oyanedel et al., 2015).

The composition of the VFAs shows a higher prominence of shorter chain VFAs at higher OLRs. Additionally, the production of shorter chain VFAs requires less metabolic energy compared to longer chain VFAs like caproic acid, resulting in lower metabolic energy losses and a higher concentration of these shorter chain VFAs. It was hypothesized, that higher availability of substrate at higher OLRs allowed for the hydrolytic and fermentative microbes to produce VFAs faster. However, to establish the validity of this hypothesis, microbial analysis and kinetics would be required.

A similar trend was evident for butyric acid but was not as pronounced: C5 (3,368 mg. L^{-1}), C10 (3,167 mg. L^{-1}), and C15 (2,956 mg. L^{-1}) ($p>0.05$) (see Table 5.2). The associated specific butyric acid yield was: C5 – 52 mg. g^{-1} VS; C10 - 50 mg. g^{-1} VS; and C15 – 46 mg. g^{-1}VS ($p > 0.05$). Interestingly, valeric acid concentrations increased with increasing OLR: C5 (1,132 mg. L^{-1}), C10 (1,589 mg. L^{-1}), and C15 (2,010 mg. L^{-1}) (see Table 5.2) ($p<0.05$).

As the operational conditions such as pH and OLR have been shown to influence the fermentation pathways, and as the pH for both C10 and C15 were similar, the OLR can also be used to steer the concentrations of the desired VFAs (Yang et al., 2022). This is significant for PHA production, as different VFA compositions result in different PHA materials. For example, fermentation broth with primarily butyric acid and no valeric acid could yield polyhydroxybutyrate (PHB) (Al Battashi et al., 2021). In contrast, fermentation broth with significant levels of butyric acid and valeric acid could yield poly-3-hydroxybutyrate-co-3-hydroxyvalerate (PHB-co-

PHV) (Al Battashi et al., 2021). Further research is required to establish the viability of producing PHAs from the fermentation broth within this study.

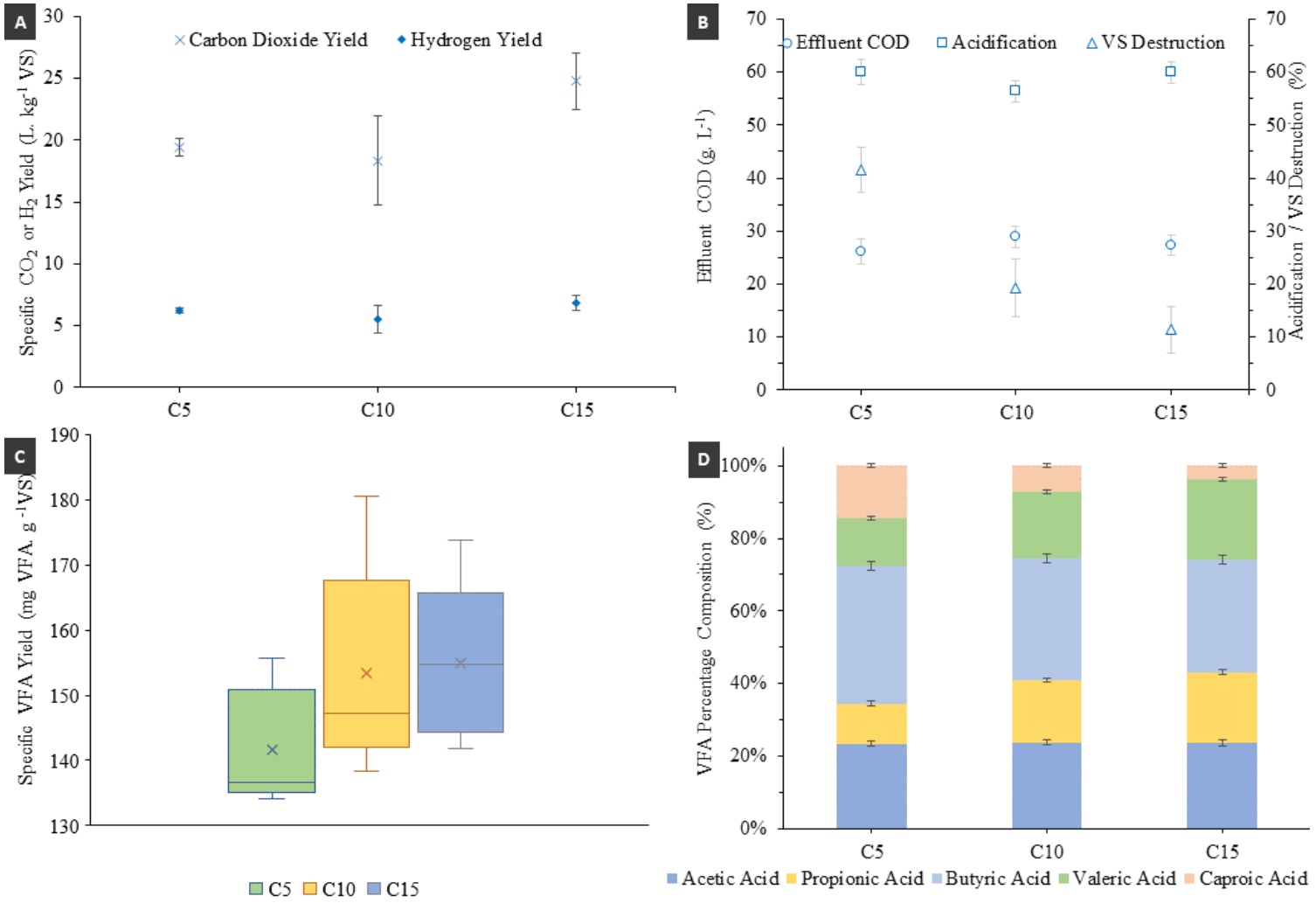


Figure 5.3: Dark fermentation yields and performance metrics at various organic loading rates

5.3.3 Acidogenesis performance

The COD reduction across the three reactors was C5 (23 %), as compared to C10 (15 %) and C15 (19 %). However, there was no significant difference in the effluent COD across the three reactors (Figure 5.3B) ($p > 0.05$). As the mixed whiskey by-products consist of solids and liquids, the level of acidification was evaluated in two ways: firstly, based on the COD within the reactor (referred to as the acidification) and secondly, based on the COD of the liquids of the mixed whiskey by-products (referred to as the COD-to-VFA efficiency) (see Section 5.2.3). While the acidification was slightly higher in C15 (60 %) than in C10 (56 %), the COD equivalent of VFAs was similar (ca. 16.4 g COD_{VFA}. L^{-1}). This effectively results in the same COD-to-VFA efficiency for C10 and C15 (48 %). The COD-to-VFA efficiency of C5 was slightly lower (46 %) due to the higher reduction in COD ($p > 0.05$). There was no significant difference in the COD-to-VFA efficiency across the three reactors. The acidification for C5 was 60 %.

The specific VFA yield for the reactors was C5 – 141.7 mg VFA. g^{-1} VS; C10 – 153.3 mg VFA. g^{-1} VS; C15 – 155.0 mg VFA. g^{-1} VS ($p> 0.05$) (see Figure 5.3C). Interestingly, more butyric acid and caproic acid can be generated per gram of substrate at a lower OLR of 5 g VS. L^{-1}. d^{-1} (50% of the VFA yield) than at higher OLRs of 10 g VS. L^{-1}. d^{-1} (40 % of the VFA yield) and 15 g VS. L^{-1}. d^{-1} (34 % of the VFA yield) (Figure 5.3D).

The biogas composition was primarily CO_2 (up to 75 $\%_{vol}$) for all three reactors (Table 5.2). The remainder was predominantly H_2 with traces of CH_4 (<1 $\%_{vol}$). There was no significant difference in the specific CO_2 yield and specific H_2 yield across the three reactors (Table 5.2) ($p>0.05$). Even though the specific CO_2 and H_2 yields were similar, the volumetric yields increased with increasing OLR (data not

shown). In other words, more feedstock produced more H_2 and CO_2 by volume. Overall, there was no significant difference between the specific gas yields and specific VFA yields with the increasing OLR. The impact of increasing OLR was evident in the VFA composition.

5.3.4 Considerations of dark fermentation of whiskey by-products

Significant differences were observed in the TAN concentrations, specific valeric acid yield and specific caproic acid yield across the three OLRs investigated. As three products are generated from the process, defining the primary objective of the fermentation process is required. Regarding VFAs, if caproic acid and butyric acid are more of interest, a lower OLR may be better suited for the process. If valeric acid and butyric acid are of interest, higher OLRs are better suited (see Table 5.2). Process-oriented OLR selection is of significant interest for the proposed biorefinery as the OLR can be used to produce different types of PHA polymers, such as PHB-co-PHV, which have different physical properties and higher economic value than PHB (Al Battashi et al., 2021). The proposed biorefinery focused on PHA production; however, VFA separation may be an attractive alternative approach for the biorefinery. Different VFAs have different market prices and could produce different end products. For example, caproic acid is partially insoluble in water, making it easier to separate and isolate from the fermentation broth than the other prominent VFAs in this study (Bastidas-Oyanedel et al., 2015). The lowest OLR in this study would be better suited to this approach than the higher OLRs, as more caproic acid was observed at lower loading rates.

Another potential valorisation pathway may be to extract the desired VFAs from the effluent, and the remaining solids from the fermentation broth could be used as feedstock for a subsequent methanogenic reactor to produce biogas (methane and CO_2), effectively resulting in a two-phase digestion system. The lower OLR would be better suited for this approach, as lower propionic acid concentrations were observed at lower OLRs.

5.3.5 Biogenic carbon dioxide for beer carbonisation

As a whiskey distillery is within the food and beverage industry, the biogenic CO_2 produced in fermentation can offset CO_2 utilisation. Carbonated beers were selected to illustrate the potential CO_2 offset. The potential of the CO_2 offset produced through dark fermentation can be estimated based on the following assumptions:

- A commercial whiskey distillery of 50 million L_{OLA} produces 516.5 kt. a^{-1} of mixed whiskey by-products (Hackula et al., 2023b).
- The CO_2 can be converted to beverage-grade CO_2 (99.9 %).
- The density of CO_2 is 1.9768 kg. m^{-3} CO_2 (National Institute of Standards and Technology, 2023).
- The price of CO_2 is between 50-70 €. t^{-1} (Salomone et al., 2019; Uddin et al., 2022).
- Carbonated beers require 3.9-5.5 g CO_2. L^{-1} (Liger-Belair and Cilindre, 2021).
- The standard volume for a small beer can is 330 ml.

- The analysis only considers CO_2 from dark fermentation, which has an average specific CO_2 yield of 1.34 m^3 CO_2. t^{-1} ww of mixed whiskey by-products (average of values reported in Table 5.2)
- The exchange rate from euro (€) to US dollar (US$) was set at 1.10 US$. $€^{-1}$ (Central Bank of Ireland, 2023).

The specific CO_2 yield of 1.34 m^3 CO_2. t^{-1} ww equates to 692,110 m^3 CO_2. a^{-1} (13.8 L CO_2. L^{-1}_{OLA}). The annual mass of CO_2 is approximately 1,368 t CO_2. a^{-1}. The value of this amount of CO_2 is between € 68,400 - 95,760 (US$ 75,240 - 105,336). The generated CO_2 is enough to carbonate up to 351 million L (1,064 million cans) of beer. For context, 710 million L of beer was produced in Ireland in 2020 (IBEC, 2021). The CO_2 generated from whiskey by-products of a 50 million L_{OLA} facility could offset up to 49 % of the annual CO_2 demand for beer production in Ireland. This is significant as only one distillery was considered for this analysis. Table 5.3 shows the CO_2 offset potential for beers from dark fermentation.

Table 5.3: CO_2 offset potential of whiskey by-products within Ireland		
	Units	**Value**
Whiskey by-products production [a]	kt. a^{-1}	516.5
Specific CO_2 yield[b]	m^3. t^{-1} ww	1.34
CO_2 mass yield[c]	t. a^{-1}	1,368
CO_2 monetary value[d]	€. a^{-1} ($. a^{-1})	68,400 - 95,760 (75,240 -105,336)
Beer carbonated using biogenic CO_2 [efg]	million L	249 - 351
	million cans	755 - 1,064
Potential for biogenic CO_2 as a substitute for beer carbonation in Ireland[h]	%	35 - 49

[a] Annual production rate of the mixed whiskey by-products assumed from (Hackula et al., 2023b); [b] CO_2 yield based on experimental data; [c] CO_2 density is 1.9768 kg. m^{-3} CO_2 (National Institute of Standards and Technology, 2023); [d] The price of CO_2 is assumed to be between 50-70 €. t CO_2^{-1} (Salomone et al., 2019; Uddin et al., 2022); [e] number of beverages carbonated with biogenic CO_2; [f] A carbonated beer requires 3.9 - 5.5 g CO_2. L^{-1} (Liger-Belair and Cilindre, 2021); [g] Volume of a can = 330 ml; [h] Share of total CO_2 used for beer produced in Ireland at 710 million L of beer in 2020 (IBEC, 2021);

5.3.6 Biogenic hydrogen for heating and distribution transport

Hydrogen can be used to offset fossil fuel usage at the distillery. The analysis provides the utilisation potential of the biogenic H_2 for the distillery's process heating or distribution transport. The following assumptions were made to establish the potential usage:

- Only H_2 usage for heating or as a transport fuel for the distillery was considered.
- A commercial whiskey distillery of 50 million L_{OLA} results in 516.5 kt. a^{-1} of mixed whiskey by-products (Hackula et al., 2023b).
- The average specific H_2 yield was taken to be 0.38 m^3 H_2. t^{-1} ww of mixed whiskey by-products (average of values reported in Table 5.2).

- The energy value of H_2 is 33.3 kWh. kg^{-1} (Transport & Environment, 2020).
- The density and price of H_2 are 0.089 kg. m^{-3} and 5 €. kg^{-1} H_2, respectively (Muzny et al., 2013; Dinh et al., 2021).
- The distillery's processes are heated with natural gas with a CO_2e emission intensity of 202 g CO_2e. kWh^{-1} (DEFRA, 2022).
- 40 t trucks (25 t load capacity) operating on compressed H_2 (700 bar) fuel cells would be used for transporting whiskey nationally with a hydrogen energy consumption of 2.5 kWh. km^{-1} (Gray et al., 2022).
- The average distance travelled per tonne of national road freight is 95.1 km. t^{-1}. $truck^{-1}$ (Eurostat, 2022).
- The alcohol by volume (ABV) for whiskey is 40 %, and the density of ethanol is 0.78 kg. L^{-1} (National Institute of Standards and Technology, 2023).
- Whiskey is transported 365 days a year with 50 million L of whiskey being sold annually.
- The distillery's fleet is currently fuelled by diesel, with a diesel energy consumption of 3.18 kWh. km^{-1} and CO_2e emission intensity of 263.9 g CO_2e. kWh^{-1} (Gray et al., 2022; DEFRA, 2022).
- The exchange rate from euro (€) to US dollar (US$) was set at 1.10 US$. $€^{-1}$ (Central Bank of Ireland, 2023).

The detailed calculations are shown in Appendix C.3. The results from the analysis are shown in Table 5.4.

Table 5.4: Biogenic hydrogen utilisation potential for heating and transport

Section	Parameters	Units	Value
Hydrogen energy and monetary value	Distillery size	million L_{OLA}. a^{-1}	50
	Distillery H_2 yield	million L H_2. a^{-1}	196.3
	Specific distillery H_2 yield	L H_2. L^{-1}_{OLA}	3.9
	H_2 energy equivalent	MWh. a^{-1}	586
	Value of H_2[a]	€ ($)	88,000 (96,800)
Transport	Daily number of trucks required	trucks. d^{-1}	10
	Annual distance travelled by fleet	million km. a^{-1}	8.7
	Distance fuelled by H_2	km	234,432
	Potential for H_2 as a substitute fuel for distillery transport	%	2.7
Heating	Distillery thermal energy demand	GWh	208
	Hydrogen thermal replacement at the distillery	%	0.3
	Whiskey produced using H_2 as the heat source	L_{OLA}	140,885
Emissions offset	Avoided emissions from diesel substitution in transport	**t CO_2 Eq. a^{-1}**	**197**
	Avoided emissions from natural gas replacement in heating	**t CO_2 Eq.a^{-1}**	**118**

[a] the exchange rate taken to be 1.10 US$ per € (Central Bank of Ireland, 2023)

The emissions reduction for transport was evaluated to be 66 % more than using the H_2 for heating. Replacing fossil fuels in distribution transport with H_2 could be an effective decarbonisation option for the distillery. Indirect emissions, which include downstream transportation and distribution, from a large distillery can contribute up to 75 % of the total GHG emissions (O'Shea et al., 2020). However, the H_2 produced from dark fermentation would only satisfy 2.7 % of the transport requirements. Thus, implementing a two-phase digestion system, where some effluent is used to produce biomethane, may be a better decarbonisation strategy. In relation to the recast Renewable Energy Directive (REDII), biomethane can be considered preferable for transport as opposed to heat due to the less stringent sustainability criteria for transport as opposed to heat (Long et al., 2021).

The analysis shows biogenic H_2 produced through dark fermentation from whiskey by-products is better suited for transport than heating for decarbonisation at a large distillery. However, using H_2 for heating would require less investment and infrastructural changes if blended with natural gas or biomethane to produce hythane, a mixture of biomethane and biohydrogen (Riahi et al., 2022).

5.3.7 Volatile fatty acid usage for beer packaging

To assess the application of VFAs within the food and beverage industry, the VFAs from the fermentation broth were assumed to be converted to PHAs for bioplastic production and subsequent use as plastic shrinkwrap packaging for six beers. Six beers are colloquially referred to as a six-pack. The following assumptions were made:

- A commercial whiskey distillery of 50 million L_{OLA} results in 516.5 kt. a^{-1} of mixed whiskey by-products (Hackula et al., 2023b).
- An average specific VFA yield of 9.6 kg VFA. t^{-1} ww of mixed whiskey by-products (average of values reported in Table 5.2).
- The liquid-solid separation efficiency of the fermentation broth was 80 % (Moses, 2014).
- The PHA production process yields 0.3 g PHA. g^{-1} VFA broth (Al Battashi et al., 2021).
- The market price for PHAs is 5,000 €. t^{-1} (Crutchik et al., 2020).
- The standard volume for a small beer can is 330 ml, the ABV for a beer can is 5 %, and the density of ethanol is 0.78 kg. L^{-1}.

- The PHA mass required for a standard carrying bag is 9.03 g for a 20 kg capacity bag (Al Battashi et al., 2021). The equivalent bioplastic for packaging six beers (1.96 kg) is estimated to require 0.85 g PHA per beer shrinkwrap package (see Appendix C.4).

Table 5.5 summaries the calculations of converting VFAs to PHA for use as beer packaging.

Table 5.5: VFA to PHA utilisation potential through Irish beer packaging

Parameters	Units	Value
Distillery size	million L_{OLA}. a^{-1}	50
Annual by-products produced	kt. a^{-1}	516.5
PHA yield	t PHA. a^{-1}	1,189.8
Value of PHA[a]	million € (US$). a^{-1}	5.9 (6.5)
Number of six-pack beer packages produced from PHAs	million bags	1,322

[a] the exchange rate taken to be 1.10 US$ per € (Central Bank of Ireland, 2023)

If all beer produced in Ireland in 2020 (710 million L) was packaged into 6 x 330 ml beer packages, the distillery could supplement 369 % of the demand for beer packing with biobased packaging (see Appendix C.4) (IBEC, 2021). This may interest the distillery as they could collaborate with the beer industry to provide biodegradable packaging and diversify the distiller's revenue stream while decarbonising another industry.

5.3.8 Limitations and future research

A biorefinery that produces VFAs (and subsequently PHAs as in this study), H_2 and CO_2 from the distillery by-products would have products valued at a combined € 6.1 million (€ 0.12 L^{-1}_{OLA} produced). PHAs were the primary revenue source; however, the characterisation and quantification of PHAs was not part of the experimental

process and was deemed beyond the scope of this study. Subsequent research is necessary to generate PHAs from VFAs and comprehensively characterise and quantify the resulting PHAs. Gas separation and purification techniques are already implemented at an industrial scale, posing less investment ‘risk’. In contrast, PHA production through biogenic VFAs is not implemented at scale yet. The investment for PHA production would pose a higher investment ‘risk’ for a distiller.

It should be noted that the work presented does not include all of the associated costs of infrastructure, process modifications and other logistical costs outside the scope of this analysis. A complete life-cycle and techno-economic analysis would be required to evaluate the environmental and economic impact of the products generated in this study. Further research is required to establish the ideal valorisation pathway from the VFAs, separation techniques, and potential upgrading pathways such as chain elongation.

5.4 Conclusion

A biorefinery concept via dark fermentation was explored to valorise distillery by-products. Continuous experimental trials evaluated the impact of the organic loading rate and established a specific VFA yield of 164.5 mg VFA. g^{-1} VS, and a CO_2 yield of 24.8 L CO_2. kg^{-1} VS, which were observed at the highest OLR of 15 gVS. L^{-1}. d^{-1}. The biogenic CO_2 from a 50 million L_{OLA} distillery was calculated to have the potential to supplement almost half of the CO_2 requirements of the Irish brewing industry. Hydrogen as a transport fuel had greater decarbonisation potential than use for heating in a distillery context. The potential offset of CO_2 emissions from the use of biogenic H_2 and CO_2 from dark fermentation was estimated to be up to 1,565 t CO_2e. a^{-1}. The proposed biorefinery's potential value in terms of the products was

estimated to be € 6.1 million (US$ 6.7 million). The biorefinery supports the distillery's transition to circular production systems.

References

1. Al Battashi, H., Al-Kindi, S., Gupta, V.K., Sivakumar, N., 2021. Polyhydroxyalkanoate (PHA) Production Using Volatile Fatty Acids Derived from the Anaerobic Digestion of Waste Paper. J Polym Environ 29, 250–259. https://doi.org/https://doi.org/10.1007/s10924-020-01870-0
2. Angenent, L.T., Karim, K., Al-Dahhan, M.H., Wrenn, B.A., Domíguez-Espinosa, R., 2004. Production of bioenergy and biochemicals from industrial and agricultural wastewater. Trends Biotechnol 22, 477–485. https://doi.org/10.1016/j.tibtech.2004.07.001
3. APHA, 2023. Standard Methods for the Examination of Water and Wastewater™, 24th ed. American Public Health Association, American Water Works Association, and Water Environment Federation. Lipps WC, Braun-Howland EB, Baxter TE, eds.
4. Atasoy, M., Owusu-Agyeman, I., Plaza, E., Cetecioglu, Z., 2018. Bio-based volatile fatty acid production and recovery from waste streams: Current status and future challenges. Bioresour Technol 268, 773–786. https://doi.org/10.1016/j.biortech.2018.07.042
5. Bastidas-Oyanedel, J.-R., Bonk, F., Thomsen, M.H., Schmidt, J.E., 2015. Dark fermentation biorefinery in the present and future (bio)chemical industry. Rev Environ Sci Biotechnol 14, 473–498. https://doi.org/10.1007/s11157-015-9369-3
6. Blonskaja, V., Menert, A., Vilu, R., 2003. Use of two-stage anaerobic treatment for distillery waste. Advances in Environmental Research 7, 671–678. https://doi.org/10.1016/S1093-0191(02)00038-2

7. Buitrón, G., Martínez-Valdez, F.J., Ojeda, F., 2019. Biogas Production from a Highly Organic Loaded Winery Effluent Through a Two-Stage Process. Bioenergy Res 12, 714–721. https://doi.org/10.1007/s12155-019-09984-7
8. Carrillo-Reyes, J., Tapia-Rodríguez, A., Buitrón, G., Moreno-Andrade, I., Palomo-Briones, R., Razo-Flores, E., Aguilar Juárez, O., Arreola-Vargas, J., Bernet, N., Maluf Braga, A.F., Braga, L., Castelló, E., Chatellard, L., Etchebehere, C., Fuentes, L., León-Becerril, E., Méndez-Acosta, H.O., Ruiz-Filippi, G., Tapia-Venegas, E., Trably, E., Wenzel, J., Zaiat, M., 2019. A standardised biohydrogen potential protocol: An international round robin test approach. Int J Hydrogen Energy 44, 26237–26247. https://doi.org/10.1016/j.ijhydene.2019.08.124
9.
10. Candry, P., Radić, L., Favere, J., Carvajal-Arroyo, J.M., Rabaey, K., Ganigué, R., 2020. Mildly acidic pH selects for chain elongation to caproic acid over alternative pathways during lactic acid fermentation. Water Res 186, 116396. https://doi.org/10.1016/J.WATRES.2020.116396
11. Central Bank of Ireland, 2023. Euro Exchange Rate | Central Bank of Ireland [WWW Document]. Annual Averages / Meáin bhliantúla 2001-present | xls 291 KB. URL https://www.centralbank.ie/statistics/interest-rates-exchange-rates/exchange-rates (accessed 5.3.23).
12. Crutchik, D., Franchi, O., Caminos, L., Jeison, D., Belmonte, M., Pedrouso, A., Val del Rio, A., Mosquera-Corral, A., Campos, J.L., 2020. Polyhydroxyalkanoates (PHAs) Production: A Feasible Economic Option for the Treatment of Sewage Sludge in Municipal Wastewater Treatment Plants? Water (Basel) 12, 1118. https://doi.org/10.3390/w12041118

13. DATAtab Team, 2023. DATAtab: Online Statistics Calculator. DATAtab e.U. Graz, Austria. URL https://datatab.net
14. Dauptain, K., Schneider, A., Noguer, M., Fontanille, P., Escudie, R., Carrere, H., Trably, E., 2021. Impact of microbial inoculum storage on dark fermentative H2 production. Bioresour Technol 319, 124234. https://doi.org/10.1016/j.biortech.2020.124234
15. de Groof, V., Coma, M., Arnot, T., Leak, D.J., Lanham, A.B., 2021. Selecting fermentation products for food waste valorisation with HRT and OLR as the key operational parameters. Waste Management 127, 80–89. https://doi.org/10.1016/j.wasman.2021.04.023
16. DEFRA. (2022). *Greenhouse gas reporting: conversion factors 2022*. https://www.gov.uk/government/publications/greenhouse-gas-reporting-conversion-factors-2022
17. Deng, C., Lin, R., Cheng, J., Murphy, J.D., 2019. Can acid pre-treatment enhance biohydrogen and biomethane production from grass silage in single-stage and two-stage fermentation processes? Energy Convers Manag 195, 738–747. https://doi.org/10.1016/j.enconman.2019.05.044
18. Department of Environment, C. and C., 2023. Ireland's Long-term Strategy on Greenhouse Gas Emissions Reduction. URL https://www.gov.ie/en/publication/e4e81-long-term-strategy-on-greenhouse-gas-emissions-reductions/
19. Dinh, V.N., Leahy, P., McKeogh, E., Murphy, J., Cummins, V., 2021. Development of a viability assessment model for hydrogen production from dedicated offshore wind farms. Int J Hydrogen Energy 46, 24620–24631. https://doi.org/10.1016/j.ijhydene.2020.04.232

20. IBEC, 2021. Irish Beer Market Report 2021. URL https://www.ibec.ie/drinksireland/news-insights-and-events/news/2022/05/09/beer-market-report-2021
21. Eurostat, 2022. Road freight transport by journey characteristics [WWW Document]. Statistics Explained. URL https://ec.europa.eu/eurostat/statistics-explained/index.php?title=Road_freight_transport_by_journey_characteristics#Empty_runnings_of_road_freight_vehicles (accessed 5.31.23).
22. Gerardi, M.H., 2003. The Microbiology of Anaerobic Digesters. The Microbiology of Anaerobic Digesters. https://doi.org/10.1002/0471468967
23. Gray, N., O'Shea, R., Wall, D., Smyth, B., Lens, P.N.L., Murphy, J.D., 2022. Batteries, fuel cells, or engines? A probabilistic economic and environmental assessment of electricity and electrofuels for heavy goods vehicles. Advances in Applied Energy 8, 100110. https://doi.org/10.1016/J.ADAPEN.2022.100110
24. Gunes, B., Stokes, J., Davis, P., Connolly, C., Lawler, J., 2019. Pre-treatments to enhance biogas yield and quality from anaerobic digestion of whiskey distillery and brewery wastes: A review. Renewable and Sustainable Energy Reviews 113, 109281. https://doi.org/10.1016/j.rser.2019.109281
25. Hackula, A., O'Shea, R., Murphy, J.D., Wall, D.M., 2023a. Design, Construction, and Concept Validation of a Laboratory-Scale Two-phase Reactor to Valorize Whiskey Distillery By-products. ACS Engineering Au. https://doi.org/10.1021/ACSENGINEERINGAU.3C00006
26. Hackula, A., Shinde, R., Hickey, D., O'Shea, R., Murphy, J.D., Wall, D.M., 2023b. Two-phase anaerobic digestion for enhanced valorisation of whiskey distillery by-products. Bioresour Technol 129239. https://doi.org/10.1016/J.BIORTECH.2023.129239

27. IndiaMART. (2023, December 1). *IndiaMART*. https://www.indiamart.com/proddetail/valeric-acid-4300649448.html?pos=7&kwd=valeric%20acid&tags=CC||||7533.29|Price|product|||TS
28. International Energy Agency, 2019. Putting CO2 to Use Creating value from emissions. URL https://www.iea.org/reports/putting-co2-to-use
29. Kang, X., Lin, R., Li, L., Wu, B., Deng, C., O'Shea, R., Sun, Y., Murphy, J.D., 2021. Assessment of pretreatment and digestion temperature on anaerobic digestion of whiskey byproducts and microbial taxonomy. Energy Convers Manag 243, 114331. https://doi.org/10.1016/j.enconman.2021.114331
30. Liger-Belair, G., Cilindre, C., 2021. How Many CO2Bubbles in a Glass of Beer? ACS Omega 6, 9672–9679. https://doi.org/10.1021/ACSOMEGA.1C00256
31. Long, A., Bose, A., O'Shea, R., Monaghan, R., Murphy, J.D., 2021. Implications of European Union recast Renewable Energy Directive sustainability criteria for renewable heat and transport: Case study of willow biomethane in Ireland. Renewable and Sustainable Energy Reviews 150, 111461. https://doi.org/10.1016/j.rser.2021.111461
32. Moses, D.R., 2014. Performance evaluation of continuous screw press for extraction soybean oil. American Journal of Science and Technology 1, 238–242.
33. Muzny, C.D., Huber, M.L., Kazakov, A.F., 2013. Correlation for the Viscosity of Normal Hydrogen Obtained from Symbolic Regression. J Chem Eng Data 58, 969–979. https://doi.org/10.1021/je301273j

34. National Institute of Standards and Technology, 2023. Isobaric Properties for Carbon dioxide [WWW Document]. https://webbook.nist.gov/cgi/fluid.cgi?P=1&TLow=0&THigh=0&TInc=&Digits=5&ID=C124389&Action=Load&Type=IsoBar&TUnit=C&PUnit=atm&DUnit=kg%2Fm3&HUnit=kJ%2Fmol&WUnit=m%2Fs&VisUnit=uPa*s&STUnit=N%2Fm&RefState=DEF (accessed 3.7.23).
35. O'Shea, R., Lin, R., Wall, D.M., Browne, J.D., Murphy, J.D., 2020. Using biogas to reduce natural gas consumption and greenhouse gas emissions at a large distillery. Appl Energy 279, 115812. https://doi.org/10.1016/j.apenergy.2020.115812
36. Owusu-Agyeman, I., Plaza, E., & Cetecioglu, Z., 2020. Production of volatile fatty acids through co-digestion of sewage sludge and external organic waste: Effect of substrate proportions and long-term operation. *Waste Management*, *112*, 30–39. https://doi.org/10.1016/j.wasman.2020.05.027
37. Riahi, Z., Hraiech, I., Sautet, J.C., Ben Nasrallah, S., 2022. Experimental and numerical study of oxidant effect on hythane combustion. Int J Hydrogen Energy 47, 8105–8117. https://doi.org/10.1016/J.IJHYDENE.2021.12.155
38. Ribau Teixeira, M., Guarda, E.C., Freitas, E.B., Galinha, C.F., Duque, A.F., Reis, M.A.M., 2020. Valorization of raw brewers' spent grain through the production of volatile fatty acids. N Biotechnol 57, 4–10. https://doi.org/10.1016/j.nbt.2020.01.007
39. Salomone, F., Giglio, E., Ferrero, D., Santarelli, M., Pirone, R., Bensaid, S., 2019. Techno-economic modelling of a Power-to-Gas system based on SOEC electrolysis and CO2 methanation in a RES-based electric grid. Chemical Engineering Journal 377, 120233. https://doi.org/10.1016/j.cej.2018.10.170

40. Sganzerla, W.G., Sillero, L., Forster-Carneiro, T., Solera, R., Perez, M., 2022. Determination of Anaerobic Co-fermentation of Brewery Wastewater and Brewer's Spent Grains for Bio-hydrogen Production. Bioenergy Res 1, 1–11. https://doi.org/10.1007/S12155-022-10486-2
41. Sittijunda, S., Baka, S., Jariyaboon, R., Reungsang, A., Imai, T., Kongjan, P., 2022. Integration of Dark Fermentation with Microbial Electrolysis Cells for Biohydrogen and Methane Production from Distillery Wastewater and Glycerol Waste Co-Digestion. Fermentation 8, 537. https://doi.org/10.3390/fermentation8100537
42. Solera, R., Romero, L.I., Sales, D., 2002. The Evolution of Biomass in a Two-phase Anaerobic Treatment Process During Start-up. Chem Biochem Eng Q. 16 (1) 25-29.
43. Transport & Environment. ,2020. *How to decarbonise the UK's freight sector by 2050*. https://www.transportenvironment.org/discover/how-decarbonise-uks-freight-sector-2050/
44. Uddin, Z., Yu, B.-Y., Lee, H.-Y., 2022. Evaluation of alternative processes of CO2 methanation: Design, optimization, control, techno-economic and environmental analysis. Journal of CO2 Utilization 60, 101974. https://doi.org/10.1016/j.jcou.2022.101974
45. Vanyan, L., Cenian, A., Trchounian, K., 2022. Biogas and Biohydrogen Production Using Spent Coffee Grounds and Alcohol Production Waste. Energies (Basel) 15, 5935. https://doi.org/10.3390/en15165935
46. Wang, H., Xu, J., Sheng, L., Liu, X., Lu, Y., Li, W., 2018. A review on bio-hydrogen production technology. Int J Energy Res 42, 3442–3453. https://doi.org/10.1002/er.4044

47. Yang, M., Watson, J., Wang, Z., Si, B., Jiang, W., Zhou, B., Zhang, Y., 2022. Understanding and design of two-stage fermentation: A perspective of interspecies electron transfer. Renewable and Sustainable Energy Reviews 168, 112891. https://doi.org/10.1016/j.rser.2022.11

6.0 Assessing two-phase anaerobic digestion systems for demand-driven electricity and biobutanol transport fuel at a large distillery

Anga Hackula [a, b], Rajas Shinde [a, b, c], Richard O'Shea [a, b], Jerry D. Murphy [a b], David M. Wall [a, b]

[a] SFI MaREI Centre for Energy, Climate and Marine, Environmental Research Institute, University College Cork, Cork, Ireland

[b] Civil, Structural and Environmental Engineering, School of Engineering and Architecture, University College Cork, Cork, Ireland

[c] Crops, Environment and Land Use Program, Crop Science Department, Teagasc, Oak Park, Carlow, R93XE12 Co. Carlow, Ireland

Abstract

Decarbonisation of industry will necessitate innovative technological solutions that allow for both reduced carbon footprint and security of supply. Biogas systems can allow electricity production on-demand. This study evaluated and compared different two-phase anaerobic digestion systems for continuous volatile fatty acid (VFAs) production and demand-driven biogas production at a whiskey distillery using byproducts as feedstock. The systems analysed were a two-phase continuously stirred tank reactor (CSTR) and a leach bed-expanded granular sludge bed reactor (LBR-EGSB) system. Both systems exhibited continuous VFA production (up to 10.4 g. L^{-1}_{VFA} made up of primarily butyric acid and acetic acid) and rapid biogas production, achieving peak flow rates within 30 minutes. The peak biogas production from the demand-driven EGSB was 3.1 L. $L^{-1}_{reactor}$. d^{-1} compared to the CSTR, which recorded 1.8 L. $L^{-1}_{reactor}$. d^{-1}. Three kinetic models of both systems were assessed, which were able to describe the cumulative biogas production. A theoretical evaluation of processing butyric acid into butanol, to be blended with diesel, could produce a more sustainable transport fuel than diesel, reducing distillery-associated transport emissions by 16 %.

6.1 Introduction

To combat climate change, the European Commission released the REPowerEU plan, which seeks to increase the production and use of clean, renewable energy and reduce dependency on fossil fuels (European Commission, 2022). Geopolitical instability has highlighted the need for energy security within the EU and the importance of diversifying energy supply (Sokhanvar and Bouri, 2022). While solar and wind energy provide clean, renewable electricity, their intermittency and non-dispatchability require significant backup generation to fulfil power demand (Steinke et al., 2013). Additionally, various sectors, such as the food and beverage sector, cannot be fully electrified and require fossil fuels for their manufacturing processes (Paltsev et al., 2021). To remain competitive with the introduction of demand-side reduction measures, especially during peak hours, the adoption of alternative energy sources becomes imperative (European Parliamentary Research Service, 2022). Anaerobic digestion (AD) has the potential to fulfil the energy requirements of the food and beverage sector and provide demand-driven electricity for commercial users.

AD systems convert organic residues into valuable streams such as volatile fatty acids (VFAs) and biogas (Abad et al., 2019). Volatile fatty acids, such as acetic acid and butyric acid, can be used as platform chemicals for an array of high-value products such as bio-preservatives (Dishisha et al., 2012), bioplastics, and biofuels (Ahmad et al., 2023). For example, butyric acid can be further processed into butanol, which can be blended with diesel, up to 20 % butanol on a volume basis,

and used directly as a transport fuel without modifying the engine (Tipanluisa et al., 2021). Biogas (ca. 55 % methane (CH_4) and ca. 45 % carbon dioxide (CO_2)) can be used in combined heat and power (CHP) systems or further processed (via CO_2 removal) to biomethane comparable to natural gas quality (Hilkiah Igoni et al., 2008). Biomethane can be directly injected into the gas grid to reduce dependence on imported natural gas, thus improving energy security. Through AD, the food and beverage sector could decarbonise their processes and potentially collaborate with VFA-utilising industries, such as the pharmaceutical industry, to decarbonise their supply chains and reduce their energy insecurity.

Demand-driven AD systems seek to produce biogas to satisfy biogas demand at specific times. This approach is achieved by altering the feeding regime to the digester to produce enhanced levels of biogas when the demand is required (Szarka et al., 2013). Demand-driven biogas production is anomalous to traditional AD systems, which are typically continuously fed (Szarka et al., 2013); demand-driven biogas involves feeding digesters at enhanced levels for particular periods. Biogas storage is an alternative solution for (or an enhancement of) on-demand biogas utilisation; however, demand-driven biogas systems can potentially reduce the biogas storage capacity required at an AD facility and thus reduce capital costs (Hahn et al., 2014). The continuous operation allows for steady, constant biogas production. However, the approach would reduce the available fermentation broth for VFAs.

Operators of demand-driven AD systems can produce electricity at peak hours to benefit from peak electricity rates and, during off-peak hours, produce high-value VFAs (Wall et al., 2016). This approach would complement demand-side reduction measures introduced by electricity providers (European Parliamentary Research Service, 2022). The critical operational characteristics of such systems are the biogas lag time, the time taken to reach maximum biogas flow rates and the maximum cumulative biogas production. Shorter biogas lag times, high maximum biogas flow rates and optimised cumulative production are desired in demand-driven AD systems to enable quicker response to demand-side reduction measures. Several AD systems and feedstocks have been studied for demand-driven operation. A previous study evaluated mono-digestion of four feedstocks (grass silage, food waste, seaweed, and dairy cattle slurry) in single-phase continuously stirred tank reactors (CSTRs) for demand-driven operation and found a 30-minute lag phase to reach peak biogas flow rates from cattle slurry (O'Shea et al., 2016). The study evaluated semi-continuous reactor feeding and developed a kinetic model determining the dispatch time to operate a CHP unit. Such models provide operators with a scientific approach to demand-driven AD operation and biogas production forecasting, as opposed to conjectures in the absence of empirical data. A limitation of the study was that it focused on a single reactor type. Alternative reactors, such as the leach bed reactor, allow for hydrolysis of high-solid feedstocks and may also be suitable for such applications. Further studies have evaluated sugar beet silage, maize silage, and grass silage and reported a wide range of maximum gas production from single-phase demand-driven biogas systems from 0.5 $L_{biogas}.\ L^{-1}_{reactor}.d^{-1}$ (Ahmed and Kazda, 2017) to 5.5 $L_{biogas}.\ L^{-1}_{reactor}.d^{-1}$ (Mauky et al., 2015).

Two-phase AD systems, which split the anaerobic digestion process, seek to provide optimum conditions for the respective AD steps so that the microbial consortia can thrive (Pohland and Ghosh, 2009). Typically, hydrolysis and acidogenesis (producing hydrogen, carbon dioxide and VFAs) take place in the first reactor, and acetogenesis and methanogenesis (producing biogas) occur in the second reactor (Castilla-Archilla et al., 2021). Two-phase systems that operate in a demand-driven biogas manner have been evaluated previously in the literature. A previous study evaluated maize silage in a leach bed reactor with a downstream anaerobic filter (LBR-AF) (Linke et al., 2015). However, the focus was on optimising methane yields (330 L CH_4. kg^{-1} VS) and not VFA production. Prior studies also investigated grass silage in a leach bed reactor with a downstream upflow anaerobic sludge blanket (LBR-UASB) and hypothesized the operation of a demand-driven biogas system (Wall et al., 2016) where VFAs were produced in the LBR and when biogas demand was required, the VFA rich leachate would be fed into the UASB (Shinde et al., 2023). However, both studies did not evaluate the conversion of VFAs to other products. Within the food and beverage industry, several studies have evaluated the amenability of distillery by-products (Barrena et al., 2018) and brewery residues (Ribau Teixeira et al., 2020) in AD systems. However, there is a gap in the literature where distillery by-products are evaluated and compared in different two-phase systems for continuous VFA production and demand-driven biogas production. No prior studies have compared or modelled different AD systems processing distillery feedstocks for demand-driven biogas production. Furthermore, no prior studies have evaluated the potential of further processing the VFAs from the fermentation broth into butanol for use in transport or the potential emissions savings which could be achieved. This work aims to address this knowledge gap.

This study investigates the demand-driven biogas operation of a leach bed reactor with a downstream expanded granular sludge bed (LBR-EGSB) and a two-phase CSTR when fed with distillery by-products. This approach would benefit a distillery seeking to valorise VFAs and biogas production for electricity generation on-demand through a CHP unit. The topology for this approach is shown in Figure 6.1. The specific objectives of this study are: (1) to operate and compare a two-phase CSTR and the LBR-EGSB in a demand-driven manner; (2) to assess three kinetic models to describe cumulative biogas production from the whiskey by-products digested in the demand-driven biogas systems; and (3) to explore the potential of biobutanol production from butyric acid within the VFAs to blend with fossil fuels for transportation.

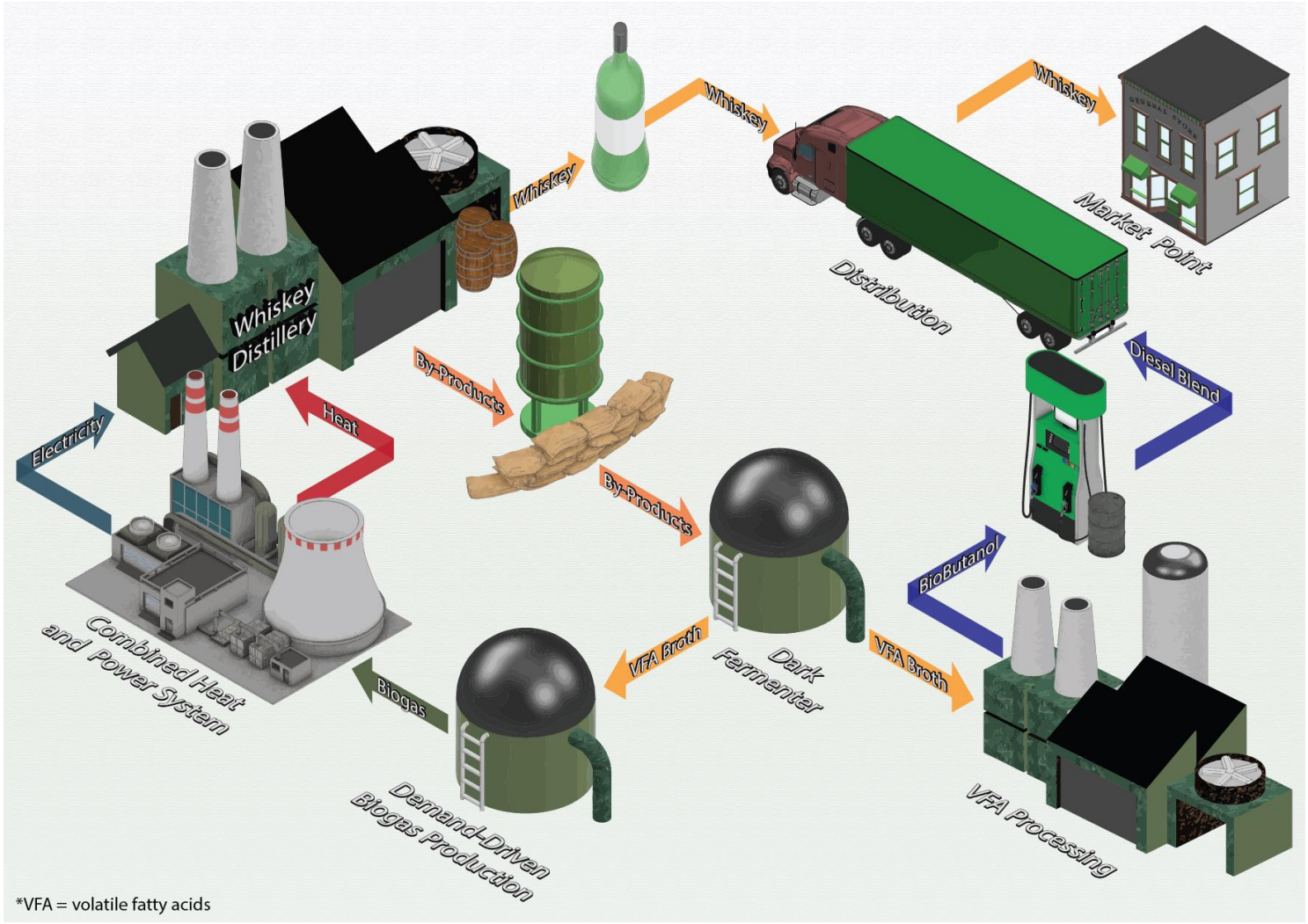


Figure 6.1: Proposed whiskey distillery topology for continuous VFAs and demand-driven biogas production

6.2 Materials and methods

6.2.1 Methods and analysis overview

The overall process of the experiments and analysis to achieve the objectives of the study are illustrated in Figure 6.2. The feedstock, whiskey by-products, and inoculum used in the study are characterised and detailed in Section 6.2.2. Two systems were assessed, namely a two-phase CSTR and an LBR-EGSB. The inoculation of all the reactors is detailed in Section 6.2.2. The operation of the CSTR and the LBR-EGSB is detailed in Sections 6.2.3 and 6.2.4, respectively.

Two-phase digestion was evaluated as follows: the feedstock was fed to the dark fermenters to produce VFA-rich effluent. The dark fermenters were monitored throughout the experimental trials, as indicated in Figure 6.2 and detailed in Section 6.2.6. The effluent from the dark fermenters was fed to the inoculated methanogenic reactors of both the CSTR and LBR-EGSB systems in a demand-driven manner. These methanogenic reactors were continuously monitored, as described in Figure 6.2 and Section 6.2.6. The data collected during the experimental trials was analysed as per Figure 6.2 and Section 6.2.6 to evaluate the performance, stability, and comparison of both systems.

A theoretical estimation of the potential to blend biobutanol for use as a transport fuel was made based on the processed data collated from the dark fermenters and assumptions from the literature (Figure 6.2). The assumptions, which provide an accurate representation of an operating distillery, are outlined in Section 3.6 and further detailed in Appendix D.2. The overall analysis estimates the potential biobutanol yield, emissions savings, and monetary savings for the distillery. Three kinetic models (Section 6.2.8) were used to assess their ability to describe and

compare the cumulative biogas production of both demand-driven methanogenic reactors.

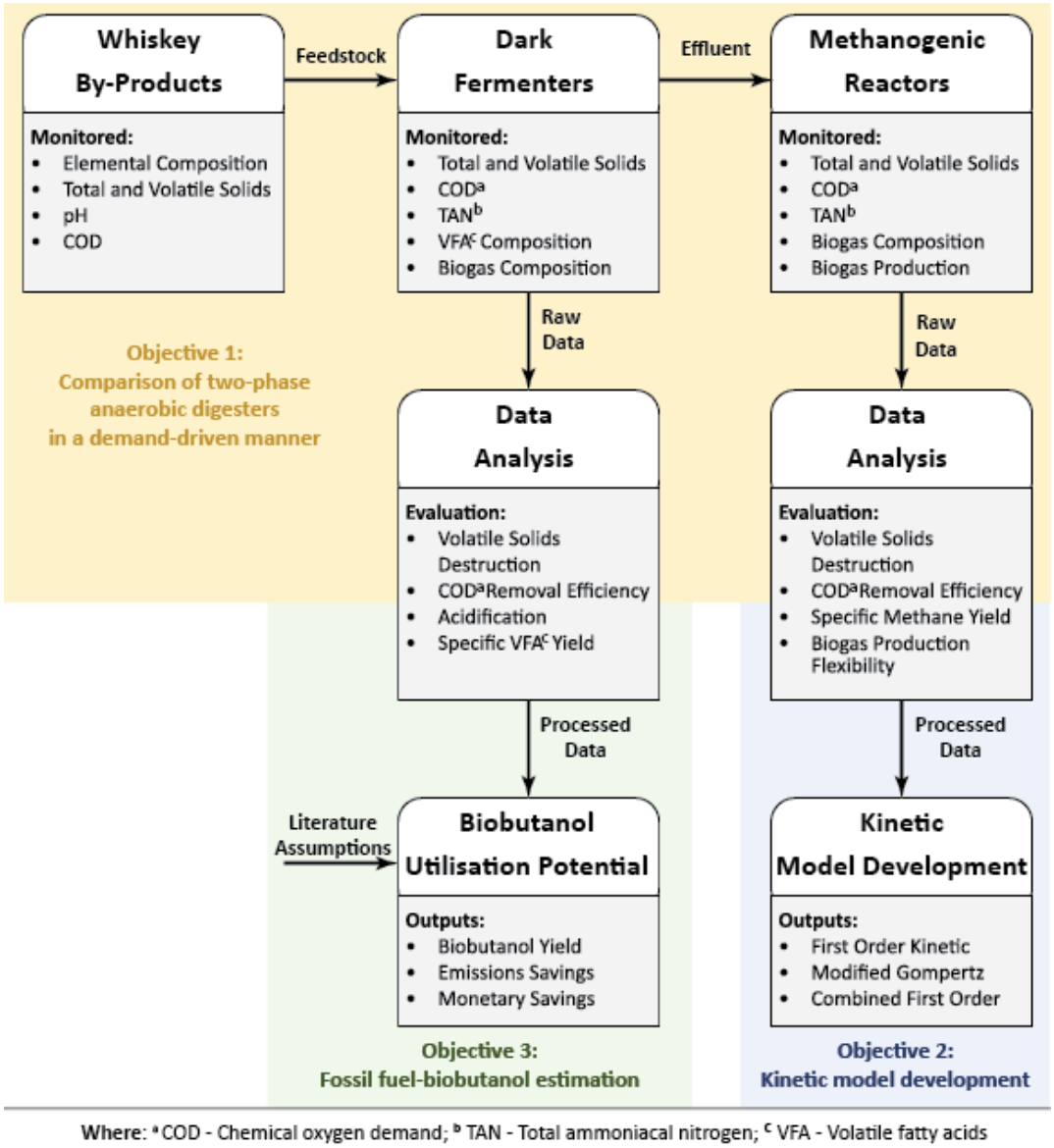


Figure 6.2: Methods and analysis overview

6.2.2 Inocula and whiskey by-product characteristics

The first CSTR (C1a) in the two-phase CSTR system, which served as the dark fermenter, was inoculated with thermally pretreated (100 ^{o}C for 30 minutes) cattle slurry to inhibit methanogens. The dark fermenter inoculum was adjusted to pH 6.0 with 1 M HCl (Mohan et al., 2012). The second CSTR, which served as the

methanogenic reactor, was seeded with raw cattle slurry sourced from a local farm in Co. Cork, Ireland. The total solids (TS) and volatile solids (VS) of the inoculum were 2 % on a wet weight basis (ww) and 1.5 %ww, respectively.

The leach bed reactor (LBR), which served as the dark fermenter of the LBR-EGSB, did not require inoculation. The expanded granular sludge bed (EGSB), which served as the methanogenic reactor and was considered for demand-driven biogas operation. The EGSB was inoculated with 3 L of granular sludge sourced from a local mesophilic EGSB processing cheese whey in Co. Cork, Ireland. The remainder of the EGSB was filled with distilled water. The TS and VS content of the granular sludge was 11 %ww and 10 %ww, respectively.

The mixed whiskey by-products were defined in a previous study (Hackula et al., 2023a). Briefly, four substates are generated at the distillery: draff (5 %ww), cake maize (the solid fraction of thick stillage) (10 %ww), centrate (the liquid fraction of thick stillage) (34 %ww) and thin stillage (51 %ww). The design attributes of the CSTR allowed for the feedstock to be introduced into the reactor as a mixture of the whiskey by-products. In contrast, with the LBR-EGSB, the feedstock was introduced as distinct solids and liquids separately. The whiskey by-product solids consist of draff and cake maize. The whiskey by-product liquids consist of centrate and thin stillage.

Nonetheless, in both reactor configurations, the proportions of these by-products reflected the annual production at the distillery. Table 6.1 shows the characteristics of the mixed whiskey by-products and the individual substrates. The pH of the

whiskey by-product liquids was adjusted to 7.5 with 6 M NaOH before experiments to maintain the reactors' pH above 5.

Table 6.1: Characteristics of the mixed whiskey by-products (adapted from ((Hackula et al., 2023a)))

		Solids		Liquids		
	Unit	**Draff**	**Cake maize**	**Centrate**	**Thin stillage**	**Mixed whiskey by-products**
TS[a]	%ww	27	29	4	3	7
VS[b]	% TS	96	97	89	89	94
pH	pH	/	/	3.8	4.3	4.0
COD[c]	g. L^{-1}	/	/	34.6	33.4	/
CHON[d]						$C_{12}H_{19.8}O_{7.9}N$

[a] TS = total solids; [b] VS = volatile solids; [c] COD = soluble chemical oxygen demand; [d] CHON = chemical composition

6.2.3 Demand-driven operation CSTR trials

Figure 6.3 shows the operation of the two-phase CSTR system. Two Bioprocess Control™ BioReactor Simulator-CSTR 2G reactors in series (C1a and C1b) were used for the CSTR experimental trials. The first CSTR (C1a) served as the dark fermenter (for VFA production) and was manually pulse-fed the mixed whiskey by-products throughout the trial. C1a was operated at an organic loading rate (OLR) of 15.0 gVS. L^{-1}. d^{-1} and a hydraulic retention time (HRT) of 4 days and pulse-fed once a day throughout the experimental trials (Hackula et al., 2024). Once the chemical oxygen demand (COD) of C1a reached stable conditions within the last 3 days (<5 % variance), which took 12 days, the effluent was manually collected each day and added to a combined VFA tank. C1a was operated for 52 days (13 HRTs).

The second CSTR (C1b) served as the methanogenic reactor and was considered for demand-driven biogas operation. C1b was pulse-fed with effluent from the VFA tank. C1b had an average OLR of ca. 3.4 g VS. L^{-1}. d^{-1} (2.3 g COD. L^{-1}. d^{-1}) and an HRT of 25 days. The HRT of the two-phase system was ca. 29 days. C1b was

acclimatised for one HRT (25 days) prior to the collection of data in the second HRT, resulting in a total of 50 days of operation (2 HRTs). The methanogenic reactor (C1b) operation for demand-driven biogas operation was achieved by pulse-feeding the maximum organic load every 24 hours. The effluent of C1b was discarded after experiments.

The operating volumes of C1a and C1b were 1L and 1.6L, respectively. Mesophilic conditions (37±0.5^{o}C) were maintained throughout the trials by partially submerging the reactors in a thermostatic water bath. A Bioprocess Control^{TM} BRS-B unit was used after the gas outlet ports to continuously measure the biogas production at a standard temperature and pressure (STP) of 0^{o}C and 101.325 kPa.

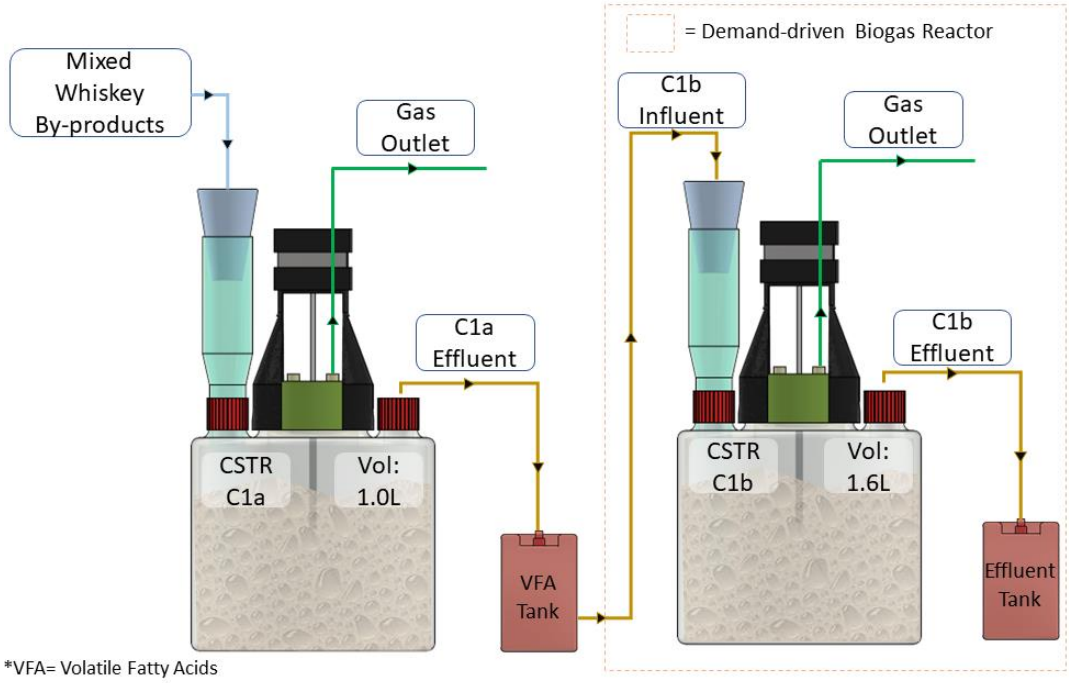


Figure 6.3: Operation of the two-phase CSTR

6.2.4 LBR-EGSB demand-driven operation trials

Figure 6.4 illustrates the LBR-EGSB system. The LBR-EGSB system was fully detailed in a previous work by the authors (Hackula et al., 2023a). In short, the

whiskey by-product liquids, also the leachate, were pumped (Figure 6.4 - pump 1) into the LBRs and leached organic matter from the whiskey by-product solids, increasing the concentration of VFAs in the leachate. The leachate was then pumped into a VFA tank (Figure 6.4 - pump 2) and subsequently (Figure 6.4 - pump 3) into the EGSB, where biogas was produced. The full system consisted of 3 LBRs (5 L operating volume each) and a single EGSB (6 L operating volume). The LBRs were sequentially batch-fed 980g of whiskey by-product solids every 7 days; for instance, on Day 0 - LBR 1 was fed; on day 7 - LBR 2 was fed; on day 14 - LBR 3 was fed; on day 21 - LBR 1 was emptied and fed, and so on. Initially, the leachate holding tank was filled with fresh whiskey by-product liquids. The leachate was recirculated into each LBR (Figure 6.4 - pump 1), resulting in flooding within the LBRs. This operation resulted in an increase of VFA content in the leachate. A peristaltic pump (Figure 6.4 - pump 2) continuously introduced 5.9 L of fresh whiskey by-product liquids per week into the leachate holding tank. The same volume of leachate was continuously pumped (Figure 6.4 - pump 2) into a VFA tank to maintain a constant volume in the leachate tank. The EGSB was operated in a demand-driven manner by pulse-feeding leachate into the reactor once every 24 hours to achieve the maximum OLR of 3.8 g COD. L^{-1}. d^{-1}. The upflow velocity of the EGSB of 0.85 m. h^{-1} was achieved through high recirculation (Figure 6.4 - pump 4). The Bioprocess Control^{TM} BRS-B unit continuously measured the biogas production from the EGSB at STP of 0 ^{o}C and 101.325 kPa. Biogas production of the LBRs was not measured as primarily CO_2 was expected; however, the biogas composition was evaluated.

6.2.5 Evaluating biogas production flexibility

Biogas production flexibility was assessed using a combination of methods described previously in the literature (Dotzauer et al., 2019). All biogas data was collected and processed in 15-minute intervals, taken from the beginning of the second HRT until the end of the experimental trials. The biogas production rate (Y_{bpr}) and the average daily biogas production rate ($Y_{bpr_{ave}}$) were calculated using the following equations (Shinde et al., 2023):

$$Y_{bpr} = \frac{Biogas\ in\ 15\ \text{min}\ intervals \times 96}{V_{reactor}} \quad (L_{biogas}.\ L^{-1}{}_{r}.\ d^{-1})$$

$$Y_{bpr_{ave}} = \frac{\sum Y_{bpr}\ daily\ 15\ \text{min}\ intervals}{96} \quad (L_{biogas}.\ L^{-1}{}_{r}.\ d^{-1})$$

Where: Y_{bpr} is the biogas production rate in $L_{biogas}.\ L^{-1}{}_{reactor}.\ d^{-1}$ ($L_{biogas}.\ L^{-1}{}_{r}.\ d^{-1}$), 96 is the number of 15-minute intervals per day, $V_{reactor}$ is the volume of the reactor in L (L_r), and $Y_{bpr_{ave}}$ is the average daily biogas production rate ($L_{biogas}.\ L^{-1}{}_{r}.\ d^{-1}$).

A 'ramp-up' phase was considered whenever Y_{bpr} increased above $Y_{bpr_{ave}}$. The 'ramp down' phase was considered as the decline back to and below $Y_{bpr_{ave}}$.

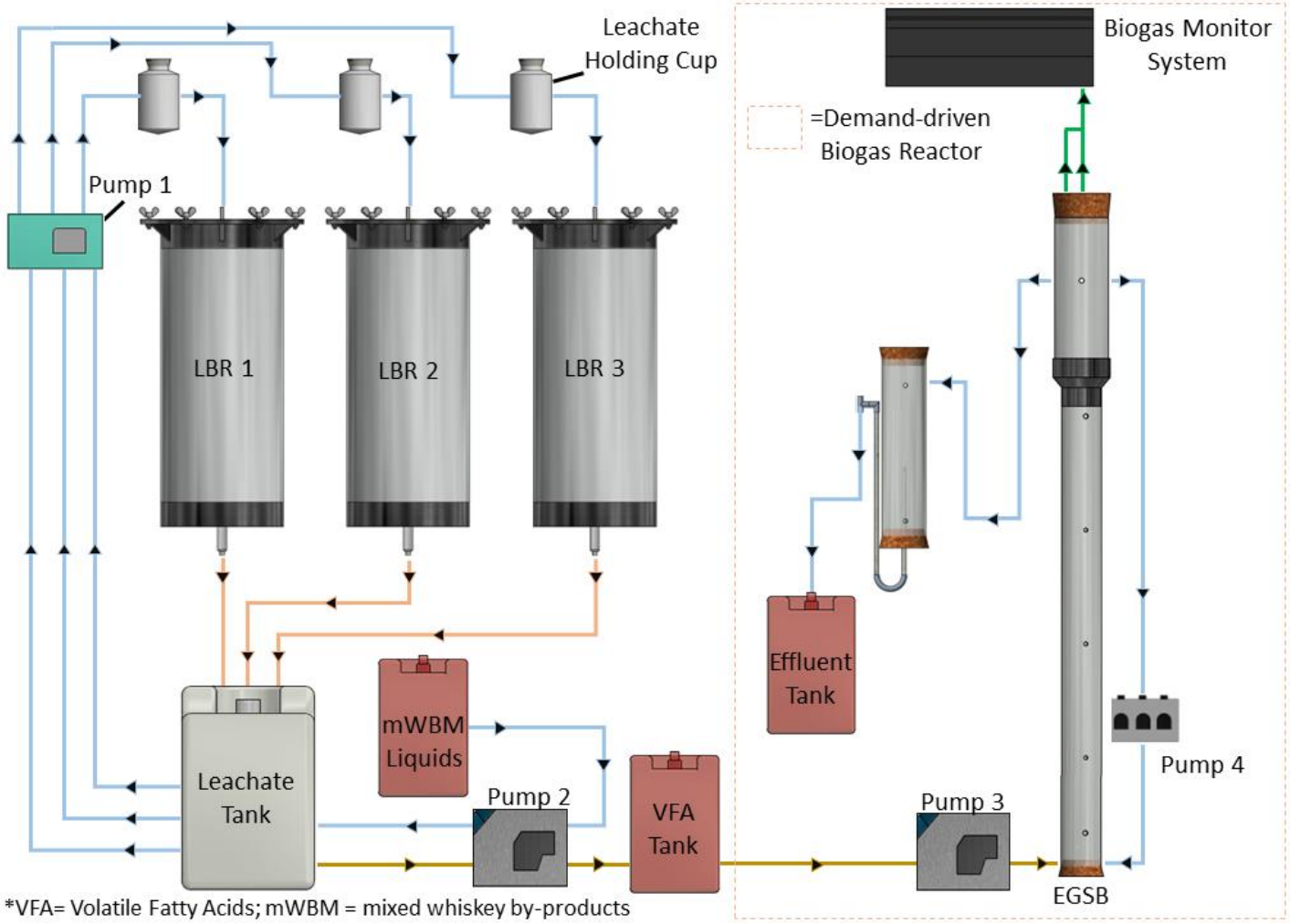


Figure 6.4: Operational overview of the LBR-EGSB (adapted from (Hackula et al., 2023b))

The flexibility indicators were calculated using the following equations (Dotzauer et al., 2019):

$$m_{bpr_{up}} = \frac{\left(Y_{bpr_{peak}} - Y_{bpr_{ave}}\right)\times 100}{Y_{bpr_{peak}} \times \Delta t} \quad (\%.\ h^{-1})$$

$$m_{bpr_{down}} = \frac{\left(Y_{bpr_{ave}} - Y_{bpr_{peak}}\right)\times 100}{Y_{bpr_{peak}} \times \Delta t} \quad (\%.\ h^{-1})$$

Where: $m_{bpr_{up}}$ is the slope of the ramp-up in percentage per hour (%. h^{-1}), $m_{bpr_{down}}$ is the slope of the ramp down (%. h^{-1}), $Y_{bpr_{peak}}$ is the maximum 15-minute biogas production rate over the average daily biogas production rate ($Y_{bpr_{ave}}$), and the difference in time (Δt) denotes the hours (h) taken to achieve the respective change.

The amplitude (the difference between peak gas production ($Y_{bpr_{peak}}$) and the lowest gas production within 24 hours) was calculated by the difference between $Y_{bpr_{peak}}$ and the minimum gas production rate ($Y_{bpr_{min}}$), divided by $Y_{bpr_{peak}}$. The peak production phase was defined as the region where gas production was above $Y_{bpr_{ave}}$.

6.2.6 Analytical methods

The TS and VS content of all samples were measured using standard methods 2540 G (APHA, 2022). An elemental analyser furnished with a thermal conductivity detector was used to evaluate the elemental composition of the substrates. Reagecon COD cuvette Vials (420721) and a Hach Lange spectrometer (DR 3900) were used to evaluate the COD concentrations of both CSTR effluents, the leachate tank, and EGSB effluent. Total ammoniacal nitrogen (TAN) was evaluated using the Hach

Lange AmVer™ Salicylate Test 'N Tube ™ Method (Hach Lange 10031) and the DR3900spectrometer.

A Mettler Toledo™ F20 pH meter was used to evaluate the effluent pH. The VFA concentration and composition of the samples were evaluated by an Agilent GC (Agilent Technologies 7890B) equipped with a DB-FFAP column (Ø 0.32mm x 50m) and a flame ionisation detector. VFA samples were collected and stored at -20°C prior to analyses. Prior to testing, the VFA samples were thawed at room temperature and centrifuged at 12,000 rpm for 10 minutes. Both the COD and TAN samples were prepared similarly prior to analysis. The COD removal efficiency (COD_{eff}) and VS destruction efficiency (VS_{eff}) of the reactors were evaluated as follows:

$$X_{eff} = \frac{(X_{in} - X_{out})}{X_{in}} \times 100$$

Where: X_{in} is the reactor influent COD or VS prior to digestion, COD_{out} is the COD or VS of the reactor effluent, and X_{eff} is the COD removal efficiency (COD_{eff}) or the VS destruction efficiency (VS_{eff})

Acidification was assessed by converting the VFAs into their COD equivalent (COD_{VFA}) using conversion factors reported in prior studies and dividing COD_{VFA} by the COD measured within the reactor (Khatami et al., 2021). The conversion factors can be found in Appendix D.1. Acidification was only assessed for C1a and the LBR.

The alkalinity ratio (FOS/TAC) was used to evaluate the stability of the mesophilic reactors (Drosg, 2013). The FOS/TAC was measured using an automatic dual-point titration method according to the Nordmann method and a Hach Lange TitraLab

AT1000 Series that evaluates the ratio between the volatile fatty acids (FOS) and the total alkalinity (TAC) (Ciotola et al., 2014).

The specific VFA yield describes the VFA production per mass of material fed to the system. The specific methane yield describes the methane production per mass of material fed to the system.

DataTAB.net, an online statistical calculator, was used to evaluate the statistical difference of the data (DATAtab Team, 2023). A two-sample, single-factor ANOVA parametric test with the significance level (p) set to 0.05 was used.

6.2.7 Demand-driven biogas kinetics

Three kinetic models of biogas production were used to assess the kinetics of the demand-driven biogas reactors: a first order exponential model, the modified Gompertz model, and a hybrid of two first order models (Strömberg et al., 2014). This approach was adapted from a prior study which evaluated demand-driven biogas production (O'Shea et al., 2016).

AD is a biological process with multiple subprocesses, with an array of different intermediates and microbial groups. These characteristics make it difficult to definitively model the kinetics of the several intermediate steps (Strömberg et al., 2014). The first order kinetic equation simplifies the whole process by assuming a single reaction is rate limiting. Hydrolysis of complex substrates is often the rate-limiting step, which can be described by the first order kinetic equation (Shahriari et al., 2012).

$$v(t) = V_{max} * (1 - \exp(-k * t))$$

Where: v(t) denotes the cumulative gas production per unit reactor volume (L_{biogas}. $L^{-1}{}_{reactor}$) at a specific time *t* (min) after feeding. V_{max} denotes the final specific biogas production (L_{biogas}. $L^{-1}{}_{reactor}$) taken 24 hours after feeding, and *k* is the rate constant of decay (1. min^{-1}).

Biological processes, such as AD, are often described using the modified Gompertz equation, particularly if the growth or decay can be described in a sigmoidal (S-shape) pattern (Shahriari et al., 2012). The pulse-feeding nature in this study is typically sigmoidal (O'Shea et al., 2016). The model was deemed suitable for demand-driven operation as it would also describe the lag phase, which is a crucial demand-driven operation parameter.

$$v(t) = V_{max} * \exp\left(-\exp\left(\left(\frac{R_m \cdot e}{V_{max}}\right)(\lambda - t) + 1\right)\right)$$

Where: the maximum specific biogas production rate *Rm* (L_{biogas}. $L^{-1}{}_{reactor}$. min^{-1}) and the lag phase λ (min).

As solids and liquids enter the methanogenic two-phase CSTR, the potential of two different degradation profiles was assessed using the combined first order model (Strömberg et al., 2014).

$$v(t) = V_{max} * (1 - x^{*}exp(-k_1 * t) - (1 - x) * \exp(-k_2 * t))$$

The equation above considers the easily degradable portion in the substrate *x*, and k_1 considers the rate constant of this portion. The second decay constant k_2 considers the remaining portion of the substrate.

The built-in solver function within Microsoft Excel was used to determine the parameters of the model by minimising the sum of square errors between the experimental data and the model output. The generalised reduced gradient (GRG) non-linear solver engine was used for all three models applied to the entire period after feeding.

6.3 Results and discussion

6.3.1 Observations on reactor stability

The pH of both dark fermenters, C1a and the LBR, remained stable above the pH of 5.0 with a slightly higher pH in C1a ($p>0.05$) (see Table 6.2). This could be due to a slightly higher prominence of pH-reducing acids, such as acetic acid, within the fermentation broth of the LBRs as compared to C1a, which was evidenced in the VFA composition in Table 6.2. Higher COD was observed in C1a compared to the LBRs ($p<0.05$). This could be attributed to the anoxic nature of the LBRs, which would result in aerobic respiration and CO_2 production, which was evident in the greater CO_2 concentration observed in the trials (see Table 6.2) (Gerardi, 2003).

The pH of demand-driven methanogenic reactors, C1b and the EGSB remained above 7.5, with the EGSB above the recommended methanogenesis pH range of 7.0-

8.0 (Drosg, 2013). Even though the pH of the EGSB was above the recommended range, the EGSB was considered stable based on the FOS/TAC ratio. The FOS/TAC value of the EGSB was significantly lower than C1b ($p<0.05$) due to a lower accumulation of VFAs within the EGSB than C1b (see Table 6.2). The EGSB remained within the recommended reactor stability FOS/TAC values (<0.3). Conversely, C1b was within the potentially unstable values (0.3-0.8) (Drosg, 2013). Higher FOS/TAC values in C1b could be attributed to an accumulation of VFAs, particularly acetic acid (see Table 6.2). Higher TAN concentrations were observed in C1b (1.3 g. L^{-1}) as compared to the EGSB (0.3 g. L^{-1}) ($p<0.05$). This would suggest higher degradation of the feedstock in C1b than the LBR-EGSB configuration as protein degradation increases TAN concentrations.

Similar findings have previously been reported in literature (Hackula et al., 2023b). Methanogenic reactors can remain stable at TAN concentrations of up to 5 g. L^{-1}, however, acclimatisation to higher TAN concentrations is usually required (Drosg, 2013). A similar FOS/TAC observation with pulse-fed CSTRs processing similar feedstocks was observed in the literature (Jackson et al., 2020). Overall, in terms of stability, C1b is more likely to succumb to instability as determined by the FOS/TAC and higher levels of TAN as compared to the EGSB.

6.3.2 Reactor and methane production efficiency

Acidification was used to describe how much of the measured COD is a constituent of the VFAs. The acidification was significantly higher in C1a (64 %) as compared to the LBRs (42 %) ($p<0.05$) (see Table 6.2). This means the CSTR dark fermenter (C1a) was a better VFA-producing reactor when compared to the LBRs. This could

be because the anoxic nature of the LBRs may have resulted in some aerobic respiration. This hypothesis was evidenced by significantly higher CO_2 concentrations within the LBR (89 %) as compared to C1a (80 %) ($p<0.05$). The acidification of both reactors was within the range of 41 % (Guarda et al., 2021) and 81 % (Ribau Teixeira et al., 2020) for similar feedstocks. Prior studies found thermal pretreatment resulted in higher acidification due to a breakdown of recalcitrant lignin within the solid whiskey by-products (Kang et al., 2021). The specific VFA yield of C1a was significantly higher than the LBR ($p<0.05$), with butyric acid and acetic acid as the prominent VFAs (see Table 6.2). Given the prominence of butyric acid as a significant VFA in both dark fermenters, exploring valorisation pathways for this VFA may be an attractive prospect for the distillery. Caproic acid was the next prominent VFA with similar concentrations in both dark fermenters.

Higher COD removal (ca. 96 %) was observed throughout the operation of the EGSB. C1b had lower COD removal (ca. 81 %). These findings concur with results in the literature for similar reactor types (Jiraprasertwong et al., 2021). The results suggest that the demand-driven operation does not affect the COD removal efficiency of the reactors.

Table 6.2: Summary of experimental stability, reactor efficiency, and yields

		Two-phase CSTR		LBR-EGSB	
Parameter	**Unit**	**C1a**	**C1b**	**LBR**	**EGSB**
Function		VFA Production	Demand-Driven Biogas	VFA Production	Demand-Driven Biogas
pH		5.3 ± 0	7.6 ± 0	5.0 ± 0	8.2 ± 0
FOS/TAC[a]			0.5 ± 0		0.2 ± 0
Effluent COD	g. L^{-1}	29.4 ± 4	6.1 ± 3	25.3 ± 1	0.8 ± 0
% COD Rem[b]	%	10 ± 0	81 ± 0	30 ± 0	96 ± 0
% VS Rem[c]	%	37 ± 0	74 ± 1	45 ± 0	
TAN[d]	g. L^{-1}	0.1 ± 0	1.3 ± 0	0.2 ± 0	0.3 ± 0
VFAs[e]	g. L^{-1}	10.4 ± 2.2	1.9 ± 1.4	9.9 ± 0.9	
Acidification	%	64 ± 0		42 ± 0	
Acetic acid	g. L^{-1}	2.1 ± 0.6	1.7 ± 1.2	3.0 ± 0.4	
Propionic acid	g. L^{-1}	1.4 ± 0.8		1.2 ± 0.1	
Butyric acid	g. L^{-1}	2.7 ± 0.9		2.7 ± 0.6	
Valeric acid	g. L^{-1}	1.7 ± 0.8		0.8 ± 0.1	
Caproic acid	g. L^{-1}	2.0 ± 0.7		1.7 ± 0.3	
Specific VFA yield	g VFA. kg^{-1} VS	163.6 ± 25		142.8 ± 13	
	g VFA. kg^{-1} ww	10.4 ± 1.6		9.1 ± 0.8	
$\%H_{2vol}$[f]	%	20 ± 6		11 ± 2	
$\%CO_{2vol}$[g]	%	80 ± 7	36 ± 2	89 ± 2	24 ± 6
$\%CH_{4vol}$[h]	%		64 ± 2		76 ± 5

Specific methane yield	L CH_4. g^{-1} COD		0.24 ± 0		0.34 ± 0
HRT (# of HRTs) [ij]	Days (Number)	4 (13)	25 (2)	18 (3)	6 (3)

[a] FOS/TAC = alkalinity ratio; [b] % COD Rem = COD removal efficiency; [c] % VS Rem = volatile solids removal efficiency; [d] TAN = total ammoniacal nitrogen; [e] VFAs = volatile fatty acids; [f] $\%H_{2vol}$ = hydrogen content in the biogas on a volumetric basis; [g] $\%CO_{2vol}$ = carbon dioxide content in the biogas on a volumetric basis; [h] $\%CH_{4vol}$ = methane content in the biogas on a volumetric basis; [i]HRT = hydraulic retention time; [j] number of HRTs operated shown in brackets, data excludes initial HRT.

A significantly higher specific methane yield was observed in the EGSB (0.34 L CH_4. g COD^{-1}_{added}) as compared to the C1b (0.24 L CH_4. $g^{-1}COD_{added}$) ($p<0.05$) (see Table 6.2). The specific methane yield of the whole system for LBR-EGSB was 288 L CH_4. kg^{-1}VS (18.4 L CH_4. kg^{-1}ww), and for the two-phase CSTR was 160 L CH_4. kg^{-1}VS (10.2 L CH_4. kg^{-1}ww). The difference in the methane yields can be attributed to higher COD removal within the EGSB and an accumulation of VFAs within C1b (Han et al., 2020). Significantly higher methane content (76 %) was observed in the EGSB than in C1b (64 %) ($p<0.05$). Two-phase systems have been reported to achieve higher methane content within the biogas (Fuentes et al., 2021). Based on the results, the EGSB offered superior methane yields and methane content within the biogas. In effect, the biogas from the EGSB would require less energy for biogas upgrading than C1b, which would reduce the operational costs of an upgrading unit. Combined with the higher organic loading rate of the EGSB, the EGSB may be the better-suited reactor for a distillery's longer-term operation. The higher organic loading rate would effectively result in a smaller reactor, which may reduce capital investment. However, the familiarity of the CSTR system amongst developers and AD users provides comfort and a knowledge base for potential system failures.

The CSTR dark fermenter exhibited higher VFA yields, H_2 compositions, and acidification levels than the LBRs. Based on these VFA production metrics, the CSTR dark fermenter was the better VFA-producing reactor for the mixed whiskey by-products. However, simplicity and no moving components are attractive design features of the LBR.

6.3.3 Flexibility of the two-phase reactors

The CSTR system was able to reach peak gas quicker (<15 min) than the EGSB (ca. 2.75 hrs) (see Figure 6.5A). However, a steeper ramp-up slope was observed in the EGSB (40 %. h^{-1}) than in the CSTR (18 %. h^{-1}), suggesting a more rapid response in the EGSB and a higher peak biogas production rate (see Table 6.3). The lower ramp-up slope in C1b could be due to the requirement for solids degradation (within the influent) prior to methane production within C1b. In contrast, only liquids were processed in the EGSB. The EGSB could enter the peak production phase, the region above the average daily production rate, within 30 minutes. The CSTR was able to enter the peak production phase within 15 minutes. The ramp-up of the EGSB was slightly higher than various studies evaluating a demand-driven operation on UASBs, which reported ramp-up slopes between 10 %. h^{-1} (Dotzauer et al., 2019) and 39 %. h^{-1} (Shinde et al., 2023). The higher ramp-up rate compared to UASBs in the literature can be attributed to higher recirculation rates and upflow velocities within the EGSB (0.85 m. h^{-1}) as opposed to the UASB as documented in the literature (0.2 m. h^{-1}) by (Chernicharo, 2007), which increases the substrate-to-inoculum contact within the reactor.

Table 6.3: Biogas production flexibility comparison between the CSTR and EGSB

Parameter	Unit	C1b	EGSB
Average daily biogas production rate ($Y_{bpr_{ave}}$)	L. $L^{-1}_{reactor}$. d^{-1}	1.0	1.5
Peak biogas production rate ($Y_{bpr_{peak}}$)	L. $L^{-1}_{reactor}$. d^{-1}	1.8	3.1
Ramp upslope ($m_{bpr_{up}}$)[a]	%. h^{-1}	18	40
Ramp downslope ($m_{bpr_{down}}$)[b]	%. h^{-1}	-6	-4
Amplitude[c]	%	62	98
Peak biogas production phase[d]	h	7.8	13.5

[a] Ramp-up slope time taken after pulse-feeding; [b] Ramp-down slope time taken after peak biogas production [c] amplitude – the degree the biogas production increases by, taken from the lowest biogas production point to the peak; [d] duration when biogas production rate was above the average daily biogas production rate

The average daily biogas production rate ($Y_{bpr_{ave}}$) was higher in the EGSB (1.5 L_{biogas}. L^{-1}_{r}. d^{-1}) than C1b (1.0 L_{biogas}. L^{-1}_{r}. d^{-1}). The average daily biogas production rate of both reactors was within the range of 0.4 L_{biogas}. L^{-1}_{r}. d^{-1} (O'Shea et al., 2016) and 2.7 L_{biogas}. L^{-1}_{r}. d^{-1} (Shinde et al., 2023) of various demand-driven studies previously undertaken. The EGSB produced a higher peak biogas production than the CSTR (3.1 L_{biogas}. L^{-1}_{r}. d^{-1} versus 1.8 L_{biogas}. L^{-1}_{r}. d^{-1}). Both reactors were within the range of 0.5 L_{biogas}. L^{-1}_{r}. d^{-1} (Ahmed and Kazda, 2017) and 5.5 L_{biogas}. L^{-1}_{r}. d^{-1} (Mauky et al., 2015) reported in the literature. The EGSB had a slightly lower ramp-down slope (-4 %. h^{-1}) than the CSTR (-6 %. h^{-1}). The ramp-down slope of both reactors was within the range of -25 %. h^{-1} (Dotzauer et al., 2019) and -2 %. h^{-1} (Shinde et al., 2023), which was reported in the literature. However, the EGSB was able to remove almost all of the COD introduced (96 % COD destroyed), resulting in a lower minimum biogas production (<0.1 L_{biogas}. L^{-1}_{r}. d^{-1}) as opposed to C1b (ca. 0.8 L_{biogas}. L^{-1}_{r}. d^{-1}) by the end of 24 hours (see Figure 6.5A).

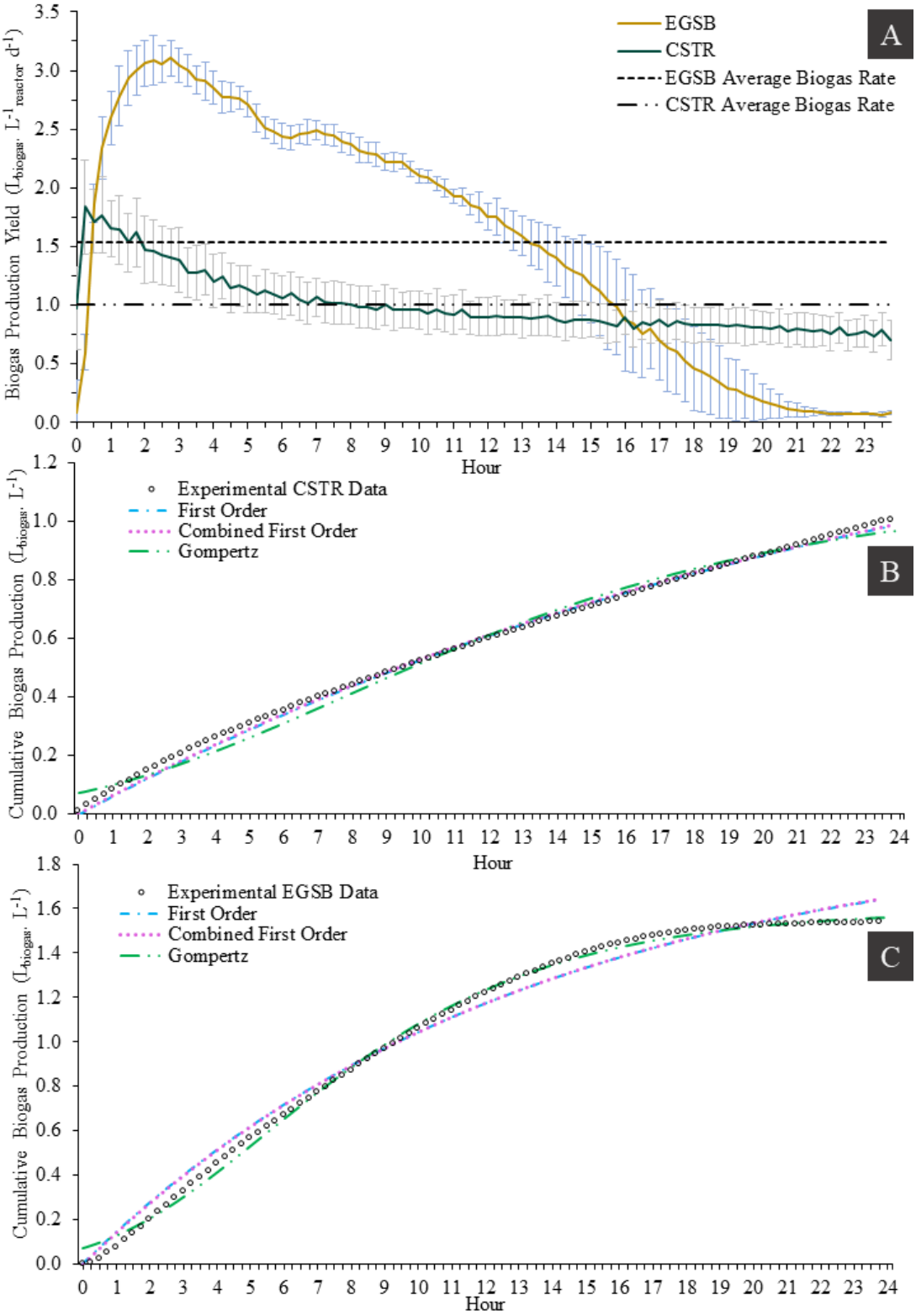


Figure 6.5: A-Biogas production yields; B-cumulative biogas production, with the first order model, combined first order model and modified Gompertz model for demand-driven CSTR biogas reactors and C – for EGSB reactors

In effect, C1b started at a higher gas production point than the EGSB before the demand-driven operation (see Figure 6.5A). This was highlighted by the higher amplitude of 98 % in the EGSB as opposed to 62 % in the C1b (see Table 6.3). A less steep ramp-down slope rate (%. h^{-1}) was observed in the EGSB, resulting in a longer peak biogas production phase (13.5 hours), as opposed to 7.8 hours in the CSTR. The ramp down of both reactors may not be a significant flexibility concern to a distillery as the excess biogas can be redirected for the production of heat and power within the distillery.

Based on the experiments, the CSTR was able to reach peak biogas flow rates quicker. At the same time, the EGSB showed higher peak biogas flow rates, more rapid biogas response, and higher cumulative biogas production rates.

6.3.4 Kinetics and biogas production of two-phase demand-driven systems

The cumulative biogas production curves and associated kinetic models, the first order model, modified Gompertz model and combined first order model, for the demand-driven methanogenic reactors, C1b and the EGSB, are shown in Figure 6.5B and 4C. The parameters of the model are shown in Table 6.4. The average cumulative biogas production (L_{biogas}. $L^{-1}_{reactor}$) values at every 15-minute interval of the last HRT were plotted over 24 hours.

All kinetic models fit the experimental data with an adjusted R^2 value of >0.97. The first k-values for the first-order model and combined first-order model were highest in the EGSB compared to C1b, implying a more rapid rate at which biogas production occurs. The x-value in the combined first-order model was higher in the EGSB than in C1b, implying a greater portion of readily degradable organics within

the leachate in the LBR. The x-value for the EGSB was almost 1, which implies that the two-term, combined first-order model may not be needed. This was expected as only liquids are introduced into the EGSB, as opposed to a solid-liquid mixture in C1b. The comparison should be taken with caution as different inoculum was used in the reactors. For C1b, all kinetic models slightly understated the final biogas production by less than 4 %. Conversely, for the EGSB, the models slightly overestimated the final biogas production by less than 6 %. Overall, all models could be important for the distillery as they can be used for forecasting, supply-demand balance, and integration of renewables if the distillery decides to sell excess electricity to the electricity provider or install other intermittent energy sources on site. This approach may interest countries like Ireland, where energy trading is implemented. The models could inform decision-making as to the best time to pulse-fed the reactors to meet peak energy requirements and reduce internal demand.

Table 6.4: Demand-driven biogas trial kinetics

Data source	Parameter	Unit	C1b	EGSB
Experimental data	Daily biogas yield	$L_{biogas}. L^{-1}_{reactor}. d^{-1}$	1.0	1.5
First order model	Vmax	$L_{biogas}. L^{-1}_{reactor}. d^{-1}$	1.6	2.0
	k	1. min^{-1}	0.6×10^{-3}	1.3×10^{-3}
	Adjusted R^2		0.995	0.976
Gompertz model	Vmax	$L_{biogas}. L^{-1}_{reactor}. d^{-1}$	1.1	1.6
	R_m	$L_{biogas}. L^{-1}_{reactor}. d^{-1}$	0.9×10^{-3}	2.0×10^{-3}
	λ	min.	0	38.2
	Adjusted R^2		0.980	0.995
Combined first-order model	Vmax	$L_{biogas}. L^{-1}_{reactor}. d^{-1}$	1.9	2.0
	x	%	0.8	1.0
	k_1	1. min^{-1}	0.7×10^{-3}	1.3×10^{-3}
	k_2	1. min^{-1}	0.2×10^{-6}	0
	Adjusted R^2		0.995	0.976

6.3.5 Demand-driven thermal and electrical production

A demand-driven approach, enabled through two-phase AD systems, can co-produce VFAs and biogas. Box 6.1 shows the approximate thermal and electrical energy produced if a CHP unit converted all the mixed whiskey by-products into energy.

Box 6.1: Evaluating thermal and electrical production through a CHP unit

The following assumptions were made to evaluate the thermal and electrical production if all the substrate was used to produce biogas for thermal and electrical production through a CHP unit:

- A large distillery with a whiskey production capacity of 50 million L_{OLA}. a^{-1}.
- A typical whiskey distillery has thermal energy demand (4.16 kWh_{th}. L^{-1}_{OLA}) and electrical energy demand (0.69 kWh_e. L^{-1}_{OLA}) (O'Shea et al., 2020).
- This size distillery produces 516.5 kt. a^{-1} of mixed whiskey by-products (Hackula et al., 2023b).
- The TS and VS of the mixed whiskey by-products are 7 %ww and 94 % TS (see Table 6.1)
- The VS destruction and COD-to-methane conversion of the LBR-EGSB system were taken to be 45 % and 0.34 L CH_4. g^{-1}COD. Giving a specific methane yield of 288 m^3. t^{-1} VS (see Appendix D.3).
- A CHP unit will be used to produce thermal and electrical energy.
- The thermal and electrical efficiencies are 50 % and 40 %, respectively (Hakawati et al., 2017).
- Methane has an energy content of 10 kWh. m^{-3}.

The thermal energy demand and electrical demand can be calculated as follows:

$$\text{Thermal energy demand} = 50 \text{ million } L_{OLA}.a^{-1} \times 4.16\ kW_{th}h.L_{OLA}^{-1} = 208\ GWh_{th}$$

$$\text{Electrical energy demand} = 50 \text{ million } L_{OLA}.a^{-1} \times 0.69\ kW_{th}h.L_{OLA}^{-1} = 34.5\ GWh_e$$

The available volatile content for biogas production can be calculated as follows:

$$516.5\ kt.a^{-1} \times 7\ \%ww \times 94\ \%TS = 33.99\ kt.a^{-1}$$

The methane produced from the LBR-EGSB system can be estimated as follows:

$$\text{Annual Methane Yield} = 288\ \text{m}^3.\ \text{t}^{-1}\ \text{VS}\ \times 33.99\ \text{kt VS.a}^{-1}$$
$$= 9.8 \text{ x } 10^6\ \text{m}^3\text{CH}_4$$

The thermal and electrical energy output of the CHP system can be calculated as follows:

$\text{Thermal energy output} = 9.8 \text{ x } 10^6\ \text{m}^3\text{CH}_4\ \times$
$10\ \text{kWh.m}^{-3} \text{ x } 50\ \%_{\text{thermal efficiency}} = 49\ \text{GWh}_{\text{thermal}}$ which is 24 % of the thermal demand

$\text{Electrical energy output} = 10.1 \text{ x } 10^6\ \text{m}^3\text{CH}_4\ \times$
$10\ \text{kWh.m}^{-3} \text{ x } 40\ \%_{\text{thermal efficiency}} = 39\ \text{GWh}_{\text{electrical}}$ which is 113 % of the electrical demand

If fulfilling the electricity demand is an essential objective for the distillery, almost all (88 %) of the available feedstock would have to be used for electricity generation. Thus, producing VFAs while maintaining and fulfilling the electricity baseload through a CHP unit would not be feasible as little feedstock would be available for VFAs. However, the distillery may opt for a more dynamic electricity generation approach, where electricity is only generated once the price of electricity reaches a threshold price. The various scenarios require further research on the cost-benefits of supplementing electricity and VFA extraction. It must be noted that the analysis only considers the EGSB as it exhibited a higher specific methane yield, but a similar analysis can be adopted for C1b (see Table 6.2).

The demand-driven electricity approach, whereby the distiller would only meet the electricity demand during peak hours, for 2 hours (typically between 5-7 pm), would reduce the required electricity production from the CHP unit to 2.9 GWh with an associated heat output of 3.7 GWh_{th}. The required feedstock to satisfy this demand is approximately 8 %, thus availing the remainder of the fermentation broth from VFA production for further processing. This approach would reduce the size required for

the EGSB and biogas storage, which could reduce the capital outlay required for the mentioned systems.

6.3.6 Biobutanol for distribution transport

Valorisation of the VFAs can be achieved by isolating butyric acid and further processing it into biobutanol. Biobutanol can be produced from butyric acid and blended with diesel for use in transport, thus reducing the emissions associated with the distillery transport distribution (Scope 3 emissions). The following assumptions were used to estimate the use of biobutanol in the transportation of whiskey:

- Biobutanol will be used to create an 80:20 diesel-butanol blend on a volumetric basis, which will be used as a transport fuel (Tipanluisa et al., 2021).
- Diesel is currently used for whiskey distribution transport. The fleet travels 8.7 million km. a^{-1} (Hackula et al., 2024) with a fuel consumption of 0.37 L_{diesel}. km^{-1} (Gray et al., 2021).
- The density of biobutanol was taken to be 813.4 kg. m^{-3} with a lower heating value of 35.744 MJ. kg^{-1} (Tipanluisa et al., 2021).
- The density of diesel was taken to be 844.1 kg. $m^{-3,}$ and for the diesel-butanol blend, it was considered to be 838.9 kg. m^{-3} (Tipanluisa et al., 2021).
- The energy density of diesel was taken to be 43.85 MJ. $kg^{-1,}$ and for the diesel-butanol blend, it was 42.14 MJ. kg^{-1} (Tipanluisa et al., 2021).
- 516.5 kt of mixed whiskey by-products are produced per annum by a 50 million L_{OLA} facility (Hackula et al., 2023b).

- The specific VFA yield for C1a was 10.4 kgVFA. t^{-1}ww, and for the LBR 9.1 kgVFA. t^{-1}ww (see Table 6.2).
- The liquids can be isolated with a separation efficiency of 80 % (Moses, 2014), and butyric acid can be separated from the liquids with a 95 % efficiency (Aydin et al., 2018).
- A two-step catalytic process converts butyric acid to butanol with an efficiency of 48 % (Cho et al., 2019).
- The emissions from diesel combustion are 3.21 t CO_2e. t^{-1}_{diesel} (DEFRA, 2022).
- The average price of diesel was taken to be 1.51 €. L^{-1}_{diesel} (GlobalPetrolPrices, 2023).

The calculations of the analysis are shown in Table 6.5, with detailed calculations in Appendix D.2.

Table 6.5: Biobutanol utilisation potential in transport

Parameters	Units	Dark Fermenter	
		CSTR	LBR
Annual distance travelled by the distillery fleet	million km. a^{-1}	8.7	
Annual diesel requirement to fulfil transport demand	million kg. a^{-1}	2.72	
	MJ	119,212,160	
Distillery size	million L_{OLA}. a^{-1}	50	
Specific VFA yield	kg VFA. t^{-1}_{mWBM}	10.4	9.1
Distillery VFA yield	kt VFAs. a^{-1}	4.08	3.57
The portion of butyric acid within VFAs	kt Butyric Acid. a^{-1}	1.22	1.1
Biobutanol yield after processing butyric acid	t Butanol. a^{-1}	585.6	513.6
Distillery biobutanol volume	L Butanol. a^{-1}	719,941	631,424
Volume of 80:20 diesel-biobutanol blend using all biobutanol fuel	million L Diesel blend. a^{-1}	3.6	3.16
Total energy of 80:20 diesel-biobutanol blend	MJ	127,262,800	111,671,000
Total distillery transport energy fulfilled by 80:20 diesel-biobutanol blend	%	107	94
Additional fossil diesel energy required to meet distillery transport energy demand	MJ	0	7,541,160
Additional fossil diesel mass required to meet distillery transport demand	t Diesel. a^{-1}	0	171.98
Diesel mass reduction through blending with biobutanol	t Diesel. a^{-1}	440	358
Distillery transport emissions offset from 80:20 diesel-biobutanol blend	t CO_2e. a^{-1}	1,412	1,149
Volume of diesel reduced through blending with biobutanol	L Diesel. a^{-1}	521,265	424,144
Monetary savings from diesel reduction at the distillery	€ ($)	787,110 (865,821)	640,457 (704,503)

Where: CSTR - Continuously stirred tank reactor; LBR – Leach bed reactor; the exchange rate taken to be 1.10 US$ per € (Central Bank of Ireland, 2023)

Blending biobutanol with diesel would not require significant infrastructural changes at the distillery, making it a more straightforward decarbonisation strategy than biomethane or biohydrogen for a large distillery in the interim. The CO_2 emissions saved from this approach in the CSTR dark fermenter (C1a) would be a 16 % CO_2 emission reduction associated with Scope 3 emissions. Given that Scope 3 emissions are major carbon contributors at a distillery, the utilisation of a diesel-biobutanol blend transport fuel provides a potential environmentally conscious solution for the distillery (O'Shea et al., 2020). Various studies have evaluated diesel-butanol blends, and only a slight decrease (<3 %) in power and torque has been reported at a blend of 20 % (Tipanluisa et al., 2021).

6.4 Conclusion

The demand-driven operation of two anaerobic digestion systems processing whiskey by-products was assessed and compared. Overall, the two-phase CSTR produced higher VFA yields and a shorter lag phase to reach peak biogas production rates than the LBR-EGSB system. The EGSB had higher biogas production, average daily biogas production rates, and more rapid biogas response. Three kinetic models of both systems were evaluated, which could be used for biogas production forecasting. A theoretical analysis evaluated blending biobutanol with diesel, which showed the potential to displace 16 % of diesel in Scope 3 transport emissions. Both systems were able to operate in a demand-driven manner.

References

1. Abad, V., Avila, R., Vicent, T., Font, X., 2019. Promoting circular economy in the surroundings of an organic fraction of municipal solid waste anaerobic digestion treatment plant: Biogas production impact and economic factors. Bioresour Technol 283, 10–17. https://doi.org/10.1016/J.BIORTECH.2019.03.064
2. Ahmad, J., Awais, M., Rashid, U., Ngamcharussrivichai, C., Raza Naqvi, S., Ali, I., 2023. A systematic and critical review on effective utilization of artificial intelligence for bio-diesel production techniques. Fuel 338, 127379. https://doi.org/10.1016/J.FUEL.2022.127379
3. Ahmed, S., Kazda, M., 2017. Characteristics of on-demand biogas production by using sugar beet silage. Anaerobe 46, 114–121. https://doi.org/10.1016/j.anaerobe.2017.04.016
4. APHA, 2022. Standard Methods for the Examination of Water and Wastewater™, 24th ed. American Public Health Association, American Water Works Association, and Water Environment Federation.
5. Aydin, S., Yesil, H., Tugtas, A.E., 2018. Recovery of mixed volatile fatty acids from anaerobically fermented organic wastes by vapor permeation membrane contactors. Bioresour Technol 250, 548–555. https://doi.org/10.1016/j.biortech.2017.11.061
6. Barrena, R., Traub, J.E., Gil, C.R., Goodwin, J.A.S., Harper, A.J., Willoughby, N.A., Sánchez, A., Aspray, T.J., 2018. Batch anaerobic digestion of deproteinated malt whisky pot ale using different source inocula. Waste Management 71, 675–682. https://doi.org/10.1016/J.WASMAN.2017.06.025
7. Castilla-Archilla, J., Papirio, S., Lens, P.N.L., 2021. Two step process for volatile fatty acid production from brewery spent grain: Hydrolysis and direct acidogenic fermentation using anaerobic granular sludge. Process Biochemistry 100, 272–283. https://doi.org/10.1016/j.procbio.2020.10.011
8. Chernicharo, C.A. de L., 2007. Anaerobic Reactors. IWA Publishing, London.
9. Cho, S.-H., Kim, J., Han, J., Lee, D., Kim, H.J., Kim, Y.T., Cheng, X., Xu, Y., Lee, J., Kwon, E.E., 2019. Bioalcohol production from acidogenic products via a two-step process: A case study of butyric acid to butanol. Appl Energy 252, 113482. https://doi.org/10.1016/j.apenergy.2019.113482

10. Ciotola, R.J., Martin, J.F., Tamkin, A., Castańo, J.M., Rosenblum, J., Bisesi, M.S., Lee, J., 2014. The influence of loading rate and variable temperatures on microbial communities in anaerobic digesters. Energies (Basel) 7, 785–803. https://doi.org/10.3390/en7020785
11. DATAtab Team, 2023. DATAtab: Online Statistics Calculator.
12. DEFRA, 2022. Greenhouse gas reporting: conversion factors 2022.
13. Dishisha, T., Alvarez, M.T., Hatti-Kaul, R., 2012. Batch- and continuous propionic acid production from glycerol using free and immobilized cells of Propionibacterium acidipropionici. Bioresour Technol 118, 553–562. https://doi.org/10.1016/J.BIORTECH.2012.05.079
14. Dotzauer, M., Pfeiffer, D., Lauer, M., Pohl, M., Mauky, E., Bär, K., Sonnleitner, M., Zörner, W., Hudde, J., Schwarz, B., Faßauer, B., Dahmen, M., Rieke, C., Herbert, J., Thrän, D., 2019. How to measure flexibility – Performance indicators for demand driven power generation from biogas plants. Renew Energy 134, 135–146. https://doi.org/10.1016/j.renene.2018.10.021
15. Drosg, B., 2013. Process monitoring in biogas plants. IEA Bioenergy.
16. European Commission, 2022. Renewable energy targets [WWW Document]. Renewable energy targets.
17. European Parliamentary Research Service, 2022. Energy saving and demand reduction.
18. Fuentes, K.L., Torres-Lozada, P., Chaparro, T.R., 2021. Beverage wastewater treatment by anaerobic digestion in two-stages for organic matter removal and energy production. Biomass Bioenergy 154, 106260. https://doi.org/10.1016/J.BIOMBIOE.2021.106260
19. Gerardi, M.H., 2003. The Microbiology of Anaerobic Digesters. The Microbiology of Anaerobic Digesters. https://doi.org/10.1002/0471468967
20. GlobalPetrolPrices, 2023. Ireland Diesel prices, 07-Aug-2023 [WWW Document]. URL https://www.globalpetrolprices.com/Ireland/diesel_prices/ (accessed 8.14.23).
21. Gray, N., McDonagh, S., O'Shea, R., Smyth, B., Murphy, J.D., 2021. Decarbonising ships, planes and trucks: An analysis of suitable low-carbon fuels for the maritime, aviation and haulage sectors. Advances in Applied Energy 1, 100008. https://doi.org/10.1016/j.adapen.2021.100008

22. Guarda, E.C., Oliveira, A.C., Antunes, S., Freitas, F., Castro, P.M.L., Duque, A.F., Reis, M.A.M., 2021. A Two-Stage Process for Conversion of Brewer's Spent Grain into Volatile Fatty Acids through Acidogenic Fermentation. Applied Sciences 11, 3222. https://doi.org/10.3390/app11073222
23. Hackula, A., O'Shea, R., Murphy, J.D., Wall, D.M., 2024. Developing distillery biorefineries through dark fermentation of whiskey production by-products: the effect of organic loading rate on decarbonisation pathways. Energy Convers Manag 301, 118064. https://doi.org/10.1016/j.enconman.2024.118064
24. Hackula, A., O'Shea, R., Murphy, J.D., Wall, D.M., 2023a. Design, Construction, and Concept Validation of a Laboratory-Scale Two-phase Reactor to Valorize Whiskey Distillery By-products. ACS Engineering Au. https://doi.org/10.1021/ACSENGINEERINGAU.3C00006
25. Hackula, A., Shinde, R., Hickey, D., O'Shea, R., Murphy, J.D., Wall, D.M., 2023b. Two-phase anaerobic digestion for enhanced valorisation of whiskey distillery by-products. Bioresour Technol 129239. https://doi.org/10.1016/J.BIORTECH.2023.129239
26. Hahn, H., Krautkremer, B., Hartmann, K., Wachendorf, M., 2014. Review of concepts for a demand-driven biogas supply for flexible power generation. Renewable and Sustainable Energy Reviews 29, 383–393. https://doi.org/10.1016/j.rser.2013.08.085
27. Hakawati, R., Smyth, B.M., McCullough, G., De Rosa, F., Rooney, D., 2017. What is the most energy efficient route for biogas utilization: Heat, electricity or transport? Appl Energy 206, 1076–1087. https://doi.org/10.1016/j.apenergy.2017.08.068
28. Han, Y., Green, H., Tao, W., 2020. Reversibility of propionic acid inhibition to anaerobic digestion: Inhibition kinetics and microbial mechanism. Chemosphere 255, 126840. https://doi.org/10.1016/j.chemosphere.2020.126840
29. Hilkiah Igoni, A., Ayotamuno, M.J., Eze, C.L., Ogaji, S.O.T., Probert, S.D., 2008. Designs of anaerobic digesters for producing biogas from municipal solid-waste. Appl Energy 85, 430–438. https://doi.org/10.1016/J.APENERGY.2007.07.013
30. Jackson, S.A., Kang, X., O'Shea, R., O'Leary, N., Murphy, J.D., Dobson, A.D.W., 2020. Anaerobic digestion performance and microbial community

structures in biogas production from whiskey distillers organic by-products. Bioresour Technol Rep 12, 100565. https://doi.org/10.1016/j.biteb.2020.100565

31. Jiraprasertwong, A., Karnchanapaisal, P., Seneesrisakul, K., Rangsunvigit, P., Chavadej, S., 2021. High process activity of a two-phase UASB (upflow anaerobic sludge blanket) receiving ethanol wastewater: Operational conditions in relation to granulation development. Biomass Bioenergy 148, 106012. https://doi.org/10.1016/j.biombioe.2021.106012
32. Kang, X., Lin, R., Li, L., Wu, B., Deng, C., O'Shea, R., Sun, Y., Murphy, J.D., 2021. Assessment of pretreatment and digestion temperature on anaerobic digestion of whiskey byproducts and microbial taxonomy. Energy Convers Manag 243, 114331. https://doi.org/10.1016/j.enconman.2021.114331
33. Khatami, K., Atasoy, M., Ludtke, M., Baresel, C., Eyice, Ö., Cetecioglu, Z., 2021. Bioconversion of food waste to volatile fatty acids: Impact of microbial community, pH and retention time. Chemosphere 275, 129981. https://doi.org/10.1016/j.chemosphere.2021.129981
34. Linke, B., Rodríguez-Abalde, Á., Jost, C., Krieg, A., 2015. Performance of a novel two-phase continuously fed leach bed reactor for demand-based biogas production from maize silage. Bioresour Technol 177, 34–40. https://doi.org/10.1016/j.biortech.2014.11.070
35. Mauky, E., Jacobi, H.F., Liebetrau, J., Nelles, M., 2015. Flexible biogas production for demand-driven energy supply – Feeding strategies and types of substrates. Bioresour Technol 178, 262–269. https://doi.org/10.1016/j.biortech.2014.08.123
36. Mohan, S.V., Chiranjeevi, P., Mohanakrishna, G., 2012. A rapid and simple protocol for evaluating biohydrogen production potential (BHP) of wastewater with simultaneous process optimization. Int J Hydrogen Energy 37, 3130–3141. https://doi.org/10.1016/j.ijhydene.2011.10.109
37. Moses, D.R., 2014. Performance evaluation of continuous screw press for extraction soybean oil. American Journal of Science and Technology 1, 238–242.
38. O'Shea, R., Lin, R., Wall, D.M., Browne, J.D., Murphy, J.D., 2020. Using biogas to reduce natural gas consumption and greenhouse gas emissions at a large distillery. Appl Energy 279, 115812. https://doi.org/10.1016/j.apenergy.2020.115812

39. O'Shea, R., Wall, D., Murphy, J.D., 2016. Modelling a demand driven biogas system for production of electricity at peak demand and for production of biomethane at other times. Bioresour Technol 216, 238–249. https://doi.org/10.1016/j.biortech.2016.05.050
40. Paltsev, S., Morris, J., Kheshgi, H., Herzog, H., 2021. Hard-to-Abate Sectors: The role of industrial carbon capture and storage (CCS) in emission mitigation. Appl Energy 300. https://doi.org/10.1016/j.apenergy.2021.117322
41. Pohland, F.G., Ghosh, S., 2009. Developments in Anaerobic Stabilization of Organic Wastes - The Two-Phase Concept. http://dx.doi.org/10.1080/00139307109434990 1, 255–266. https://doi.org/10.1080/00139307109434990
42. Ribau Teixeira, M., Guarda, E.C., Freitas, E.B., Galinha, C.F., Duque, A.F., Reis, M.A.M., 2020. Valorization of raw brewers' spent grain through the production of volatile fatty acids. N Biotechnol 57, 4–10. https://doi.org/10.1016/j.nbt.2020.01.007
43. Shahriari, H., Warith, M., Hamoda, M., Kennedy, K.J., 2012. Anaerobic digestion of organic fraction of municipal solid waste combining two pretreatment modalities, high temperature microwave and hydrogen peroxide. Waste Management 32, 41–52. https://doi.org/10.1016/j.wasman.2011.08.012
44. Shinde, R., Hackula, A., O'Shea, R., Barth, S., Murphy, J.D., Wall, D.M., 2023. Demand-driven biogas production from Upflow Anaerobic Sludge Blanket (UASB) reactors to balance the power grid. Bioresour Technol 385, 129364. https://doi.org/10.1016/j.biortech.2023.129364
45. Sokhanvar, A., Bouri, E., 2022. Commodity Price Shocks Related to the War in Ukraine and Exchange Rates of Commodity Exporters and Importers. Borsa Istanbul Review. https://doi.org/10.1016/J.BIR.2022.09.001
46. Steinke, F., Wolfrum, P., Hoffmann, C., 2013. Grid vs. storage in a 100% renewable Europe. Renew Energy 50, 826–832. https://doi.org/10.1016/J.RENENE.2012.07.044
47. Strömberg, S., Nistor, M., Liu, J., 2014. Towards eliminating systematic errors caused by the experimental conditions in Biochemical Methane Potential (BMP) tests. Waste Manag 34, 1939–48. https://doi.org/10.1016/j.wasman.2014.07.018
48. Szarka, N., Scholwin, F., Trommler, M., Fabian Jacobi, H., Eichhorn, M., Ortwein, A., Thrän, D., 2013. A novel role for bioenergy: A flexible, demand-

oriented power supply. Energy 61, 18–26. https://doi.org/10.1016/J.ENERGY.2012.12.053

49. Tipanluisa, L., Fonseca, N., Casanova, J., López, J.-M., 2021. Effect of n-butanol/diesel blends on performance and emissions of a heavy-duty diesel engine tested under the World Harmonised Steady-State cycle. Fuel 302, 121204. https://doi.org/10.1016/j.fuel.2021.121204
50. Wall, D.M., Allen, E., O'Shea, R., O'Kiely, P., Murphy, J.D., 2016. Investigating two-phase digestion of grass silage for demand-driven biogas applications: Effect of particle size and rumen fluid addition. Renew Energy 86, 1215–1223. https://doi.org/10.1016/j.renene.2015.09.049

7.0 Investigating the effects of whiskey-barrel derived biochar addition to anaerobic digestion at a distillery: a study on energy yield and system efficiency

Anga Hackula [a b], Xue Ning [a b], Gillian Collins [a c], Stephen A. Jackson [a d], Niall D. O'Leary [a d], Chen Deng [e], Richard O'Shea [a b], Jerry D. Murphy [a b], David M. Wall [a b]

[a] SFI MaREI Centre for Energy, Climate and Marine, Environmental Research Institute, University College Cork, Cork, Ireland

[b] Civil, Structural and Environmental Engineering, School of Engineering and Architecture, University College Cork, Cork, Ireland

[c] School of Chemistry, University College Cork, Cork, Ireland

[d] School of Microbiology, University College Cork, Cork, Ireland

[e] School of Chemistry and Chemical Engineering, Southeast University, Nanjing, PR China

Abstract

Closed-loop systems enable circular economy systems and applications in the food and beverage sector to enhance decarbonisation. Whiskey distillation by-products are amenable to anaerobic digestion and thus facilitate resource recovery and circularity. Furthermore, biochar derived from whiskey barrels can be used as a carbonaceous additive within anaerobic digestion to enhance biomethane production. In this paper, biochar produced from the pyrolysis of discarded whiskey barrels at 300 ^{o}C, was shown to enhance biomethane production by up to 15 %. A kinetic analysis revealed that the biochar reduced the biomethane lag time by up to 42 %. The mass and energy balance of this integrated anaerobic digestion-pyrolysis system was evaluated. The overall system efficiency was assessed at 68 % of all input energy (expressed on a primary energy basis); utilisation of renewable electricity could increase this efficiency to 71 %. Biochar from discarded whiskey barrels can provide a decarbonisation pathway for whiskey distilleries but may be constrained by the total resources available.

7.1 Introduction

Valorising wastes into commercial products offers an important pathway to climate change mitigation and circular economy systems. Repurposing waste streams is strongly emphasised and promoted in the European Union (EU); EU waste recycling targets of at least 60 % of municipal waste must be achieved by 2030 (European Commission. Directorate-General for Environment., 2023). Organic waste valorisation can be achieved through anaerobic digestion (AD), a mature technology that produces biogas and bio-fertiliser. The biogas can be used directly to produce renewable electricity and heat, or it can be upgraded to biomethane (with an equivalent calorific value to natural gas) and used as a renewable transport fuel. The upgrading of biogas also leads to a co-product of biogenic carbon dioxide (CO_2).

Organic residues generated in the food and beverage industry, such as those in whiskey production, can be processed via AD. The implementation of AD systems can decarbonise energy production in such industries. However, the digestion of by-products from the whiskey industry may be impaired due to issues such as ammonia inhibition (Kang et al., 2022). Various methods have previously been tested to enhance the efficiency of AD, such as thermal and chemical pretreatments (Wei et al., 2022). Wei et al. (2022) observed up to 27 % improvement in biomethane yields from chemical pretreatment of feedstocks.

Biochar is a carbonaceous material produced from pyrolysis and may be used as an enhancement additive in AD (Świechowski et al., 2023). Pyrolysis is an oxygen-deprived, thermal decomposition process of high-solid organic residues, typically

effected at temperatures between 300-900 ^{o}C (Deng et al., 2021). The process also produces bio-oil and syngas, which can both be processed further (Weber and Quicker, 2018). Biochar addition to anaerobic digestion has been shown to mitigate inhibitory toxins, improve buffer capacity, absorb biogas impurities such as hydrogen sulphide (H_2S) and reduce carbon dioxide concentrations within the biogas (Zhao et al., 2021). As such, it can potentially improve the operational efficiency and stability of AD systems. Biochar may also improve the direct interspecies electron transfer (DIET), acting as an electron bridge between microorganisms in the AD process (Zhao et al., 2021). Biochar is considered more economically effective than alternative carbonaceous materials such as activated carbon and carbon nanotubes used to improve DIET in AD (Ning et al., 2023). The biomass used in pyrolysis and the process conditions (holding temperature, heating rate, residence time, atmosphere) are crucial in determining the properties of biochar (Singh et al., 2020). In turn, these properties influence the synergistic effect of biochar addition on the AD system.

Various feedstocks from the food and beverage industry, such as rice straw and walnut shells, have previously been used to produce biochar (Hoang et al., 2022; Lahijani et al., 2018). The addition of biochar to the digestion of food waste was reported to increase biomethane yields by 10 % (Sunyoto et al., 2016). Within the brewery and whiskey industries, studies have assessed the digestion of solid distillery residues (such as brewer's spent grains and draff) with biochar addition and reported increases in biomethane yields of up to 10 % (Deng et al., 2021; Świechowski et al., 2023). Wooden whiskey barrels are one by-product of the whiskey production process that may be used for biochar production. Processing

whiskey barrels directly through AD would not be viable due to the high lignin content of wood (Deng et al., 2021). Direct burning may provide the most accessible form of utilisation, but carbon and particulate emissions may be undesirable at a distillery (Kirchsteiger et al., 2021). Pyrolysis may, however, provide an attractive valorisation pathway for such whiskey barrels.

The efficacy of biochar addition (produced at various temperatures) to AD varies across the literature. Shen et al., (2021) reported a decline in biomethane yield with biochar addition (generated from corn stover) as the temperature at which the biochar was produced increased from 300 to 700 ^{o}C. Wang and co-workers observed a positive effect on biomethane yield (ca.11 % increase) with the addition of biochar derived from Douglas-fir; however, a negligible difference in biomethane yield (<1 %) was observed from various biochars produced at temperatures between 400-730^{o}C (Wang et al., 2020). The variability of biomethane production following biochar addition highlights the need for further analysis and the use of experimental trials for specific case assessments. Biochar derived from whiskey barrels has not been previously evaluated in terms of its performance enhancing features when used as an additive to AD systems. Application of biochar to agricultural land is also deemed a negative emissions technology as it increases soil organic content (European Academies Science Advisory Council., 2018), and as such, can improve photosynthesis and crop yields. Wu et al., (2023) utilised the detail of the recast Renewable Energy Directive (attribution of a carbon savings of 45 g $CO_{2\text{-equiv}}$. MJ^{-1}) to generate a carbon credit of 900 g CO_2. kg^{-1} for biochar (with an energy value of 20 MJ. kg^{-1}) when applied to agricultural land.

To the best of the authors' knowledge, evaluating whiskey barrel-derived biochar with AD of whiskey by-products has not yet been explored in the literature. The addition of biochar generated from whiskey barrels may be of interest to a distillery in enacting a circular economy strategy, improving AD process efficiencies, and lowering the carbon footprint of the whiskey product. The precise aims of this investigation are as follows:

(1) Produce and characterise biochar produced from whiskey barrels at three pyrolysis holding temperatures (300 ^{o}C, 500 ^{o}C, and 700 ^{o}C);

(2) Evaluate and compare the impact of whiskey barrel-derived biochar addition (generated at different temperatures) on biomethane production in batch AD experimental trials;

(3) Quantify the energy efficiency, a value derived from the energy output (biomethane and pyrolysis products) divided by the energy inputs (whiskey by-products, whiskey barrels, and primary input energy) of an integrated AD-pyrolysis system using mass and energy balances.

7.2 Materials and methods

7.2.1 Biochar production

Used whiskey barrels (46.7 %TS carbon) were sourced from a local distillery and were processed into sawdust using a table saw with a dedicated collection system. The sawdust was dried at 105 ^{o}C for 24 hours and filtered to particle sizes smaller than 2 mm. A compact tube furnace (R50/250/12, Nabertherm, Germany) was used

to produce the biochar. Three types of biochar were produced at three different holding temperatures (300, 500, and 700 ^{o}C as per Shen et al. (2021)) in a nitrogen atmosphere under a heating rate of 10 ^{o}C. min^{-1}, and a residence time of one hour. The produced biochar was termed Char300, Char500, and Char700, respectively, corresponding to the holding temperature. The biochar was cooled to room temperature, followed by grinding and filtering to a particle size of 0.5 mm or less (Shen et al., 2021). Samples of each biochar were placed in separate plastic bags, which were stored in a desiccator before use.

7.2.2 Inoculum and feedstocks

Effluent from a laboratory-scale anaerobic digester processing mixed whiskey by-products was used as inoculum for the AD experimental trials. Prior to use, filtration of the inoculum was undertaken (5 mm mesh sieve) to extract undigested solid residues (see Table 7.1 for the inoculum properties). The inoculum was stored and degassed for 21 days in a laboratory scale continuously stirred tank reactor (CSTR) at mesophilic conditions (37 ^{o}C) until the time of use.

'Mixed whiskey by-products' were processed at the distillery from draff, cake maize, centrate, and thin stillage. The by-products were combined and evaluated in the laboratory, with a composition based on the production volumes at the distillery as previously described by (Hackula et al., 2023a). The chemical composition and properties of the whiskey by-products are shown in Appendix E.1.

7.2.3 Batch biomethane experiments

To evaluate the impact of various biochar dosages on the biomethane production of mixed whiskey by-products, batch biochemical methane potential (BMP) assays were conducted. The BMP assays were operated with an inoculum-to-substate ratio of 2:1 on a volatile solids (VS) basis (Johannesson et al., 2020).

The BMP assays were assessed for different ratios between the mass of the biochar and the VS content of the substrate to investigate the effect of the biochar-to-substrate ratio. Groups M1-4 were dosed with Char300 at increasing biochar-to-substrate ratios of 0.25, 0.5, 1.0, and 2.0 g biochar. g^{-1}VS, respectively. Groups M5-8 were dosed with Char500 with the same biochar-to-substrate ratio regime as groups M1- 4. Similarly, groups M9-12 consisted of Char700 dosed the same as the previous groups. A group (group M0) consisting of whiskey by-products and no biochar was operated to assess the methane potential without biochar addition. A blank group (group M13) with just inoculum was also operated to subtract any residual gasses produced from the inoculum.

A positive control group (group M14) with cellulose (2.18 g) was also operated. Each group was run in triplicate. In setting up the BMP, 350 ml of inoculum was added to each assay, along with the required mass of sample and biochar. To accommodate for the varying bulk densities and dosages of the different biochars, the volume of the BMPs was adjusted to 400 ml with deionised water. The pH of the BMP assays was adjusted to 7.5 with 6M sodium hydroxide and purged with nitrogen before experiments (Kang et al., 2022). Figure 7.1 shows the experimental setup of the BMP assays.

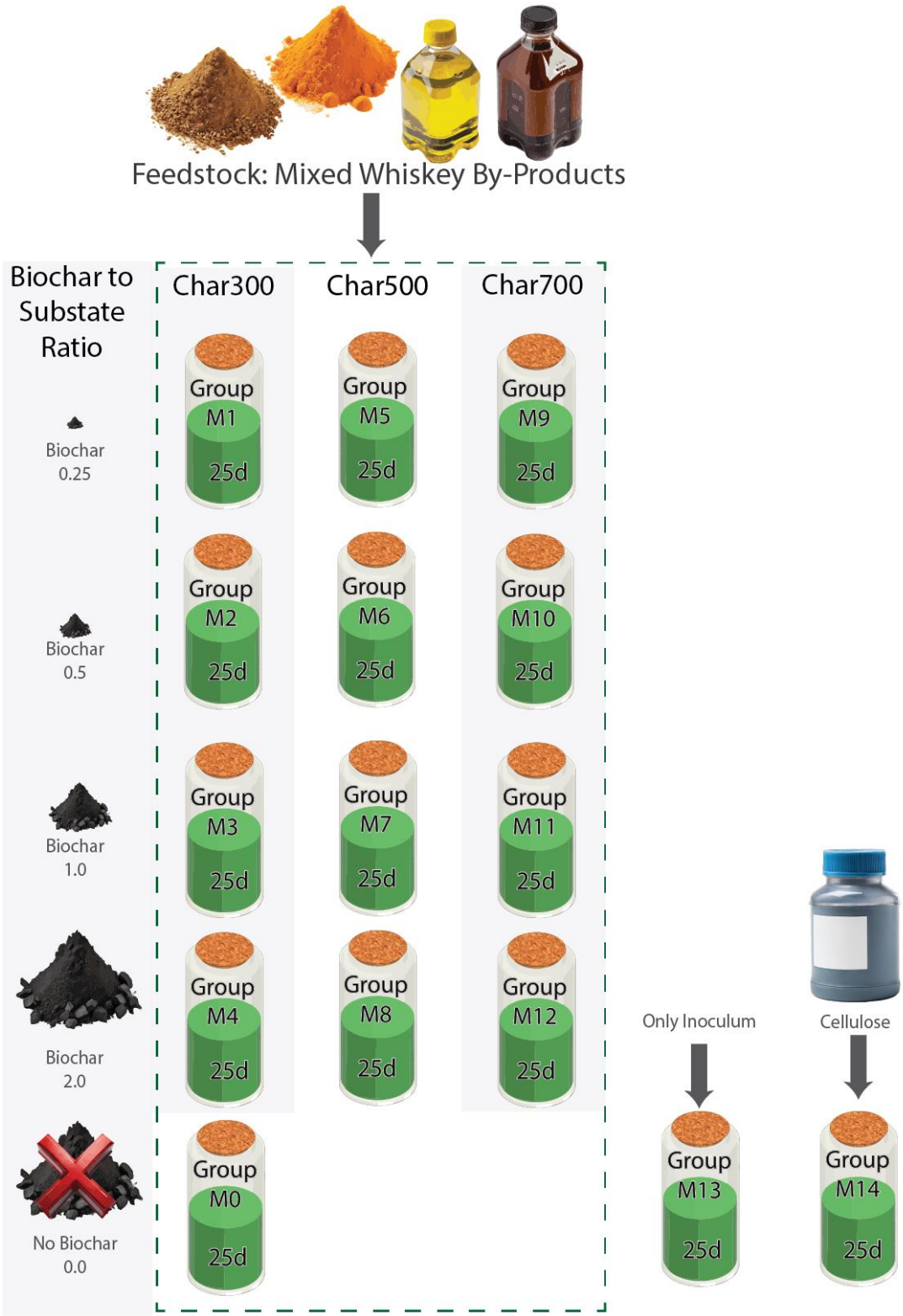


Figure 7.1: BMP assays experimental setup.

Mesophilic temperatures (37±1 ^{o}C) were maintained for all experiments by a thermostatic water bath.

Dry gas volumes at standard temperature and pressure (STP – 0 ^{o}C and 101.325 kPa) were measured by the Automatic Bioprocess Control ^{TM} AMPTS II system.

7.2.4 Characterisation of biomass and biochar

The total solids (TS) and volatile solids (VS) content of the materials were established using 2540G APHA standard methods (APHA, 2022). The carbon, hydrogen and nitrogen content were attained by an elemental analyser and were expressed as a percentage of TS. Elemental composition on a VS basis was obtained by using the VS/TS ratio. Two ratios, namely the oxygen-to-carbon (O/C) molar ratio and the hydrogen-to-carbon (H/C) molar ratio, were used to estimate the degree of carbonisation after pyrolysis. The biochars underwent evaluation of their pH and electrical conductivity (EC) in a suspended state, following the methodology outlined in existing literature (Deng et al., 2021) using a Mettler Toledo^{TM} F20 pH meter and a VWR CO310 conductivity meter, respectively. The Brunauer-Emmett-Teller (BET) method was used to determine the specific surface area (SSA) and porosity of the biochars. The biochar surface functional groups were qualitatively evaluated using a Perkin Elmer Spectrum Two FT-IR Spectrometer to generate Fourier Transform Infrared Spectroscopy (FTIR) spectra with an operating range of 4000-450 cm^{-1} and a 4 cm^{-1} resolution. 20 scans were averaged for the spectra.

7.2.5 Gas production kinetic analysis

The modified Gompertz equation was deemed as an appropriate kinetic model to examine the lag phase of biomethane production since cumulative biomethane production was deemed to be “S-shaped” (Shahriari et al., 2012):

$$v(t) = V_{max} * \exp\left(-\exp\left(\left(\frac{R_m \times e}{V_{max}}\right)(\lambda - t) + 1\right)\right)$$

Where: Vmax is the final cumulative biomethane yield; *Rm* is the maximum specific biomethane production rate (in $L_{biomethane}$. g^{-1} VS_{added}. d^{-1}); λ is the lag phase (in days); *t* is time (in days).

7.2.6 Biodegradability index and substrate energy yield calculation

The ratio between the achieved experimental biomethane yield (BMP) and the theoretical methane yield (see Table 7.1) was expressed as the biodegradability index (BI).

The energy yields were calculated by multiplying the biomethane yield with the respective lower heating value (LHV) of methane. The LHV of methane was assumed to be 50 MJ. kg^{-1} at STP. The modified Dulong formula was used to calculate the higher heating value (HHV) and the LHV of the biomass as follows:

$$HHV = 337 \times C + 1419 \times \left(H - \frac{O}{8}\right) + 93 \times S + 23.26 \times N$$

$$LHV = HHV - 212 \times H - 8 \times O$$

Where: HHV is the higher heating value (kJ. kg^{-1}TS), LHV is the lower heating value (kJ. kg^{-1}TS). C, H, O, N, and S are the TS percentage of carbon, hydrogen, oxygen, nitrogen, and sulphur, respectively.

The LHV and HHV were converted into a VS basis using the percentage of volatile solids within the total solids.

7.2.7 DNA extraction and sequencing

The BMP assays were sampled at the end of the experiments for DNA extraction and microbial community 16S rRNA gene sequencing. The BMP assay with the highest specific methane yield for each biochar temperature variant was selected for evaluation. In addition, the group with no biochar amendment (M0) was also analysed. Samples were frozen at -80 ºC until use. The methodology for DNA extraction and sequencing was comprehensively described in a prior study (Jackson et al., 2020). Similarly, the taxonomic marker gene amplicon sequence processing and analysis was adopted from a prior study (Jackson et al., 2020). The methodology is also included in Appendix E.2.

7.2.8 Conventional AD system and integrated AD-pyrolysis system energy efficiency

Two AD systems were evaluated for energy efficiency with biochar utilisation, as detailed below.

System 1 represents a conventional AD system without biochar addition that consists of an anaerobic digester and a digestate separation process. In this system, biochar is not added to the system and reflects the experimental results of Group M0. The digestate produced is considered a biofertiliser. However, the energy of offsetting synthetic fertiliser production was considered outside the system boundary. The energy inputs of system 1 were the feedstock, electricity, and heating energy. The biomethane energy was this system's energy output. The energy efficiency was calculated using Equation 7.1. Figure 7.2 illustrates the mass and energy balance undertaken for this analysis.

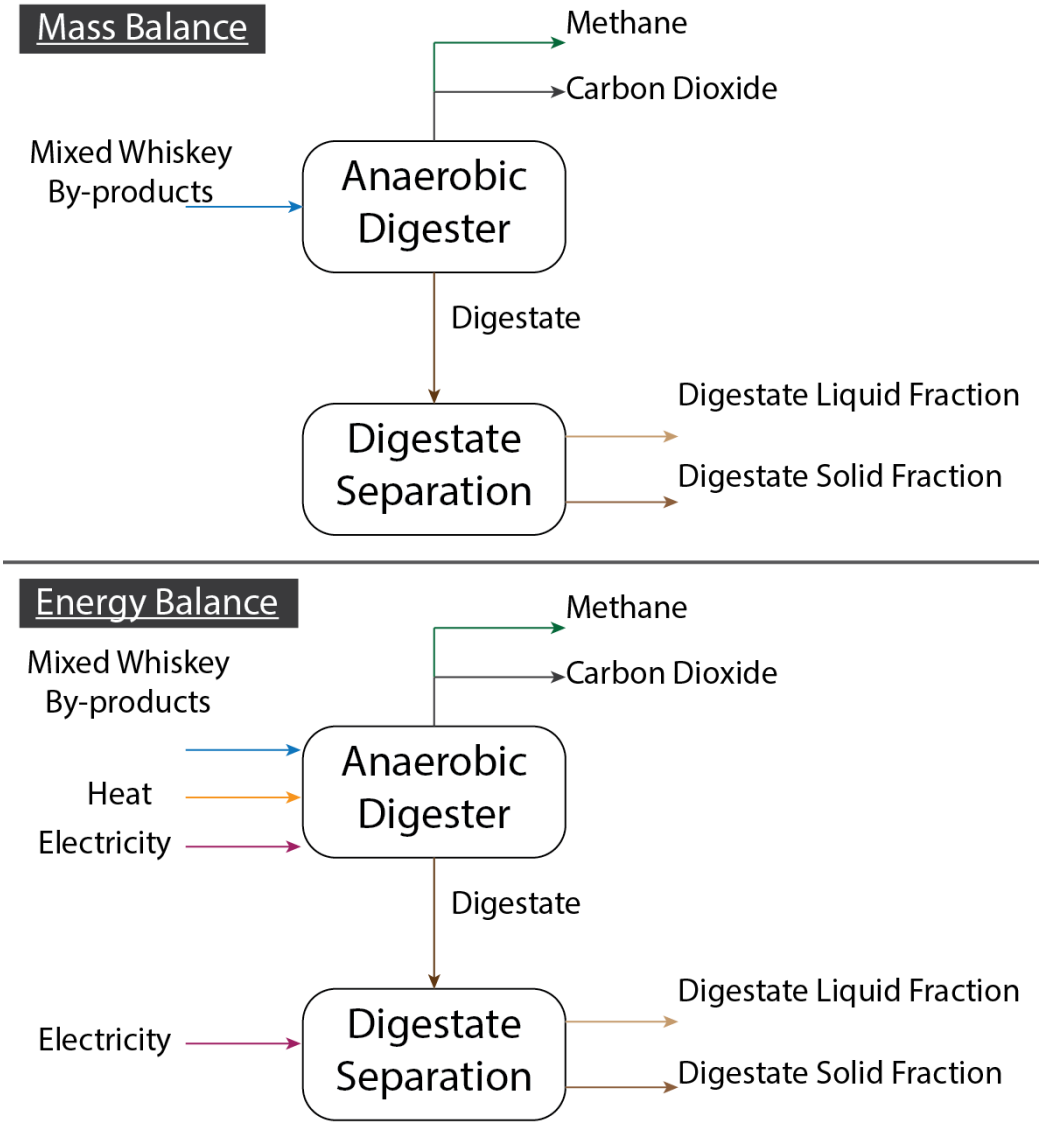


Figure 7.2: Mass and energy balance schematic of conventional AD system without biochar addition

System 2 exemplifies an integrated AD-pyrolysis system whereby whiskey barrels are pyrolysed to meet the biochar addition investigated in this study. Similar to System 1, the digestate from the AD process was considered a biofertiliser. The primary product of this system was biomethane, with the pyrolysis products considered as secondary products. Only the optimum biochar dosage for each pyrolysis temperature was considered for this system. The system comprises of an anaerobic digester, a digestate separation process, and a pyrolyser (and the various steps required to prepare the whiskey barrels for pyrolysis), as illustrated in Figure

7.3. The energy inputs of System 2 were the feedstock, electricity, heating energy, and the whiskey barrels. The energy outputs consisted of the biomethane, biochar, syngas, and bio-oil. The energy efficiency of System 2 was calculated using Equation 7.2. Figure 7.3 shows the schematic of the mass and energy balance undertaken in this analysis.

$$h_{AD} = \frac{Qout}{Qin} = \frac{Q_{out_{CH4}}}{Q_{in_{feedstock}} + Q_{in_P}} \quad \text{(Equation 7.1)}$$

$$h_{AD-PY} = \frac{Qout}{Qin} = \frac{Q_{out_{CH4}} + Q_{bio-oil} + Q_{syngas} + Q_{biochar}}{Q_{in_{feedstock}} + Q_{WB} + Q_{in_P}} \quad \text{(Equation 7.2)}$$

Where: h_{AD}= the AD energy efficiency of the conventional AD system (System 1); Q_{out} = energy outputs of the system; Q_{in} = energy inputs of the system; $Q_{out_{CH4}}$ = energy from methane produced by the system; $Q_{in_{feedstock}}$= energy of the feedstock; Q_{in_P} = energy of electricity and heating, which were converted into primary energy. The primary energy factors for electricity and heat were 2.3 and 1.1, respectively (Esser and Sensfuss, 2016); h_{AD-PY}= the AD energy efficiency of the integrated AD-pyrolysis system (System 2); $Q_{bio-oil}$ = energy from bio-oil produced from the system; Q_{syngas} = energy of syngas; $Q_{biochar}$ = energy of biochar Q_{WB} = energy from whiskey barrels.

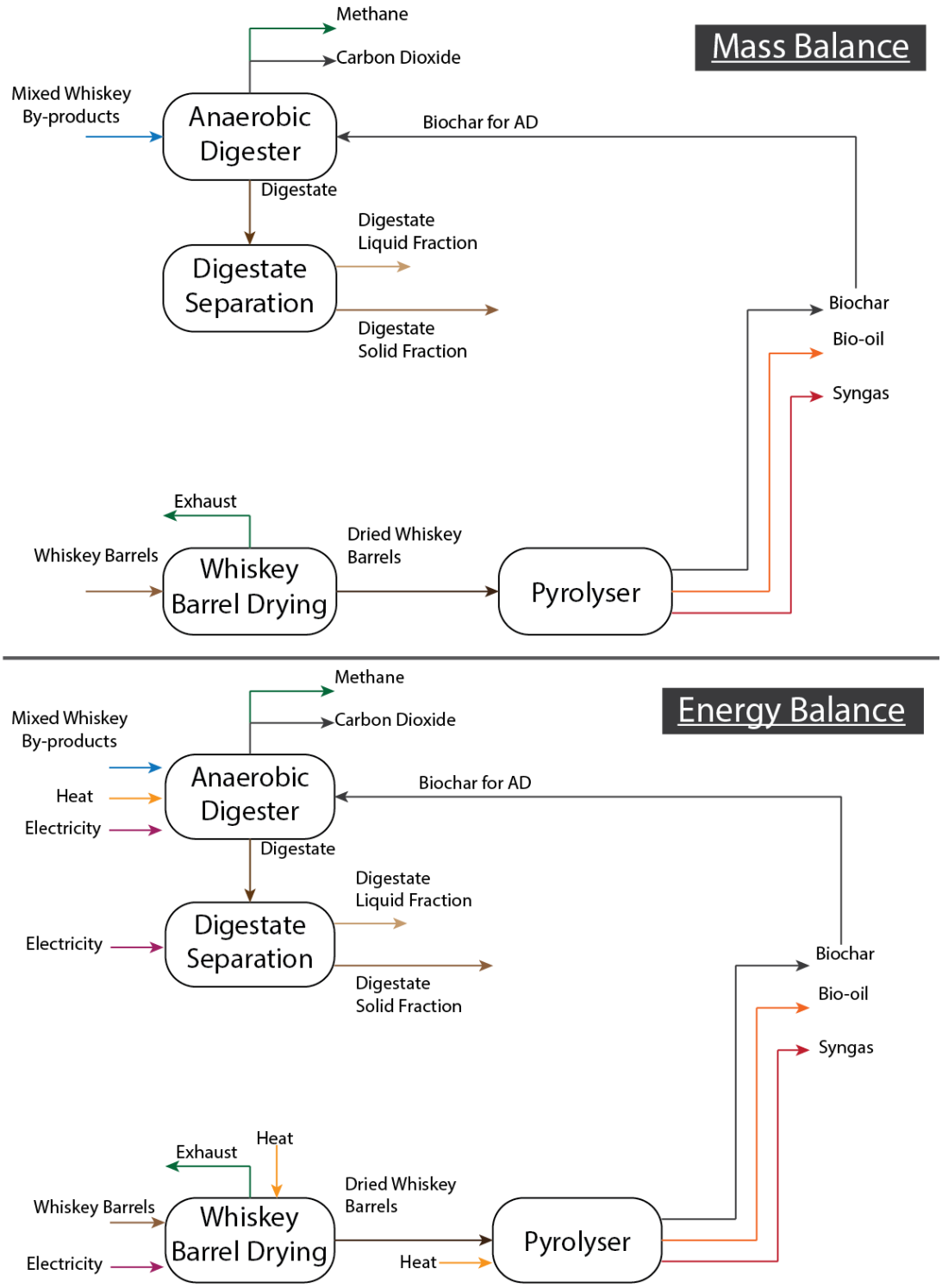


Figure 7.3: Mass and energy balance schematic of an integrated anaerobic digester and pyrolysis system processing whiskey barrels and whiskey by-products.

In addition, the following assumptions were made for the conventional AD system:

1. A mesophilic AD system processing a tonne of mixed whiskey by-products was assumed.
2. The system produces the same methane yield as the BMP assays. 60 $\%_{vol}$ of the biogas was biomethane, and the remaining 40 $\%_{vol}$ was carbon dioxide.
3. The electricity demand for the AD system was taken to be 10 kWh. t^{-1} of biomass (Vo et al., 2018). The thermal demand (H_{inAD}) to maintain mesophilic temperatures was calculated as follows:

   $$H_{in\ AD} = m_{mWBM} \times C_{p_{\mathrm{H2O}}} \times \Delta T$$

   Where: m_{mWBM} is the mass of wet mixed whiskey by-products; $C_{p_{\mathrm{H2O}}}$ is the specific heat capacity of water, and ΔT is the change in temperature between the digester temperature (37 ^{o}C) and the average ambient temperature (15 ^{o}C).
4. A decanter centrifuge (70 % efficiency) was used to separate the digestate into the liquid and solid fractions. The electrical demand for the digestate separation process was 3.5 kWh. t^{-1}digestate (Tampio et al., 2016).
5. The lower heating value (LHV) of biomethane was assumed to be 50 MJ. kg^{-1}, and no energy contribution came from the carbon dioxide.
6. The consumption of heat and electricity were transformed into primary energy consumption within the European framework, employing the primary energy conversion factors of 1.1 and 2.3 for heat and electricity, respectively (Esser and Sensfuss, 2016). This was done to account for the typical energy mix within Europe and to future-proof the calculation methodology if renewable energy sources, such as solar or other fuels, are used.

For the integrated AD-pyrolysis system, the assumptions regarding the conventional AD system were retained for consistency with the following additional assumptions considered:

1. Whiskey barrels were readily available to produce the required biochar dosage for AD.
2. The thermal demand of the pyrolysis units (H_{inPY}) was calculated as follows:

$$H_{in\,PY} = m_{DriedMass} \times C_{p_{dried}} \times \Delta T$$

Where: $m_{DriedMass}$ is the mass of the whiskey barrels; $C_{p_{dried}}$ was the specific heat capacity of the dried pyrolysis matter and was assumed to be 1.8 MJ. kg^{-1}. $^{o}C^{-1}$ (Radmanović et al., 2014); and ΔT is the change in temperature between the pyrolysis holding temperature and the average ambient temperature (15 ^{o}C).

3. The electricity demand was taken to be 0.5 MJ. kg^{-1} (Monlau et al., 2015).
4. The biochar yields from the whiskey barrels were based on the experimental results from this study (Table 7.1). The different temperatures evaluated in this study would result in different bio-oil and syngas yields. The combined mass and energy of the bio-oil and syngas were approximated by subtracting the whiskey barrel TS content/energy content entering the pyrolyser with the biochar yield (see Table 7.1). For the mass balance, the bio-oil and syngas production were assumed to be 58.4 % and 32.8 % of the remaining TS content/energy content entering the pyrolyser, respectively (Monlau et al., 2015). For the energy balance, the syngas heating value was assumed to be 10.3 MJ. kg^{-1} and the remaining energy made up the bio-oil (Monlau et al., 2015).

5. The LHV of the different biochars were used for the analysis see Table 7.1.

7.2.9 Statistical significance

Statistical significance was assessed using a one-way analysis of variance (ANOVA) using the MS Excel data analysis Tool-Pak feature. The significance level was set to 0.05, with results $p<0.05$ evaluated as statistically significant. The statistical significance results were verified by an online statistic calculator, DataTAB.net (DATAtab Team, 2023). For significant differences between pairwise groups, the Fisher's Least Significant Difference (LSD) test was used to evaluate pairwise group comparison on DataTAB.net.

7.3 Results and discussion

7.3.1 Biochar production and properties

The biochar yield (%) reflects the mass of biochar produced from the total solids of the whiskey barrels. A decreasing biochar yield with increasing pyrolysis temperature was evident (see Table 7.1); this is ascribed to a loss of volatile components with increasing temperature. A similar trend in biochar yield with increasing temperature is evident in the literature (Kaur et al., 2020). The pH values of the biochars were slightly acidic and lower than biochars previously produced from soft-wood pellets (pH 7.91-8.44), indicating a diminished buffering capacity from whiskey barrel-derived biochar. The reported pH of biochar has a broad range (pH 4.6-10.4) due to variations between production processes and biomass characteristics (Jahromi et al., 2019; Shen et al., 2021).

The biochar carbon content increased with increasing pyrolysis temperature (see Table 7.1). Conversely, the hydrogen and oxygen content of the biochar decreased

with increasing pyrolysis temperature. These two trends have an impact on the carbonisation ratios (O/C and H/C molar ratios) of biochar. Both carbonisation ratios exhibited a decreasing trend as temperature increased, suggesting improved carbonisation with increasing temperature (see Table 7.1). Similar trends in biochar yield, carbonisation ratios, and pH values have been observed in the literature evaluating biochar production at various temperatures (Shen et al., 2021). The electrical conductivity for Char300 was higher than both Char500 and Char 700. The electrical conductivity values were within the typical ranges reported in the literature of 60-3110 µS. cm^{-1} (Kaur et al., 2020).

Table 7.1: Compositional characteristics and surface properties of whiskey-barrel derived biochar at various temperatures

	Char300	**Char500**	**Char700**
Ash (%TS)	<1	<1	<1
Biochar yield (%)[a]	46	35	20
pH	5.96	6.16	6.18
C (%TS)	60	78	86
H (%TS)	4	2	1
N (%TS)	~0	~0	~0
O (%TS)	36	20	13
O/C	0.60	0.26	0.15
H/C	0.07	0.03	0.01
Specific surface area (m^2. g^{-1})	0.481	298.1	401.8
Pore volume (cm^3. g^{-1})	~0	0.122	0.171
Electrical conductivity (µS. cm^{-1})	195.2	122.8	126.4
Higher heating value (MJ. kg^{-1}TS)	18.1	24.9	27.7
Lower heating value (MJ. kg^{-1}TS)	16.9	24.3	27.4

Where: [a] Biochar yield = total mass of biochar per total solid mass of whiskey barrel added

Contradictory trends in electrical conductivity with increasing temperature have been observed previously (Shen et al., 2021; Wang et al., 2020). The electrical conductivity results suggest that Char300 may have the highest ability to transfer

electrons in suspension (Deng et al., 2021). Increasing specific surface area and pore volume were observed with increasing temperature (see Table 7.1), which suggests higher adsorption capacity for biochars produced at higher temperatures (Yin et al., 2017). The unique characteristics of the different biochars suggest that each could have different effects on the AD process. Char300, due to higher electrical conductivity, may be best suited for increased biomethane production by facilitating enhanced direct interspecies electron transfer (DIET) (Zhao et al., 2021). Char700 provides better absorbent qualities with its higher specific surface area and pore volume and thus could be used with substrates containing inhibitory elements such as ammonia.

7.3.2 Fourier transform infrared spectroscopy observations

The FTIR spectra of the biochars are illustrated in Figure 7.4. Char700 had the least functionality of the three biochars evaluated, suggesting less functional groups were present in Char700. The flattening of the peaks with increasing pyrolysis temperature, observed in Char500 as compared to Char300, suggest a loss of O-containing functional groups with increasing temperature (Deng et al., 2021). The following transmittance peaks were observed in Char300 and Char500: the broad transmittance peak of ca. 950-1,490 cm^{-1} is associated with overlapping peaks from C-O, C-C and C-N stretching and C-H bending vibrations. As negligible N was detected to be present in the biochars by elemental analysis (as per Table 7.1), the C-N bond was most likely not present. Peaks in the region of 1,490 - 1,750 cm^{-1} were associated with C=O and aromatic C=C stretching. The Char300 and Char500 both display peaks at 1700 cm^{-1}, characteristic of the C=O stretching vibration, which is absent in the Char700 biochar. A minor peak at 2,980 cm^{-1} was only observed in

Char700, attributed to the C-H stretching vibrations. As functional groups play a pivotal role in DIET, it can be hypothesized that Char700 may be the least effective biochar in facilitating DIET due to the lower degree of O-containing surface functional groups, as indicted by FTIR and elemental analysis (see Table 7.1) (Deng et al., 2021).

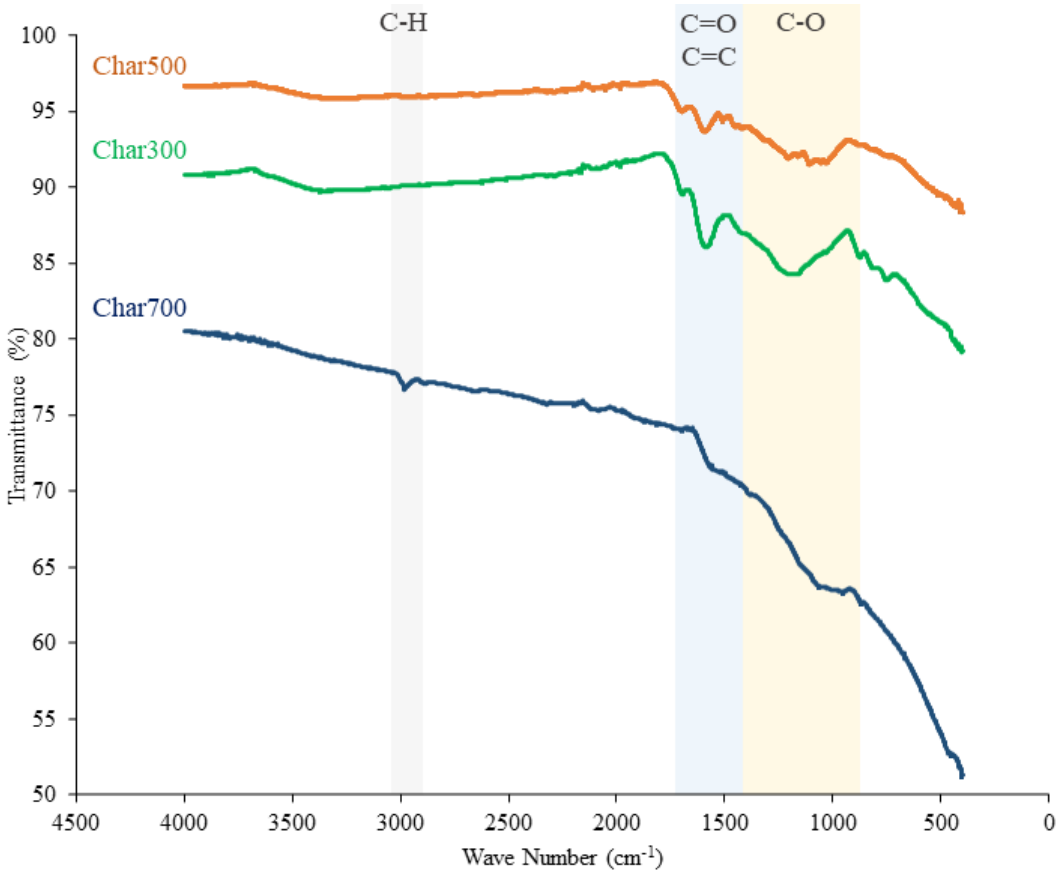


Figure 7.4: Biochar FTIR analysis produced at different pyrolysis temperatures.

7.3.3 Whiskey barrel-derived biochar and biomethane production

Figure 7.5 exhibits the various biochar dosages and their impact on biomethane potential. The control group, Group M0, reached a specific biomethane yield of 325 L CH_4. kg^{-1} VS, which equated to a BI of 65 %. This specific biomethane yield was lower than various yields observed in the literature processing similar feedstocks

(384-389 L CH_4. kg^{-1}VS) (Hackula et al., 2023b; Kang et al., 2021). This could be due to reduced activity of the inoculum, which was observed in the cellulose control, Group M14, which produced 251±13 L CH_4. kg^{-1} cellulose as opposed to the theoretical maximum of 350 L CH_4. kg^{-1}cellulose (Raposo et al., 2011). It was hypothesized the inoculum change in operation from continuous operation to batch operation resulted in a shift in microbial community composition and/or predation patterns, ultimately reducing the inoculum activity (Kundu et al., 2013).

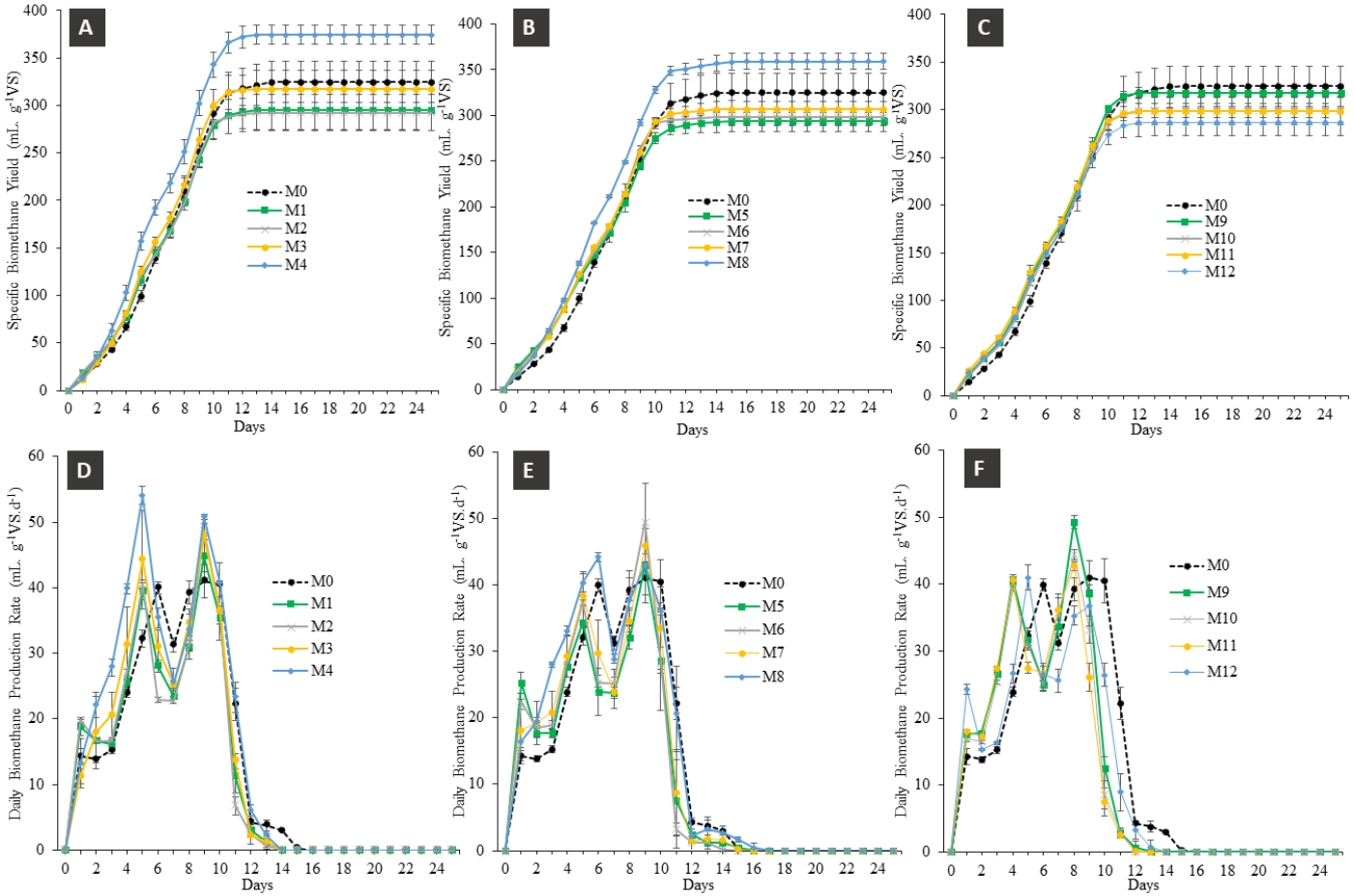


Figure 7.5: Specific biomethane yield (A-Char300, B-Char500 and C-Char700) and the daily biomethane production (D-Char300, E-Char500 and F-Char700) for whiskey by-products with variable biochar additions: M0 was the control group with no biochar addition; M1 to M4 biochar to substrate ratio of 0.25, 0.5, 1 & 2 g $_{biochar}$. $g^{-1}VS_{substrate}$, respectively; M5 to M8 contained 0.25, 0.5, 1 & 2 g $_{biochar}$. $g^{-1}VS_{substrate}$, respectively M9 to M12 biochar to substrate ratios of 0.25, 0.5, 1 & 2 g $_{biochar}$. $g^{-1}VS_{substrate}$, respectively.

Only the highest dosages of Char300 and Char500, groups M4 and M8, statistically enhanced the specific biomethane yield in comparison to the group without biochar addition (M0), producing 374 and 359 L CH_4. kg^{-1}VS, respectively ($p<0.05$). The remaining doses of Char300 and Char500 had no significant effect on the specific biomethane yield, suggesting the doses were insufficient in promoting DIET ($p>0.05$). Lower specific biomethane yields were observed across the different doses of Char700. Other than the highest dosage applied for Char700, Char700 had no statistically significant effect on the specific biomethane yield as compared to Group M0 ($p>0.05$). It was hypothesized that the lower electrical conductivity as compared to Char300 and reduced functionality observed in the FTIR analysis (see Table 7.1 and Figure 7.4) could not facilitate DIET; thus, no enhancement of biomethane was observed from the addition of Char700. The adsorptive properties of Char700, such as high porosity and specific surface area, may have reduced the available volatile content and adsorbed available organic content for methanogenesis; thus, an inhibitory effect was observed at the highest dosage. A separate study that investigated another carbonaceous material, activated carbon with high porosity, also reported a similar effect due to VFA adsorption (Xie et al., 2022). No statistical difference between the specific biomethane yield of Group M4 (Char300 with a biochar to substrate ratio of 2:1) and Group M8 (Char500 with a biochar to substrate ratio of 2:1) was observed ($p>0.05$). However, both groups were statistically higher than the control group, Group M0, improving the specific biomethane yield by up to 15 % ($p<0.05$).

In relation to the daily production of biomethane, three peaks were evident across all assays (see Figure 7.5D, E, and F). The initial peak on day 1 could be associated with the readily degradable organic fraction within the mixed whiskey by-product

feedstock. The initial peak was least pronounced in group M0. The second peak, between days 4-6, could be associated with the degradation of the liquid fraction of the feedstock. For the most part, this peak was evident later in group M0 as compared to the groups with biochar addition. This suggests a reduced lag phase for groups with biochar addition, which can be ascribed to improved hydrolysis and acidogenesis. Finally, the peak between days 8 - 10 could be associated with the degradation of the solid fraction of the mixed whiskey by-products. In general, this peak was lowest in group M0, which again indicates enhanced hydrolysis and acidogenesis in the biochar-containing groups.

Based on the experimental results, Group M4 (Char300 at a biochar to substrate ratio of 2 g biochar. g^{-1}VS) and Group M8 (Char500 at a biochar to substrate ratio of 2 g biochar. g^{-1}VS) were favourable for biomethane production. Char700 had a statistically insignificant impact on the specific methane yield. However, the adsorptive properties of Char700 may negate inhibitory effects during continuous reactor operation, which may be a reason to consider the use of this biochar.

7.3.4 Assessing the kinetics of biochar addition on the biomethane potential

The modified Gompertz equation was used to evaluate the kinetic parameters for biomethane production trials, as shown in Table 7.2.

The peak biomethane production rate (*Rm*) with Char300 and Char500 increased with increasing biochar dosage (as per Table 7.2), and the highest dosage exhibited the highest peak biomethane production rate. The opposite trend was observed for Char700. Overall, all biochars reduced the lag phase by up to 42 % compared to Group M0. These observations in the lag phase are dissimilar to results from biochar

derived from draff, which was previously observed to have a negligible effect as a biochar amendment on the lag phase (Deng et al., 2021). In general, shorter lag phases describe faster biomethane production. Shorter lag phases may have desirable implications in demand-driven biomethane production systems whereby biomethane is generated on-demand. This type of operational approach benefits from a more rapid response; thus, shorter lag phases are desired (Hackula et al., 2024). A high adjusted R^2 value was observed across all the variations of biochar addition for biomethane (>0.97).

Table 7.2: Biomethane kinetic parameters of mixed whiskey by-products at various biochar temperatures and dosages

			Experimental results			Kinetic model parameters				
	Group	Biochar to substrate ratio	Biochemical methane potential (ml. g^{-1}VS)	BI[a] %	Specific energy yield (MJ. kg^{-1}VS)	V_{max}[b] (ml. g^{-1}VS)	R_m[c] (ml. g^{-1}VS. d^{-1})	λ[d] (d)	T_m[e] (d)	Adj. R^2
Control	M0	/	325 *	65	11.7	337	43.5	2.6	10.4	0.98
Char300	M1	0.25	295 *	59	10.6	306	38.2	2.0	10.0	0.98
	M2	0.5	292 *	58	10.5	304	37.7	1.9	9.9	0.97
	M3	1	317 *	63	11.4	328	43.2	2.2	9.8	0.98
	M4	2	374 **	75	13.4	387	48.4	1.9	9.9	0.99
Char500	M5	0.25	293 *	57	10.5	305	35.8	1.5	10.0	0.98
	M6	0.5	298 *	59	10.7	309	39.2	1.7	9.6	0.97
	M7	1	307 *	61	11.0	317	39.9	1.8	9.8	0.98
	M8	2	359 **	72	12.9	371	46.1	1.9	9.9	0.99
Char700	M9	0.25	318 *	63	11.4	331	41.2	2.0	10.0	0.98
	M10	0.5	299 *	60	10.7	310	39.9	2.0	9.7	0.98
	M11	1	299 *	60	10.7	309	39.1	1.6	9.5	0.98
	M12	2	287 ***	57	10.3	297	37.7	1.7	9.6	0.98

Where: a = BI – biodegradability index; b = V_{max} – maximum biomethane yield; c = R_m - peak biomethane production rate; d = λ - lag phase in days; e = T_m - digestion process peak time in days;
*; **; * statistically similar pairwise groups are denoted by the number of asterisks.

7.3.5 Observations in microbial taxonomy

No consistent correlations were observed between taxonomic abundances and cumulative biomethane yields (see Appendix E.6). The correlations between bacterial taxon relative abundances and cumulative biomethane yields were observed in the BMP assays for the Phylum Chloroflexi, the Classes Anaerolineae and δ-Proteobacteria, the Orders Anaerolineales and Syntrophobacterales, the Families Porphyromonadaceae, Anaerolinaceae and for the Genus Bacteroides. No correlations between cumulative biomethane yields and archaeal taxon abundances at any level of classification in the BMP assays were observed.

Surprisingly, no archaeal acetoclastic methanogens were identified from any of the trials (see Appendix E.6). Whether or not the presence of these taxa was obscured in the cohort of sequences that were not classified or not classified below the Kingdom level is not known. If they were truly absent, and if biomethane production was strictly through methylotrophic and hydrogenotrophic pathways, then this is not an effect of biochar supplementation, as acetoclastic taxa were also absent from BMP assays with no such supplement. Notwithstanding the unclassified sequencing reads, the correlations observed between cumulative biomethane yields and taxon relative abundances suggest that the positive mechanistic effects are on the bacterial communities and in the hydrolysis and acidogenesis stages of biomethane production and not on the archaeal methanogenesis. A previous study hypothesized enhanced hydrolysis and acidogenesis with biochar addition in two-phase digestion of grass and slurry (Ning et al., 2023).

7.3.6 Evaluation of system energy efficiencies

The energy efficiency of a conventional AD system was assessed based on the experimental results shown in Table 7.2 and the characteristics of the feedstock in Table 7.1 (see Section 7.2.8 for assumptions used for the analysis). The comprehensive energy and mass balance of the conventional AD system can be found in Appendix E.3. The comparative energy efficiency analysis is summarised in Table 7.3.

Based on the mass and energy analysis of biochar addition, the highest energy efficiency was observed when biochar produced at 300 ^{o}C was used. The lowest efficiency was observed in the system without biochar addition. The energy efficiencies from the analysis were higher compared to a previously analysed integrated AD-pyrolysis system processing different materials by (Deng et al.,2020); in that work, an AD-pyrolysis unit treating seaweed as the AD feedstock, with biochar produced from forest residues and digestate at a biochar dosage-to-substrate ratio of 0.25 g biochar. g^{-1}VS reported an energy efficiency of 57 % (Deng et al., 2020). Deng et al., (2020) evaluated further processing of the digestate, which required additional heating and electricity demands, such as digestate drying, and which may decrease the system efficiency. The financial and environmental aspects of implementing biochar addition were deemed out of the scope of this analysis; instead, priority was given to the system's energy benefits. Critically, the availability of whiskey barrels to implement such a system may be a limitation at the highest dosages.

Table 7.3: Comparative analysis of energy efficiency of biochar addition in anaerobic digesters

Parameters	Symbol	Units	No biochar	Char 300	Char 500	Char 700
System			1	2	2	2
Feedstock mass	$m_{feedstock}$	t	1	1	1	1
Whiskey barrel volatile solids		t		0.278	0.366	0.08
Feedstock volatile solids		t	0.064	0.064	0.064	0.064
Pyrolysis holding temperature		^oC		300	500	700
Biochar to substrate ratio[a]			0	2	2	0.25
Biochar addition	$m_{biochar}$	t	0	0.128	0.128	0.016
Methane production	m_{CH4}	t	0.015	0.017	0.016	0.015
Carbon dioxide production	m_{CO2}	t	0.027	0.032	0.030	0.027
Digestate production	$m_{AD\ digestate}$	t	0.96	1.08	1.08	0.98
Energy value of feedstock and whiskey barrels	$Q_{feedstock}$	MJ	963	4,484	5,589	1975
Total primary energy consumption in the process	$Q_{primary\ E}$	MJ	223	1,974	2,666	777
Energy output of the system		MJ	744	4,372	5,426	1,763
Net energy output; excluding feedstock energy[b]		MJ	521	2,398	2,764	986
Specific energy yield[c]		MJ. $kg^{-1}VS$	8.1	7.0	6.4	6.8
Process energy efficiency[d]		%	63	68	66	64

Where: a = biochar to substrate ratio, on a wet weight of biochar to volatile solids basis of substrate introduced into the reactor, of best-performing dosage achieved during experimental trials. b = energy output of the system subtracted by the total primary energy consumption of the system; c = the specific energy yield considers the net energy output divided by the feedstock and whiskey barrel where applicable; d = process energy efficiency considers the energy output of the system divided by the energy inputs, which include the feedstock, biochar, and primary input energy, of the system.

For a 50 million L_{OLA} facility based in Ireland, the whiskey barrels available for pyrolysis are approximately 0.7 $g_{\text{whiskey barrels}}$. $g^{-1}VS_{\text{mixed whiskey by-products}}$. The resource would only be sufficient for the lowest AD dosages of biochar pyrolysed at 300 ^oC and 500 ^oC applied in this study if a continuous dosage strategy is required. A

proposed solution would be to purchase additional whiskey barrels from the United States of America (USA), where whiskey barrels from bourbon are only permitted for singular use (National Archives and Records Administration, 2023). The large distillery considered in this study already imports whiskey barrels from the United States of America as part of their process. Therefore, the practicality and logistic considerations of purchasing additional whiskey barrels is already in place. Alternatively, implementing an AD system that has a high solids retention mechanism, such as the expanded granular sludge bed, may not require continuous dosing and thus may not necessitate as high quantities of biochar (Yang et al., 2018). Adopting an integrated AD-pyrolysis approach whereby the digestate, which contains both digestate and biochar, is further processed to create biochar, would also reduce the amount of whiskey barrels required for the system. The integrated AD-pyrolysis system would be able to overcome the resource limitation as the biochar would be recycled within the system.

Furthermore, such an approach may become necessary in the future to aid digestate management. As such, the digestate solid fraction would be pyrolysed, leaving only the digestate liquid fraction for further digestate management. In such a case, the integrated system would now valorise the solid digestate into the pyrolysis products: biochar, syngas, and bio-oil.

Various options are available to improve the system's energy efficiency, such as the integration of renewables. For example, the use of heat pumps to utilise heat from other processes within the distillery may also improve the overall system efficiency. Renewable energy integration was evaluated on Char300 at the highest dosage by

changing the primary energy factor of electricity from 2.3 to 1. The overall energy efficiency was increased from 68 % to 71 %. This study does not highlight the other benefits of biochar addition, such as alleviating inhibitory effects of ammonia accumulation, which have been observed with anaerobic digesters processing whiskey by-products (Kang et al., 2022). Nor does this study examine the benefits of carbon sequestration associated with biochar addition to land, which can equate to 900 kg $CO_{2\text{-equiv}}$. $t^{-1}_{biochar}$ (Wu et al., 2023). Evaluating the self-sustainability and environmental aspects of implementing such a system is required. Establishing the system configuration that will meet the distillery's objectives requires further investigation. A lifecycle analysis and techno-economic analysis are required to evaluate the optimum use of the pyrolysis products from the proposed process.

7.4 Conclusion

Whiskey barrel-derived biochar, produced at different temperatures, was utilised in anaerobic digestion (AD). Biochar pyrolysed at 300 ^{o}C enhanced biomethane production by up to 15 %. Kinetic analysis revealed biochar, at all temperatures, reduced the biomethane lag time by up to 42 %. An investigation of the taxonomy suggested that the positive mechanistic effects are on the bacterial communities and in the hydrolysis and acidogenesis stages of biomethane production and not on the archaeal methanogenesis. The integrated AD-pyrolysis system was evaluated to have an overall system energy efficiency of 64-68 % across the different pyrolysis temperatures (300-700 ^{o}C).

Data availability

All sequencing data has been deposited in the GenBank Short Read Archive (SRA) and are publicly available with accession numbers SRX23538931-SRX23538937, under BioProject number PRJNA1072329.

https://www.ncbi.nlm.nih.gov/sra/PRJNA1072329

References

1. APHA, 2022. Standard Methods for the Examination of Water and Wastewater™, 24th ed. American Public Health Association, American Water Works Association, and Water Environment Federation.
2. DATAtab Team, 2023. DATAtab: Online Statistics Calculator.
3. Deng, C., Lin, R., Kang, X., Wu, B., O'Shea, R., Murphy, J.D., 2020. Improving gaseous biofuel yield from seaweed through a cascading circular bioenergy system integrating anaerobic digestion and pyrolysis. Renewable and Sustainable Energy Reviews 128, 109895. https://doi.org/10.1016/j.rser.2020.109895
4. Deng, C., Lin, R., Kang, X., Wu, B., Wall, D.M., Murphy, J.D., 2021. What physicochemical properties of biochar facilitate interspecies electron transfer in anaerobic digestion: A case study of digestion of whiskey by-products. Fuel 306, 121736. https://doi.org/10.1016/j.fuel.2021.121736
5. Esser, A., Sensfuss, F., 2016. Review of the default primary energy factor (PEF) reflecting the estimated average EU generation efficiency referred to in Annex IV of Directive 2012/27/EU and possible extension of the approach to other energy carriers. Karlsruhe.
6. European Academies Science Advisory Council., 2018. Nagative emission technologies : what role in meeting Paris agreement targets? ESAC Secretariat.
7. European Commission. Directorate-General for Environment., 2023. Ireland, 2025 EU waste recycling targets : state of play. Publications Office of the European Union. https://doi.org/10.2779/378751
8. Hackula, A., O'Shea, R., Murphy, J.D., Wall, D.M., 2023a. Design, Construction, and Concept Validation of a Laboratory-Scale Two-phase Reactor

to Valorize Whiskey Distillery By-products. ACS Engineering Au. https://doi.org/10.1021/ACSENGINEERINGAU.3C00006

9. Hackula, A., Shinde, R., Hickey, D., O'Shea, R., Murphy, J.D., Wall, D.M., 2023b. Two-phase anaerobic digestion for enhanced valorisation of whiskey distillery by-products. Bioresour Technol 129239. https://doi.org/10.1016/J.BIORTECH.2023.129239
10. Hackula, A., Shinde, R., O'Shea, R., Murphy, J.D., Wall, D.M., 2024. Assessing two-phase anaerobic digestion systems for demand-driven electricity and biobutanol transport fuel at a large distillery. J Clean Prod 140974. https://doi.org/10.1016/j.jclepro.2024.140974
11. Hoang, A.T., Goldfarb, J.L., Foley, A.M., Lichtfouse, E., Kumar, M., Xiao, L., Ahmed, S.F., Said, Z., Luque, R., Bui, V.G., Nguyen, X.P., 2022. Production of biochar from crop residues and its application for anaerobic digestion. Bioresour Technol 363, 127970. https://doi.org/10.1016/j.biortech.2022.127970
12. Jackson, S.A., Kang, X., O'Shea, R., O'Leary, N., Murphy, J.D., Dobson, A.D.W., 2020. Anaerobic digestion performance and microbial community structures in biogas production from whiskey distillers organic by-products. Bioresour Technol Rep 12, 100565. https://doi.org/10.1016/j.biteb.2020.100565
13. Jahromi, N.B., Fulcher, A., Walker, F., 2019. What Is Biochar and How Different Biochars Can Improve Your Crops. Knoxville 829.
14. Johannesson, G.H., Crolla, A., Lauzon, J.D., Gilroyed, B.H., 2020. Estimation of biogas co-production potential from liquid dairy manure, dissolved air flotation waste (DAF) and dry poultry manure using biochemical methane potential (BMP) assay. Biocatal Agric Biotechnol 25, 101605. https://doi.org/10.1016/j.bcab.2020.101605

15. Kang, X., Lin, R., Li, L., Wu, B., Deng, C., O'Shea, R., Sun, Y., Murphy, J.D., 2021. Assessment of pretreatment and digestion temperature on anaerobic digestion of whiskey byproducts and microbial taxonomy. Energy Convers Manag 243, 114331. https://doi.org/10.1016/j.enconman.2021.114331
16. Kang, X., Lin, R., Wu, B., Li, L., Deng, C., Rajendran, K., Sun, Y., O'Shea, R., Murphy, J.D., 2022. Towards green whiskey production: Anaerobic digestion of distillery by-products and the effects of pretreatment. J Clean Prod 357, 131844. https://doi.org/10.1016/j.jclepro.2022.131844
17. Kaur, G., Johnravindar, D., Wong, J.W.C., 2020. Enhanced volatile fatty acid degradation and methane production efficiency by biochar addition in food waste-sludge co-digestion: A step towards increased organic loading efficiency in co-digestion. Bioresour Technol 308, 123250. https://doi.org/10.1016/j.biortech.2020.123250
18. Kirchsteiger, B., Kubik, F., Sturmlechner, R., Stressler, H., Schwabl, M., Kistler, M., Kasper-Giebl, A., 2021. Real-life emissions from residential wood combustion in Austria: From TSP emissions to PAH emission profiles, diagnostic ratios and toxic risk assessment. Atmos Pollut Res 12, 101127. https://doi.org/10.1016/J.APR.2021.101127
19. Kundu, K., Sharma, S., Sreekrishnan, T.R., 2013. Changes in microbial communities in a hybrid anaerobic reactor with organic loading rate and temperature. Bioresour Technol 129, 538–547. https://doi.org/10.1016/j.biortech.2012.11.118
20. Lahijani, P., Mohammadi, M., Mohamed, A.R., 2018. Metal incorporated biochar as a potential adsorbent for high capacity CO2 capture at ambient

condition. Journal of CO2 Utilization 26, 281–293. https://doi.org/10.1016/J.JCOU.2018.05.018

21. Monlau, F., Sambusiti, C., Antoniou, N., Barakat, A., Zabaniotou, A., 2015. A new concept for enhancing energy recovery from agricultural residues by coupling anaerobic digestion and pyrolysis process. Appl Energy 148, 32–38. https://doi.org/10.1016/j.apenergy.2015.03.024
22. National Archives and Records Administration, 2023. Title 27-Alcohol, Tobacco Products and Firearms Chapter I-Alcohol and Tobacco Tax and Trade Bureau, Department of the Treasury Subchapter A-Alcohol.
23. Ning, X., Deng, C., Hickey, D.T., Hackula, A., O'Shea, R., Wall, D.M., Lin, R., Murphy, J.D., 2023. Improving biomethane production from biochar-supplemented two-stage anaerobic digestion of on-farm feedstocks. J Clean Prod 423, 138723. https://doi.org/10.1016/j.jclepro.2023.138723
24. Radmanović, K., Đukić, I., Pervan, S., 2014. Specific Heat Capacity of Wood. Drvna industrija 65, 151–157. https://doi.org/10.5552/drind.2014.1333
25. Raposo, F., Fernández-Cegrí, V., De la Rubia, M.A., Borja, R., Béline, F., Cavinato, C., Demirer, G., Fernández, B., Fernández-Polanco, M., Frigon, J.C., Ganesh, R., Kaparaju, P., Koubova, J., Méndez, R., Menin, G., Peene, A., Scherer, P., Torrijos, M., Uellendahl, H., Wierinck, I., de Wilde, V., 2011. Biochemical methane potential (BMP) of solid organic substrates: evaluation of anaerobic biodegradability using data from an international interlaboratory study. Journal of Chemical Technology & Biotechnology 86, 1088–1098. https://doi.org/10.1002/jctb.2622
26. Shahriari, H., Warith, M., Hamoda, M., Kennedy, K.J., 2012. Anaerobic digestion of organic fraction of municipal solid waste combining two

pretreatment modalities, high temperature microwave and hydrogen peroxide. Waste Management 32, 41–52. https://doi.org/10.1016/j.wasman.2011.08.012

27. Sunyoto, N.M.S., Zhu, M., Zhang, Z., Zhang, D., 2016. Effect of biochar addition on hydrogen and methane production in two-phase anaerobic digestion of aqueous carbohydrates food waste. Bioresour Technol 219, 29–36. https://doi.org/10.1016/j.biortech.2016.07.089
28. Świechowski, K., Rasaq, W.A., Syguła, E., 2023. Anaerobic digestion of brewer's spent grain with biochars—biomethane production and digestate quality effects. Front Energy Res 11, 225. https://doi.org/10.3389/FENRG.2023.1141684/BIBTEX
29. Tampio, E., Marttinen, S., Rintala, J., 2016. Liquid fertilizer products from anaerobic digestion of food waste: mass, nutrient and energy balance of four digestate liquid treatment systems. J Clean Prod 125, 22–32. https://doi.org/10.1016/J.JCLEPRO.2016.03.127
30. Vo, T.T.Q., Wall, D.M., Ring, D., Rajendran, K., Murphy, J.D., 2018. Techno-economic analysis of biogas upgrading via amine scrubber, carbon capture and ex-situ methanation. Appl Energy 212, 1191–1202. https://doi.org/10.1016/j.apenergy.2017.12.099
31. Wang, P., Peng, H., Adhikari, S., Higgins, B., Roy, P., Dai, W., Shi, X., 2020. Enhancement of biogas production from wastewater sludge via anaerobic digestion assisted with biochar amendment. Bioresour Technol 309, 123368. https://doi.org/10.1016/j.biortech.2020.123368
32. Weber, K., Quicker, P., 2018. Properties of biochar. Fuel 217, 240–261. https://doi.org/10.1016/j.fuel.2017.12.054

33. Wei, Y., Gao, Y., Yuan, H., Chang, Y., Li, X., 2022. Effects of organic loading rate and pretreatments on digestion performance of corn stover and chicken manure in completely stirred tank reactor (CSTR). Science of The Total Environment 815, 152499. https://doi.org/10.1016/j.scitotenv.2021.152499
34. Wu, B., Lin, R., Bose, A., Huerta, J.D., Kang, X., Deng, C., Murphy, J.D., 2023. Economic and environmental viability of biofuel production from organic wastes: A pathway towards competitive carbon neutrality. Energy 285, 129322. https://doi.org/10.1016/j.energy.2023.129322
35. Xie, Z., Cao, Q., Chen, Y., Luo, Y., Liu, X., Li, D., 2022. The biological and abiotic effects of powdered activated carbon on the anaerobic digestion performance of cornstalk. Bioresour Technol 343, 126072. https://doi.org/10.1016/j.biortech.2021.126072
36. Yang, B., Wang, M., Wang, J., Song, X., Wang, Y., Xu, H., Bai, J., 2018. Mechanism of high contaminant removal performance in the expanded granular sludge blanket (EGSB) reactor involved with granular activated carbon for low-strength wastewater treatment. Chemical Engineering Journal 334, 1176–1185. https://doi.org/10.1016/J.CEJ.2017.11.072
37. Yin, Q., Zhang, B., Wang, R., Zhao, Z., 2017. Biochar as an adsorbent for inorganic nitrogen and phosphorus removal from water: a review. Environmental Science and Pollution Research 24, 26297–26309. https://doi.org/10.1007/s11356-017-0338-y
38. Zhao, W., Yang, H., He, S., Zhao, Q., Wei, L., 2021. A review of biochar in anaerobic digestion to improve biogas production: Performances, mechanisms and economic assessments. Bioresour Technol 341, 125797. https://doi.org/10.1016/j.biortech.2021.125797

University College Cork, Ireland
Coláiste na hOllscoile Corcaigh

CORA
Cork Open Research Archive
Cartlann Taighde Oscailte Chorcaí

Hackular, A. A. 2024. Decarbonisation of whiskey distilleries in a circular economy: investigating biorefinery systems for valorisation of distillery by-products. PhD Thesis, University College Cork.

Please note that Chapters 8-10 (pp. 246-332) are unavailable due to a request by the author.

CORA Cork Open Research Archive http://cora.ucc.ie

11.0 Conclusions and recommendations

11.1 Conclusions

This thesis explores various biorefinery technologies as a means of valorising whiskey by-products generated at a large distillery in Ireland while simultaneously providing a decarbonisation pathway. The objectives described in Section 1.2 have been addressed as follows:

- A two-phase anaerobic reactor leach bed reactor connected to an expanded granular sludge bed (termed LBR-EGSB) was designed, constructed, and conceptually validated to valorise liquid and solid whiskey distillery by-products. Several design modifications, including the integration of a cost-effective siphon-actuated leachate attenuation system, enhanced the configuration beyond that of comparable designs. High volatile fatty acid yields (10.3 g. $L^{-1}_{Leachate}$) and methane-rich biogas (75%$_{vol}$ CH_4) were produced.
- Three anaerobic digestion systems were evaluated and compared to valorise by-products generated at a whiskey distillery. From an energy perspective, any of the proposed systems are suitable as similar specific methane yields were evident. However, two-phase systems could provide additional valorisation opportunities through volatile fatty acid production. All three systems demonstrated benefits and limitations that may vary depending on a distillery's objectives.
- A biorefinery concept via dark fermentation was explored to valorise distillery by-products. The biogenic CO_2 produced through dark fermentation from a 50 million L_{OLA} facility was calculated to have the potential to supplement almost

half of the CO_2 requirements of the Irish brewing industry. The proposed biorefinery's potential value in terms of the products was estimated to be € 6.1 million (US$ 6.7 million). The biorefinery supports the distillery's transition to circular production systems.

- The demand-driven operation of two anaerobic digestion systems processing whiskey by-products was assessed and compared. Overall, the two-phase CSTR produced higher VFA yields and a shorter lag phase to reach peak biogas production rates than the LBR-EGSB system. The EGSB had higher biogas production, average daily biogas production rates, and more rapid biogas response. A theoretical analysis evaluated blending biobutanol with diesel, which showed the potential to displace 16 % of diesel in Scope 3 transport emissions. Both systems were able to operate in a demand-driven manner.
- Whiskey barrel-derived biochar, produced at different temperatures, was utilised in anaerobic digestion (AD). Biochar pyrolysed at 300 ^{o}C enhanced biomethane production by up to 15 %. Kinetic analysis revealed biochar, at all temperatures, reduced the biomethane lag time by up to 42 %. The integrated AD-pyrolysis system was evaluated to have an overall system energy efficiency of 64-68 % across the different pyrolysis temperatures (300-700 ^{o}C).
- The whiskey barrel-derived biochar (pyrolyzed at 300 ^{o}C) was compared to commercial biochar and activated carbon for their efficacy in enhancing the two-phase anaerobic digestion of whiskey by-product to produce biohythane. The highest energy-yielding combination was observed when whiskey barrel-derived biochar was used at a dosage of 2.0 g biochar. g^{-1}VS. Biohythane used as a transport fuel and in a CHP unit could reduce CO_2 emissions of the industry

site by 44 %. This approach enhances the scientific understanding of the circular applications of whiskey barrels.

- Two-phase anaerobic digestion comprising a CSTR-UASB was used to process whiskey by-products. High concentrations of caproic acid (ca. 3.6 g. L^{-1}) were observed in the CSTR digestate, with acidification reaching 70 %. Biochar addition can increase demand-driven biogas production. The distillery's current process, which produces cattle feed and whiskey, would be converted to produce caproic acid (for revenue), biochar (for methane enhancement), demand-driven biogas (for demand-side electricity reduction during peak hours) and whiskey.

11.2 Notable scientific contributions

The following notable scientific contributions that were made within this thesis are:

- Chapter 3 was the first study to evaluate an LBR-EGSB system for processing whiskey by-products, utilising principles of fluid mechanics to enhance leachate dispensing.
- Chapter 4 addressed a gap in the literature by accounting for and assessing both liquid and solid whiskey by-products across different AD system configurations, focusing on their potential to produce VFAs and biogas.
- Chapter 5 established the effects of different organic loading rates of whiskey by-products on the production of VFAs, biohydrogen, and biogenic carbon dioxide through dark fermentation, with a notable focus on quantifying the potential of these products for use in heating and transport within the distillery context.

- Chapter 6 was the first study to explore the further processing of VFAs into biobutanol for use in transport or potential emissions savings from blending biobutanol with diesel.
- Chapter 7 and 8 were the first studies to produce and utilise biochar derived from whiskey barrels in the anaerobic digestion of whiskey by-products, comparing its effectiveness with that of commercial carbonaceous materials.
- Chapter 9 was the first study to produce and utilise digestate-derived biochar specifically for demand-driven biogas production.

11.3 Recommendations and research implications

This body of work demonstrates the decarbonisation potential of a large distillery through the valorisation of by-products processed in different biorefinery concepts and anaerobic digestion systems. Based on the conclusions of this work, as highlighted in Section 11.1 in line with the Science Foundation Ireland (SFI) MaREI research centre's three impact priorities of 1. informing policy, 2. supporting industry, and 3. empowering society, the following recommendations are:

11.3.1 Policy

Based on the insights from the thesis, the following policy recommendations can be considered:

- Encourage circular economy models: policymakers should consider providing financial incentives, such as tax breaks or subsidies, for distilleries adopting circular economy processes. These incentives could target the uptake of the technologies explored in this thesis, such as two-phase anaerobic digestion.

- Promotion of energy self-sufficiency: policies that advocate and promote industries to be energy self-sufficient through biorefinery approaches are encouraged. For example, the implementation of processes that can satisfy a significant amount of the distillery's energy demand through biomethane or biohydrogen could be promoted through policy measures that recognise and reward energy self-sufficiency.
- Development of biobased products: establishing a framework or certification standards for biobased products such as bioplastics derived from industrial by-products is recommended. Ensuring the bio-products help with decarbonisation and national sustainability objectives while remaining safe for the environment and community is essential.

By adopting these recommendations, policymakers would be able to advance the shift to industry decarbonisation while simultaneously meeting the national sustainability goals and combating climate change.

11.3.2 Industry

Based on the insights from the thesis, the following recommendations for industry can be considered:

- Consider two-phase anaerobic digestion: traditional anaerobic digestion may be less of a financial undertaking initially, but two-phase anaerobic digestion provides more valorisation opportunities through VFAs production. VFAs can be processed to numerous other products, which could further decarbonise beyond the distillery’s immediate needs.

- Integrate cascading biorefinery approaches: the distillery has an abundant biogenic carbon dioxide resource which could be valuable in the future as fossil fuel use declines. The distillery should start adapting its current processes to consider the future use of this resource in a cascading biorefinery approach.
- Utilise biochar technology: biochar can be used in the cereal production process on agricultural lands and may enhance yields. Furthermore, the biochar from process by-products can be used to enhance biomethane and biohydrogen production, which could be considered if a distillery decides to implement two-phase anaerobic digestion.
- Investigate demand-driven biogas production: utilise demand-driven biogas production during peak demand hours, which can lead to better alignment with energy markets and improve the economic viability of the AD system.

Industry can significantly enhance their sustainability and reduce their carbon footprint through the use of their process by-products.

11.3.3 Community

Based on the insights from the thesis, the following recommendations for consumers and community stakeholders, such as educational institutes, can be considered:

- Consumer awareness: increasing awareness about the benefits of sustainable whiskey production process and the importance of supporting brands that adopt circular economy strategies is recommended. Educational campaigns should emphasise how these practices contribute to combating climate change.
- Policy engagement: local communities are encouraged to advocate for policies that support the development of sustainable practices. This can be achieved

through lobbying for regulations that incentivise the adoption of technologies such as anaerobic digestion.

The community has a key role in steering a transition for sustainable practices. Adopting these recommendations would lead to enhanced community engagement and environmental benefits.

11.3.4 Future research

The following recommendations are proposed for further research and practical implementation:

1. Optimisation of two-phase anaerobic digestions:
   a. Further refinements on the design and operation of the LBR-EGSB system to maximise the production of VFAs and biogas. This can be done through pretreatment, torrefaction, and/or carbonaceous additives.
   b. Long-term operational studies (years) to assess the stability and variability of the system. This is particularly important with the VFA profile, as the composition may influence any potential products generated from the process.
   c. Modernise the systems by integrating technology, such as sensory technology, real-time monitoring systems, and reactive artificial intelligence to adjust system operation for smooth operation.

2. Expand comparative study of anaerobic digestion systems:

a. The comparative analysis can be extended to encompass a broader range of anaerobic digestion technologies, such as microbial electrolysis cells, or alternative configurations, such as the membrane bioreactor.
b. The comparative analysis can be expanded to incorporate scalability, cost-effectiveness, and adaptability to different distillery requirements. For example, if the distillery only requires the treatment of liquid residues, the analysis may seek to incorporate the outputs of such an approach.

3. Volatile fatty acid extraction and utilisation:
   a. Various options were explored for VFAs from the study; however, the extraction and utilisation were only theoretical. Continuous extraction of high value caproic acid or butyric acid requires further investigation of the effects on biogas production and overall stability of the systems.
   b. The VFAs production route may be an attractive opportunity within the thesis. However, a comprehensive stakeholder engagement is required to evaluate the distillery's desire to pursue this valorisation path. This can be done through various qualitative methods such as focus groups, interviews, and surveys with open-ended questions or through various quantitative methods, such as conjoint analysis and preference ranking.
   c. Caproic acid was generated at notably higher yields in dark fermentation than usual without any additional ethanol. As the distillery already produces ethanol, a portion of the ethanol could be redirected for chain-elongation. This pathway requires further investigation.
   d. Indirect emissions may make up most of the emissions at a distillery. VFAs, which can be further processed into biofuels for blending with diesel, may

provide an interim decarbonisation solution. However, the other emissions, such as NOx emissions and particulates, would require further investigation. The ability of the fleet to blend diesel with the VFA derivatives also requires consideration.

4. Demand-driven system implications
   a. The distillery has a continuous thermal and electrical load. The demand-driven operation may solve their electrical demand-side reduction issues. However, their thermal demand would still require decarbonisation. Utilising some of the VFAs for biomethane may provide some of the thermal requirements, and an optimal strategy should be developed.
   b. Various topologies and energy storage systems are available to the distillery. Thus, a further study to better manage and utilise the biogas and combined heat and power (CHP) unit is required. This could be through a mass and energy balance of the possible configurations.
   c. The “stop-start” nature of the demand-driven system may have undesirable consequences on the CHP unit. For example, increased maintenance or replacement of parts. These additional expenses may negate the increased revenue generated from operating the system during peak hours. An investigation of the durability of a CHP unit operated in a demand-driven manner is required.

5. Progressing biochar utilisation:
   a. Evaluating the adsorption capacity of the biochar and adsorption selectivity may be of interest. For example, if the biochar effectively adsorbs all the VFAs

except butyric acid, it may provide a cost-effective pre-isolation system. This may also be a function of the different pyrolysis production parameters.

b. The use of biochar in solid retention systems, such as the UASB, potentially reduces the need for continuous addition. However, the biochar may have an adsorption capacity which may change the efficacy of the biochar. A dosage optimisation strategy based on the long-term adsorption capacity of the biochar needs to be developed.

c. While the biochar was used in AD in the thesis, an exploration of other applications, such as a soil amendment or as a sacrificial electrode for water electrolysis, is required. The objective should be to fully leverage the properties of the biochar and contribute to an environmentally sustainable solution, which may exist outside the scope of the distillery.

6. Comprehensive assessment of integrated systems:

   a. A techno-economic analysis (TEA) and life cycle assessment (LCA) of the various systems is required to evaluate their overall environmental and financial impacts.

   b. Development of guidelines and best practices for the implementation of such systems in other industries with organic residues may be of interest.

   c. A comprehensive integration approach whereby whiskey by-products are co-digested with other feedstocks generated, such as brewery by-products and cider pomace, may be of interest in regions with significant industries.

7. Development of policy and regulatory frameworks:

a. Further research through collaboration with industry stakeholders, and policymakers is required to develop a supportive regulatory framework that stimulates circular economy practices and the growth of biorefinery technologies.
b. Incentives for distilleries and similar industries to invest in waste reduction, energy self-sufficiency, and green production practices are required.

The recommendations can advance the distillery industry towards a more sustainable and economically viable future, while progressing applied science with regards to biorefinery systems. By leveraging their by-products through biorefinery technologies, distilleries can transform their by-product into valuable resources.

Appendices

Appendix A

Appendix A.1: Theoretical substrate composition calculation of mWBM

Box A.1: mWBM substrate composition on a TS, VS and total weight basis.

Table A.1: Whiskey by-products and characteristics used to calculate cake maize and centrate annual production

	Unit	Draff	Thin stillage	Thick stillage	Cake maize	Centrate
Per annum	(tww)	31251	322813	277503	$m_{ww_{cake}}$	$m_{ww_{cent}}$
%ww of mWBM	(%)	4.95	51.11	43.94		
Wet ratio		1	10	9		
Total solids	(%)	27.38	2.94	8.87	29.02	3.54
TS amount	(t TS)	8557	9500	24615		
Volatile solids	(% TS)	95.99	88.77	95.62	97.22	89.25
Volatile solids	(%ww)	26.28	2.61	8.48	28.21	3.16
VS amount	(t VS)	8213	8433	23536		
VS Ratio		1	1.03	2.87		
% VS ratio of mWBM		20	21	59		

The total wet weight of thick stillage ($m_{ww_{thick}}$) must equal the combined wet weight of cake maize ($m_{ww_{cake}}$) and centrate ($m_{ww_{cent}}$). $m_{ww_{cake}}$ and $m_{ww_{cent}}$ can be rewritten with the known volatile content of the wet weight (Table S1):

$$m_{ww_{thick}} = m_{ww_{cake}} + m_{ww_{cent}}$$

$$m_{ww_{thick}} = \frac{m_{vs_{cake}}}{X_{vs_{cake}}} + \frac{m_{vs_{cent}}}{X_{vs_{cent}}}$$

$$277503\ t = \frac{m_{vs_{cake}}}{0.2821} + \frac{m_{vs_{cent}}}{0.0316}$$

- Multiply by 0.2821

$$78284 = m_{vs_{cake}} + \frac{2821}{316} m_{vs_{cent}}$$

$$m_{vs_{cake}} = 78284 - \frac{2821}{316} m_{vs_{cent}} \quad \textit{- equation 1}$$

Where:

$X_{vs_{cake}}$: $\%VS\ of\ cake\ maize$

$X_{vs_{cent}}$: $\%VS\ of\ centrate$

The VS of thick stillage ($m_{vs_{thick}}$) must equal the combined VS of Cake Maize($m_{vs_{cake}}$) and Centrate($m_{vs_{cent}}$).

$$m_{vs_{thick}} = m_{vs_{cake}} + m_{vs_{cent}}$$

$$23536\ t = m_{vs_{cake}} + m_{vs_{cent}}$$

$$m_{vs_{cake}} = 23536 - m_{vs_{cent}} \text{ - } \textit{equation 2}$$

Substitute equation 1 into 2:

$$78284\ - \frac{2821}{316} m_{vs_{cent}} = 23536 - m_{vs_{cent}}$$

$$78284 - 23536 = (\frac{2821}{316} - 1) m_{vs_{cent}}$$

$$m_{vs_{cent}} = 6906\ t\ VS\ per\ annum$$

$$\therefore m_{ww_{cent}} = \frac{m_{vs_{cent}}}{0.0316} = \frac{6906}{0.0316} = 218544\ t\ WW\ per\ annum$$

Substitute $m_{vs_{cent}}$ into equation 1:

$$m_{vs_{cake}} = 23536 - m_{vs_{cent}} = 23536 - 6906 = 16630\ t\ VS\ per\ annum$$

$$\therefore m_{ww_{cake}} = \frac{m_{vs_{cake}}}{0.2821} = \frac{16630}{0.2821} = 58951\ t\ WW\ per\ annum$$

The annual total solids can be calculated from the wet weight and the %TS from Table 3.1:

$$m_{ts_{cake}} = m_{ww_{cake}} \times 0.2902 = 58951 \times 0.2902 = 17108\ t\ TS\ per\ annum$$

$$m_{ts_{cent}} = m_{ww_{cent}} \times 0.0354 = 218544 \times 0.0354 = 7736\ t\ TS\ per\ annum$$

The percentage composition of mWBM on a wet weight basis and volatile solid basis can be calculated using the annual production rate.

$$\%\ Centrate_{VS\ basis} = \frac{m_{vs_{cent}}}{m_{vs_{draff}} + m_{vs_{thin}} + m_{vs_{cake}} + m_{vs_{cent}}} =$$

$$\frac{6906}{8213+8433+16630+6906} = 17.2\ \%\ \text{Centrate VS in mWBM}$$

$$\%\ Centrate_{ww\ basis} = \frac{m_{ww_{cent}}}{m_{ww_{draff}} + m_{ww_{thin}} + m_{ww_{cake}} + m_{ww_{cent}}}$$

$$\%\ Centrate_{ww\ basis} = \frac{218544}{31251 + 322813 + 58951 + 218544} = 34.6\%$$

The same method was used to calculate the percentage of cake maize produced per annum. Table S1 Shows the VS and WW composition and theoretical quantities of the substrates that make up mWBM

Table A.2: mWBM composition on a VS and WW basis

	Draff	Thin Stillage	Cake Maize	Centrate
VS Basis (% VS mWBM)	20	21	41	17
VS Mass (t VS per annum)	8213	8433	16630	6906
WW Basis (% WW mWBM)	5	51	9	35
Wet Weight (t WW per annum)	31251	322813	58951	218544

The theoretical VS content of mWBM can be calculated from Table S2:

$$\%VS = \frac{m_{VS}\ of\ substrates}{m_{ww}\ of\ substrates} = \frac{8213 + 8433 + 16630 + 6906}{31251 + 322813 + 58951 + 218544}$$

$$\%VS = 6.36\ \approx \mathbf{6.4}\ \%\boldsymbol{VS\ in\ mWBM}$$

The theoretical TS content of mWBM was calculated similarly.

Appendix A.2: Specific methane activity (SMA) of granular sludge

The specific methane activity (SMA) test is used to establish the methane-producing capacity of the inoculum. The SMA provides insight into the reactor's organic loading rate, particularly during an anaerobic reactor's start-up (Nizami et al., 2011). The SMA was determined by adding a known amount of volatile solids content in the inoculum (1.61 gVS) into a glass bottle and a known amount of acetic acid (2.2 g COD. L^{-1}) (Hussain & Dubey, 2017). The gas production was monitored during this period using the Bioprocess Control ™ AMPTS II. The bottles were kept at 37ºC in a water bath. The SMA is approximated by plotting the g COD equivalent of methane production against time (in hours) and dividing it by the gVS.

SMA = methane produced (g COD-CH_4). g^{-1}VS

Equations B.1 and B.2 are required to convert methane to the COD equivalent (Chernicharo, 2007):

$$K(t) = (P.K)/[R.(273 + T)] \text{ – Equation B.1}$$

$$V_{CH4} \times K(t) = Methane\ produced\ in\ sCOD\ equivalent\ (gCH_4 - COD) \text{ – Equation B.2}$$

Where:

K(t) = correctional factor due to reactor operating temperature (g COD.L_{CH4}^{-1})

P = atmospheric pressure (1 atm)

K = One mole of CH_4 in COD (64 g COD per mole)

R = gas constant (0.08206 atm.L/mole.ºK)

T = temperature of the reactor (^{o}C)

V_{CH4}= volume of methane produced (L)

Box A.2: Specific Methane Activity (SMA) of Granular Sludge Used in EGSBs.

The correction factor was calculated using equation B.1

$$K(t) = \frac{P.K}{[R.(273+T)]} = \frac{1\times64}{[0.08206\times(273+37)]} = 2.52 \text{ g COD. L}_{CH_4}^{-1}$$

Figure A.1 shows the cumulative methane production.

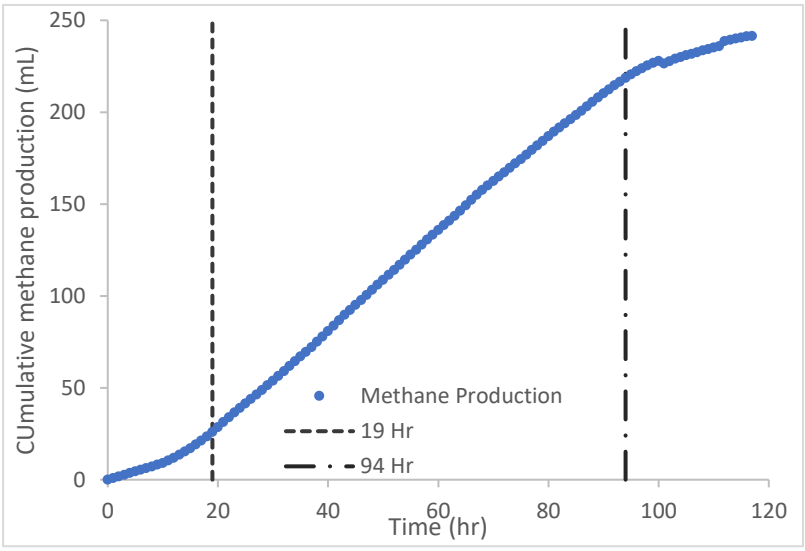


Figure A.1: Cumulative methane production from the SMA test.

The SMA was estimated by using the gradient at the steepest region (Chernicharo, 2007) in Figure S1, which is between 19-94 hrs. The corresponding change in methane in this region is 192.63 L CH_4 (218.53-25.90 L CH_4). The hourly rate during this 75-hr period (94-19hrs) equates to 2.57 L CH_4. hr^{-1} or 61.64 L CH_4. d^{-1}.

Using the correction factor (K(t) = 2.52 g COD. $L_{CH_4}^{-1}$) the COD equivalent of methane produced is 155.33 mg COD-CH_4. d^{-1}. Using the volatile solids

introduced in the SMA assay (1.61 gVS), the SMA of the inoculum is ± **0.1 g COD-CH_4. g^{-1}VS. d^{-1}**. Several studies have shown SMAs above 0.6 g COD. g^{-1}VS. d^{-1} (Nizami et al., 2011). This SMA is low, but studies have suggested that it could increase as inert particles tend to float and exit the reactor system (Hussain and Dubey, 2017a). A study evaluating UASBs that treated raw domestic sewage had a low SMA value (0.01 gCOD-CH_4. g^{-1}VS. d^{-1}) that increased over time to 0.1 gCOD-CH_4. g^{-1}VS. d^{-1} due to the long start-up time (22 weeks) (Kalogo et al., 2001). Thus, it is expected that the start-up of the EGSBs using this sludge may take a long time.

Approximately 367ml of acetic acid (2.2 g COD. L^{-1}) was used in the SMA test, which equates to 807.4 mg COD. Using Equations B.1 and B.2, it can be shown that the theoretical maximum gas production from acetic acid is 320.40 L CH_4 (807.4 mg COD /2.52 g $COD.L_{CH_4}^{-1}$). The actual gas production from the SMA test was 241.4 L CH_4. Therefore, the conversion efficiency of the inoculum is **±75 %.**

Appendix A.3: Optimum HRT to produce VFA-rich leachate

The HRT is the average duration the liquid fraction remains within a reactor. The dilution rate (Φ) is the volumetric flow rate (Q) that enters the working volume (V_e) and is the inverse of the HRT for LBRs. A high dilution rate, which equates to a low HRT, is desired. However, a dilution rate that is too high may result in flooding of the substrate and/or washing out of essential microbes. Flooding and microbial washout may negatively impact the leaching process; therefore, a balance must be

established. The HRT for LBRs can be calculated as per Eq.C.1 (Browne et al., 2013).

$HRT = V_e/Q$ **Equation C.1**

Where: HRT is the hydraulic retention time, V_e is the working volume of the reactor, and Q is the volumetric flow rate of the LBR influent.

To establish the optimum HRT that produces VFA-rich leachate, three different configurations were evaluated. Each LBR was loaded with the solid fraction and liquid fraction of mWBM; 0.67kg of mWBM 'dry' was added to each LBR, and 4.02kg of mWBM 'wet' was loaded into three separate 5L leachate holding tanks. To reflect low, medium and high recirculation rates, 60, 100 and 140 $L.day^{-1}$ were chosen, achieving HRTs of approximately 72 minutes, 43 minutes and 31 minutes, respectively. The EGSBs were disconnected during this period. Previous studies by Nizami et al. (2010), Wall et al. (2015) and Browne et al. (2013) operated at an HRT of approximately 3.8hrs, 4.4hrs and 3.8hrs respectively, for a 16L (working volume) LBR system. However, a study found that HRTs lower than 9hrs lead to pooling on the substrate surface, but this is dependent on the reactor configuration and the substrate. The leaching trial was operated in pooling/flooding conditions. Figure S2 shows the VFA composition during the preliminary leaching trials.

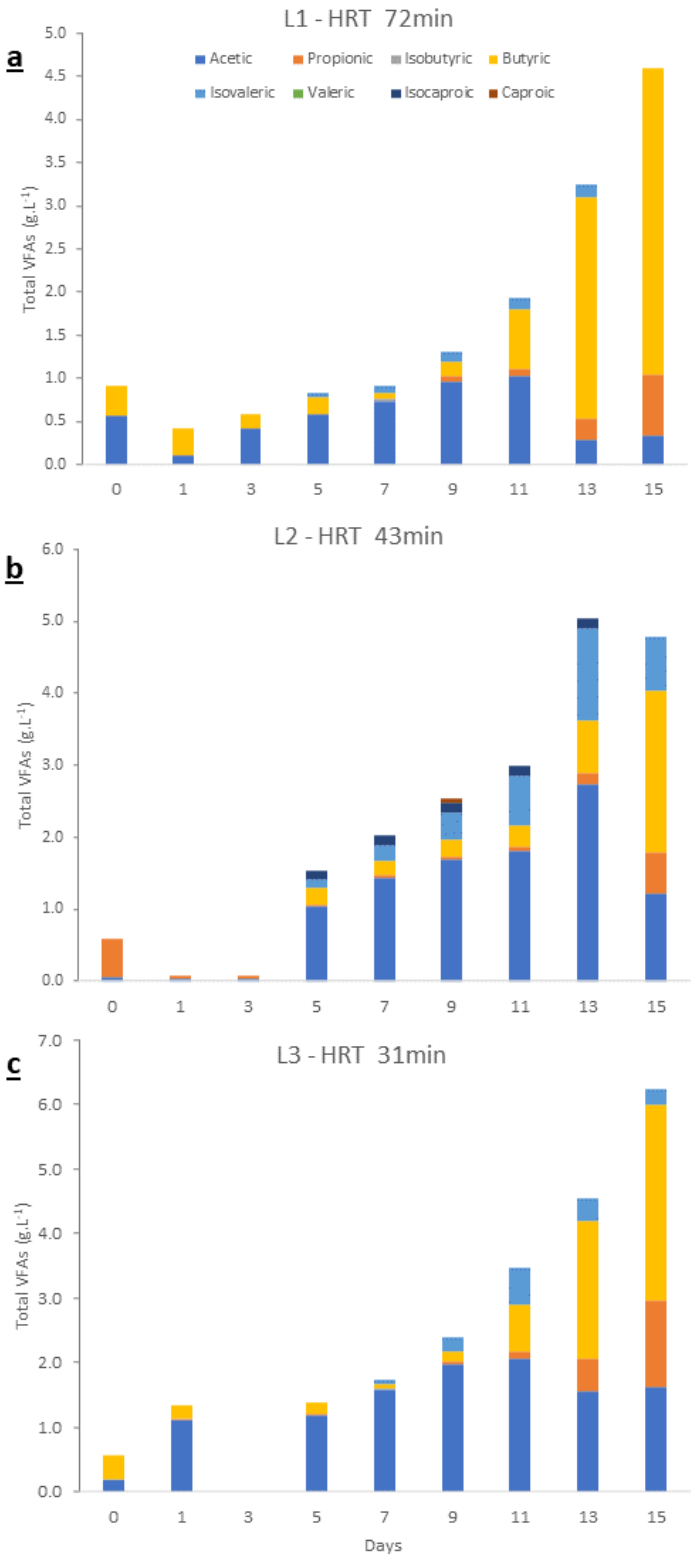


Figure A.2: VFA profiles of short leaching trials.

The lowest HRT (31 min) yielded the highest VFA yield but resulted in pooling within the LBR. As VFA yield was the primary objective, the 31 min HRT, 140 $L.d^{-1}$ recirculation rate, was used for the commissioning of the LBRs.

Appendix A.4: EGSB acclimatisation experimental trials

The EGSBs were acclimatized through experimental trials and operated over two distinct phases over 82 days as follows (Figure A.3):

- Phase 1 (Day 0-56): the EGSB was fed directly with raw mWBM 'wet' independently of the LBRs. This was done to acclimatize the inoculum to mWBM 'wet' and allow inactive sludge to be washed out from the EGSB. Initially, the OLR was 0.7 g COD. L^{-1}. d^{-1} (HRT of 23 days) and gradually increased to a maximum OLR of ±2.6 g COD. L^{-1}. d^{-1} (HRT of 6 days).
- Phase 2 (Day 57-82): the EGSB was fed VFA-rich leachate generated from the LBR preliminary trials (see Appendix A.3) but was still disconnected from the LBRs. This was done to acclimatize the inoculum to the VFA-rich leachate. The OLR started at 2.2 g COD. L^{-1}. d^{-1} (HRT of 6 days) for 22 days and increased to ±2.6 g COD. L^{-1}. d^{-1} (HRT of 6 days). While the OLR changed, the HRT remained the same due to the increased COD concentration of the VFA-rich leachate.
- Phase 3 (Day 83-112): the EGSB was connected directly to the LBR leachate after the LBR leaching trials. The EGSB influent flow rate was the same as the settings on day 82. As the COD of the leachate varied, the average COD over the previous 7 days was used to set the OLR to ±2.6 g COD. L^{-1}. d^{-1} (HRT of 6 days) for the following week.

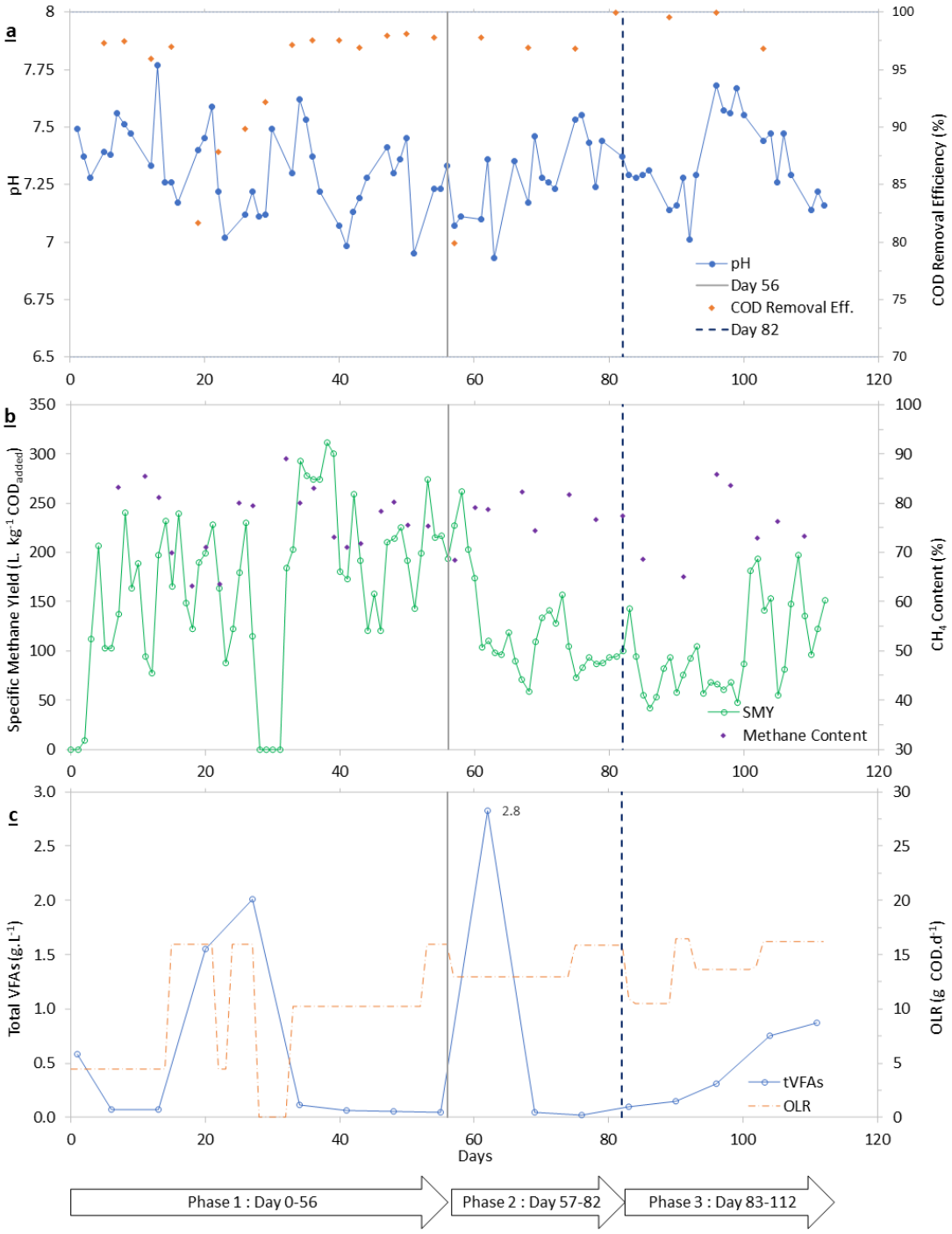


Figure A.3: (a) Expanded granular sludge bed (EGSB) pH and COD removal efficiencies, (b) specific methane yield and biogas methane content, (c) EGSB effluent total VFAs and the organic loading rate.

Appendix A.5: Theoretical LBR-EGSB biogas yield

The theoretical biogas, methane, and COD yield for the treatment of mWBM in the LBR-EGSB is shown in Box S3

Box A.3: Estimation of COD, Biogas and CH_4 production in the LBR-EGSB (adapted from (Nizami et al., 2011)).

±4.67 kg of mWBM (4.00 kg mWBM 'wet' + 0.67 kg mWBM 'dry') was loaded into the reactor sequentially every 5 days. The solid retention time (SRT) of mWBM 'dry' was therefore 15 days (3 LBRs x 5 days).

I. Breakdown of volatile matter in 3 LBRs

mWBM 'dry' in 3 LBRs	3 x 0.67 kg mWBM 'dry'	=	2.01	kg mWBM 'dry'
mWBM 'dry' %TS at	28.9% – see Table 3.1	=	581	g of TS
VS (% of TS) at	96.3%	=	560	g of VS
VS destruction	33%	=	185	g of VS
Solid retention time (SRT)		=	21	days

II. COD production from mWBM

It can be shown that 1 g of VS produces 1.4 g of COD. The COD production from mWBM 'dry' introduced to the LBRs can be calculated as follows:

VS-to-COD conversion	=	1.4	g COD g^{-1} VS
		185	g VS x 1.4 g COD g^{-1}VS
VS conversion at 70 %	=		(see **I.**)
		259	**g COD from mWBM**
Total COD from mWBM dry	=		**'dry'**

The leachate COD consists of the COD originating in mWBM 'wet' and the COD generated from mWBM 'dry'. mWBM 'wet' consists of centrate (±40 %) and thin stillage (±60 %). Therefore, the total COD produced after 1 SRT (15 days) can be calculated as follows:

Thin stillage added every 7 days	= 60 %ww of mWBM 'wet'= 2.4 kg (4kg x 0.6) ≈ 2.4 L
Thin stillage added after 15 days	= 3.5 L x 3 = 7.2L
Total COD from thin stillage added	= 7.2 L x 33.4 g COD. L^{-1} of thin stillage (see Table 3.1) = 240 g COD

A similar calculation for the COD contributed by centrate = 168 g COD

Total COD from mWBM 'wet'	= 240 g COD (from thin stillage) + 168 g COD (from centrate) **= 408 g COD**

The total COD of mWBM is the sum of the COD of mWBM 'wet' and mWBM 'dry'.

Total COD in mWBM	= 240 g COD mWBM 'dry' + 408 g COD mWBM 'wet'	
	= **648**	**g COD mWBM** after 21 days

III. Biogas Production from mWBM

1 kg of COD destroyed generates 350 L of CH_4. The methane production can be estimated from the COD production and efficiency of the EGSB (95 %) (Chernicharo. 2007). The methane production from the estimated COD produced from the LBR is as follows:

∴ 350 L CH_4 kg^{-1} COD x 648 g COD x 95 % efficiency
Methane produced after 21 days = 215 L CH_4

The theoretical specific methane yield of mWBM in the LBR-EGSB can be estimated by using the amount of VS introduced into the system after 3 feeds of mWBM and the methane produced after 21 days:

Theoretical VS introduced = 4.67 kg of mWBM x 3 Feeds x VS of mWBM (see Box A.1)
Theoretical VS introduced = 4.67 kg x 3 x 6.37 % = 892 g VS mWBM introduced after 21 days.

Theoretical methane yield for LBR-EGSB = 215 L CH_4 / 892 g VS mWBM
Theoretical methane yield for LBR-EGSB **= 241 L CH_4. kg^{-1} VS**
Theoretical methane yield for LBR-EGSB = **172 L CH_4. kg^{-1} COD** (using 1.4 kg COD. kg^{-1}VS)

The maximum yield **(459 L CH_4. kg^{-1} VS)** was calculated assuming 100 % VS destruction and 100 % COD removal efficiency.

Appendix References

1. Nizami, A.-S., Singh, A., & Murphy, J. D. (2011). Design, Commissioning, and Start-Up of a Sequentially Fed Leach Bed Reactor Complete with an Upflow Anaerobic Sludge Blanket Digesting Grass Silage. *Energy & Fuels*, *25*(2), 823–834. https://doi.org/10.1021/ef101739d
2. Hussain, A., & Dubey, S. K. (2017). Specific methanogenic activity test for anaerobic degradation of influents. *Applied Water Science*, *7*(2), 535–542. https://doi.org/10.1007/S13201-015-0305-Z/TABLES/2

3. Chernicharo, C. A. de L. (2007). *Anaerobic Reactors* (Vol. 3). IWA Publishing. https://www.iwapublishing.com/sites/default/files/ebooks/9781780402116.pdf
4. Kalogo, Y., MBouche, J. H., & Verstraete, W. (2001). Physical and Biological Performance of Self-Inoculated UASB Reactor Treating Raw Domestic Sewage. *Journal of Environmental Engineering*, *127*(2), 179–183. https://doi.org/10.1061/(ASCE)0733-9372(2001)127:2(179)
5. Browne, J. D., Allen, E., & Murphy, J. D. (2013). Improving hydrolysis of food waste in a leach bed reactor. *Waste Management*, *33*(11), 2470–2477. https://doi.org/10.1016/j.wasman.2013.06.025
6. Wall, D. M., Allen, E., O'Shea, R., O'Kiely, P., & Murphy, J. D. (2016). Investigating two-phase digestion of grass silage for demand-driven biogas applications: Effect of particle size and rumen fluid addition. *Renewable Energy*, *86*, 1215–1223. https://doi.org/10.1016/j.renene.2015.09.049

Appendix B

Appendix B.1: Biochemical methane production (BMP) of the whiskey by-products

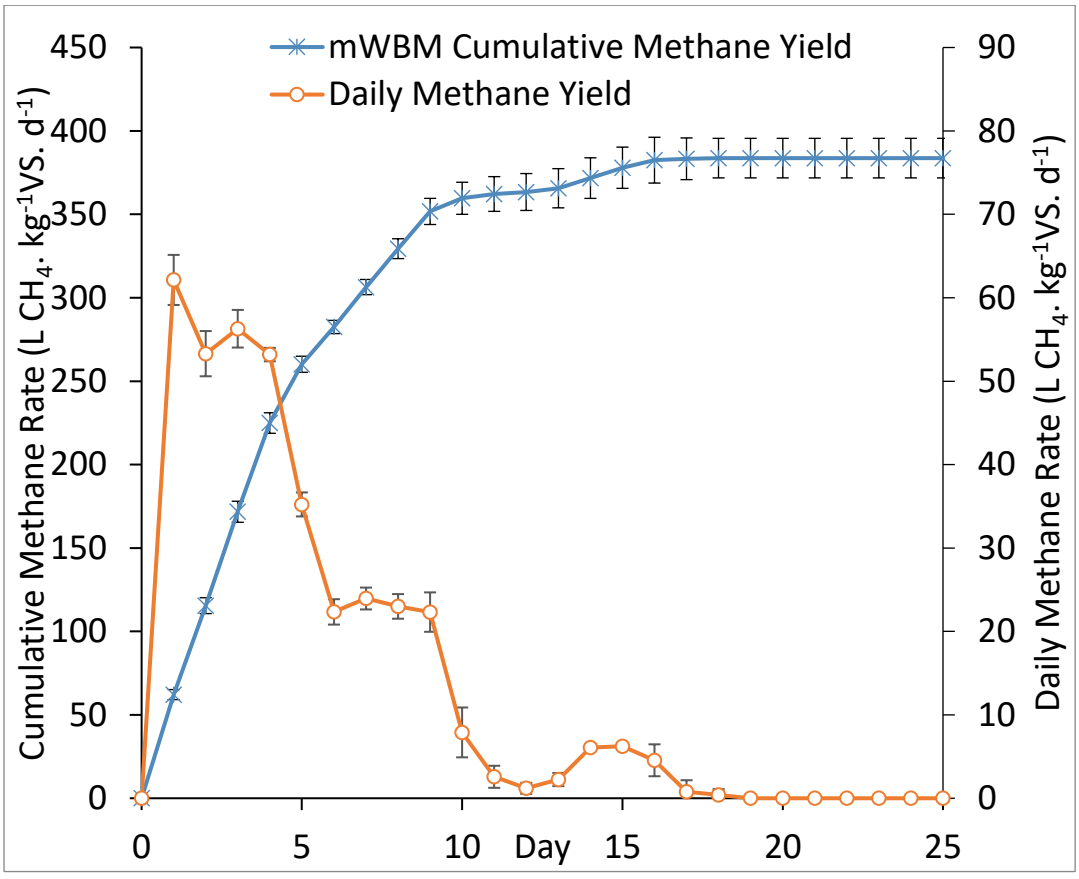


Figure B.1: Cumulative and daily methane yield of whiskey by-products under mesophilic condition

Appendix B.2: Continuous trials experimental data

Table B1: Single-phase CSTR (C1) experimental trial results at an OLR of 2.5 gVS. L^{-1}. d^{-1}

Wk[a]	pH	F/T[b]	Out	% Rem[c]	NH_3-N[d]	Free NH_3[e]	tVFAs	%HAc[f]	%HPr[g]	HAc: HPrh	Methane Yield		BI[k]	% CH_4[l]
											VS[i]	COD[j]		
			g. L^{-1}		mg. L^{-1}	mg. L^{-1}	mg. L^{-1}							
1	7.3	0.2	3.7	89	1,218	37	40	100	0	-	278.5	185.7	55	51
2	7.3	0.3	3.8	89	1,263	40	51	100	0	-	281.2	187.5	56	54
3	7.3	0.3	3.2	91	1,323	45	105	65	13	5	277.7	185.1	55	52
4	7.3	0.3	3.5	90	1,308	44	488	41	30	1.4	266.0	177.3	53	56
5	7.4	0.3	3.4	90	1,323	48	365	48	23	2.1	258.1	172.1	51	55
Ave[m]	7.3	0.3	3.5	90	1,287	43	210	71	13	2.8	272.3	181.5	54	54

[a] Wk = week at organic loading rate during the second hydraulic retention time; [b] F/T = alkalinity ratio (FOS/TAC); [c] % Red = COD removal efficiency; [d] NH_3-N = ammoniacal nitrogen; [e] Free NH_3 = free ammonia; [f] %HAc = percentage of acetic acid in the total VFAs; [g] %HPr = percentage of propionic acid in the total VFAs; [h] HAc:HPr = acetic acid-to-propionic acid ratio; [i] VS = specific methane yield on a volatile solids basis (L CH_4. kg^{-1} VS_{added}); [j] COD = specific methane yield equivalent on a COD basis using a conversion factor of 1.5 kg COD. kg^{-1} VS mWBM; [k] BI = biodegradability index as compared to the theoretical maximum. [l] %CH_4 = Percentage of methane in biogas on a volume basic; [m] Ave = average

Table B.2: Experimental trial results of the acidogenic phase of the two-phase CSTR (C2a) at an OLR of 2.5 gVS. L^{-1}. d^{-1}

Wk[a]	pH	Out	% Rem[c]	NH_3-N[d]	tVFAs	%HAc[f]	%HPr[g]	%HBu[n]	%HVa[n]	%HCa[o]	Acid. [p]	VFA Yield
		g. L^{-1}		mg. L^{-1}	mg. L^{-1}						%	mgVFA. g^{-1}VS
1	4.9	31.7	6	920	12,218	36	10	29	8	11	61	192.4
2	4.8	31.4	7	740	11,480	30	11	33	10	12	60	180.8
3	4.8	29.2	14	528	12,168	21	11	37	12	13	71	191.6
4	4.8	32.2	5	420	11,508	21	11	37	13	15	62	181.2
5	4.8	31.9	6	589	8,590	18	10	36	15	18	48	135.3
Ave[m]	4.8	31.3	8	639	11,193	25	11	35	12	14	60	176.3

Table B.3: Experimental trial results of the methanogenic phase of the two-phase CSTR (C2b) at an OLR of 2.5 gVS. L^{-1}. d^{-1}

Wk[a]	pH	F/T[b]	In	Out	% Rem[c]	NH_3-N[d]	Free NH_3[e]	tVFAs	%HAc[f]	%HPr[g]	HAc: HPrh	SMY		BI[k]	% CH_4[l]
			g. L^{-1}	g. L^{-1}		mg. L^{-1}	mg. L^{-1}	mg. L^{-1}				VS[i]	COD[j]	%	
1	7.4	0.2	31.7	3.3	89	1,468	67.1	378	96	1.9	45.4	274.4	182.9	55	78
2	7.5	0.2	31.4	3.0	90	1,438	64.3	268	99	0		271.9	181.3	54	71
3	7.5	0.2	29.2	2.6	92	1,105	40.5	176	98	0		274.4	182.9	55	77
4	7.4	0.2	32.2	4.5	86	760	31.1	345	99	0		257.0	171.3	51	76
5	7.4	0.2	31.9	4.3	87	1,423	77.6	524	98	0		266.6	177.7	53	77
Ave[m]	7.5	0.2		3.5	89	1,239	29.7	338	98	0.4		268.9	179.2	53	76

[a] Wk = week at organic loading rate during the second hydraulic retention time; [b] F/T = alkalinity ratio (FOS/TAC); [c] % Rem = COD removal efficiency; [d] NH_3-N = ammoniacal nitrogen; [e] Free NH_3 = free ammonia; [f] %HAc = percentage of acetic acid in the total VFAs; [g] %HPr = percentage of propionic acid in the total VFAs; [h] HAc:HPr = Acetic acid-to-propionic acid ratio; [i] VS = specific methane yield on a volatile solids basis (L CH_4. kg^{-1} VS_{added}); [j] COD = specific methane yield equivalent on a COD basis using a conversion factor of 1.5 kg COD. kg^{-1} VS mWBM; [k] BI = biodegradability index as compared to the theoretical maximum. [l] %CH_4 = Percentage of methane in biogas on a volume basic; [m] Ave = average; [n] %HBu = percentage of butyric acid in the effluent tVFAs; [o] %HBu = percentage of caproic acid in the effluent tVFAs; [p] Acidification = percentage of COD equivalent of VFAs in the COD

Table S4: Experimental trial results of the acidogenic phase of the LBR-EGSB (LBR)

		COD		Ammonia	Effluent VFAs								
Wk[a]	pH	Out	% Rem[c]	NH_3-N[d]	tVFAs	%HAc[f]	%HPr[g]	%HBu[n]	%HVa[n]	%HCa[o]	Acid.[p]	VFA Yield	VS Dest.
		g. L^{-1}	%	mg. L^{-1}	mg. L^{-1}						%	mgVFA. g^{-1}VS	%
1	4.4	26.3	22	100	10,117	20	17	45	8	7	62	136.1	50
2	4.4	26.9	20	140	10,221	19	16	45	8	7	67	137.5	41
3	4.4	27.0	20	100	10,247	19	17	45	8	7	66	137.9	37
Ave[m]	4.4	26.7	21	113	10,195	19	17	45	8	7	65	137.2	42

Table S5: Experimental trial results of the methanogenic phase of the LBR-EGSB (EGSB) at an OLR of 3.5 gVS. L^{-1}. d^{-1}

			COD			Ammonia		Effluent VFAs				Gas Production			
Wk[a]	pH	F/T[b]	In	Out	% Rem[c]	NH_3-N[d]	Free NH_3[e]	tVFAs	%HAc[f]	%HPr[g]	HAc:HPr[h]	SMY		BI[k]	% CH_4[l]
												VS[i]	COD[j]		
			g. L^{-1}	g. L^{-1}	%	mg. L^{-1}	mg. L^{-1}	mg. L^{-1}						%	
1	7.1	0.4	21.6	1.3	94	263	6.0	432	51	49	1.0	-	338.2	48	74
2	7.0	0.3	22.8	1.3	95	360	6.1	255	57	29	2.0	-	331.0	47	74
3	7.0	0.4	24.1	1.3	95	400	5.9	445	51	32	1.6	-	334.8	48	79
Ave[m]	7.0	0.4		1.3	94	341	6.0	378	53	37	1.5	-	334.8	48	76

[a] Wk = week at organic loading rate during the second hydraulic retention time; [b] F/T = alkalinity ratio (FOS/TAC); [c] % Rem = COD removal efficiency; [d] NH_3-N = ammoniacal nitrogen; [e] Free NH_3 = free ammonia; [f] %HAc = percentage of acetic acid in the total VFAs; [g] %HPr = percentage of propionic acid in the total VFAs; [h] HAc:HPr = Acetic acid-to-propionic acid ratio; [i] VS = specific methane yield equivalent on a volatile solids basis (L CH_4. kg^{-1} VS_{added}); [j] COD = specific methane yield on a COD basis (L CH_4. kg^{-1} COD_{added}) ; [k] BI = biodegradability index as compared to the theoretical maximum. [l] %CH_4 = Percentage of methane in biogas on a volume basic; [m] Ave = average; [n] %HBu = percentage of butyric acid in the effluent tVFAs; [o] %HBu = percentage of caproic acid in the effluent tVFAs; [p] Acidification = percentage of COD equivalent of VFAs in the COD; [q] VS Dest. = Volatile solids destruction efficiency.

Appendix C

Appendix C.1: Experimental results from dark fermentation trials at different loading rates

Table C.1: Experimental results from dark fermentation trials at an organic loading rate of 5 gVS. L^{-1}. d^{-1}

Wk	Eff. COD	% COD Rem[a]	TAN[b]	tVFAs[c]	%HAc[d]	%HPr[e]	%HBu[f]	%HVa[g]	%HCa[h]	Acid.[i]	COD_{VFA}[j]	COD-To-VFA	Specific VFA Yield	% H_2[k]	Specific H_2 Yield	Specific CO_2 Yield	VS Des[l]
	g. L^{-1}	%	mg. L^{-1}	mg. L^{-1}	%	%	%	%	%	%	g. L^{-1}	%	mgVFA. g^{-1}VS	%	L H_2. kg^{-1}VS	L CO_2. kg^{-1}VS	%
5	23.3	31	555	9,906	25	9	38	11	13	72	16.7	49	155.7	27	6.1	19	45
6	26.4	22	490	8,535	22	10	39	12	13	55	14.6	43	134.2	22	6.4	19.8	41
7	25.6	25	455	9,284	21	10	38	13	13	63	16	47	145.9	26	5.7	17.7	47
8	27.8	18	440	8,692	22	12	34	13	15	55	14.9	44	136.6	18	7	21.8	49
9	27.7	18	400	8,650	22	12	33	14	15	55	14.9	44	136	26	6.1	19	25
Ave[m]	**26.1**	**23**	**468**	**9,013**	**22**	**11**	**36**	**13**	**14**	**60**	**15.4**	**46**	**141.7**	**24**	**6.3**	**19.4**	**42**

[a] % COD Rem = Percentage COD removal; [b] TAN = total ammoniacal nitrogen; [c] tVFAs = total volatile fatty acids; [d]%HAc = percentage of acetic acid; [e]%HPr = percentage of propionic acid; [f]%HBu= percentage of butyric acid; [g]%HVa= percentage of valeric acid; [h]%HCa= percentage of caproic acid; [i]Acid.= acidification; [j]COD_{VFA}.= COD equivalent of VFAs; [k]% H_2 = percentage hydrogen in biogas; [l] VS des. = volatile solids destruction; [m]Ave = average

Table C.2: Experimental results from dark fermentation trials at an organic loading rate of 10 gVS. L^{-1}. d^{-1}

Wk	Eff COD	% COD Rem[a]	TAN[b]	tVFAs[c]	%HAc[d]	%HPr[e]	%HBu[f]	%HVa[g]	%HCa[h]	Acid.[i]	COD_{VFA}[j]	COD-To-VFA	Specific VFA Yield	% H_2[k]	Specific H_2 Yield	Specific CO_2 Yield	VS Des.[l]
	g. L^{-1}	%	mg. L^{-1}	mg. L^{-1}	%	%	%	%	%	%	g. L^{-1}	%	mgVFA. g^{-1}VS	%	L H_2. kg^{-1}VS	L CO_2. kg^{-1}VS	%
5	27.3	20	485	8,808	21	14	42	13	9	55	14.9	44	138.4	23	8.7	28.6	38
6	28	17	365	9,368	23	16	34	15	9	56	15.7	46	147.2	24			19
7	28.5	16	333	11,484	22	18	32	19	5	67	19.2	57	180.5	21	4.9	16.2	20
8	31.4	8	358	9,267	25	17	28	22	6	49	15.4	45	145.7	24	5.1	16.9	6
9	29.3	14	218	9,852	24	20	27	22	5	55	16.3	48	154.8	24	3.5	11.6	13
Ave[m]	**28.9**	**15**	**352**	**9,756**	**23**	**17**	**33**	**18**	**7**	**56**	**16.3**	**48**	**153.3**	**23**	**5.5**	**18.3**	**19**

[a] % COD Rem = Percentage COD removal; [b] TAN = total ammoniacal nitrogen; [c] tVFAs = total volatile fatty acids; [d]%HAc = percentage of acetic acid; [e]%HPr = percentage of propionic acid; [f]%HBu= percentage of butyric acid; [g]%HVa= percentage of valeric acid; [h]%HCa= percentage of caproic acid; [i]Acid.= acidification; [j]COD_{VFA}.= COD equivalent of VFAs; [k]% H_2 = percentage hydrogen in biogas; [l] VS des. = volatile solids destruction; [m]Ave = average

Table C.3: Experimental results from dark fermentation trials at an organic loading rate of 15 gVS. L^{-1}. d^{-1}

Wk	Effluent COD	% COD Rem[a]	TAN[b]	tVFAs[c]	%HAc[d]	%HPr[e]	%HBu[f]	%HVa[g]	%HCa[h]	Acid.[i]	COD_{VFA}[j]	COD-To-VFA	Specific VFA Yield	% H_2[k]	Specific H_2 Yield	Specific CO_2 Yield	VS Des.[l]
	g. L^{-1}	%	mg. L^{-1}	mg. L^{-1}	%	%	%	%	%	%	g. L^{-1}	%	mgVFA. g^{-1}VS	%	L H_2. kg^{-1}VS	L CO_2. kg^{-1}VS	%
5	28.5	16	373	9,341	22	16	36	20	3	55	15.6	46	146.8	16	7.8	28.3	4
6	28.2	17	373	9,018	24	17	30	21	5	50	15	44	141.7	18	7.9	28.5	2
7	26.2	23	338	11,056	25	23	26	20	3	68	18	53	173.8	14	7.9	28.6	8
8	25.3	25	370	10,041	23	20	28	23	3	66	16.6	49	157.8	24	4.9	17.6	16
9	28.5	16	230	9,845	20	19	30	24	3	61	16.6	49	154.7	24	5.8	20.9	26
Ave[m]	**27.3**	**19**	**337**	**9,860**	**23**	**19**	**30**	**22**	**4**	**60**	**16.4**	**48**	**155**	**19**	**6.9**	**24.8**	**11**

[a] % COD Rem = Percentage COD removal; [b] TAN = total ammoniacal nitrogen; [c] tVFAs = total volatile fatty acids; [d]%HAc = percentage of acetic acid; [e]%HPr = percentage of propionic acid; [f]%HBu= percentage of butyric acid; [g]%HVa= percentage of valeric acid; [h]%HCa= percentage of caproic acid; [i]Acid.= acidification; [j]COD_{VFA}.= COD equivalent of VFAs; [k]% H_2 = percentage hydrogen in biogas; [l] VS des. = volatile solids destruction; [m]Ave = average

Appendix C.2: Biogenic carbon dioxide utilisation potential

Table C.4: CO_2 offset potential of whiskey by-products within Ireland

Parameters	Acronyms	Units	Value	Equations	Ref.
Distillery Size	V_{dist}	million $L_{whiskey}$. a^{-1}	50		
Whiskey By-Products Production	$mWBM_{yearly}$	kt. a^{-1}	516.5		(1)
CO_2 Volume Yield	Y_{CO2}	million L CO_2. a^{-1}	692.1	$Y_{H2} = 1.34m^3\ CO_2.t^{-1} \times mWBM_{yearly}$	this study
Specific distillery hydrogen yield	SY_{H2}	L CO_2. $L^{-1}{}_{OLA}$	1.34	$SY_{CO2} = Y_{CO2} \div V_{dist}$	
CO_2 Mass Yield	M_{CO2}	t H_2. a^{-1}	1,368	$M_{CO2} = Y_{CO2} \times 1.9768\ kg^{-1}.m^3$	(2)
CO_2 monetary value[a]	Val_{lower}	€ ($). a^{-1}	68,400 (75,241)	$Val_{upp} = M_{CO2} \times 50€.\ t^{-1}CO_2$	(3)
	Val_{upper}	€ ($). a^{-1}	95,760 (105,336)	$Val_{lower} = M_{CO2} \times 70€.\ t^{-1}CO_2$	(3)
Beer carbonated using biogenic CO_2 (upper limit)	$Beers_{LtrU}$	million L of beer	351	$Beers_{LtrU} = M_{CO2} \div 3.9g\ CO_2.\ L^{-1}$	(4)
Beer carbonated using biogenic CO_2 (lower limit)	$Beers_{LtrL}$	million L of beer	249	$Beers_{LtrL} = M_{CO2} \div 5.5g\ CO_2.\ L^{-1}$	(4)
Beer carbonated using biogenic CO_2 (upper limit)	$Beers_{CansU}$	million cans of beer	1,064	$Beers_{CansU} = Beers_{LTRU} \div 0.33\ L.\ Can^{-1}$	
Beer carbonated using biogenic CO_2 (lower limit)	$Beers_{Cans}L$	million cans of beer	755	$Beers_{CansL} = Beers_{LTRL} \div 0.33\ L.\ Can^{-1}$	

[a] the exchange rate taken to be 1.10 US$ per € (Central Bank of Ireland, 2023)

References: (1) - (Hackula et al., 2023); (2) - (National Institute of Standards and Technology, 2023); (3) (Salomone et al., 2019; Uddin et al., 2022)(4) - (Liger-Belair and Cilindre, 2021)

Appendix C.3: Biogenic hydrogen utilisation potential

Table C.5: Biogenic hydrogen utilisation potential through heating and transport

Section	Parameters	Acronyms	Units	Value	Equations	Ref.
Hydrogen energy and monetary value	Distillery Size	V_{dist}	million $L_{whiskey}$. a^{-1}	50		
	Annual by-products produced	$mWBM_{yearly}$	kt. a^{-1}	516.5		(1)
	Distillery H_2 yield	Y_{H2}	million L H_2. a^{-1}	196.3	$Y_{H2} = 0.38\ m^3\ H_2.\ t^{-1} \times mWBM_{yearly}$	this study
	Specific distillery H_2 yield	SY_{H2}	L H_2. $L^{-1}{}_{OLA}$	3.93	$SY_{H2} = Y_{H2} \div V_{dist}$	
	Annual Mass of H_2	M_{H2}	t H_2. a^{-1}	17.6	$M_{H2} = Y_{H2} \times 0.089\ kg.\ m^{-3}$	
	H_2 Energy Equivalent	E_{H2}	kWh	586,080	$M_{H2} = M_{H2} \times 1000$ x 33.3 kWH/kg H_2	(3)
	Value of H_2[a]	V_{H2}	€ ($)	88,000 (96,800)	$V_{H2} = M_{H2} \times 5$ €. $kg^{-1}H_2$; Assuming 1.1 US$/€	(2)
Transport	Density of Whiskey	$m_{whiskey}$	$kg.m^{-3}$ whiskey	915.6	$m_{whiskey}$ =0.6 × 1000 $kg.m^3{}_{H2O}$ + 0.4 × 780 $kg.m^3{}_{ETH}$; assuming 40 ABV and the density of ethanol to be 780 $kg.m^3$	
	Weight whiskey and bottle	S.F	kg bottled whiskey. L^{-1}	1.67	(0.47kg. $bottle^{-1}$ ÷ 0.7 $L_{whiskey}$. $bottle^{-1}$ x 1 $L_{whiskey}$) + 1$L_{whiskey}$ × $m_{whiskey}$; where 0.47kg. $bottle^{-1}$ is the weight of a 0.7L whiskey bottle	
	Truck Capacity	$TR_{capacity}$	t. $truck^{-1}$	25		(3)
	Daily mass of bottle whiskey	V_{daily}	t bottled whiskey. d^{-1}	228.8	$V_{daily} = V_{dist} \times S.F \div 365$ days per year	
	Daily number of trucks required	Tks	trucks. d^{-1}	10	Trucks = $V_{daily} \div TR_{capacity}$	
	Daily distance travelled by fleet	D_{daily}	km. d^{-1}	23,775	$D_{daily} = Tks \times 95.1\ km.t^{-1} \times TR_{capacity}$	(4)
	Annual distance travelled by fleet	D_{yearly}	million km. a^{-1}	8.7	$D_{year} = D_{daily} \times 365$ days per year	
	Distance fuelled by H_2	DH_2	km	234,432	$DH_2 = E_{H2} \div 2.5\ kWh.\ km^{-1}$	(3)
	H_2 transport replacement	D		3	$D = DH_2 / Dyearly \times 100$	

Heating	Distillery thermal energy demand	$TH_{whiskey}$	GWh	208	$TH_{whiskey} = V_{dist} \times 4.16\ kWh.L^{-1}_{OLA}$; where $4.16\ kWh.L^{-1}_{OLA}$ is the thermal demand per L OLA	(5)
	Potential for H_2 as a substitute fuel for distillery transport	TH	%	0.3	$TH = E_{H2} \div TH_{whiskey} \times 100$	
	Whiskey produced using H_2 as the heat source	WB	L $_{whiskey}$	140,885	$WB = TH_{H2} \div 4.16\ kWh.L^{-1}_{OLA}$	(5)
Emissions offset	Transport Diesel Replaced by H_2	E_{diesel}	kWh	745,493.7	$M_{diesel} = DH_2 \times 3.18\ kWh.\ km^{-1}$	(3,6)
	Avoided emissions from diesel substitution in transport	$CO2_{diesel}$	kg CO_2 eq.a^{-1}	196,736	$M_{diesel} = E_{diesel} \times 0.2639\ kg\ CO_2eq.\ kWh^{-1}$	(6)
	Avoided emissions from natural gas replacement in heating	$CO_{nat.gas}$	kg CO_2eq.a^{-1}	118,388	$CO_{nat.gas} = E_{H2} \times 0.202\ kgCO_2e.\ kWh^{-1}$ natural gas	(6)

[a] the exchange rate taken to be 1.10 US$ per € (Central Bank of Ireland, 2023)

References: (1) - (Hackula et al., 2023); (2) - (Dinh et al., 2021); (3) - (Gray et al., 2021); (4) - (Eurostat, 2022); (5) - (O'Shea et al., 2022); (6) – (DEFRA, 2023)

Appendix C.4: Volatile fatty acid utilisation potential

Table C.6: VFA to PHA utilisation potential through Irish beer packaging

Parameters	Acronyms	Units	Value	Equations	Ref.
Distillery Size	V_{dist}	million $L_{whiskey}$. a^{-1}	50		
Annual by-products produced	$mWBM_{yearly}$	kt. a^{-1}	516.5		(1)
Distillery VFA yield	Y_{VFA}	t VFA. a^{-1}	4,958	$Y_{VFA} = 9.6kg_{VFA}.t^{-1} \times mWBM_{yearly}$	this study
Effective VFA yield after processing	EY_{VFA}	t VFA. a^{-1}	3,966	$EY_{VFA} = Y_{VFA}. \times 0.8$; assuming 80 liquid-solid separation efficiency.	(2-3)
PHA Yield	Y_{PHA}	t PHA. a^{-1}	1,189.8	$Y_{PHA} = EY_{VFA} \times 0.3\ t_{PHA}.\ t_{VFA}^{-1}$	(3)
Value of PHA[a]	E_{PHA}	million € (US$). a^{-1}	5.9 (6.5)	$E_{PHA} = Y_{PHA} \times 5000$ €. t_{PHA}^{-1}	(4)
Number of six-pack beer packages	N_{20_BAGS}	million bags	131.8	$N_{20_BAGS} = Y_{PHA} \div 9.03g$ PHA. 20kg-bag^{-1}	(3)
Potential Value of six-pack beer packages [a]	E_{20_BAGS}	million € (US$). a^{-1}	6.6 (7.2)	$E_{20_bags} = N_{20_bags} \times 0.05$ €. 20kg-bag^{-1}	
Mass of a can of beer	m_{can}	g. can^{-1}	10.6	$m_{can} = 16$ g.can^{-1} x 330ml ÷ 500 ml; where a 500ml can requires 16 grams of aluminium	
Density of beer	m_{beer}	$kg.m^3_{beer}$	989	$m_{beer} = 0.95 \times 1000$ kg.m^3_{H2O} + 0.05×780 kg.m^3_{ETH}; assuming 5 ABV and the density of ethanol to be 780 kg.m^3	
Mass of a six-pack of beer	m_{6_BAGS}	$kg_{six\text{-}pack}$	1.96	$V_{6_BAGS} = 6\ beer_{can} \times 0.33L.\ beer^{-1}_{can} \times m_{beer}$	

PHA Required for six-pack of beer	V_{6_BAGS}	g PHA. six-pack bag^{-1}	0.9	$V_{6_BAGS} = m_{6_BAGS} \div 20kg\ capacity\ bag_{PHA} \times 9.03g\ PHA.bag$; where 9.03 g PHA is required for a 20 kg capacity bag, accounting for the reduced mass required for a 6 pack of beer.	(3)
Number of six-pack beer packages produced from PHAs	N_{6pk_BAGS}	million bags	1,322	$N_{pk_BAGS} = Y_{PHA} \div V_{6_BAGS}$	(3)
	N_{BEERS_CANS}	million cans of beer	7,932	$N_{BEERS_BCANS} = N_{6pk_BAGS} \times 6$ beers per six-pack bag	
	N_{beers_ltr}	million L of beer	2618	$N_{beers_ltr} = N_{BEERS_CANS}$ x 0.33L per beer; where 0.33L is the volume of a beer can	
% PHA six-pack beer packages that can supplement Irish beer	$_{PHA}$	%	369	$PHA = N_{beers_ltr} \div 710$ million L of beer; where 710 million L of beer were produced in Ireland in 2020.	(5)

[a] The exchange rate taken to be 1.10 US$ per € (Central Bank of Ireland, 2023)

References: (1) - Hackula et al., 2023; (2) - Moses, 2014; (3) - Al Battashi et al., 2021; (4) - Crutchik et al., 2020; (5) - IBEC, 2021

Appendix D

Appendix D.1: VFA to COD conversion factors

Table D.1: VFA-COD Conversion Factors		
Acetic	1.07	g COD. g acid^{-1}
Propionic	1.51	g COD. g acid^{-1}
Isobutyric	1.82	g COD. g acid^{-1}
Butyric	1.82	g COD. g acid^{-1}
Isovaleric	2.04	g COD. g acid^{-1}
Valeric	2.04	g COD. g acid^{-1}
Isocaproic	2.21	g COD. g acid^{-1}
Caproic	2.21	g COD. g acid^{-1}
Heptanoic	2.34	g COD. g acid^{-1}

Appendix D.2: Potential butanol production and diesel blend from VFA production

The average VFA concentration for C1a was 10.4 g. L^{-1}. The OLR was maintained at 15 gVS.L^{-1}. d^{-1}. The reactor volume of C1a is 1.0 L. Approximately 0.236 L of effluent was removed per day. The specific VFA yield for C2a is 163.6 mgVFA. g^{-1}VS:

(10.4 g. L^{-1} x 0.236 L) / (15 gVS.L^{-1}. d^{-1} x1.0 $L_{reactor}$)

The VS content of mWBM is 6.37 %ww. Therefore, the Specific VFA yield of C2a was **10.4 mg VFA. g^{-1}WW**.

The average VFA concentration for the LBR was 9.9 g. L^{-1}. 0.9 L. d^{-1} of leachate was removed from the leachate tank. Approximately 6.86 kg of mWBM per week was introduced in the system, which equates to 62.426 gVS per day. The specific VFA yield for the LBR was **142.7 mgVFA.g^{-1}VS**:

(9.9 g. L^{-1} x 0.9 L. d^{-1}) / (62.426 gVS. d^{-1})

The VS content of mWBM is 6.37 %ww. Therefore, the Specific VFA yield is **9.1 mg VFA. g^{-1}WW**.

Table D.2: Biogenic butanol utilisation potential in transport

Parameters	Acronyms	Units	Reactor		Equations	Ref.
			CSTR	LBR		
Annual distance travelled by distillery fleet	D_{diesel}	million km. a^{-1}	8.7			(1)
Annual diesel requirement to fulfil transport demand	V_{diesel}	million L. a^{-1}	3.22		$V_{diesel} = D_{diesel} \times 0.37\ L_{diesel}.\ km^{-1}$	(2)
	M_{diesel}	million kg. a^{-1}	2.72		$M_{diesel} = D_{diesel} \times 0.8441\ kg_{diesel}.\ L^{-1}$	(3)
	E_{diesel}	MJ	119,212,160		$M_{diesel} = D_{diesel} \times 43.848\ MJ_{diesel}.\ kg^{-1}$	(3)
Distillery size	V_{dist}	million $L_{whiskey}.\ a^{-1}$	50	50		
Annual by-products produced	$mWBM_{yearly}$	$kt_{mWBM}.\ a^{-1}$	516.5	516.5		(1)
Specific VFA yield	SY_{VFA}	kg VFA. t^{-1}_{mWBM}	10.4	9.1		this study
Distillery VFA yield	Y_{VFA_X}	kt VFAs. a^{-1}	4.08	3.57	$Y_{VFA_X} = SY_{VFA} \times mWBM_{yearly} \times 80\% \times 95\%$; where 80% is the solid-liquid separation efficiency, 95% is the VFA separation efficiency	(4,5)
The portion of butyric acid within VFAs	Y_{HBu}	kt Butyric Acid. a^{-1}	1.22	1.1	$Y_{HBu} = Y_{VFA_X} \times 30\%$ Butyric acid in both reactors	this study
Biobutanol yield after processing butyric acid	Y_{nBut}	t Butanol. a^{-1}	585.6	513.6	$Y_{nBut} = Y_{HBu} \times 48\%$; where 48% is the butyric acid-to-butanol process conversion efficiency	(6)

Table D.2: Biogenic butanol utilisation potential in transport

Parameters	Acronyms	Units	Reactor		Equations	Ref.
			CSTR	LBR		
Distillery biobutanol volume	V_{nBut}	L Butanol. a^{-1}	719,941	631,424	$V_{nBut} = SY_{nBut} / 0.8134$ kg. L^{-1}	(3)
Volume of 80:20 diesel-biobutanol blend using all the biobutanol product	V_{Bu20D}	million L Diesel Blend. a^{-1}	3.6	3.16	$V_{Bu20D} = V_{nBut} / 20\%$	
80:20 diesel-biobutanol blend blend mass	M_{Bu20D}	kt Diesel Blend. a^{-1}	3.02	2.65	$M_{Bu20D} = V_{Bu20D} \times 0.8389$ $kg_{Diesel\ Blend}$. L^{-1}	(3)
Total energy of 80:20 diesel-biobutanol blend	E_{Bu20D}	MJ	127,262,800	111,671,000	$E_{Bu20D} = M_{Bu20D} \times 42.14$MJ. kg^{-1}	(3)
Total distillery transport energy fulfilled by 80:20 diesel-biobutanol blend	$\%E_{Bu20D}$	% Fulfill	107%	94%	$\%E_{Bu20D} = E_{Bu20D} / E_{Diesel}$	
Corrected Diesel blend Mass to meet transport demand	$Cor.M_{Bu20D}$	kt Diesel Blend. a^{-1}	2.83	/	$Cor.M_{Bu20D} = E_{diesel}$ / 42.14MJ. kg^{-1}; LBR doesn't fulfil demand, thus additional diesel will be required to meet demand	(3)
Volume of fossil diesel in blend	V_{blend_Diesel}	million L Diesel. a^{-1}	2.70[a]	2.53[b]	[a] $V_{blend_diesel_CSTR} = Cor.M_{Bu20D} / 0.8389$ $kg_{Diesel\ Blend}$. $L^{-1} \times 0.80$ %; [b] $V_{blend_diesel_LBR} = V_{Bu20D} \times 0.80$ %; where 80% is the volumetric percentage in the diesel blend.	(3)
Mass of fossil diesel in blend	M_{blend_Diesel}	million kg Diesel. a^{-1}	2.28	2.19	$M_{diesel} = V_{blend_diesel} \times 0.8441$ kg_{diesel}. L^{-1}	(3)

Table D.2: Biogenic butanol utilisation potential in transport

Parameters	Acronyms	Units	Reactor		Equations	Ref.
			CSTR	LBR		
Additional fossil diesel energy required to meet distillery transport energy demand	$Add.E_{diesel}$	MJ	0	7,541,160	$Add.E_{diesel} = E_{diesel} - E_{Bu20D}$	
Additional fossil diesel mass required to meet distillery transport demand	$Add.\ M_{diesel}$	t Diesel. a^{-1}	0	171.98	$Add.M_{diesel} = Add.E_{diesel} / 43.848\ MJ_{diesel}.\ kg^{-1}$	(3)
Diesel mass reduction through blending with biobutanol	M_{diesel_saved}	t Diesel. a^{-1}	440.00	358.02	$M_{diesel_saved_CSTR} = M_{diesel} - (M_{blend_diesel} + Add.\ M_{diesel})$	
Distillery transport emissions offset from 80:20 diesel-biobutanol blend	EM_{saved}	t CO_2e. a^{-1}	1,412	1,149	$M_{diesel_saved} = M_{diesel_saved} \times 3.21$ t $CO_2e.t^{-1}$ Diesel	(7)
Volume of diesel reduced through blending with biobutanol	V_{diesel_saved}	L Diesel. a^{-1}	521,265	424,144	$V_{diesel_saved} = M_{diesel_saved} / 0.8441\ kg_{diesel}.\ m^{-3}$	(3)
Monetary savings from diesel reduction at distillery	$Val._{diesel}$	€ ($)	787,110 (865,821)	640,457 (704,503	$Val._{diesel} = V_{diesel_saved} \times 1.51$ €. $L^{-1}{}_{diesel}$	(8)

[a] the exchange rate taken to be 1.10 US$ per € (Central Bank of Ireland, 2023)

Table D.2: Biogenic butanol utilisation potential in transport						
Parameters	**Acronyms**	**Units**	**Reactor**		**Equations**	**Ref.**
			CSTR	**LBR**		

References: (1) - (Hackula et al., 2023c); (2) - (Gray et al., 202); (3) - (Tipanluisa et al., 2021); (4) - (Aydin et al., 2018); (5) - (Moses, 2014); (6) - (Cho et al., 2023); (7) - (DEFRA, 2023); (8) - (GlobalPetrolPrices, 2023)

Appendix D.3: LBR-EGSB specific methane yield estimation

The specific methane yield is shown in Box D.1.

Box D.1: LBR-EGSB Specific methane yield (adapted from(Nizami et al., 2011)*.)*

6.86 kg of mWBM (5.88 kg mWBM 'wet' + 0.98 kg mWBM 'dry') was loaded into the LBR|-EGSB system sequentially every 7 days. mWBM 'dry' was loaded into the LBRs, and mWBM 'wet' was pumped into the leachate tank. The solid retention time (SRT) of mWBM 'dry' was therefore 21 days (3 LBRs x 7 days). The potential volatile solids (VS) from the feedstock was calculated based on the data in Table 6.1

IV. Breakdown of volatile matter in 3 LBRs

mWBM 'dry' is placed in the LBR and through the leaching process the organic matter (VFAs and COD) is increased in the leachate.

mWBM 'dry' per	LBR	=	0.98 kg	
mWBM 'dry' in 3 LBRs	3 x 0.98 kg mWBM 'dry'	=	2.94	kg mWBM 'dry'
mWBM 'dry' %TS at	28.9% – see Table 6.1	=	850	g of TS
VS (% of TS) at	96.3%	=	819	g of VS
VS conversion at	45%	=	369	g of VS
Solid retention time (SRT)		=	21	days

V. COD Production from mWBM

Note that 1 g of VS produces 1.5 g of COD (Hackula et al 2023b). The COD production from mWBM 'dry' introduced to the LBRs can be calculated as follows:

VS-to-COD conversion	=	1.5	g COD g^{-1} VS
VS conversion at 45%	=	369	g VS x 1.5 g COD g^{-1}VS (see **I.**)
Total COD from mWBM dry	=	**554**	**g COD from mWBM 'dry'**

The leachate COD consists of organics within mWBM 'wet' and the COD generated from the VS removed from mWBM 'dry'. mWBM 'wet' consists of centrate (±40%) and thin stillage (±60%). Therefore, the total COD produced after 1 SRT (21 days) can be calculated as follows:

Thin stillage added every 7 days	= 60 %ww of mWBM 'wet'= 3.50 kg (5.88kg x 0.6) ≈ 3.50 L
Thin stillage added after 21 days	= 3.5 L x 3 = 10.5 L
Total COD from thin stillage added	= 10.5 L x 33.4 g COD. L^{-1} of thin stillage see Table 4.1) = 351 g COD

A similar calculation for the COD contributed by centrate = 242 g COD

Total COD from mWBM 'wet'	= 351 g COD (from thin stillage) + 242 g COD (from centrate) **= 593 g COD**

The total COD of mWBM is the sum of the COD of mWBM 'wet' and mWBM 'dry'.

Total COD in mWBM	= 554 g COD mWBM 'dry' + 593g COD mWBM 'wet'

	=	**1,147**	**g COD mWBM** after 21 days

VI. Biogas Production from mWBM

The average methane production from EGSB was 0.34 m^3 CH_4 kg^{-1} COD_{added} (see Table 6.2). The methane production from the estimated COD produced from the LBR is as follow:

∴ 0.34 m^3 CH_4 kg^{-1} COD x 1,147 g COD
Methane produced after 21 days = 390 L CH_4

The theoretical specific methane yield of mWBM in the LBR-EGSB can be estimated by using the amount of VS introduced into the system after 3 feeds of mWBM and the methane produced after 21 days:

VS introduced = 6.86 kg of mWBM x 3 Feeds x VS of mWBM (see Table 6.1)
VS introduced = 6.86 kg x 3 x 7% x 94% TS = 1,354 g VS mWBM introduced after 21 day.
Methane yield for LBR-EGSB = 390 L CH_4 / 1,354 g VS $mWBM_{@\ 70\ VS\ conversion}$
Methane yield for LBR-EGSB **= 288 L CH_4. kg^{-1} VS added**
Methane yield for LBR-EGSB = 288 L CH_4. kg^{-1} VS added / 1.5 g COD g^{-1} VS
Methane yield for LBR-EGSB **= 192 L CH_4. kg^{-1} COD added**
Methane yield for LBR-EGSB = 288 L CH_4. kg^{-1} VS added x 0.064 kg VS. kg^{-1}ww

Methane yield for LBR-EGSB = **18.4 L CH_4. kg^{-1} ww added**

Appendix D.4: CSTR specific methane yield

The OLR of C15 was 15 g VS. L^{-1}. d^{-1} which equates to 10.0 g COD. L^{-1}. d^{-1} (15 g VS. L^{-1}. d^{-1} x 1.5 g COD g^{-1} VS). The reactor volume was 1L resulting in 10.0 g COD introduced in the system. The second phase system has a specific methane yield of 0.24 L CH_4. g^{-1} COD resulting in 2.4 L of CH_4 (10.0 g COD x 0.24 L CH_4. g^{-1} COD). The specific methane yield would be 160 L CH_4. kg^{-1} VS (2.4 L of CH_4 x 15 g VS. L^{-1}. d^{-1} x 1 $L_{reactor}$). On a wet weight basis, this equates to 10.2 L CH_4. kg^{-1} ww.

Appendix E

Appendix E.1: Properties of the mixed whiskey by-products and inoculum

Table E.1: Properties of the mixed whiskey by-products and inoculum

	Draff	Cake Maize	Centrate	Thin Stillage	Mixed whiskey by-products	Inoculum
Total solids (% ww)	27.4	29.0	3.5	2.9	6.8	3.8
Volatile solids (% ww)	26.3	28.2	3.4	2.6	6.4	2.6
COD[a] (g. L^{-1})			34.6	33.4		
Theoretical biomethane potential (L CH_4. kg^{-1}VS) [b]					501	
Elemental composition					$C_{12}H_{19.8}O_{7.9}N$	

[a] COD = chemical oxygen demand; [b] calculated from a prior study (adapted from (Hackula et al., 2023a, 2023b))

Appendix E.2: DNA extraction and sequencing

Samples were frozen at -80 ºC until use. Digestate samples were thawed and aliquoted to Eppendorf tubes. Lysozyme was added to the tubes and then incubated at 37 ºC for 30 min. TENP buffer (5% 1 M Tris, 4% 0.5 M EDTA, 50% 5 M NaCl, 10% (10% (w/v) PVPP) and Proteinase K (20 μg/mL) were added to the tubes which were then incubated at 70 °C for 2 h with occasional manual agitation. One-tenth volume of 10% CTAB buffer (10% (w/v) CTAB in 0.7 M NaCl) was added to each tube, and the incubation was continued for a further 15 min. Tubes were then centrifuged at 18,000 *g*, and supernatants were transferred to fresh sterile Eppendorf tubes. An equal volume of phenol:chloroform: isoamyl (25:24:1) (Merck) was added and mixed well and then centrifuged at 18,000 *g* for 30 min. The upper phase was transferred to fresh Eppendorf tubes. Isopropanol (0.7 vols) and 3 M sodium acetate (0.1 vols) were added to each tube and centrifuged for 30 min to pellet DNA. Supernatants were discarded, and the pellets were washed with cold (4 °C) 70% EtOH. The DNA was dissolved in Tris-HCL pH 8.0, was visualized on a 1% agarose gel, and was quantified by NanoDrop. Equimolar amounts of DNA from appropriate triplicate extractions were pooled for sequencing.

Taxonomic marker (16S rRNA) gene amplicons were sequenced for both bacteria and archaea, separately, on the MiSeq Illumina platform (v3 chemistry, 2 x 300 bp paired-end sequencing) by Eurofins Genomics Ltd. (Konstanz, Germany) using their proprietary protocols with ISO 17025 accreditation. For bacteria, the V3-V5 region was targeted for sequencing, and for archaea, the V3-V4 region was targeted.

Appendix E.3: Taxonomic marker gene amplicon sequence processing and analysis

Raw sequencing reads were demultiplexed and primer sequences were trimmed from reads by Eurofins Genomics Ltd. using custom in-house scripts. Briefly, adapter and primer sequences were removed using Cutadapt (Martin, 2011). For quality filtering, reads were pre-processed using fastp (Chen et al., 2018). Paired-end reads were merged with a minimum overlap of 10 bp using FLASH v2.2.00 (Magoč and Salzberg, 2011). Subsequent processing and analyses were performed using the Quantitative Insights Into Microbial Ecology (QIIME) 2 v2019.10 package (https://qiime2.org). The 'Deblur' plugin was used to filter datasets for quality, for trimming, for chimera removal and to dereplicate sequences (Amir et al., 2017). Sequences were trimmed to 280 bases and were aligned using the 'MAFFT' plugin (Katoh and Standley, 2013). Diversity analyses were performed using the 'core metrics phylogenetic' plugin. Taxonomy and phylogeny were assigned using the 'feature-classifier' plugin with reference to the Greengenes database release 13_8 trained on the 515F/806R region for bacterial classifications and trained on the full-length gene for archaeal classifications (DeSantis et al., 2006, McDonald et al., 2012). OTUs were clustered at 99% similarities.

Appendix E.4: Mass and energy balance of single-phase anaerobic digestion system without biochar

Table E.2: Mass and energy balance of single-phase anaerobic digestion system without biochar

Parameters	Acronyms	Units	Values	Equations	References
Mass of the feedstock *Whiskey By-products* (mWBM) (wwt)	m_{mWBM}	t	1		
mWBM VS Content	VS_{mWBM}	t	0.064	The VS content in mWBM is measured as 6.4%.	This study
TS in mWBM	TS_{mWBM}	t	0.068	The TS content in mWBM is measured as 6.8%.	This study
CH_4 production (accounting for biogas composition)	Y_{CH4}	m^3	20.8	$Y_{CH4} = VS_{mWBM} \times SMY\ m^3/t\ VS$; where the specific methane yield (SMY) is 325 m^3/t VS	This study
Mass of CH_4	m_{CH4}	t	0.015	$m_{CH4} = Y_{CH4} \times 0.716\ kg/m^3 \div 1000$; where 0.716 is the density of CH_4.	[1]
CO_2 production (accounting for biogas composition)	Y_{CO2}	m^3	13.867	$Y_{CO2} = Y_{CH4} \div 60\% \times 40\%$; where 60% is the percentage of CH_4 and 40% is the CO_2.	
Mass flow of CO_2	m_{CO2}	t	0.027	$m_{CO2} = Y_{CO2} \times 1.98\ kg/m^3 \div 1000$; where 1.98 kg/m^3 is the density of CO_2	[1]
Mass of digestate	$m_{digestate}$	t	0.958	$m_{digestate} = m_{mWBM} - m_{CH4} - m_{CO2}$	
VS in wet solid digestate	$VS_{WS\ digestate}$	t	0.022	$VS_{WS\ digestate} = VS_{AD\ mWBM} - m_{CH4} - m_{CO2}$	This study
TS in wet solid digestate	$TS_{WS\ digestate}$	t	0.026	$TS_{WS\ digestate} = TS_{mWBM} - m_{CH4} - m_{CO2}$	This study

Mass of wet solid digestate	$m_{WS\ digestate}$	t	0.082	$m_{WS\ digestate} = TS_{digestate} \div (1–70\%) \times$ (1-4.92%; where 70% is the moisture content, 4.92% of solids lost to liquids	[2]
Energy value of mWBM	$Q_{in\ mWBM}$	MJ	962.56	$Q_{IN\ mWBM} = VS_{mWBM} \times 1000 \times$15.04 MJ/kg VS, in which 15.04 MJ/kg VS is the lower heating value (LHV) of mWBM.	This study
Energy value of CH_4	Q_{CH4}	MJ	750	$Q_{CH4} = m_{CH4} \times$ 50 MJ/kg, in which 50 MJ/kg is the LHV of CH_4.	
Energy value of wet solid digestate	Q WS digestate	MJ	212.56	Q WS digestate = $Q_{in\ mWBM} – Q_{CH4}$	
Electricity consumption for biogas production	$E_{IN\ AD}$	MJ	36.0	$E_{IN\ AD} = m_{mWBM} \times$ (10kWh/t × 3.6 MJ/kWh) MJ/t; where 10 kWh/t is the electricity consumption	[3]
Heat consumption for biogas production	$H_{IN\ AD}$	MJ	92.0	$H_{IN\ AD} = Cp \times (37 – 15)$ °C × m mWBM × 1000, in which Cp (4.18×10^{-3} MJ/kg/°C) is the specific heat capacity of water; (37 – 15) °C is the difference between the digestion temperature and the ambient temperature.	[3]
Electricity consumption for digestate segregation	$E_{IN\ digestate\ segregation}$	MJ	12.07	$E_{IN\ digestate\ segregation} = m_{digestate} \times$ (3.5 × 3.6) MJ/t; where 10 kWh/t is the electricity consumption	[4]
Total primary energy consumption in the AD system	$Q_{IN\ P\ AD}$	MJ	223.0	$Q_{IN\ P\ AD} = (E_{IN\ AD} + E_{IN\ digestate\ segregation}) \times 2.3 + H_{IN\ AD} \times 1.1 \div 90\%$, in which 2.3 and 1.1 are primary energy conversion factors for electricity and heat, respectively; 90% is the boiler efficiency.	[5]
Energy output of the system	$Q_{OUT\ AD}$	MJ	750	$Q_{OUT\ AD} = Q_{CH4}$	
AD process efficiency	η_{AD}	%	63	AD efficiency = $Q_{OUT\ AD} \div (Q_{IN\ mWBM} + Q_{IN\ P\ AD}) \times 100$	

Appendix E.5: Mass and energy balance of integrated anaerobic digestion system and pyrolysis system with biochar at 300 ºC

Table E.3: Mass and energy balance of integrated anaerobic digestion system and pyrolysis system, whiskey barrels pyrolyzed at 300ºC at digestate

Acronyms	Units	Values	Equations	References
$m_{AD\ mWBM}$	t	1		
$VS_{AD\ mWBM}$	t	0.064	$VS_{AD\ mWBM} = m_{AD\ mWBM} \times 6.4\%$, in which 6.4% is the VS content in mWBM.	This study
$TS_{AD\ mWBM}$	t	0.068	$TS_{AD\ mWBM} = m_{AD\ mWBM} \times 6.8\%$, in which 6.8% is the TS content in mWBM.	This study
$m_{char\ addition}$	t	0.128	$m_{char\ addition} = VS_{AD\ mWBM} \times 2$; where 2 is the biochar-to-substrate ratio	This study
$Y_{CH4\ AD\text{-}PY}$	m^3	23.94	$Y_{CH4\ AD\text{-}PY} = VS_{AD\ mWBM} \times 374\ m^3.\ t^{-1}$ VS; where 374 $m^3.\ t^{-1}$ VS the specific methane yield	This study
$m_{CH4\ AD\text{-}PY}$	t	0.017	$m_{CH4\ AD\text{-}PY} = Y_{CH4\ AD\text{-}PY} \times 0.716\ kg.\ m^{-3} \div 1000$; where 0.716 kg. m^{-3} is the density of CH_4	[1]
$Y_{CO2\ AD\text{-}PY}$	m^3	15.96	$Y_{CO2\ AD\text{-}PY} = Y_{CH4\ AD\text{-}PY} \div 60\ \% \times 40\ \%$; where 60 % is the CH_4 content; 40 % is the CO_2 content on a volume basis	
$m_{CO2\ AD\text{-}PY}$	t	0.032	$m_{CO2\ AD\text{-}PY} = Y_{CO2\ AD\text{-}PY} \times 1.980\ kg.\ m^{-3} \div 1000$; where 1.980 kg. m^{-3} is the density of CO_2	[1]
$m_{digestate}$	t	1.079	$m_{digestate} = m_{AD\ mWBM} + m_{char\ addition} - m_{CH4\ AD\text{-}PY} - m_{CO2\ AD\text{-}PY}$	
$TS_{digestate}$	t	0.147	$TS_{digestate} = TS_{AD\ mWBM} + m_{char\ addition} - m_{CH4\ AD\text{-}PY} - m_{CO2\ AD\text{-}PY}$	This study
$m_{WS\ digestate}$	t	0.466	$m_{WS\ digestate} = TS_{digestate} \div (1–70\%); \times (1\text{-}4.92\%)$; where 70% is the moisture content after separation, 4.92% of solids lost to liquids	[2]
$VS_{AD\ digestate}$	t	0.015	$VS_{AD\ digestate} = VS_{AD\ mWBM} \times (1 –75\%) – m_{CH4\ AD\text{-}PY} – m_{CO2\ AD\text{-}PY}$	This study
$m_{L\ digestate}$	t	0.613	$m_{L\ digestate} = m_{digestate} – m_{WS\ digestate}$	
$Q_{IN\ AD\ mWBM}$	MJ	962.56	$Q_{IN\ AD\ mWBM} = VS_{AD\ mWBM} \times 15.04\ MJ.\ kg^{-1}$ VS, in which 15.04 MJ. kg^{-1}VS is the LHV of mWBM.	This study
$Q_{Biochar}$	MJ	2163.2	$Q_{IN\ AD\ Char} = m_{char\ addition} \times 16.9\ MJ.\ kg^{-1} \times 1000$, in which 16.9 MJ. kg^{-1}VS is the LHV of the biochar	This study
$Q_{OUT\ CH4}$	MJ	850	$Q_{OUT\ CH4} = m_{CH4} \times 50\ MJ.\ kg^{-1}$, in which 50 MJ. $kg^{-1}$is the LHV of CH_4.	

$Q_{AD\ digestate}$	MJ	2276.76	$Q_{AD\ digestate} = Q_{IN\ AD\ mWBM} + Q_{IN\ AD\ Char} - Q_{OUT\ CH4}$	This study
$E_{IN\ AD}$	MJ	40.61	E IN AD = $(m_{AD\ mWBM} + m_{char\ addition}) \times (10 kWh/t \times 3.6\ MJ.\ kWh^{-1})$; where 10 kWh/t is the energy consumption from AD.	[3]
$H_{IN\ AD}$	MJ	103.73	H IN AD = Cp × (37 – 15) °C × (m AD mWBM + m char addition) × 1000, in which Cp (4.18×10^{-3} MJ/kg/°C) is the specific heat capacity of water; (37 – 15) °C is the difference between the digestion temperature and the ambient temperature.	[3]
$E_{IN\ digestate\ separation}$	MJ	13.60	$E_{IN\ digestate\ segregation} = m_{digestate} \times (3.5\ kWh.\ t^{-1} \times 3.6\ MJ.\ kWh^{-1})$; where 3.5 kWh. t^{-1} is the energy consumption from digestate separation.	[4]
$m_{dry\ WB}$	t	0.278	$m_{dry\ WB} = m_{char\ addition} \div$ %biochar yield; where %biochar yield is the biochar yield of 46% for Char300	This study
$Y_{char\ AD\text{-}PY}$	t	0.128	$Y_{char\ AD\text{-}PY} = m_{dry\ WB} \times$ %biochar yield; where %biochar yield is the biochar yield of 46% for Char300	This study
$Y_{oil\ AD\text{-}PY}$	t	0.128	$Y_{oil\ AD\text{-}PY} = m_{dry\ WB} \times [(1\text{-}46\%) \times (66.7\% / (66.7\% + 11.1\%))]$; where 30% is the yield mWBM from biochar in the experiments, 66.7% is the bio-oil production and 11.1% is the syngas yield mWBM both taken from literature. Note the mass of biochar addition from AD won't contribute to syngas production	[5, 6]
$Y_{syngas\ AD\text{-}PY}$	t	0.022	$Y_{syngas\ AD\text{-}PY} = m_{dry\ WB} \times [(1\text{-}46\%) \times (11.1\% / (66.7\% + 11.1\%))]$; where 30% is the yield mWBM from biochar in the experiments, 66.7% is the bio-oil production and 11.1% is the syngas yield mWBM both taken from literature. Note the mass of biochar addition from AD won't contribute to syngas production	[5, 6]
$Q_{IN\ WB}$	MJ	3516.7	$Q_{IN\ WB} = m_{dry\ WB} \times 1000 \times 12.65\ MJ.\ kg^{-1}VS$, in which 12.65 MJ. $kg^{-1}VS$ is the LHV of whiskey barrels	This study
$Q_{IN\ DRY\ WB}$	MJ	3516.7	$Q_{IN\ dry\ WB} = Q_{IN\ WB}$	This study
$Q_{char\ AD\text{-}PY}$	MJ	2163.2	$Q_{char\ AD\text{-}PY} = Y_{char\ AD\text{-}PY} \times 1000 \times LHV_{biochar}$; where $LHV_{biochar}$ is the lower energy value of the whiskey barrel biochar 24.3 MJ. $kg^{-1}TS$	This study

$Q_{\text{syngas AD-PY}}$	MJ	229.1	$Q_{\text{syngas AD-PY}} = Y_{\text{syngas AD-PY}} \times 1000 \times LHV_{syngas}$; where LHV_{syngas} is the lower energy value of the syngas 10.3 MJ. kg^{-1} TS	[5]
$Q_{\text{oil AD-PY}}$	MJ	1124.4	$Q_{\text{oil AD-PY}} = Q_{\text{in WB}} - Q_{\text{Char AD-PY}} - Q_{\text{syngas AD-PY}}$	
$H_{\text{IN WB drying}}$	MJ	1112	$H_{\text{IN WB drying}} = m_{\text{dry WB}} \times 1000 \times 4.0$ MJ. kg^{-1} TS; where 4.0 MJ. kg^{-1} TS is the energy required to dry the whiskey barrels.	[6]
$H_{\text{IN PY}}$	MJ	142.61	H IN PY = Cp × (Temp – 15) °C × m dry WB× 1000, in which Cp (1.8×10^{-3} MJ/kg/°C) is the specific heat capacity of the whiskey barrels; (Temp – 15) °C is the difference between the pyrolysis temperature and the ambient temperature.	[6]
$E_{\text{IN WB treating}}$	MJ	152.75	$E_{\text{IN WB treating}} = m_{\text{dry WB}} \div 0.91 \times 1000 \times 0.5$ MJ. kg^{-1}; where 0.5 MJ. kg^{-1} is the electricity input for pretreating WB, 0.91 is the TS content of whiskey barrels	[6]
$Q_{\text{IN P AD-PY}}$	MJ	1970	$Q_{\text{IN P AD-PY}} = (E_{\text{IN AD}} + E_{\text{IN digestate segregation}} + E_{\text{IN WB treating}}) \times 2.3 + (H_{\text{IN PY}} + H_{\text{IN WB drying}} + H_{\text{IN AD}}) \times 1.1$; where 2.3 is the primary energy consumption for electricity	
$Q_{\text{OUT P AD-PY}}$	MJ	4366.5	$Q_{\text{OUT P AD-PY}} = Q_{\text{oil AD-PY}} + Q_{\text{syngas AD-PY}} + Q_{\text{char AD-PY}} + Q_{\text{OUT CH4}}$	
$h_{\text{AD-PY}}$	%	68	$h_{\text{AD-PY}} = Q_{\text{OUT AD-PY}} \div (Q_{\text{IN AD mWBM}} + Q_{\text{IN DRY WB}} + Q_{\text{IN P AD-PY}}) \times 100$	

References:
[1] NIST Chemistry WebBook. Available from: https://webbook.nist.gov/chemistry/: National Institute of Standards and Technology.
[2] Al Seadi T, Drosg B, Fuchs W, Rutz D, Janssen R. 12 - Biogas digestate quality and utilization. In: Wellinger A, Murphy J, Baxter D, editors. The Biogas Handbook: Woodhead Publishing; 2013. p. 267-301.
[3] Vo TTQ, Wall DM, Ring D, Rajendran K, Murphy JD. Techno-economic analysis of biogas upgrading via amine scrubber, carbon capture and ex-situ methanation. Appl Energy. 2018;212:1191-202.
[4] Tampio E, Marttinen S, Rintala J. Liquid fertilizer products from anaerobic digestion of food waste: mass, nutrient and energy balance of four digestate liquid treatment systems. J Clean Prod. 2016;125:22-32.
[5] Monlau F, Sambusiti C, Antoniou N, Barakat A, Zabaniotou A. A new concept for enhancing energy recovery from agricultural residues by coupling anaerobic digestion and pyrolysis process. Appl Energy. 2015;148:32-8.
[6] Onarheim K, Solantausta Y, Lehto J. Process Simulation Development of Fast Pyrolysis of Wood Using Aspen Plus. Energy Fuels. 2014;29:205-17.

Appendix E.6: Observations in microbial taxonomy

Table E.4: Number of retained reads per sample after quality filtering and paired-end read merging

Sample ID	Retained Bacterial Sequences	Retained Archaeal Sequences
M0	44,240	61,250
M4	39,640	64,305
M8	45,137	56,544
M9	38,084	58,094

Table E.5: Relative abundances of Kingdom level taxonomic classification of sequencing reads targeting the V3-V5 region of the bacterial 16S rRNA gene

	M0	M4	M8	M9
k__Archaea	0.130890052	0.52867	0.338409	0
k__Bacteria	99.19596111	98.86133	98.83672	99.84314
Unassigned	0.673148841	0.610004	0.824873	0.156863

Table E.6: Relative abundances of Phylum level taxonomic classification of sequencing reads targeting the V3-V5 region of the bacterial 16S rRNA gene

	M0	M4	M8	M9
k__Archaea;__	0.13089	0.52867	0.338409	0
k__Bacteria;__	31.17053	41.70394	36.31557	43.94118
k__Bacteria;p__Actinobacteria	1.757666	2.236682	3.532149	2.921569
k__Bacteria;p__Bacteroidetes	48.7285	40.80927	37.39425	35.29412
k__Bacteria;p__Chloroflexi	3.926702	5.754372	4.29357	2.392157
k__Bacteria;p__Firmicutes	5.777861	3.477023	4.208968	9.156863
k__Bacteria;p__Planctomycetes	0.093493	0.040667	0.063452	0
k__Bacteria;p__Proteobacteria	7.703815	4.839366	13.02876	5.509804
k__Bacteria;p__Spirochaetes	0.037397	0	0	0.45098
k__Bacteria;p__Tenericutes	0	0	0	0.176471
Unassigned;__	0.673149	0.610004	0.824873	0.156863

Table E.7: Relative abundances of Class level taxonomic classification of sequencing reads targeting the V3-V5 region of the bacterial 16S rRNA gene

	M0	M4	M8	M9
k__Archaea;__;__	0.13089	0.52867	0.338409	0
k__Bacteria;__;__	31.17053	41.70394	36.31557	43.94118
k__Bacteria;p__Actinobacteria;__	0	0	0.126904	0
k__Bacteria;p__Actinobacteria;c__Actinobacteria	1.757666	2.236682	3.405245	2.921569
k__Bacteria;p__Bacteroidetes;__	24.64473	18.54412	19.75465	21.09804
k__Bacteria;p__Bacteroidetes;c__Bacteroidia	24.08377	22.26515	17.61844	13.70588
k__Bacteria;p__Bacteroidetes;c__Cytophagia	0	0	0.021151	0.490196
k__Bacteria;p__Chloroflexi;c__Anaerolineae	3.926702	5.754372	4.29357	2.392157
k__Bacteria;p__Firmicutes;__	0.093493	0	0.105753	0.156863
k__Bacteria;p__Firmicutes;c__Bacilli	2.412117	1.159008	2.220812	7.235294
k__Bacteria;p__Firmicutes;c__Clostridia	3.272251	2.318015	1.882403	1.764706
k__Bacteria;p__Planctomycetes;c__Planctomycetia	0.093493	0.040667	0.063452	0
k__Bacteria;p__Proteobacteria;__	0.617053	0.183001	0.465313	0.215686
k__Bacteria;p__Proteobacteria;c__Betaproteobacteria	6.432311	2.765352	11.92893	3.078431
k__Bacteria;p__Proteobacteria;c__Deltaproteobacteria	0.430067	0.447336	0.232657	0.176471
k__Bacteria;p__Proteobacteria;c__Gammaproteobacteria	0.224383	1.443676	0.401861	2.039216
k__Bacteria;p__Spirochaetes;c__Spirochaetes	0.037397	0	0	0.45098
k__Bacteria;p__Tenericutes;c__Mollicutes	0	0	0	0.176471
Unassigned;__;__	0.673149	0.610004	0.824873	0.156863

Table E.8: Relative abundances of Order level taxonomic classification of sequencing reads targeting the V3-V5 region of the bacterial 16S rRNA gene

	M0	M4	M8	M9
k__Archaea;__;__;__	0.13089	0.52867	0.338409	0
k__Bacteria;__;__;__	31.17053	41.70394	36.31557	43.94118
k__Bacteria;p__Actinobacteria;__;__	0	0	0.126904	0
k__Bacteria;p__Actinobacteria;c__Actinobacteria;o__Actinomycetales	1.757666	2.236682	3.405245	2.921569
k__Bacteria;p__Bacteroidetes;__;__	24.64473	18.54412	19.75465	21.09804
k__Bacteria;p__Bacteroidetes;c__Bacteroidia;o__Bacteroidales	24.08377	22.26515	17.61844	13.70588
k__Bacteria;p__Bacteroidetes;c__Cytophagia;o__Cytophagales	0	0	0.021151	0.490196
k__Bacteria;p__Chloroflexi;c__Anaerolineae;__	0.037397	0	0	0
k__Bacteria;p__Chloroflexi;c__Anaerolineae;o__Anaerolineales	3.889304	5.754372	4.29357	2.392157
k__Bacteria;p__Firmicutes;__;__	0.093493	0	0.105753	0.156863
k__Bacteria;p__Firmicutes;c__Bacilli;o__Bacillales	2.412117	1.159008	2.220812	7.235294
k__Bacteria;p__Firmicutes;c__Clostridia;__	0.673149	0	0	0.45098
k__Bacteria;p__Firmicutes;c__Clostridia;o__Clostridiales	2.599102	2.318015	1.882403	1.313725
k__Bacteria;p__Planctomycetes;c__Planctomycetia;o__Pirellulales	0.093493	0.040667	0.063452	0
k__Bacteria;p__Proteobacteria;__;__	0.617053	0.183001	0.465313	0.215686
k__Bacteria;p__Proteobacteria;c__Betaproteobacteria;__	3.926702	2.033347	7.84687	2.960784
k__Bacteria;p__Proteobacteria;c__Betaproteobacteria;o__Burkholderiales	2.50561	0.732005	4.082064	0.117647
k__Bacteria;p__Proteobacteria;c__Deltaproteobacteria;__	0.317876	0.203335	0.126904	0.078431
k__Bacteria;p__Proteobacteria;c__Deltaproteobacteria;o__Syntrophobacterales	0.112191	0.244002	0.105753	0.098039
k__Bacteria;p__Proteobacteria;c__Gammaproteobacteria;__	0.112191	0.264335	0.063452	1.529412
k__Bacteria;p__Proteobacteria;c__Gammaproteobacteria;o__Enterobacteriales	0.037397	1.05734	0.253807	0.333333
k__Bacteria;p__Proteobacteria;c__Gammaproteobacteria;o__Xanthomonadales	0.074794	0.122001	0.084602	0.176471

k__Bacteria;p__Spirochaetes;c__Spirochaetes;o__Spirochaetales	0.037397	0	0	0.45098
k__Bacteria;p__Tenericutes;c__Mollicutes;o__Acholeplasmatales	0	0	0	0.176471
Unassigned;__;__;__	0.673149	0.610004	0.824873	0.156863

Table E.9: Relative abundances of Family level taxonomic classification of sequencing reads targeting the V3-V5 region of the bacterial 16S rRNA gene

	M0	M4	M8	M9
k__Archaea;__;__;__;__	0.13089	0.52867	0.338409	0
k__Bacteria;__;__;__;__	31.17053	41.70394	36.31557	43.94118
k__Bacteria;p__Actinobacteria;__;__;__	0	0	0.126904	0
k__Bacteria;p__Actinobacteria;c__Actinobacteria;o__Actinomycetales;__	1.757666	2.236682	3.405245	2.921569
k__Bacteria;p__Bacteroidetes;__;__;__	24.64473	18.54412	19.75465	21.09804
k__Bacteria;p__Bacteroidetes;c__Bacteroidia;o__Bacteroidales;__	5.422588	3.355022	4.039763	0.333333
k__Bacteria;p__Bacteroidetes;c__Bacteroidia;o__Bacteroidales;f__Marinilabiaceae	2.150337	1.972346	1.734349	3.72549
k__Bacteria;p__Bacteroidetes;c__Bacteroidia;o__Bacteroidales;f__Porphyromonadaceae	16.51085	16.93778	11.84433	9.647059
k__Bacteria;p__Bacteroidetes;c__Cytophagia;o__Cytophagales;__	0	0	0.021151	0.490196
k__Bacteria;p__Chloroflexi;c__Anaerolineae;__;__	0.037397	0	0	0
k__Bacteria;p__Chloroflexi;c__Anaerolineae;o__Anaerolineales;f__Anaerolinaceae	3.889304	5.754372	4.29357	2.392157
k__Bacteria;p__Firmicutes;__;__;__	0.093493	0	0.105753	0.156863
k__Bacteria;p__Firmicutes;c__Bacilli;o__Bacillales;__	2.412117	1.159008	2.220812	7.235294
k__Bacteria;p__Firmicutes;c__Clostridia;__;__	0.673149	0	0	0.45098
k__Bacteria;p__Firmicutes;c__Clostridia;o__Clostridiales;__	0.635752	0.122001	0.655668	0.392157
k__Bacteria;p__Firmicutes;c__Clostridia;o__Clostridiales;f__Lachnospiraceae	0	0.244002	0.169205	0.098039
k__Bacteria;p__Firmicutes;c__Clostridia;o__Clostridiales;f__Ruminococcaceae	1.963351	1.952013	1.05753	0.823529

k__Bacteria;p__Planctomycetes;c__Planctomycetia;o__Pirellulales;f__Pirellulaceae	0.093493	0.040667	0.063452	0
k__Bacteria;p__Proteobacteria;__;__;__	0.617053	0.183001	0.465313	0.215686
k__Bacteria;p__Proteobacteria;c__Betaproteobacteria;__;__	3.926702	2.033347	7.84687	2.960784
k__Bacteria;p__Proteobacteria;c__Betaproteobacteria;o__Burkholderiales;__	2.50561	0.732005	4.082064	0.117647
k__Bacteria;p__Proteobacteria;c__Betaproteobacteria;o__Burkholderiales;f__Comamonadaceae	0	0	0	0
k__Bacteria;p__Proteobacteria;c__Deltaproteobacteria;__;__	0.317876	0.203335	0.126904	0.078431
k__Bacteria;p__Proteobacteria;c__Deltaproteobacteria;o__Syntrophobacterales;f__Syntrophaceae	0.112191	0.142334	0.042301	0.098039
k__Bacteria;p__Proteobacteria;c__Deltaproteobacteria;o__Syntrophobacterales;f__Syntrophorhabdaceae	0	0.101667	0.063452	0
k__Bacteria;p__Proteobacteria;c__Gammaproteobacteria;__;__	0.112191	0.264335	0.063452	1.529412
k__Bacteria;p__Proteobacteria;c__Gammaproteobacteria;o__Enterobacteriales;f__Enterobacteriaceae	0.037397	1.05734	0.253807	0.333333
k__Bacteria;p__Proteobacteria;c__Gammaproteobacteria;o__Xanthomonadales;f__Xanthomonadaceae	0.074794	0.122001	0.084602	0.176471
k__Bacteria;p__Spirochaetes;c__Spirochaetes;o__Spirochaetales;f__Spirochaetaceae	0.037397	0	0	0.45098
k__Bacteria;p__Tenericutes;c__Mollicutes;o__Acholeplasmatales;f__Acholeplasmataceae	0	0	0	0.176471
Unassigned;__;__;__;__	0.673149	0.610004	0.824873	0.156863

Table E.10: Relative abundances of Genus level taxonomic classification of sequencing reads targeting the V3-V5 region of the bacterial 16S rRNA gene

	M0	M4	M8	M9
k__Archaea;__;__;__;__;__	0.1308901	0.5286702	0.3384095	0
k__Bacteria;__;__;__;__;__	31.170531	41.703945	36.315567	43.941176
k__Bacteria;p__Actinobacteria;__;__;__;__	0	0	0.1269036	0

k__Bacteria;p__Actinobacteria;c__Actinobacteria;o__Actinomycetales;__;__	1.7576664	2.2366816	3.4052453	2.9215686
k__Bacteria;p__Bacteroidetes;__;__;__;__	24.644727	18.544124	19.754653	21.098039
k__Bacteria;p__Bacteroidetes;c__Bacteroidia;o__Bacteroidales;__;__	5.4225879	3.3550224	4.0397631	0.3333333
k__Bacteria;p__Bacteroidetes;c__Bacteroidia;o__Bacteroidales;f__Marinilabiaceae;g__Ruminofilibacter	2.1503366	1.9723465	1.7343486	3.7254902
k__Bacteria;p__Bacteroidetes;c__Bacteroidia;o__Bacteroidales;f__Porphyromonadaceae;g__Macellibacteroides	0.5235602	1.1996747	1.2478849	0
k__Bacteria;p__Bacteroidetes;c__Bacteroidia;o__Bacteroidales;f__Porphyromonadaceae;g__Petrimonas	15.800299	15.555104	10.34264	7.3921569
k__Bacteria;p__Bacteroidetes;c__Bacteroidia;o__Bacteroidales;f__Porphyromonadaceae;g__Proteiniphilum	0.1869858	0.1830012	0.2538071	2.254902
k__Bacteria;p__Bacteroidetes;c__Cytophagia;o__Cytophagales;__;__	0	0	0.0211506	0.4901961
k__Bacteria;p__Chloroflexi;c__Anaerolineae;__;__;__	0.0373972	0	0	0
k__Bacteria;p__Chloroflexi;c__Anaerolineae;o__Anaerolineales;f__Anaerolinaceae;__	3.8893044	5.7543717	4.2935702	2.3921569
k__Bacteria;p__Firmicutes;__;__;__;__	0.0934929	0	0.105753	0.1568627
k__Bacteria;p__Firmicutes;c__Bacilli;o__Bacillales;__;__	2.4121167	1.1590077	2.2208122	7.2352941
k__Bacteria;p__Firmicutes;c__Clostridia;__;__;__	0.6731488	0	0	0.4509804
k__Bacteria;p__Firmicutes;c__Clostridia;o__Clostridiales;__;__	0.6357517	0.1220008	0.6556684	0.3921569
k__Bacteria;p__Firmicutes;c__Clostridia;o__Clostridiales;f__Lachnospiraceae;__	0	0.2440016	0.1692047	0.0980392
k__Bacteria;p__Firmicutes;c__Clostridia;o__Clostridiales;f__Ruminococcaceae;__	0.0747943	0.1830012	0	0.0980392

k__Bacteria;p__Firmicutes;c__Clostridia;o__Clostridiales;f__Ruminococcaceae;g__Bacteroides	0.6544503	0.7726718	0.5922166	0.372549
k__Bacteria;p__Firmicutes;c__Clostridia;o__Clostridiales;f__Ruminococcaceae;g__Clostridium	1.2341062	0.99634	0.465313	0.3529412
k__Bacteria;p__Planctomycetes;c__Planctomycetia;o__Pirellulales;f__Pirellulaceae;__	0.0934929	0.0406669	0.0634518	0
k__Bacteria;p__Proteobacteria;__;__;__;__	0.6170531	0.1830012	0.465313	0.2156863
k__Bacteria;p__Proteobacteria;c__Betaproteobacteria;__;__;__	3.9267016	2.0333469	7.8468697	2.9607843
k__Bacteria;p__Proteobacteria;c__Betaproteobacteria;o__Burkholderiales;__;__	2.5056096	0.7320049	4.0820643	0.1176471
k__Bacteria;p__Proteobacteria;c__Betaproteobacteria;o__Burkholderiales;f__Comamonadaceae;__	0	0	0	0
k__Bacteria;p__Proteobacteria;c__Deltaproteobacteria;__;__;__	0.3178758	0.2033347	0.1269036	0.0784314
k__Bacteria;p__Proteobacteria;c__Deltaproteobacteria;o__Syntrophobacterales;f__Syntrophaceae;g__Syntrophus	0.1121915	0.1423343	0.0423012	0.0980392
k__Bacteria;p__Proteobacteria;c__Deltaproteobacteria;o__Syntrophobacterales;f__Syntrophorhabdaceae;g__Syntrophorhabdus	0	0.1016673	0.0634518	0
k__Bacteria;p__Proteobacteria;c__Gammaproteobacteria;__;__;__	0.1121915	0.2643351	0.0634518	1.5294118
k__Bacteria;p__Proteobacteria;c__Gammaproteobacteria;o__Enterobacteriales;f__Enterobacteriaceae;__	0.0373972	1.0573404	0.2538071	0.3333333
k__Bacteria;p__Proteobacteria;c__Gammaproteobacteria;o__Xanthomonadales;f__Xanthomonadaceae;__	0.0747943	0.0610004	0.0211506	0
k__Bacteria;p__Proteobacteria;c__Gammaproteobacteria;o__Xanthomonadales;f__Xanthomonadaceae;g__Pseudoxanthomonas	0	0.0610004	0.0634518	0.1764706
k__Bacteria;p__Spirochaetes;c__Spirochaetes;o__Spirochaetales;f__Spirochaetaceae;g__HAW-RM37	0.0373972	0	0	0.4509804
k__Bacteria;p__Tenericutes;c__Mollicutes;o__Acholeplasmatales;f__Acholeplasmataceae;g__Acholeplasma	0	0	0	0.1764706

Unassigned;__;__;__;__;__	0.6731488	0.6100041	0.8248731	0.1568627

Table E.11: Relative abundances of Kingdom level taxonomic classification of sequencing reads targeting the V3-V4 region of the archaeal 16S rRNA gene.

	M0	M4	M8	M9
Unassigned	55.57731959	41.83389075	53.01375405	30.02272
k__Archaea	36.27835052	47.89576366	37.97532362	58.22751
k__Bacteria	8.144329897	10.2703456	9.01092233	11.74977

Table E.12: Relative abundances of Phylum level taxonomic classification of sequencing reads, classified as Archaea, targeting the V3-V4 region of the archaeal 16S rRNA gene

	M0	M4	M8	M9
k__Archaea;__	46.43365	40.18039	47.66977	7.575758
k__Archaea;p__Crenarchaeota	1.30719	0.465522	1.225033	1.538108
k__Archaea;p__Euryarchaeota	52.25916	59.35409	51.10519	90.88613

Table E.13: Relative abundances of Class level taxonomic classification of sequencing reads, classified as Archaea, targeting the V3-V4 region of the archaeal 16S rRNA gene.

	M0	M4	M8	M9
k__Archaea;__;__	46.43365	40.18039	47.66977	7.575758
k__Archaea;p__Crenarchaeota;__	0.284172	0.087285	0.319574	0.596878
k__Archaea;p__Crenarchaeota;c__Thaumarchaeota	1.023018	0.378237	0.905459	0.94123
k__Archaea;p__Euryarchaeota;__	12.5888	4.276986	7.536618	0.482094
k__Archaea;p__Euryarchaeota;c__Methanobacteria	7.558966	5.440791	8.149134	4.660239
k__Archaea;p__Euryarchaeota;c__Methanomicrobia	24.26826	43.03171	26.23169	75.94123
k__Archaea;p__Euryarchaeota;c__Thermoplasmata	7.843137	6.604597	9.18775	9.802571

Table E.14: Relative abundances of Order level taxonomic classification of sequencing reads, classified as Archaea, targeting the V3-V4 region of the archaeal 16S rRNA gene

	M0	M4	M8	M9
k__Archaea;__;__;__	46.43365	40.18039	47.66977	7.575758
k__Archaea;p__Crenarchaeota;__;__	0.284172	0.087285	0.319574	0.596878
k__Archaea;p__Crenarchaeota;c__Thaumarchaeota;__	1.023018	0.378237	0.905459	0.94123
k__Archaea;p__Euryarchaeota;__;__	12.5888	4.276986	7.536618	0.482094
k__Archaea;p__Euryarchaeota;c__Methanobacteria;o__Methanobacteriales	7.558966	5.440791	8.149134	4.660239
k__Archaea;p__Euryarchaeota;c__Methanomicrobia;o__Methanomicrobiales	15.2316	32.9066	19.17443	45.08724
k__Archaea;p__Euryarchaeota;c__Methanomicrobia;o__YC-E6	9.036658	10.12511	7.057257	30.85399
k__Archaea;p__Euryarchaeota;c__Thermoplasmata;o__E2	7.843137	6.604597	9.18775	9.802571

Table E.15: Relative abundances of Family level taxonomic classification of sequencing reads, classified as Archaea, targeting the V3-V4 region of the archaeal 16S rRNA gene.

	M0	M4	M8	M9
k__Archaea;__;__;__;__	46.43365	40.18039	47.66977	7.575758
k__Archaea;p__Crenarchaeota;__;__;__	0.284172	0.087285	0.319574	0.596878
k__Archaea;p__Crenarchaeota;c__Thaumarchaeota;__;__	1.023018	0.378237	0.905459	0.94123
k__Archaea;p__Euryarchaeota;__;__;__	12.5888	4.276986	7.536618	0.482094
k__Archaea;p__Euryarchaeota;c__Methanobacteria;o__Methanobacteriales;f__Methanobacteriaceae	7.558966	5.440791	8.149134	4.660239
k__Archaea;p__Euryarchaeota;c__Methanomicrobia;o__Methanomicrobiales;__	0.341006	0	0.186418	0
k__Archaea;p__Euryarchaeota;c__Methanomicrobia;o__Methanomicrobiales;f__Methanocorpusculaceae	0.227337	0.029095	0.079893	0.068871
k__Archaea;p__Euryarchaeota;c__Methanomicrobia;o__Methanomicrobiales;f__Methanomicrobiaceae	10.08809	28.97876	11.15846	44.83471
k__Archaea;p__Euryarchaeota;c__Methanomicrobia;o__Methanomicrobiales;f__Methanospirillaceae	4.575163	3.898749	7.749667	0.183655
k__Archaea;p__Euryarchaeota;c__Methanomicrobia;o__YC-E6;f__	9.036658	10.12511	7.057257	30.85399

k__Archaea;p__Euryarchaeota;c__Thermoplasmata;o__E2;f__[Methanomassiliicoccaceae]	7.843137	6.604597	9.18775	9.802571

Table E.16: Relative abundances of Genus level taxonomic classification of sequencing reads, classified as Archaea, targeting the V3-V4 region of the archaeal 16S rRNA gene

index	M0	M4	M8	M9
k__Archaea;__;__;__;__;__	46.43365	40.18039	47.66977	7.575758
k__Archaea;p__Crenarchaeota;__;__;__;__	0.284172	0.087285	0.319574	0.596878
k__Archaea;p__Crenarchaeota;c__Thaumarchaeota;__;__;__	1.023018	0.378237	0.905459	0.94123
k__Archaea;p__Euryarchaeota;__;__;__;__	12.5888	4.276986	7.536618	0.482094
k__Archaea;p__Euryarchaeota;c__Methanobacteria;o__Methanobacteriales;f__Methanobacteriaceae;__	0.454675	0.174571	0.745672	0.114784
k__Archaea;p__Euryarchaeota;c__Methanobacteria;o__Methanobacteriales;f__Methanobacteriaceae;g__Methanobacterium	6.649616	4.858889	7.110519	4.109275
k__Archaea;p__Euryarchaeota;c__Methanobacteria;o__Methanobacteriales;f__Methanobacteriaceae;g__Methanobrevibacter	0.454675	0.407332	0.292943	0.43618
k__Archaea;p__Euryarchaeota;c__Methanomicrobia;o__Methanomicrobiales;__;__	0.341006	0	0.186418	0
k__Archaea;p__Euryarchaeota;c__Methanomicrobia;o__Methanomicrobiales;f__Methanocorpusculaceae;g__	0.227337	0.029095	0.079893	0.068871
k__Archaea;p__Euryarchaeota;c__Methanomicrobia;o__Methanomicrobiales;f__Methanomicrobiaceae;__	5.399261	8.990399	5.912117	12.87879
k__Archaea;p__Euryarchaeota;c__Methanomicrobia;o__Methanomicrobiales;f__Methanomicrobiaceae;g__Methanofollis	0	0.058192	0	0
k__Archaea;p__Euryarchaeota;c__Methanomicrobia;o__Methanomicrobiales;f__Methanomicrobiaceae;g__Methanomicrobiaceae	4.688832	19.93017	5.246338	31.95592

k__Archaea;p__Euryarchaeota;c__Methanomicrobia;o__Methanomicrobiales;f__Methanospirillaceae;g__	4.575163	3.898749	7.749667	0.183655
k__Archaea;p__Euryarchaeota;c__Methanomicrobia;o__YC-E6;f__;g__	9.036658	10.12511	7.057257	30.85399
k__Archaea;p__Euryarchaeota;c__Thermoplasmata;o__E2;f__[Methanomassiliicoccaceae];g__Coxiella	0.284172	0.174571	0.319574	0
k__Archaea;p__Euryarchaeota;c__Thermoplasmata;o__E2;f__[Methanomassiliicoccaceae];g__Methanomassiliicoccus	7.558966	6.430026	8.868176	9.802571

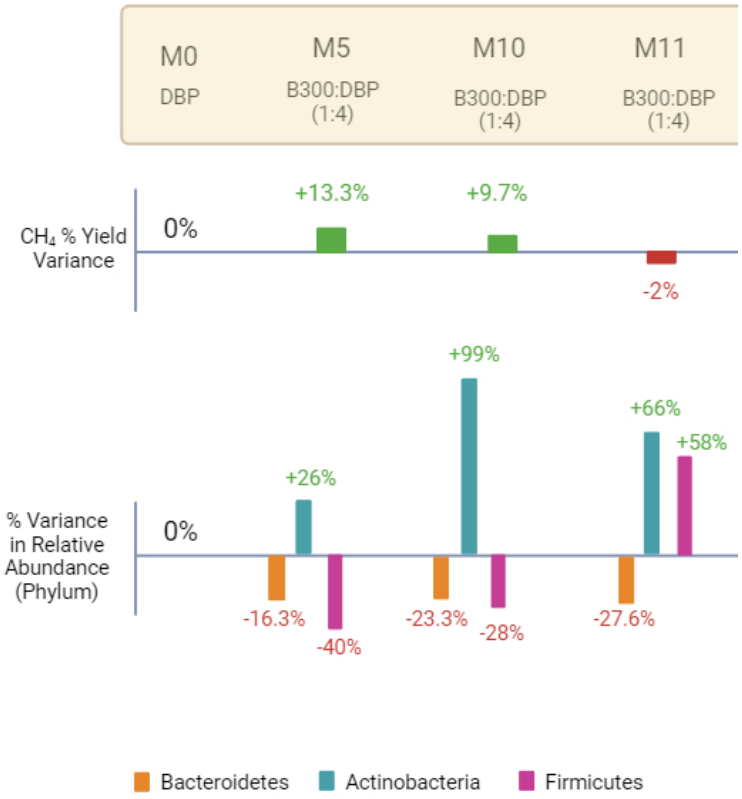


Figure E.1: Percentage methane yield variances of biochar supplemented anaerobic digesters compared to those with no biochar supplementation and percentage variance of the relative abundances of major bacterial phyla in supplemented and unsupplemented digesters

Appendix F

Appendix F.1: Biohythane energy consumption

Table F.1: Range and energy consumption fo

Description	Acronym		Value	Unit	Equations
Truck range	T_{Range}	=	1250	km	(Gray et al., 2022)
Tank size	T_{vol}	=	440	L	(Gray et al., 2022)
Vol of H_2	H_{2Vol}	=	51.35	L	TRange =T_{vol}*11.66 %H_{2vol}; where 11.66 is the average H2 volume
Vol of CH_4	CH_{4Vol}	=	388.65	L	CH_{4vol}=T_{vol} - H_{2Vol}
Density of H_2	p_{H2}	=	0.089	kg. m^{-3}	
Density of CH_4	p_{CH4}	=	0.716	kg. m^{-3}	
Mass of H_2	m_{H2}	=	4.57	kg	m_{H2}= H_{2Vol} * p_{H2}
Mass of CH_4	m_{CH4}	=	278.273	kg	m_{H2}= H_{2Vol} * p_{CH4}
Energy of H_2	E_{H2}	=	152.323	kWh	E_{H2}= m_{H2} * 33.33
Energy of CH_4	E_{CH4}	=	3864.908	kWh	E_{CH4}= m_{H2} * 50 MJ. kg^{-1} / 3.6 MJ. kWh^{-1}
Total energy	T_{energy}	=	4017.231	kWh	T_{energy} = E_{H2} + E_{CH4}
Energy consumption	$E_{consumption}$	=	3.21	kWh. km^{-1}	$E_{consumption}$ = T_{energy} / T_{range}

Appendix F.2: VFA to COD conversion factors

Table F.2: VFA to COD conversion factors	
Volatile fatty acid	**Conversion factor (g COD. g^{-1}acid)**
Acetic acid	1.07
Propionic acid	1.51
Isobutyric acid	1.82
Butyric acid	1.82
Isovaleric acid	2.04
Valeric acid	2.04
Isocaproic acid	2.21
Caproic acid	2.21
Heptanoic acid	2.34

Appendix F.3: Carbon dioxide emissions reduction of different scenarios of WBChar

Table F.3: Carbon dioxide emissions reduction of different scenarios of WBChar at a dosage of 2 g. g^{-1}VS

Parameters	Acronyms	Units	Values	Equations
Volume of Distillery	$V_{distillery}$	million L_{OLA}	50	
Mass flow of the feedstock	m_{mWBM}	t wwt	516,500	m_{mWBM} = Vdistillery * 10.33 kg. $L^{-1}{}_{OLA}$
Feedstock volatile solids content	VS_{mWBM}	t	33,056	The VS content in mWBM was measured as 6.4%.
Biochar addition (based of experimental data)	$m_{char\ addition}$	t	66,112	$m_{char\ addition} = VS_{mWBM} \times$ B2S; where B2S is the biochar-to-substrate ratio on a VS basis
Hydrogen production (assuming 25%$_{volume}$ is H_2)	Y_{H2}	m^3	1,558,787.523	$Y_{CH4} = VS_{mWBM} \times$ SHY m^3/t VS; where the specific hydrogen yield
Mass flow of H_2	m_{H2}	kg	138,732.090	$m_{H2} = Y_{H2} \times 0.089$ kg. $m^{-3} \div 1000$; where 0.089 kg. m^{-3} is the density of H_2 at STP
Carbon dioxide production (assuming 75%$_{volume}$ is CO2)	Y_{CO2}	m^3	4,676,362.569	$Y_{CO2} = Y_{CH4} \div 25\% \times 75\%$; where 25% is the percentage of H_2 and 75% is the CO_2.
Mass flow of carbon dioxide	m_{CO2}	kg	9,259,197.886	$m_{CO2} = Y_{CO2} \times 1.980$ kg. $m^{-3} \div 1000$; where 1.98 kg. m^{-3} is the density of CO_2
Methane production (assuming 60%$_{volume}$ is CH_4)	Y_{CH4}	m^3	11,305,152.000	$Y_{CH4} = VS_{mWBM} \times$ SMY m^3. t^{-1} VS; where the specific methane yield
Mass flow of methane	m_{CH4}	kg	8,094,488.83	$m_{CH4} = Y_{CH4} \times 0.716$ kg. $m^{-3} \div 1000$; where 0.716 kg. m^{-3} is the density of CH_4
Carbon dioxide production (accounting for biogas composition)	Y_{CO2}	m^3	7,536,768.00	$Y_{CO2} = Y_{CH4} \div 60\% \times 40\%$; where 60% is the percentage of CH_4 and 40% is the CO_2.

Mass flow of carbon dioxide	m_{CO2}	t	14,922.801	$m_{CO2} = Y_{CO2} \times 1.98$ kg. $m^{-3} \div 1000$; where 1.98 kg. m^{-3} is the density of CO_2
Energy value of Hydrogen	Q_{H2}	MJ	16,647,850.7	$Q_{CH4} = m_{CH4} \times 120$ MJ. kg^{-1}, in which 120 MJ. kg^{-1} is the LHV of H_2.
Energy value of Hydrogen	QV_{H2}	GWh	4.6	$Q_{CH4} = Y_{CH4} \times 33.33$ kWh. kg^{-1}, in which 120 MJ. kg^{-1} is the LHV of H_2
Energy value of Methane	Q_{CH4}	MJ	404,724,441.6	$Q_{CH4} = Y_{CH4} \times 50$ MJ. kg^{-1}, in which 50 MJ. kg^{-1} is the LHV of CH_4.
Energy value of Methane (kWh)	QV_{CH4}	GWh	112.42	$Q_{CH4} = Y_{CH4} / 3600$ MJ. kWh^{-1}
Energy value of Biohythane	$Q_{H2\text{-}CH4}$	MJ	421,372,292.3	$Q_{H2\text{-}CH4} = Q_{H2} + Q_{CH4}$
Energy value of Biohythane	$QV_{H2\text{-}CH4}$	GWh	117.0	$QV_{H2\text{-}CH4} = QV_{H2} + QV_{CH4}$
Distillery thermal demand	THwhiskey	GWh	208	
		GJ	748,800	
CO2 Emissions from Natural Gas production	$CO_{2_Heating}$	kt CO_2e. a^{-1}	42	$CO_{2_Heating} = TH_{whiskey} \times 0.202$ ktCO2e. GWh^{-1}natural gas
Distillery electrical demand	Ewhiskey	GWh	35.4	
		GJ	127,440	
CO2 Emissions from Electricity consumption	CO2_Elec	kt CO_2e. a^{-1}	11.8	$CO_{2_Heating} = TH_{whiskey} \times 0.332$ ktCO2e. GWh^{-1}electricity
Total Emissions generated from Whiskey production		kt CO_2e. a^{-1}	53.8	
Distillery Transport	Dyearly	million km. a^{-1}	8.7	Paper 3
	Ediesel	GWh	27.7	Ediesel = Dyearly / 3.18 $kWh.km^{-1}$
Total Emissions generated from Distribution Transport	CO2_Transport	kt CO_2e. a^{-1}	7.3	$CO_{2_Transport}$ = Ediesel × 0.2639 ktCO2e. GWh^{-1}diesel
Total Emissions generated		kt CO_2e. a^{-1}	**61.1**	
Specific Transport Emissions	SCO2_Transport	kt CO_2e. L^{-1} whiskey	0.1	SCO2_Transport = $(CO2_{_Transport})/V_{distillery}$

Total Emissions of Production (Electricity + Heating)	CO2_Production	**kt CO_2e. L^{-1}_{OLA}**	1.1	CO2_Production = ($CO_{2_Heating}$+ $CO_{2_Electricity}$)/$V_{distillery}$
Specific Transport and Production Emissions	CO2_TnP	**kt CO_2e. L^{-1}_{OLA}**	**1.2**	CO2_TnP = CO2_Production+ SCO2_Transport
Scenario 1: Boiler thermal recovery	TH $_{scenario\ 1}$	GJ	379,235.1	$TH_{scenario\ 1}$ = $Q_{H2\text{-}CH4}$ * Boiler efficiency, where the boiler efficiency is 90%
	THW $_{scenario\ 1}$	GWh	105.3	$TH_{scenario\ 1}$ = $QV_{H2\text{-}CH4}$ * Boiler efficiency, where the boiler efficiency is 90%
% of Natural gas offset by Biohythane	Sce1%Heating	%	50.6	%Heating = TH scenario 1 / TH whiskey
Avoided emissions from Natural Gas using Biohythane	**$CO2_{_scenario\ 1}$**	**kt CO_2e. a^{-1}**	**21.3**	**$CO2_{_scenario\ 1}$ = CO2_Heating * %Heating**
New total Emissions of Production (Electricity + Heating)	**$CO2_{_SC1_Production}$**	**kt CO_2e. L^{-1}_{OLA}**	**0.65**	**CO2_Production = (CO2_Heating+ CO2_Electricity-$CO_{2_scenario\ 1}$)/$V_{distillery}$**
New Specific Transport and Production Emissions	**$CO2_{_SC1_TnP}$**	**kt CO_2e. L^{-1}_{OLA}**	**0.8**	**$CO2_{_SC1_TnP}$ = (Total Emissions generated - $CO_{2_scenario\ 1}$)/$V_{distillery}$**
Scenario 2: CHP Unit	CHP Heat	GJ	210,686.1	CHP Heat = $Q_{H2\text{-}CH4}$ ×CHP%Heating
		GWh	58.5	CHP Heat = $QV_{H2\text{-}CH4}$ × CHP%Heating
% of Natural gas offset by Biohythane	%Heating	%	28.1	%Heating = CHP Heat / TH whiskey
Avoided emissions from CHP Heating	CHP_%Heating	kt CO_2e. a^{-1}	11.8	$CO2_{_scenario\ 1}$ = CO2_Heating × CHP%Heating
	CHP Elec.	GJ	168,548.9	CHP Heat = $Q_{H2\text{-}CH4}$ ×CHP%Elec
		GWh	46.8	#CHP Heat = $QV_{H2\text{-}CH4}$ ×CHP%Heating
Avoided emissions from CHP Electricity (Only 100%)	CHP_%Heating	kt CO_2e. a^{-1}	11.8	CHP_%Heating = CO2_Elec

% of Electricity offset by CHP Biohythane	Sce2%Elec	%	132.3	Sce2%Elec = CHP Elec / Ewhiskey
% of Heating offset by CHP Biohythane	Sce2%Heat	%	28.1	Sce2%Elec = CHP Heat / Hwhiskey
Total avoided emissions from CHP Scenario 2	**$CO2_{_scenario\ 2}$**	**kt CO_2e. a^{-1}**	**23.6**	**$CO2_{_scenario\ 1}$ = CHP_%Heating + CHP_%Electricity**
New total Emissions of Production (Electricity + Heating)	**$CO2_{_SC2_Production}$**	**kt CO_2e. L^{-1}_{OLA}**	**0.6**	**$CO2_Production = (CO2_{_Heating} + CO2_{_Electricity} - CO_{2_scenario\ 1})/V_{distillery}$**
New Specific Transport and Production Emissions	**$CO2_{_SC2_TnP}$**	**kt CO_2e. L^{-1}_{OLA}**	**0.75**	**$CO2_{_SC2_TnP} = (Total\ Emissions\ generated - CO_{2_scenario\ 1})/V_{distillery}$**
Scenario 3: Transport Distance Travelled with Biohythane	$D_{biohythane}$	million km. a^{-1}	33.9	$D_{biohythane} = QV / (3.21\ kWh.\ km^{-1})$
% of transport offset by Biohythane	%Transport	%	331	$\%Transport = D_{biohythane} / D_{yearly}$
Biohythane Energy Required to Satisfy Transport	$BioHy_{_at100\%}$	GWh	27.7	$BioHy_{_at100\%} = E_{diesel}$
Biohythane heat energy left after transport boiler	SCO2_Transport	GWh	80.4	SCO2_Transport = (QV H2-CH4 - BioHy_at100%) × boiler efficiency; where the boiler efficiency is 90%
% of Natural gas offset by Biohythane	%Sce3Heating	%	38.7	%Sce3Heating = CHP Heat / TH whiskey
Total avoided emissions from Transport + Boiler	**$CO2_{_scenario\ 3}$**	**kt CO_2e. a^{-1}**	**23.54**	**$CO_{2_scenario\ 3} = THW_{scenario\ 1} \times \%Sce3Heating + CO2_Transport$**
New Specific Transport and Production Emissions	**$CO2_{_SC3_TnP}$**	**kt CO_2e. L^{-1}_{OLA}**	**0.75**	**$CO2_{_SC3_TnP} = (Total\ Emissions\ generated - CO_{2_scenario\ 1}) / V_{distillery}$**
Scenario 4: Transport + CHP unit				
Biohythane available after transport use	$QV_{H2\text{-}CH4\text{-}Scenario4}$	GWh	89.3	$QV_{H2\text{-}CH4\text{-}Scenario4} = QV_{H2\text{-}CH4} - BioHy_{_at100\%}$

Biohythane heat energy from CHP	CHP_4 Heat	GWh	44.67	CHP_4 Heat = $QV_{H2\text{-}CH4\text{-}Scenario4}$ × CHP%Heating
Biohythane electrical energy from CHP	CHP_4 Elec.	GWh	35.74	CHP_4 Elec.= $QV_{H2\text{-}CH4\text{-}Scenario4}$ × CHP%Elec
% of Natural gas offset by Biohythane	%CHP Heating Sc4	%	21.5	%CHP Heating Sc4 = CHP4 Heat / THwhiskey
% of electricity offset by Biohythane	%CHP Ele. Sc4	%	100.96	%CHP Elec. Sc4 = CHP4 Elec / Ewhiskey
Emissions savings from Scenario 4 Heat	Sce4Heat	**kt CO_2e. a^{-1}**	9.03	Sce4Heat = CO2_Heating ×%CHP Heating Sc4
Emissions savings from Scenario 4 CHP Elec	Sce4Elec	**kt CO_2e. a^{-1}**	11.8	Sce4Elec = CO2_Elec
Total avoided emissions from Transport + CHP	**$CO2_{_scenario\ 4}$**	**kt CO_2e. a^{-1}**	**28.13**	**CO2_scenario 4 = Sce4Heat + Sce4Elec + CO2_Transport**
Specific CO2 emissions	**$CO2_{_SC4_TnP}$**	**kt CO_2e. L^{-1}_{OLA}**	**0.66**	**$CO2_{_SC4_TnP}$ = (Total Emissions generated - $CO_{2_scenario\ 1}$)/$V_{distillery}$**

Appendix G

Appendix G.1: Preliminary dosage study

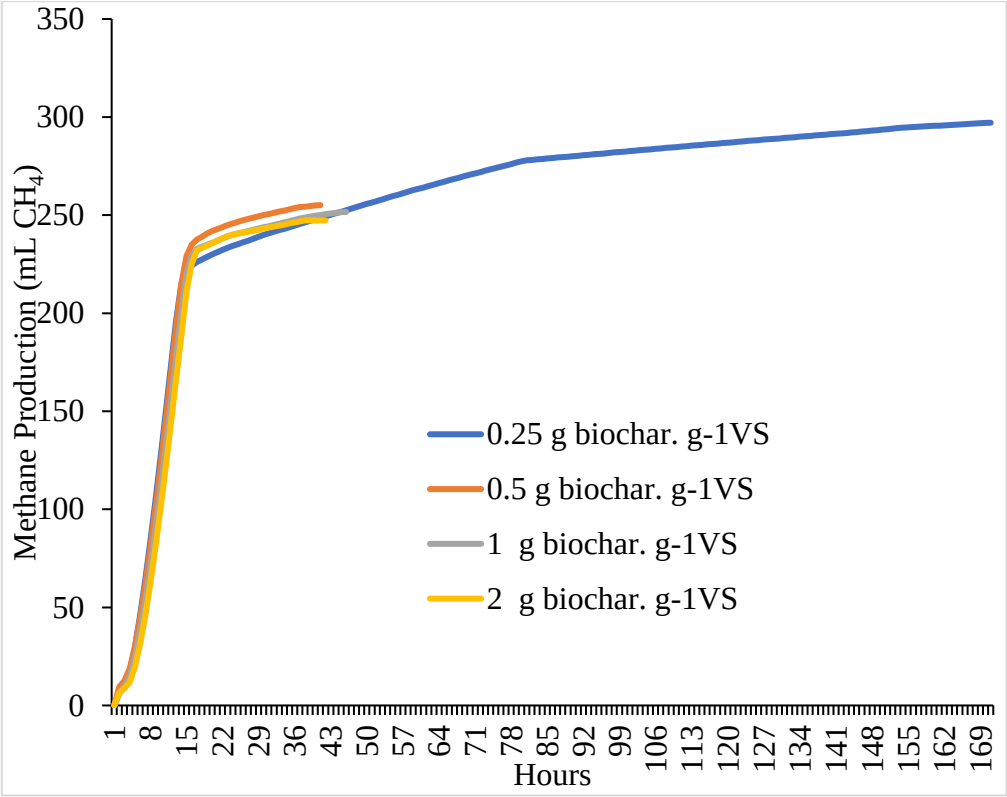


Figure G.1: Dosage study of digestate-derived biochar

Appendix G.2: FTIR analysis of digestate-derived biochar

